156045

RADC-TR-78-1[illegible], Vol I (of seven)
Final Technical Report
April 1976

APPLICATIONS OF MULTICONDUCTOR TRANSMISSION LINE THEORY TO THE PREDICTION OF CABLE COUPLING

Multiconductor Transmission Line Theory

University of Kentucky

Approved for public release;
distribution unlimited.

ROME AIR DEVELOPMENT CENTER
AIR FORCE SYSTEMS COMMAND
GRIFFISS AIR FORCE BASE, NEW YORK 13441

This report has been reviewed by the RADC Information Office (OI) and is releasable to the National Technical Information Service (NTIS). At NTIS it will be releasable to the general public including foreign nations.

This report has been reviewed and is approved for publication.

APPROVED: James C Brodock

JAMES C. BRODOCK
Project Engineer

APPROVED: Joseph J. Marsky

JOSEPH J. MARSKY
Chief, Reliability & Compatibility Division

FOR THE COMMANDER: John P. Huss

JOHN P. HUSS
Acting Chief, Plans Office

Do not return this copy. Retain or destroy.

UNCLASSIFIED

SECURITY CLASSIFICATION OF THIS PAGE (When Data Entered)

REPORT DOCUMENTATION PAGE		READ INSTRUCTIONS BEFORE COMPLETING FORM
1. REPORT NUMBER RADC-TR-76-101, Vol I (of seven)	2. GOVT ACCESSION NO.	3. RECIPIENT'S CATALOG NUMBER
4. TITLE (and Subtitle) APPLICATIONS OF MULTICONDUCTOR TRANSMISSION LINE THEORY TO THE PREDICTION OF CABLE COUPLING Vol I - Multiconductor Transmission Line Theory		5. TYPE OF REPORT & PERIOD COVERED Final Technical Report 6. PERFORMING ORG. REPORT NUMBER N/A
7. AUTHOR(s) Clayton R. Paul		8. CONTRACT OR GRANT NUMBER(s) F30602-72-C-0418
9. PERFORMING ORGANIZATION NAME AND ADDRESS University of Kentucky Department of Electrical Engineering Lexington KY 40506		10. PROGRAM ELEMENT, PROJECT, TASK AREA & WORK UNIT NUMBERS 62702F 45400130
11. CONTROLLING OFFICE NAME AND ADDRESS Rome Air Development Center (RBCT) Griffiss AFB NY 13441		12. REPORT DATE April 1976 13. NUMBER OF PAGES 183
14. MONITORING AGENCY NAME & ADDRESS(if different from Controlling Office) Same		15. SECURITY CLASS. (of this report) UNCLASSIFIED 15a. DECLASSIFICATION/DOWNGRADING SCHEDULE N/A

16. DISTRIBUTION STATEMENT (of this Report)

Approved for public release; distribution unlimited.

PRICES SUBJECT TO CHANGE

17. DISTRIBUTION STATEMENT (of the abstract entered in Block 20, if different from Report)

Same

18. SUPPLEMENTARY NOTES

RADC Project Engineer: James Brodock (RBCT)

19. KEY WORDS (Continue on reverse side if necessary and identify by block number)

Electromagnetic Compatibility
Cable Coupling
Transmission Lines
Multiconductor Transmission Lines
Wire-to-wire Coupling
Ribbon Cable
Flat Pack Cable

20. ABSTRACT (Continue on reverse side if necessary and identify by block number)

This report is the first volume in a series of reports documenting the Application of Multiconductor Transmission Line Theory to the Prediction of Cable Coupling. Modern avionics systems are becoming increasingly complex. These systems generally contain large numbers of wires connecting the various electronic equipments. The majority of the wires are in very close proximity to each other in either random cable bundles (in which the relative wire positions are not known or controlled) or in ribbon cables (in which the

(Cont'd)

DD FORM 1 JAN 73 1473 EDITION OF 1 NOV 65 IS OBSOLETE

UNCLASSIFIED

SECURITY CLASSIFICATION OF THIS PAGE (When Data Entered)

relative wire positions are known and controlled). The prediction of wire-coupled interference in these cable bundles is of considerable importance in the prediction of overall system compatibility. It is the purpose of this series of reports to examine the application of multiconductor transmission line theory to this problem.

This first volume is intended to provide a comprehensive discussion of multiconductor transmission line theory on which the remaining volumes will be based. The remaining volumes will investigate the application of this theory to specific classes of problems. Considerable experimental verification will be included in the later volumes to indicate the degree of confidence which can be placed in these models when they are applied to specific situations.

Volumes I, II, and III have been completed at this time and Volume IV is in preparation. Other volumes covering shielded wires, twisted pairs and terminal currents induced by external incident fields will be included. The completed volumes and those in preparation are:

Volume I - MULTICONDUCTOR TRANSMISSION LINE THEORY

Volume II - COMPUTATION OF THE CAPACITANCE MATRICES FOR RIBBON CABLES

Volume III - PREDICTION OF CROSSTALK IN RANDOM CABLE BUNDLES

Volume IV - PREDICTION OF CROSSTALK IN RIBBON CABLES

PREFACE

The Post-Doctoral Program at Rome Air Development Center is pursued via Project 9567 under the direction of Mr. Jacob Scherer. The Post-Doctoral Program is a cooperative venture between RADC and the participating universities: Syracuse University (Department of Electrical and Computer Engineering), the U.S. Air Force Academy (Department of Electrical Engineering), Cornell University (School of Electrical Engineering), Purdue University (School of Electrical Engineering), University of Kentucky (Department of Electrical Engineering), Georgia Institute of Technology (School of Electrical Engineering), Clarkson College of Technology (Department of Electrical Engineering), State University of New York at Buffalo (Department of Electrical Engineering), North Carolina State University (Department of Electrical Engineering), Florida Technological University (Department of Electrical Engineering), Florida Institute of Technology (College of Engineering), Air Force Institute of Technology (Department of Electrical Engineering), and the University of Adelaide (Department of Electrical Engineering) in South Australia. The Post-Doctoral Program provides, via contract, the opportunity for faculty and visiting faculty at the participating universities to spend a year full-time on exploratory development and operational problem-solving efforts with the post-doctorals splitting their time between RADC (or the ultimate customer) and the educational institutions.

The Post-Doctoral Program is totally customer-funded with current projects being undertaken for Air Defense Command (NORAD), Air Force Communications Service, Federal Aviation Administration, Defense Communications Agency, Aeronautical Systems Division (AFSC), Aero-Propulsion Laboratory

(AFSC), and Rome Air Development Center (AFSC). This effort was funded by Rome Air Development Center Electromagnetic Compatibility Branch under Project 4540, Contract F30602-72-C-0418.

Clayton R. Paul received the BSEE degree from the Citadel (1963), the MSEE degree from Georgia Institute of Technology (1964), and the PhD degree from Purdue University (1970). He served as a graduate assistant (1963-64) and as an instructor (1964-65) on the faculty of Georgia Institute of Technology. As a graduate instructor at Purdue University (1965-70) he taught courses in linear system theory, electrical circuits and electronics. From 1970-71 he was a Post Doctoral Fellow with RADC, working in the area of Electromagnetic Compatibility. His areas of research interests are in linear multivariable systems and electrical network theory with emphasis on distributed parameter networks and multiconductor transmission lines.

TABLE OF CONTENTS

LIST OF ILLUSTRATIONS

FIGURE PAGE

I. INTRODUCTION

Coupled transmission lines have continually received much attention in many diverse areas of application. Multiconductor transmission lines have been investigated in early power system studies and continue to receive attention in this area with regard to the transient behavior of power lines under fault and lightning induced conditions [1-13]. Modern emphasis on multilayer distributed circuits, strip lines and microstrip associated with integrated-circuit technology has produced a renewal of interest [14-19, 68] as has the interest in predicting transients induced on cables by external electromagnetic field sources such as high power radars or an electromagnetic pulse (EMP) from nuclear detonations [20-27]. Determining crosstalk in communication circuits [28-30] and digital computer wiring interference [30-32] are examples of other areas in which the subject of multiconductor transmission lines consistently arise.

Of particular interest within the electromagnetic compatibility (EMC) community is the prediction of coupling between wires and their associated termination-networks in closely coupled, high density cable bundles and flat pack (ribbon) cables on modern electronic systems. Control of intrasystem electromagnetic compatibility for systems within the Department of Defense is generally governed by MIL-STD-461 and 462. These are general documents which prescribe limits on emissions and susceptibilities of the individual subsystems and equipments with regard to undesired signals (interference) and do not in themselves consider the coupling paths between

the equipments and subsystems within systems. The undesired signals as used in this context are with respect to the particular equipment or subsystem, not all of which are undesired from the overall system standpoint. For example, the undesired signals may be truly undesired ones, such as transmitter harmonics, or may be the result of an essential signal, such as the fundamental frequency of a transmitter, coupling to a receptor for which such coupling is not intended.

Even if all the equipments and subsystems within a system conform to the limits in MIL-STD-461, it is, of course, not necessarily true that overall system compatibility will be achieved. Since these limits do not take into account the various coupling mechanisms and proximities of the equipments, a system whose equipments and subsystems meet MIL-STD-461 may prove to be incompatible and numerous instances of required retrofit and interference suppression measures on systems meeting these limits illustrate this fact. Thus overall system compatibility may not be achieved unless all signals (desired and undesired) and actual coupling paths within the system are considered, analytically. This deficiency has led to the development of various computer-aided intra-system (as opposed to inter-system) compatibility prediction programs which mathematically model the systems and take into account the various coupling paths for unintentional energy transfer (interference) as well as intentional energy transfer [33, 37].

The various coupling paths can generally be classified into combinations of wire, antenna and metallic box coupling, e.g., wire-to-wire, antenna-

to-antenna, antenna-to-wire, box-to-box, etc. In the case of wire-to-wire coupled interference in cable bundles, this undesired coupling of energy between circuits sharing a common bundle may be more severe than one may realize. For example, numerous cases (both experimental and analytical) may be shown where, for certain frequencies, the ratio of the received interference voltage across the terminals of a device to the voltage emitted by another device, which is coupled via wire-to-wire coupling mechanisms, exceeds unity. The two devices are not directly connected by a common pair of wires; the wires connected to each device are only in close proximity in a common cable bundle. Rarely does one encounter voltage transfer functions with magnitudes greater than unity in antenna-to-antenna interference coupling problems and this illustrates the importance of considering the mechanism of wire-coupled interference transfer.

It is the purpose of this report to provide a complete and unified discussion of multiconductor transmission line theory as it applies to the prediction of wire-coupled interference. The common approaches and assumptions which are either explicitly or implicitly used in the problem formulations which appear throughout the literature are discussed. In addition to providing a discussion of the limitations and advantages of each of these techniques, some numerically stable and efficient techniques for solving the multiconductor transmission line problem for large numbers of closely coupled, dielectric-insulated wires will be presented. Methods for computing the per-unit-length parameters will also be given. Some of the results can be

found in various places in the literature although the treatments of the subject of multiconductor lines generally either discuss the solution of the equations describing the transmission line and associated termination-networks with the entries in the transmission line equations (the per-unit-length parameters) assumed to be obtainable or they discuss the derivation of the per-unit-length parameters without regard to the solution of the equations describing the line. The purpose of this report is to provide a comprehensive discussion of the complete problem solution and in addition present some new techniques for considering large numbers of closely coupled, dielectric-insulated wires.

Throughout this report, the emphasis will be on the frequency response of the transmission lines rather than the transient response since EMC control documents currently apply predominantly to the frequency domain. If one assumes linear termination networks (no hysteresis, etc.) and assumes no nonlinear effects associated with the transmission lines such as corona discharge, then the equations describing the problem (the transmission lines and associated terminations) will be linear and thus the frequency response provides a completely general characterization.

Matrix formulation of the equations and other results of matrix analysis will be used where necessary for a logical and concise development and the reader is referred to [38] or other texts on linear algebra listed in the references.

II. THE TEM MODE FORMULATION FOR MULTICONDUCTOR LINES

Consider a Δx length section of an (n+1)-conductor, uniform transmission line in a homogeneous medium shown in Fig. 1 lying parallel to the x direction in a rectangular coordinate system. The line is said to be uniform if there is no cross-sectional variation with x either in the conductors or the characteristics of the medium, i.e., "end-on" or cross-sectional views in planes perpendicular to x are identical for all x. The medium surrounding the conductors and contained within the zero-th conductor is assumed to be linear and isotropic and therefore is describable by the scalars ϵ (permittivity), μ (permeability), and σ (conductivity) which are independent of the electric and magnetic fields in the medium but may be functions of frequency. If ϵ, μ and σ are independent of position in the medium, i.e., independent of x, y and z, the medium is said to be homogeneous. Thus for uniform lines, all (n+1) conductors have uniform cross sections along their lengths and are parallel to each other and the x direction and in the case of an inhomogeneous medium, the characteristics of the medium (ϵ, μ, σ) exhibit no cross-sectional variation with x and are therefore independent of x.

The conventional distributed-parameter, transmission line model, of course, describes only the TEM (Transverse Electro-Magnetic) mode of propagation on the line and higher order modes are not considered. The electric field intensity vector, $\vec{\mathcal{E}}(x, y, z, t)$, and the magnetic field intensity vector, $\vec{\mathcal{H}}(x, y, z, t)$, for the TEM mode of propagation both lie in planes (y, z) transverse or perpendicular to the direction of propagation (the x direction)

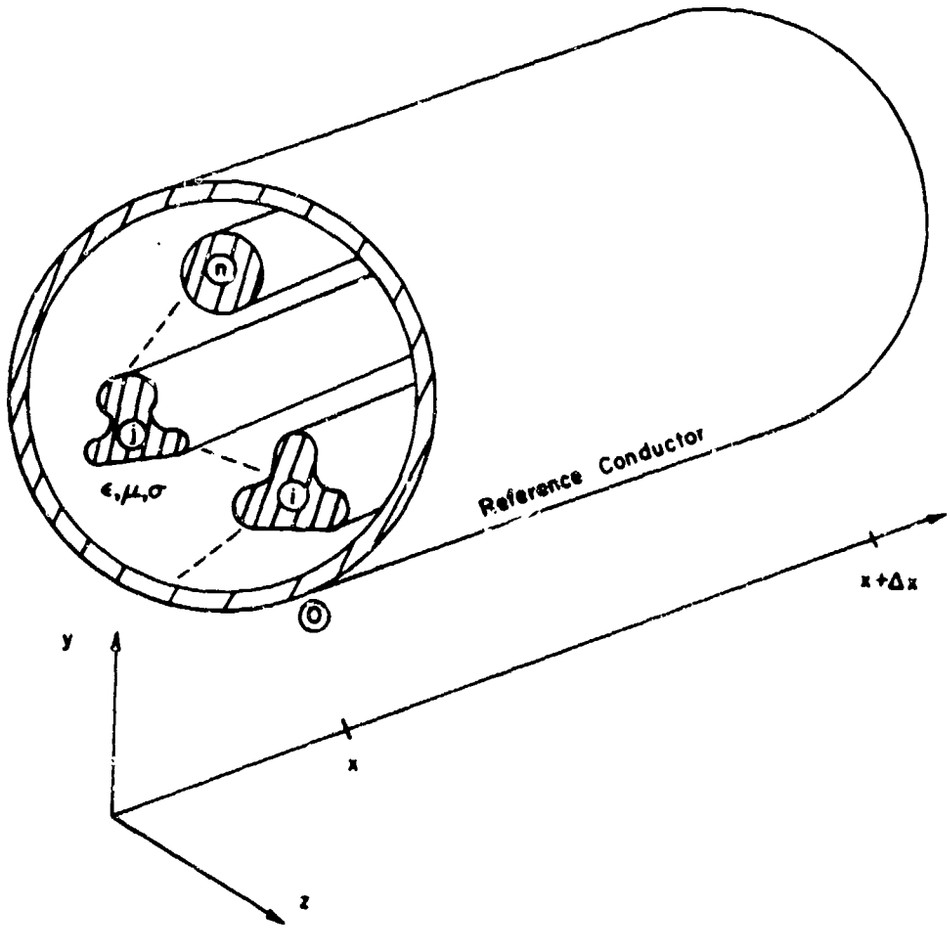

(a)

Figure 1. An (n+1)-conductor uniform transmission line (cont.).

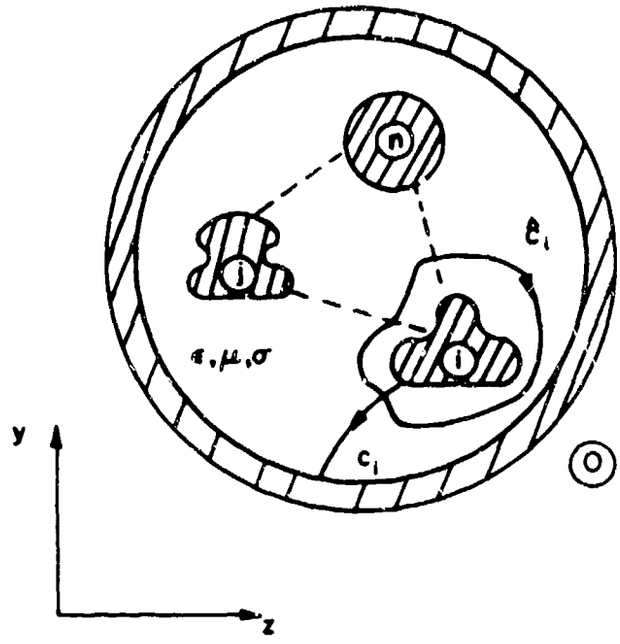

(b)

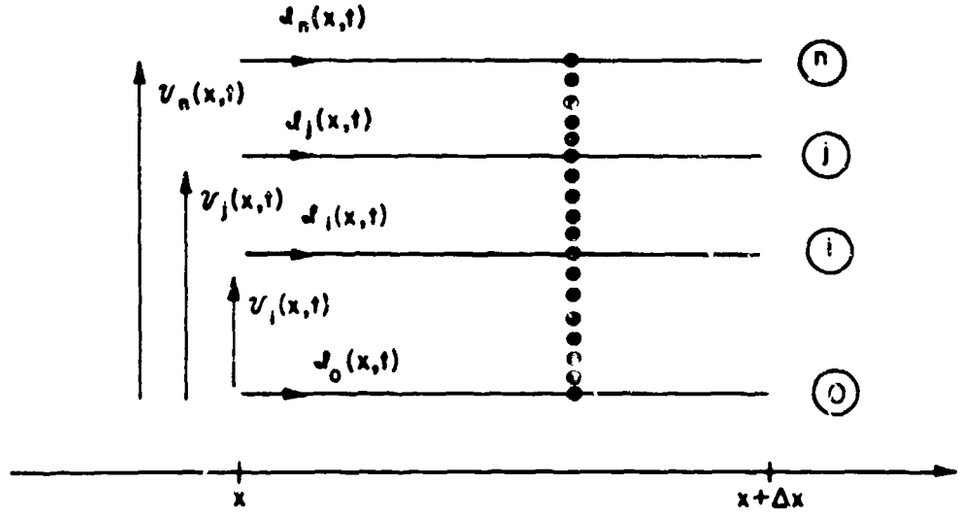

(c)

Figure 1. An (n+1)-conductor uniform transmission line.

and t is the time variable. Thus it has been shown a number of times that, assuming (n+1) perfect conductors, a homogeneous medium and the TEM mode of propagation, the nonzero components of the field vectors (the transverse electric field, $\vec{\mathcal{E}}_T(x, y, z, t)$, and the transverse magnetic field, $\vec{\mathcal{H}}_T(x, y, z, t)$) at each x along the line satisfy the same spatial distributions as static fields [40]. Therefore one can meaningfully define voltages between the conductors and currents flowing on the conductors [40]. For further clarification, see Appendix A.

The emphasis in this report will be upon determining the frequency response of the transmission lines and associated termination-networks. Therefore sinusoidal excitation is assumed with the field vectors written as $\vec{\mathcal{E}}(x, y, z, t) = \vec{E}(x, y, z)e^{j\omega t}$ and $\vec{\mathcal{H}}(x, y, z, t) = \vec{H}(x, y, z)e^{j\omega t}$ where $\vec{E}(x, y, z)$ and $\vec{H}(x, y, z)$ are complex-valued vectors independent of time t and ω is the radian frequency of excitation ($\omega = 2\pi f$). To characterize lines in a homogeneous medium such as in Fig. 1 under the TEM mode assumption, the potential, $\mathcal{V}_i(x, t)$, of the i-th conductor with respect to the reference conductor (the zero conductor) and the current, $\mathcal{I}_i(x, t)$, associated with the i-th conductor are defined for i=1,--,n (see Fig. 1c). The currents are directed in the positive x direction and the current in the reference conductor satisfies $\mathcal{I}_o(x, t) = -\sum_{i=1}^{n} \mathcal{I}_i(x, t)$ [40]. Voltages and currents for sinusoidal excitation are written as $\mathcal{V}_i(x, t) = V_i(x)e^{j\omega t}$ and $\mathcal{I}_i(x, t) = I_i(x)e^{j\omega t}$ where $V_i(x)$ and $I_i(x)$ are the phasor voltages and currents respectively and are complex-valued scalars independent of time, t. In the cross-sectional

view of Fig. 1b, the voltage of the i-th conductor with respect to the zero-th conductor chosen as a reference is defined as the line integral of $\vec{E}_T$ along contour C_i in the y, z plane and the current associated with the i-th conductor is defined as the line integral of $\vec{H}_T$ along the closed contour $\hat{C}_i$ in the y, z plane. The assumption of TEM mode propagation precludes the existence of a component of the magnetic field intensity vector in the longitudinal direction (the x direction). This assumption coupled with the assumption of perfect conductors insures that the definition of the voltages is unique [40]. The assumption of a TEM fields structure also precludes the existence of a longitudinal component of the electric field intensity vector. Therefore, no longitudinal conduction or displacement current in the dielectric is considered and any current flow in the dielectric will be confined to the transverse plane. This assumption coupled with the assumption of perfect conductors insures that the definition of the line currents is unique [40]. These results, of course, provide the basis for representing transmission lines for the TEM mode of propagation over "electrically short" Δx lengths with lumped equivalent circuits whose parameters, which are per-unit-length quantities and are derived under the condition that the transverse field vectors, $\vec{E}_T$ and $\vec{H}_T$, at each x along the line satisfy static distributions, represent the TEM mode of propagation for non-static excitation [40]. These important conclusions are demonstrated in Appendix A.

Imperfect conductors, inhomogeneous media and electrically large cross-sectional line dimensions preclude the existence of only the TEM

mode for the following reasons. With lossy conductors, there will necessarily be a longitudinal component of the electric field in the x direction due to the nonzero surface impedance of the conductors [40]. If the surrounding medium is inhomogeneous, then wave propagation can no longer be TEM as a result of the different phase velocities in the different homogeneous portions of the media. Imperfect conductors and inhomogeneous media are nevertheless considered with the distributed-parameter, transmission line model under the assumption that the conductor losses and the inhomogeneities in the media do not significantly perturb the field distribution from a TEM structure. The inclusion of inhomogeneous media which is termed the "quasi-TEM mode" assumption is particularly important in microstrip problems and other associated integrated-circuit structures [14-18, 68]. Electrically large cross-sectional dimensions of the line (conductor separation, wire radius, etc.) evidently are also capable of producing higher order modes and this can be surmised from the fact that the infinite parallel-plate transmission line, which is rigorously solvable and capable of supporting the TEM mode of propagation, will support only the TEM mode for frequencies such that the plate spacing is less than one-half wavelength. Also, it can be shown that a two-conductor coaxial line will support higher order modes when the mean circumference of the annular space between the two conductors is greater than one wavelength. Thus throughout this report, the cross-sectional dimensions of the line will be assumed to be electrically small, i.e., much less than a wavelength, so that transmission line

theory applies, i.e., the TEM mode is the dominant mode of propagation.

The specific cases of interest to be considered in this report are shown as cross-sectional views in the y, z plane in Fig. 2 and Fig. 3. In Fig. 2, n wires (circular conductors) are shown with another conductor, the reference conductor, denoted as the zero-th conductor. In Fig. 2a, the reference conductor is also a wire whereas in Fig. 2b and Fig. 2c the reference conductors are an infinite ground plane and an overall circular shield respectively. These lines are uniform and the surrounding medium is homogeneous. In Fig. 2a and Fig. 2b, the surrounding medium is free space with parameters ϵ_v and μ_v. In Fig. 2c, the medium within the circular shield is homogeneous with parameters ϵ, μ_v and σ. (The permeability of all dielectrics in this report will be considered to be that of free space, μ_v.)

In Fig. 3, similar cases are shown with the wires having circular dielectric insulations (an obviously very common situation). Thus the medium in each of these cases is inhomogeneous although the lines are nevertheless uniform. The permeabilities of the dielectric insulations are considered to be that of free space, μ_v, as is typical of dielectrics. Each dielectric insulation is described by the scalars permittivity, ϵ_i, and conductivity, σ_i, $i=0,1,----,n$ and the space surrounding the dielectric insulations is considered to be free space.

The corresponding cases for the more familiar two-conductor lines (n=1) are shown in Fig. 4 and Fig. 5. Note in Fig. 4 that the lines of $\vec{E}$ and $\vec{H}$ are shown perpendicular to each other. This is a natural consequence of

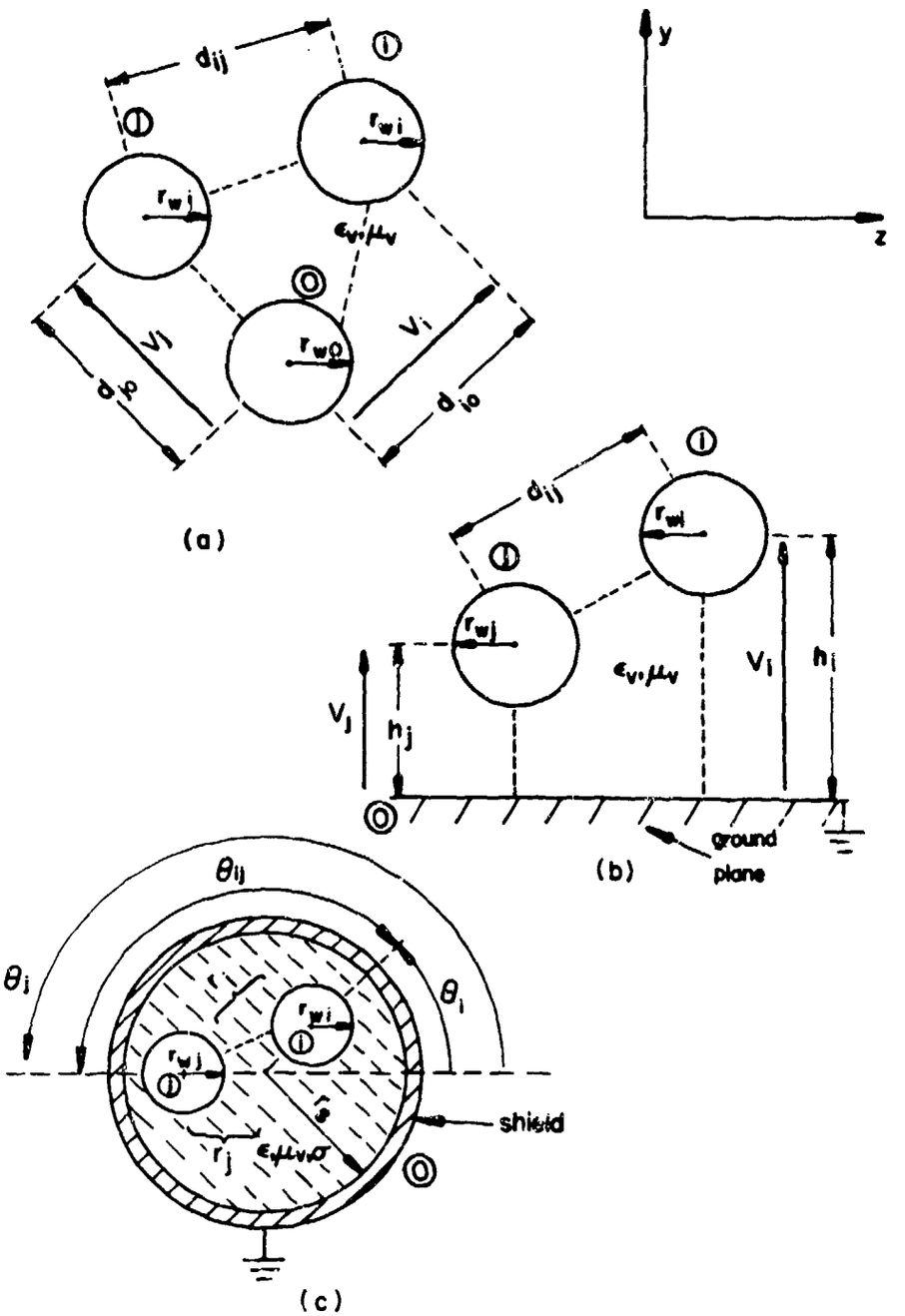

Figure 2. Multiconductor transmission lines in a homogeneous medium.

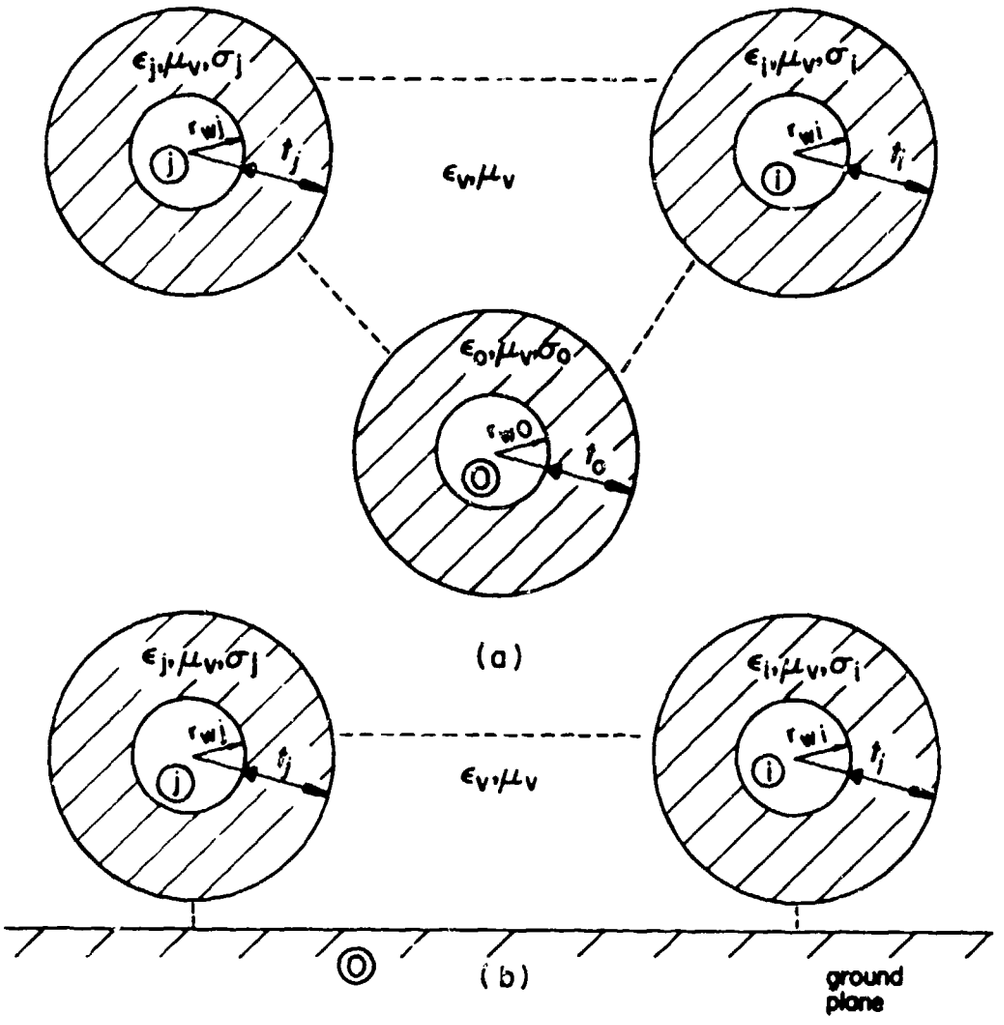

Figure 3. Multiconductor transmission lines in an inhomogeneous medium (cont.).

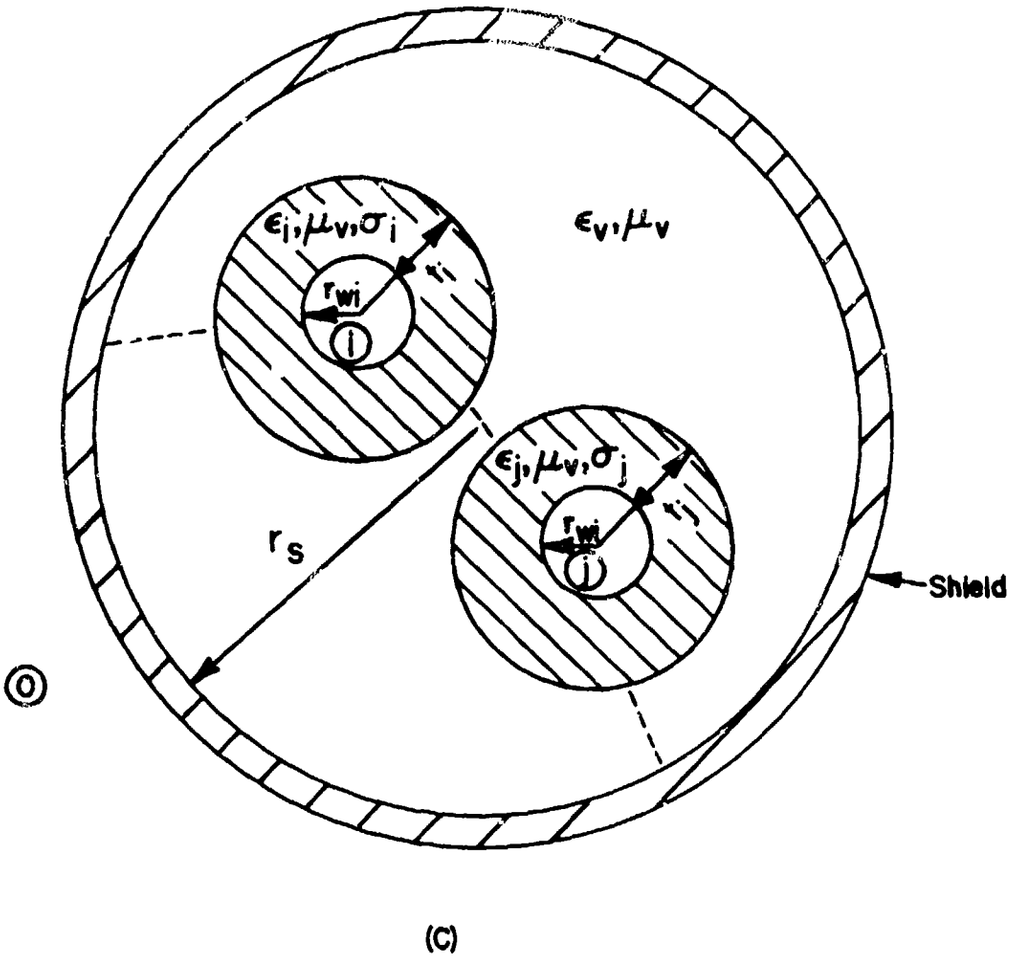

Figure 3. Multiconductor transmission lines in an inhomogeneous medium.

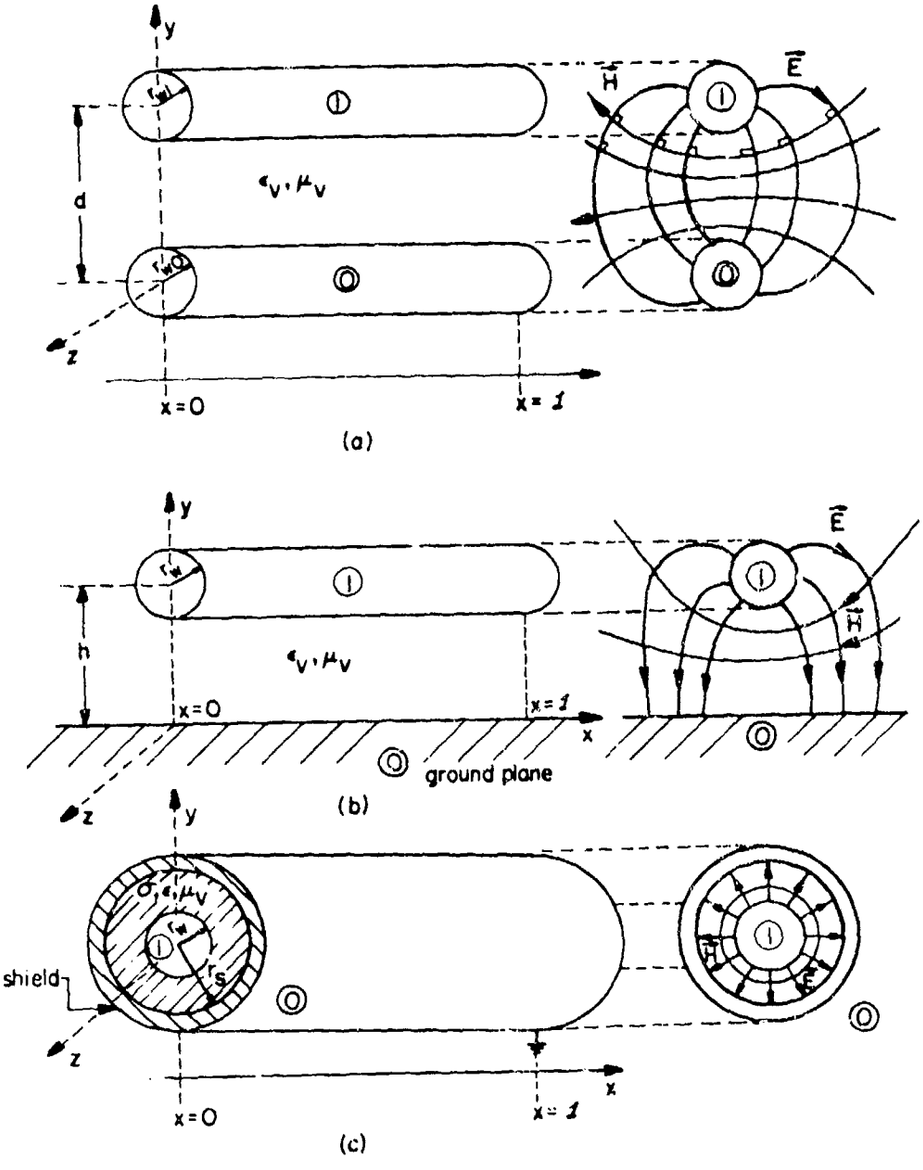

Figure 4. Two-conductor transmission lines in a homogeneous medium.

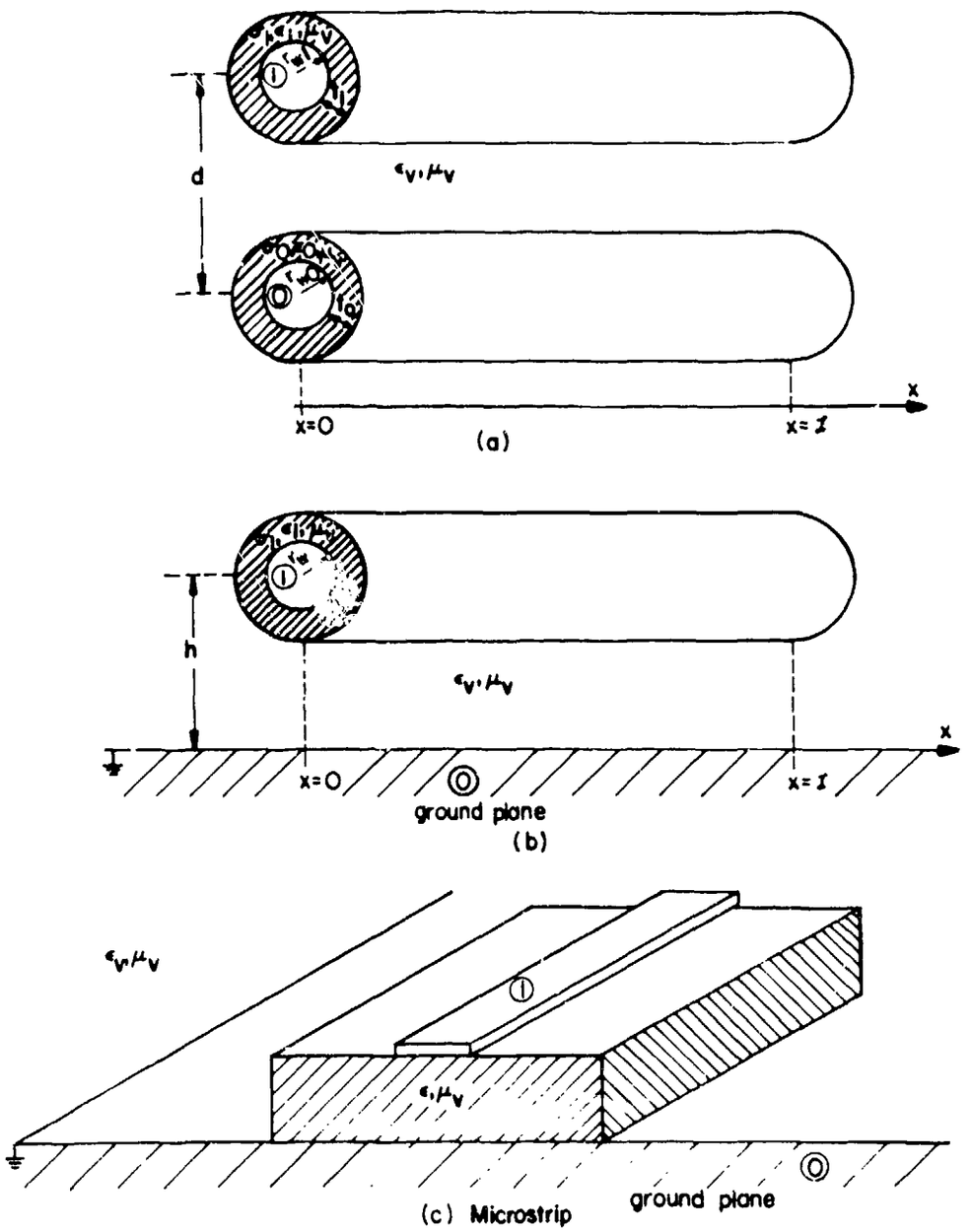

Figure 5. Two-conductor transmission lines in an inhomogeneous medium (cont.).

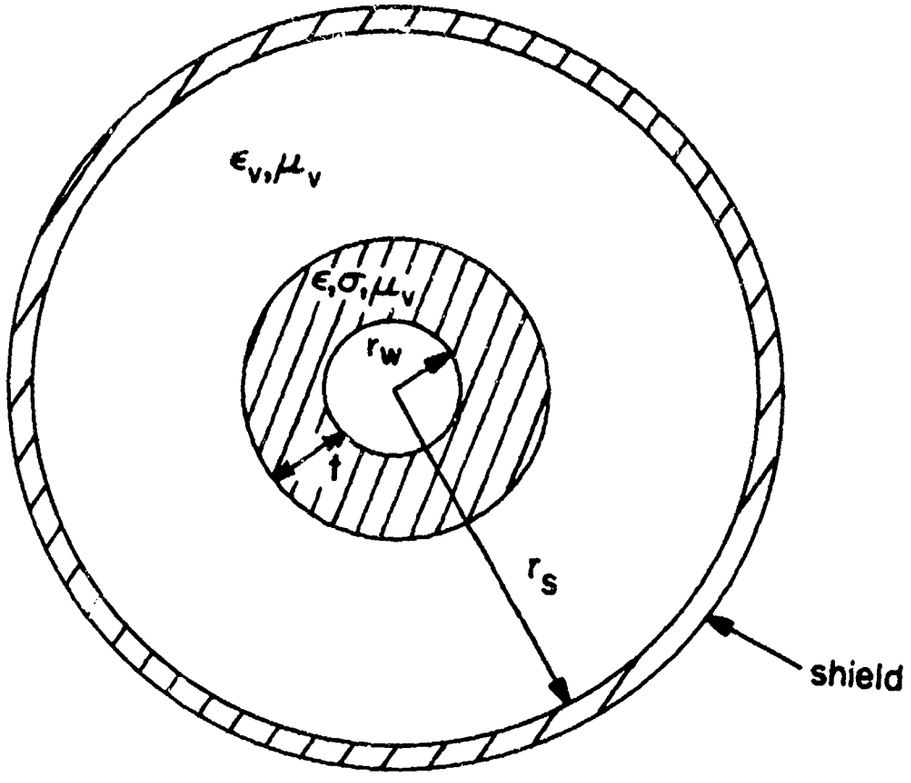

(d)

Figure 5. Two-conductor transmission lines in an inhomogeneous medium.

the TEM mode assumption [40].

If the medium is homogeneous as in Fig. 1 and Fig. 2 and all (n+1) conductors are perfect conductors, then losses in the medium can be included without violating the TEM mode assumption or the uniqueness of the voltage and current definitions [40]. However, in the case of a homogeneous medium in Fig. 2, it is only logical to consider a lossy medium for the case in Fig. 2c since the surrounding medium in Fig. 2a and Fig. 2b is considered to be free space. Dielectric losses can be introduced through a finite, nonzero ohmic conductivity, σ_d, (which generally will be quite small for typical insulation materials) and also through dipole relaxation effects [30]. To include both of these effects, we may consider the material to be characterized by a complex, effective permittivity (which is frequency dependent) instead of a real permittivity. To include dipole relaxation losses, the permittivity may be considered to be complex as [30] $\epsilon = \epsilon' - j\epsilon''$. Ampere's law in a homogeneous medium possessing both of these loss quantities becomes $\nabla X \vec{H} = \sigma_d \vec{E} + j\omega\epsilon \vec{E} = [(\sigma_d + \omega\epsilon'') + j\omega\epsilon']\vec{E} = j\omega\epsilon' \left[1-j \frac{(\sigma_d + \omega\epsilon'')}{\omega\epsilon'} \right]\vec{E}$. The real part of the complex permittivity is expressed as $\epsilon' = \epsilon_v \epsilon_r$ where ϵ_v is the permittivity of free space and ϵ_r is the relative dielectric constant. The effective conductivity of the ho ogeneous medium ther becomes $\sigma = \sigma_d + \omega\epsilon''$. Thus the losses of the medium may be accounted for by using a complex effective permittivity $\epsilon_{eff} = \epsilon_v \epsilon_r(1-j \tan \delta)$ instead of a real permittivity and $\tan \delta = \sigma/(\omega \epsilon_v \epsilon_r)$ is the loss tangent of the material [40]. Ordinarily, the loss tangent and the relative dielectric constant ϵ_r are

given for materials as a function of frequency. Therefore, it is quite clear that for (n+1) perfect conductors in a homogeneous medium, losses in the medium, i.e., $\sigma \neq 0$, can be included without violating the TEM mode assumption or the uniqueness of the voltage and current definitions since the real permittivity for the lossless case ($\sigma = 0$) is merely replaced by a complex permittivity, ε_{eff}, to account for losses in the medium. Since the TEM mode assumption is legitimate for the lossless, homogeneous case, there is no reason why the use of a complex permittivity instead of a real permittivity should change this.

The lumped-circuit model for a Δx length section of the two-conductor lines in a homogeneous medium in Fig. 4 are shown in Fig. 6. The lines have a total length ℓ and Thevenin equivalents of the linear terminations at the ends of the line are shown.

The lumped-circuit model describing the TEM mode of propagation for a Δx length section of any of the multiconductor lines in a homogeneous medium in Fig. 1 and Fig. 2 is shown in Fig. 7. All Δx length models for other sections of the line will be identical since the line is uniform. Since the cross-sectional dimensions of the line (conductor spacing, wire radius, etc.) are all assumed to be "electrically small" and Δx is assumed to be "electrically short", then it is valid to characterize a Δx section of the line with a lumped equivalent circuit.

Resistance elements r_{c_0}, r_{c_i}, r_{c_j} and conductance elements g_{i0}, g_{j0}, g_{ij} are included to represent losses associated with the conductors and

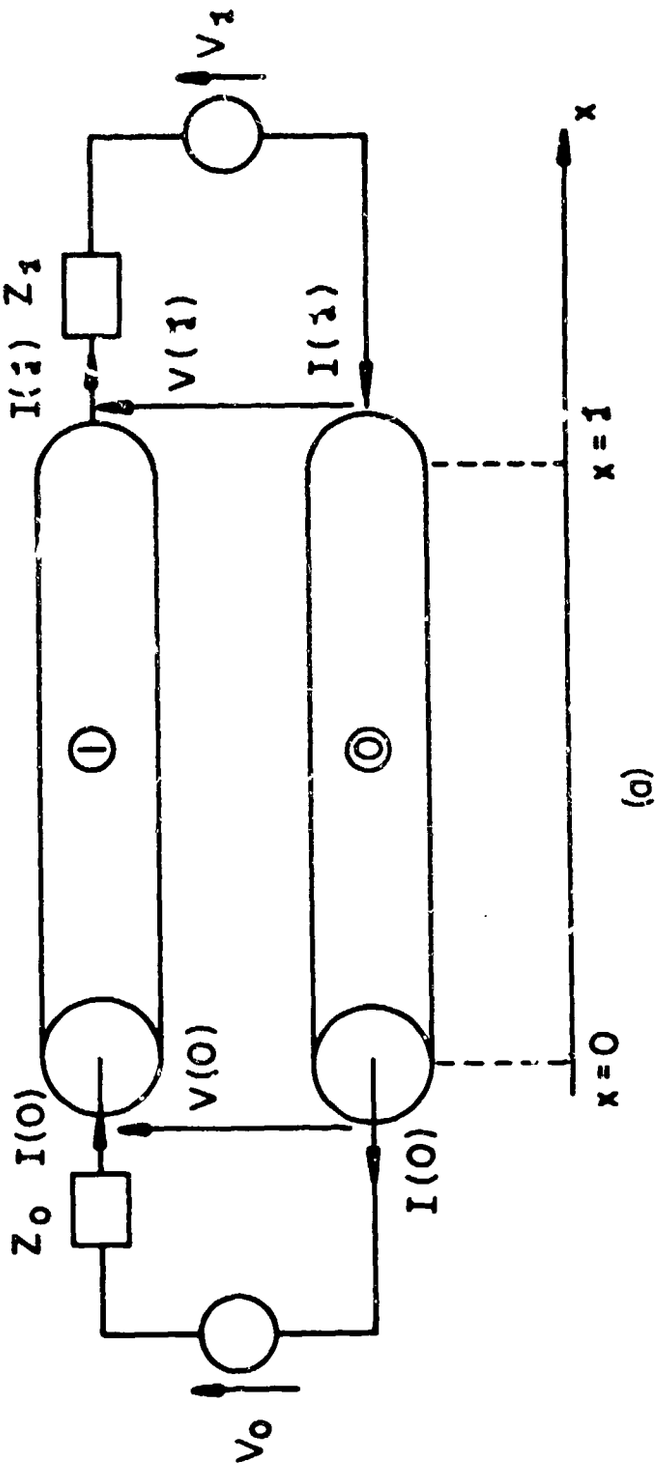

Figure 6. The termination-networks and equivalent circuits for two-conductor transmission lines (cont.).

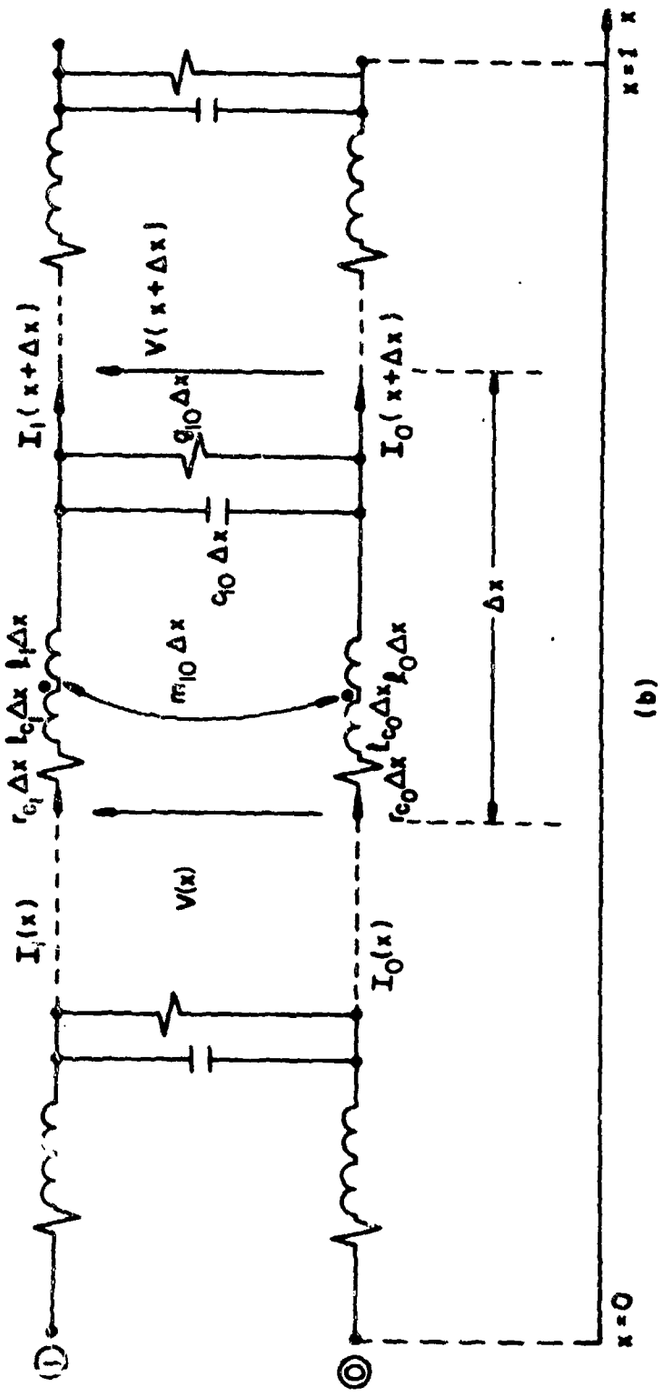

Figure 6. The termination-networks and equivalent circuits for two-conductor transmission lines (cont.).

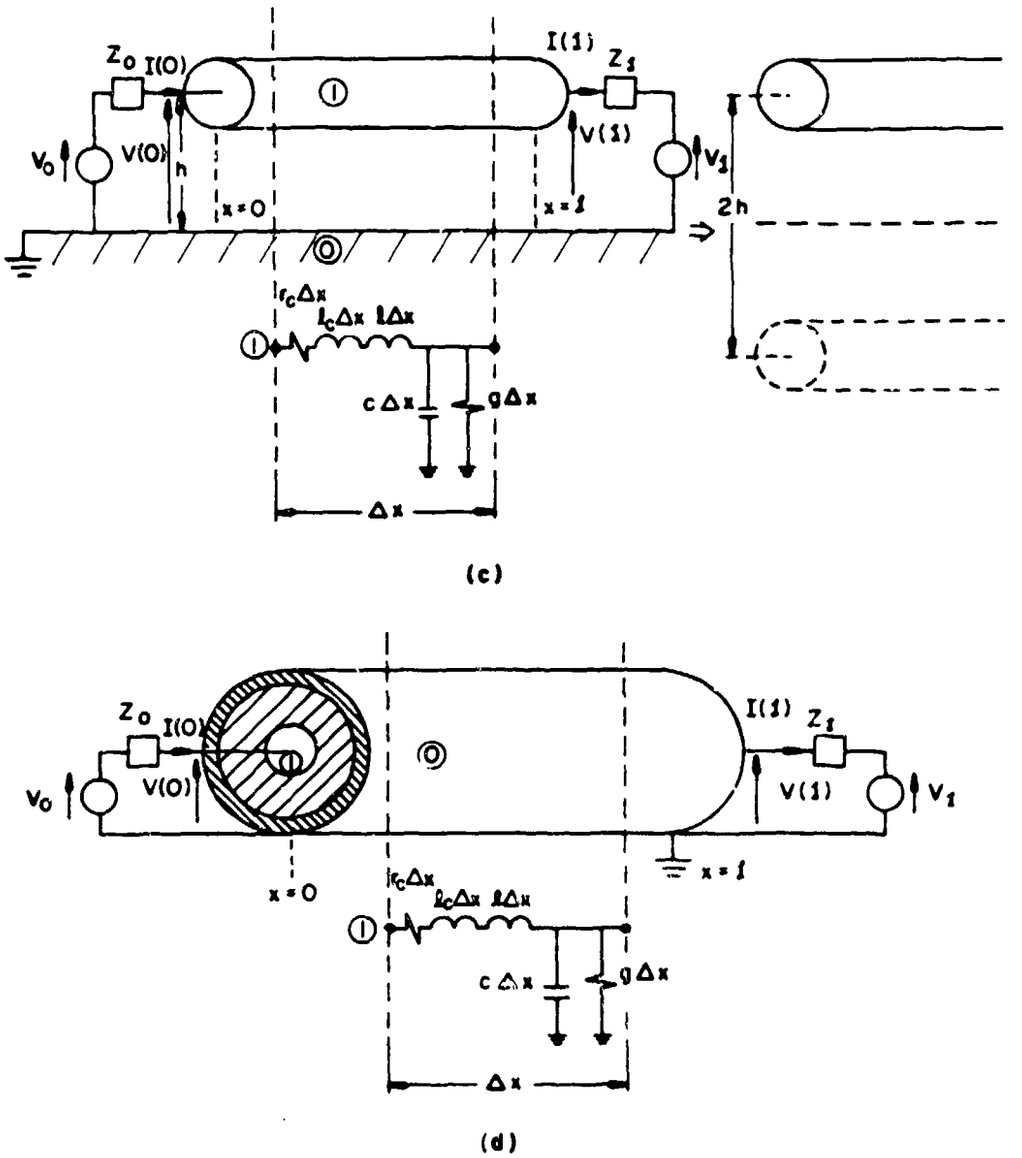

Figure 6. The termination-networks and equivalent circuits for two-conductor transmission lines.

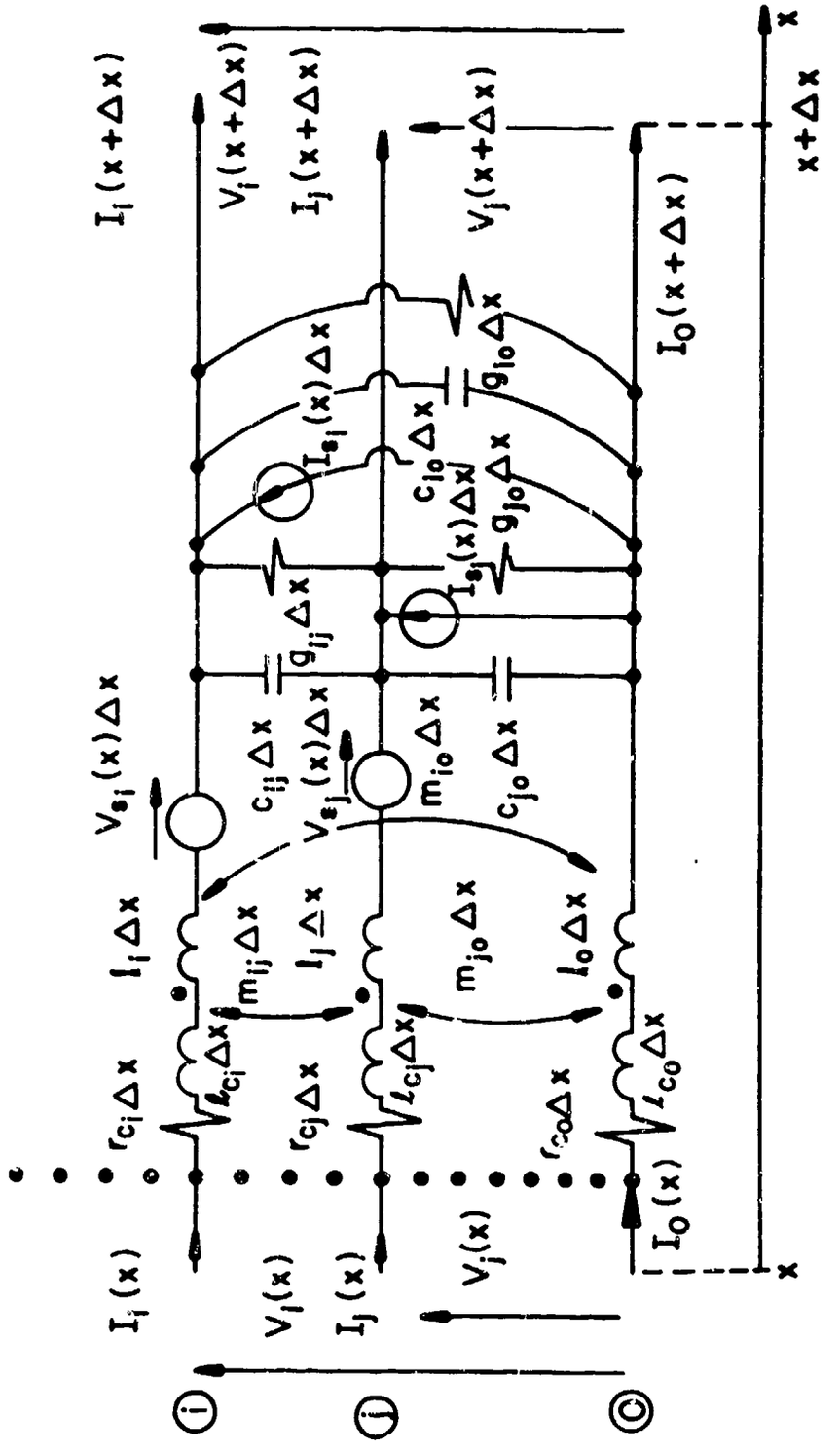

Figure 7. The per-unit-length equivalent circuit for multiconductor transmission lines.

medium respectively. The inclusion of a surrounding medium having a finite, nonzero conductivity and dipole relaxation losses with these shunt conductances is consistent with the assumption of TEM mode propagation whereby no longitudinal conduction or displacement current can flow in the dielectric and any current flow in the medium is confined to the transverse plane. The shunt conductances account for the portions of the transverse currents associated with conductive and dipole relaxation losses of the medium, i.e., the transverse displacement and conductic currents due to the imaginary part of ϵ_{eff}. Similarly, shunt capacitances account for the transverse displacement currents associated with the real part of ϵ_{eff}. Also self inductance terms for the conductors, ℓ_0, ℓ_i, ℓ_j; mutual inductances between the conductors, m_{i0}, m_{j0}, m_{ij}; and mutual capacitances between the conductors, c_{i0}, c_{j0}, c_{ij}, are shown [39]. Lossy conductors also produce a portion of the self inductances due to skin effect which is represented by the elements ℓ_{c_0}, ℓ_{c_i}, ℓ_{c_j} which are internal self inductances produced by currents internal to the lossy conductors [2, 3, 30]. The infinite ground plane and circular shield in Fig. 2b and Fig. 2c are considered to be perfect conductors and for these cases $r_{c_0} = \ell_{c_0} = 0$. A method of including a lossy ground plane is given in [29] and is frequently used to represent the earth return path in power systems [13].

Some care must be exercised in interpreting the elements ℓ_0, ℓ_i, ℓ_j and m_{i0}, m_{j0}, m_{ij} as strictly "self inductances" and "mutual inductances" respectively in the conventional sense. This interpretation relies on the

property that the sum of the currents (at a particular x) associated with all (n+1) conductors is zero, i.e., $\sum_{i=0}^{n} I_i(x) = 0$. An excellent discussion of this is presented in reference [3], Chapter 1 and the reader is referred to this for further clarification. Our results will not rely on this interpretation since we will not determine these individual external inductance parameters but will instead obtain the per-unit-length external inductance matrix, $\underset{\sim}{L}$, of the line directly. The entries in $\underset{\sim}{L}$, which are the essential items in our analysis, will be linear combinations of these per-unit-length "inductances" and once $\underset{\sim}{L}$ is determined, there is no need to separate its entries.

All of the terms resulting from losses, r_{c_0}, r_{c_i}, r_{c_j}, g_{i0}, g_{j0}, g_{ij}, ℓ_{c_0}, ℓ_{c_i}, ℓ_{c_j} are, in general, functions of frequency. The external parameters, ℓ_0, ℓ_i, ℓ_j, m_{ij}, m_{i0}, m_{j0}, c_{ij}, c_{i0}, c_{j0}, g_{i0}, g_{j0}, g_{ij}, are derived assuming perfect conductors such that the transverse fields satisfy a static distribution at each x along the line [39]. These external parameters will also be functions of frequency if the permeability, permittivity or conductivity of the surrounding medium is a function of frequency. In this case, the parameters are recomputed for each frequency assuming the transverse fields satisfy a static distribution at each x along the line. All parameters are per-unit-length quantities and therefore the total value of each parameter for a Δx length model in Fig. 7 is the per-unit-length value multiplied by the section length, Δx.

It is important to note that this is an exact representation of the TEM mode of propagation for (n+1) perfect conductors in a homogeneous medium

as in Fig. 1 and Fig. 2. Imperfect conductors are considered as an approximation through r_{c_0}, r_{c_i}, r_{c_j}, ℓ_{c_0}, ℓ_{c_i}, ℓ_{c_j} under the assumption that the conductivities of the conductors are very large and much greater that the conductivity of the dielectric medium so that the fields structure is essentially TEM. Although the presence of an inhomogeneous medium as in Fig. 3 precludes the existence of the TEM mode except perhaps in the limiting case of zero frequency, the equivalent-circuit representation in Fig. 7 will be assumed to be an adequate representation for the quasi-TEM mode for the lines in an inhomogeneous medium in Fig. 3. The parameters for this case will also be computed at each frequency by assuming (as a first-order approximation) that the field vectors are entirely transverse and satisfy a static distribution at each x along the line.

For the two-conductor cases in Fig. 4, the transmission line equations can be derived from the Δx equivalent circuits in Fig. 6 for the sinusoidal, steady state in the limit as $\Delta x \to 0$ as a pair of coupled, first-order, ordinary, complex differential equations [2, 3]

$$\frac{d\,V(x)}{dx} + \underbrace{(r_c + j\omega\ell_c + j\omega\ell)}_{Z}\, I(x) = 0 \qquad \text{(1a)}$$

$$\frac{d\,I(x)}{dx} + \underbrace{(g + j\omega c)}_{Y}\, V(x) = 0 \qquad \text{(1b)}$$

where Z and Y are the per-unit-length impedances and admittances of the line respectively. For each of these cases, $r_c = r_{c_1} + r_{c_0}$, $\ell_c = \ell_{c_1} + \ell_{c_0}$, $\ell = \ell_1 + \ell_0 - 2m_{10}$, $c = c_{10}$ and $g = g_{10}$. If an incident electromagnetic field illuminates the line of Fig. 4a, the equations in (1) are modified to include the effects of the incident field and become [20]

$$\frac{d\,V(x)}{dx} + Z\,I(x) = V_s(x) \tag{2a}$$

$$\frac{d\,I(x)}{dx} + Y\,V(x) = I_s(x) \tag{2b}$$

where $V_s(x)$ and $I_s(x)$ are distributed sources along the line induced by the spectral components of the incident field and are given by [20]

$$V_s(x) = j\omega\mu_v \int_0^d H_z^{(inc)}(y,x)dy \tag{3a}$$

$$I_s(x) = -Y \int_0^d E_y^{(inc)}(y,x)dy \quad . \tag{3b}$$

The two wires in Fig. 4a lie in the x, y plane with wire 0 at y = 0 and wire 1 at y = d. The components of the incident magnetic and electric field intensities at the radian frequency ω in the z and y directions are denoted by $H_z^{(inc)}(y,x)$ and $E_y^{(inc)}(y,x)$, respectively.

Similarly for multiconductor lines, the transmission line equations can be derived from the equivalent circuit in Fig. 7 for the sinusoidal, steady state in the limit as $\Delta x \to 0$ as a pair of n coupled, first-order, ordinary, complex differential equations in matrix form as (see Appendix B)

$$\underline{\dot{V}}(x) + \underset{\sim}{Z}\,\underline{I}(x) = \underline{V}_s(x) \tag{4a}$$

$$\underline{\dot{I}}(x) + \underset{\sim}{Y}\,\underline{V}(x) = \underline{I}_s(x) \tag{4b}$$

which may be written in an alternate form as a set of 2n coupled equations in partitioned form as

$$\begin{bmatrix} \underline{\dot{V}}(x) \\ \underline{\dot{I}}(x) \end{bmatrix} = - \begin{bmatrix} \underset{n\sim n}{0} & \underset{\sim}{Z} \\ \underset{\sim}{Y} & \underset{n\sim n}{0} \end{bmatrix} \begin{bmatrix} \underline{V}(x) \\ \underline{I}(x) \end{bmatrix} + \begin{bmatrix} \underline{V}_s(x) \\ \underline{I}_s(x) \end{bmatrix}. \tag{4c}$$

A matrix, $\underset{\sim}{M}$, with m rows and n columns is said to be m χ n and the element in the i-th row and j-th column is designated $[\underset{\sim}{M}]_{ij}$ with i=1, ---, m and j=1, ---, n. The dot (•) denotes first derivative with respect to x, i.e., $[\dot{\underline{V}}(x)]_i = \frac{d}{dx} V_i(x)$, and $\underset{m\sim n}{0}$ is the m χ n zero matrix with zeros in every position, i.e., $[\underset{m\sim n}{0}]_{ij} = 0$ for i=1, ---, m and j=1, ---, n. The elements of the n χ 1 complex column vectors $\underline{V}(x)$, $\underline{I}(x)$, $\underline{V}_s(x)$, $\underline{I}_s(x)$ are $[\underline{V}(x)]_i = V_i(x)$, $[\underline{I}(x)]_i = I_i(x)$, $[\underline{V}_s(x)]_i = V_{s_i}(x)$, $[\underline{I}_s(x)]_i = I_{s_i}(x)$ where the element of an n χ 1 column vector $\underline{V}$ with n rows in the i-th row is denoted by $[\underline{V}]_i$ for i=1, ---, n.

The per-unit-length series voltage sources, $V_{s_i}(x)$, and shunt current sources, $I_{s_i}(x)$, are induced by the spectral components of the incident field and are complex-valued and functions of frequency and position, x, along the line. For (n+1) wires in a homogeneous medium in Fig. 2a, these sources are shown in Appendix C and in [27] to be

$$V_{s_i}(x) = j\omega\mu_v \int_0^{d_{i0}} H_{n_i}^{(inc)}(\xi_i, x)\, d\xi_i \tag{5a}$$

$$I_{s_i}(x) = -\left\{(g_{i0} + j\omega c_{i0}) + \sum_{\substack{j=1 \\ j\neq i}}^{n} (g_{ij} + j\omega c_{ij})\right\} \int_0^{d_{i0}} E_{t_i}^{(inc)}(\xi_i, x)\, d\xi_i \tag{5b}$$

$$+ \sum_{\substack{j=1 \\ j\neq i}}^{n} \left\{(g_{ij} + j\omega c_{ij}) \int_0^{d_{j0}} E_{t_j}^{(inc)}(\xi_j, x)\, d\xi_j\right.$$

where ξ_i is a straight-line contour between wire 0 and wire i and perpendicular to wire 0 and wire i. $H_{n_i}^{(inc)}(\xi_i, x)$ and $E_{t_i}^{(inc)}(\xi_i, x)$ are the components of the incident field vectors normal to a plane formed by the two wires and

parallel to ξ_i (transverse field) respectively. Solutions for $V_{s_i}(x)$ and $I_{s_i}(x)$ for the other configurations are discussed in [22, 24, 25] and Appendix C.

The n χ n complex-valued matrices $\underset{\sim}{Z}$ and $\underset{\sim}{Y}$ are the per-unit-length impedance and admittance matrices respectively and are symmetric, i.e., $\underset{\sim}{Z} = \underset{\sim}{Z}^t$ and $\underset{\sim}{Y} = \underset{\sim}{Y}^t$ where the transpose of an n χ n matrix $\underset{\sim}{M}$ is denoted as $\underset{\sim}{M}^t$. These matrices are independent of x since the lines are uniform and are separable as

$$\underset{\sim}{Z} = \underset{\sim}{R}_c + j\omega \underset{\sim}{L}_c + j\omega \underset{\sim}{L} \tag{6a}$$

$$\underset{\sim}{Y} = \underset{\sim}{G} + j\omega \underset{\sim}{C} \tag{6b}$$

where $\underset{\sim}{R}_c$ and $\underset{\sim}{L}_c$ are the per-unit-length conductor resistance and conductor internal inductance matrices respectively and are real, symmetric. The external parameter matrices, $\underset{\sim}{G}$, $\underset{\sim}{L}$ and $\underset{\sim}{C}$, are real and can also be shown to be symmetric (for linear, isotropic media) regardless of whether the medium is homogeneous or inhomogeneous thus permitting the equivalent circuit representation in Fig. 7. [39]. The matrices $\underset{\sim}{G}$, $\underset{\sim}{L}$ and $\underset{\sim}{C}$ are the per-unit-length external conductance, inductance and capacitance matrices respectively. The entries in these matrices are obtained in Appendix B and are given by

$$[\underset{\sim}{R}_c]_{ii} = r_{c_i} + r_{c_0} \quad [\underset{\sim}{R}_c]_{\substack{ij \\ i\neq j}} = r_{c_0} \tag{7a}$$

$$[\underset{\sim}{L}_c]_{ii} = \ell_{c_i} + \ell_{c_0} \quad [\underset{\sim}{L}_c]_{\substack{ij \\ i\neq j}} = \ell_{c_0} \tag{7b}$$

$$[\underset{\sim}{L}]_{ii} = \ell_i + \ell_0 - 2m_{i0} \quad [\underset{\sim}{L}]_{\substack{ij \\ i\neq j}} = \ell_0 + m_{ij} - m_{i0} - m_{j0} \tag{7c}$$

$$[\underset{\sim}{G}]_{ii} = g_{i0} + \sum_{\substack{j=1 \\ i \neq j}}^{n} g_{ij} \qquad [\underset{\sim}{G}]_{\substack{ij \\ i \neq j}} = -g_{ij} \tag{7d}$$

$$[\underset{\sim}{C}]_{ii} = c_{i0} + \sum_{\substack{j=1 \\ i \neq j}}^{n} c_{ij} \qquad [\underset{\sim}{C}]_{\substack{ij \\ i \neq j}} = -c_{ij} \tag{7e}$$

for i, j = 1, ---, n. $\underset{\sim}{C}$ and $\underset{\sim}{G}$ are said to be hyperdominant since each term on the main diagonal is greater than the sum of the elements in that row [39] and they can therefore be shown to be positive definite meaning that all n eigenvalues of $\underset{\sim}{C}$ and all n eigenvalues of $\underset{\sim}{G}$ are positive and nonzero [41]. The derivation of the per-unit-length parameters will be discussed in Section V.

III. SOLUTION OF THE TRANSMISSION LINE EQUATIONS

The set of 2n first-order, complex-valued, ordinary differential equations in (4c) which describe the transmission line for the TEM mode of propagation and the sinusoidal, steady state are in the form of state variable equations [38, 42]. Systems of first-order differential equations in the state variable form have received considerable attention in recent years in the general area of linear systems and the solution to (4c) is

$$\begin{bmatrix} \underline{V}(x) \\ \underline{I}(x) \end{bmatrix} = \underset{\sim}{\Phi}(x, x_0) \begin{bmatrix} \underline{V}(x_0) \\ \underline{I}(x_0) \end{bmatrix} + \int_{x_0}^{x} \underset{\sim}{\Phi}(x, \hat{x}) \begin{bmatrix} \underline{V}_s(\hat{x}) \\ \underline{I}_s(\hat{x}) \end{bmatrix} d\hat{x} \qquad (8)$$

where $\underset{\sim}{\Phi}(x, x_0)$ is the $2n \times 2n$ complex-valued state transition matrix which is the solution to (4c) with $\underline{V}_s(x) = \underline{I}_s(x) = \underline{0}_{n-1}$ and the parameter x_0 is some arbitrary fixed point along the line [38, 42].

Obviously the difficult portion of the analysis (aside from the difficulty in computing the per-unit-length parameters and equivalent field excitation sources in $\underline{V}_s(x)$ and $\underline{I}_s(x)$) is the determination of the state transition matrix or chain parameter matrix, $\underset{\sim}{\Phi}(x, x_0)$. Fortunately, for uniform lines where $\underset{\sim}{Z}$ and $\underset{\sim}{Y}$ are not functions of x, the solution is fairly simple as will be shown (although there are some important computational problems when losses are included). For nonuniform lines where $\underset{\sim}{Z}$ and $\underset{\sim}{Y}$ are functions of x, i.e., $\underset{\sim}{Z}(x)$ and $\underset{\sim}{Y}(x)$, (4c) becomes a set of nonconstant-coefficient differential equations (Bessel's equation is an example of a nonconstant-coefficient differential equation) [43-46]. For these types of lines, (8) holds but the ultimate difficulty is the determination of the state transition matrix and

except for some very special structures one must resort to numerical methods and approximations to obtain $\underset{\sim}{\Phi}(x, x_0)$ [42]. If the line is "abruptly nonuniform" as with branched cables, i.e., consists of uniform subsections in cascade, then the overall chain parameter matrix, $\underset{\sim}{\Phi}(x, x_0)$, is the product (in the appropriate order) of the chain matrices of the individual uniform subsections between x and x_0 and thus is straightforward to obtain. As an example of this application to an "abruptly nonuniform" line, consider the line as a cascade of N uniform (n+1)-conductor transmission lines with each section between $x = x_i$ and x_{i-1} described by

$$\begin{bmatrix} \underline{V}(x_i) \\ \underline{I}(x_i) \end{bmatrix} = \underset{\sim}{\Phi}_i(x_i, x_{i-1}) \begin{bmatrix} \underline{V}(x_{i-1}) \\ \underline{I}(x_{i-1}) \end{bmatrix} + \int_{x_{i-1}}^{x_i} \underset{\sim}{\Phi}_i(x_i, \hat{x}) \begin{bmatrix} \underline{V}_{si}(\hat{x}) \\ \underline{I}_{si}(\hat{x}) \end{bmatrix} d\hat{x} \qquad (9)$$

$$x_{i-1} \leq x \leq x_i$$

for i=1, ---, N where $\underset{\sim}{\Phi}_i(x_i, x_{i-1})$ is the chain parameter matrix for the i-th section between $x = x_{i-1}$ and $x = x_i$ $(x_{i-1} \leq x \leq x_i)$ and $\underline{V}_{si}$ and $\underline{I}_{si}$ are the equivalent induced source vectors for the i-th section. By sequential substitution, the overall chain parameter matrix for the cascade of N sections between x_0 and x_N (which are not required to be identical) becomes

$$\underset{\sim}{\Phi}(x_N, x_0) \qquad (10)$$

$$\begin{bmatrix} \underline{V}(x_N) \\ \underline{I}(x_N) \end{bmatrix} = \left\{ \underset{\sim}{\Phi}_N(x_N, x_{N-1})\, \underset{\sim}{\Phi}_{N-1}(x_{N-1}, x_{N-2}) \cdots\cdots \underset{\sim}{\Phi}_2(x_2, x_1)\, \underset{\sim}{\Phi}_1(x_1, x_0) \right\} \begin{bmatrix} \underline{V}(x_0) \\ \underline{I}(x_0) \end{bmatrix}$$

$$+ \sum_{i=1}^{N-1} \left\{ \underset{\sim}{\Phi}_N(x_N, x_{N-1})\, \underset{\sim}{\Phi}_{N-1}(x_{N-1}, x_{N-2}) \cdots \underset{\sim}{\Phi}_{i+1}(x_{i+1}, x_i) \int_{x_{i-1}}^{x_i} \underset{\sim}{\Phi}_i(x_i, \hat{x}) \begin{bmatrix} \underline{V}_{si}(\hat{x}) \\ \underline{I}_{si}(\hat{x}) \end{bmatrix} d\hat{x} \right\}$$

$$+ \int_{x_{N-1}}^{x_N} \left\{ \underset{\sim}{\Phi}_N(x_N, \hat{x}) \begin{bmatrix} \underline{V}_{SN}(\hat{x}) \\ \underline{I}_{SN}(\hat{x}) \end{bmatrix} d\hat{x} \right\} \quad .$$

The overall chain parameter matrix for this cascade of nonidentical line sections between $x = x_0$ and $x = x_N$ is identified in (10) as the matrix product $\underset{\sim}{\Phi}(x_N, x_0)$. Note that the indicated order of multiplication of the individual chain parameter matrices must be preserved since they do not generally commute. Lumped-element networks at discrete points along the line can also be incorporated into the problem by writing the matrix chain parameters of these networks and including them appropriately into the product of the chain parameter matrices of the individual uniform sections in the above manner.

When the line is uniform (as is being considered here) where $\underset{\sim}{Z}$ and $\underset{\sim}{Y}$ are independent of x, the state transition matrix, $\underset{\sim}{\Phi}(x, x_0)$, can be shown to be a function of only one variable; the difference quantity $(x-x_0)$ [42]. Thus for uniform lines, we may denote the state transition or chain parameter matrix as $\underset{\sim}{\Phi}(x - x_0)$. The state transition matrix has the property that $\underset{\sim}{\Phi}(x_0, x_0) = \underset{\sim}{1}_{2n}$ where $\underset{\sim}{1}_{2n}$ is the $2n \times 2n$ identity matrix with $[\underset{\sim}{1}_{2n}]_{ii} = 1$ and $[\underset{\sim}{1}_{2n}]_{ij} = 0$ for $i, j = 1, ---, 2n$ and $i \neq j$ [38]. This should be clear from (8) by setting x equal to x_0. Additionally, it may be shown that $\underset{\sim}{\Phi}^{-1}(x, x_0) = \underset{\sim}{\Phi}(x_0, x)$ where the inverse of an $n \times n$ matrix $\underset{\sim}{M}$ is denoted by $\underset{\sim}{M}^{-1}$ and therefore the

inverse of the chain parameter matrix may be trivially determined [42]. This is quite obvious from (8) for $\underline{V}_s(x) = \underline{I}_s(x) = {}_{n}\underline{0}_{1}$ by interchanging the roles of x and x_0.

For two-conductor lines (n=1) the transmission line equations become a set of two complex-valued, ordinary differential equations given in (1). The solution of the transmission line equations for two-conductor lines can be obtained quite easily by differentiating (1b) with respect to x and substituting (1a) to yield

$$\frac{d^2 I(x)}{dx^2} = Y Z I(x) \tag{11}$$

$$= \gamma^2 I(x)$$

where the propagation constant, γ, is

$$\gamma = \sqrt{Y Z} \tag{12}$$

$$= \sqrt{Z Y} \quad .$$

The solution to (11) becomes

$$I(x) = e^{-\gamma x} I^+ - e^{\gamma x} I^- \tag{13}$$

where I^+ and I^- are complex, undetermined constants. Substituting (13) into (1b) yields

$$V(x) = Z_C \left\{ e^{-\gamma x} I^+ + e^{\gamma x} I^- \right\} \tag{14}$$

where the characteristic impedance, Z_C, is given by

$$Z_C = \gamma / Y = \sqrt{Z/Y} \quad . \tag{15}$$

To find the solutions in the time domain, multiply (13) and (14) by $e^{j\omega t}$ to obtain

$$\mathcal{V}(x,t) = \underbrace{\left[Z_C e^{(j\omega t - \gamma x)} I^+ \right]}_{\mathcal{V}^+(x,t)} + \underbrace{\left[Z_C e^{(j\omega t + \gamma x)} I^- \right]}_{\mathcal{V}^-(x,t)} \tag{16a}$$

$$\mathcal{J}(x,t) = \underbrace{[e^{(j\omega t - \gamma x)}\, I^+]}_{\mathcal{J}^+(x,t)} - \underbrace{[e^{(j\omega t + \gamma x)}\, I^-]}_{\mathcal{J}^-(x,t)} \quad . \tag{16b}$$

Therefore the total solution consists of waves traveling in the +x direction (forward-traveling waves) denoted by $\mathcal{V}^+(x,t)$ and $\mathcal{J}^+(x,t)$ and waves traveling in the -x direction (backward-traveling waves) denoted by $\mathcal{V}^-(x,t)$ and $\mathcal{J}^-(x,t)$. The characteristic impedance, Z_C, is the ratio of the voltage and current in the respective waves.

For two-conductor lines, the chain parameter matrix is 2 x 2 and can easily be shown to be [2, 3]

$$\underset{\sim}{\Phi}(x, x_0) = \begin{bmatrix} \cosh\{\gamma(x-x_0)\} & -Z_C \sinh\{\gamma(x-x_0)\} \\ -\frac{1}{Z_C}\sinh\{\gamma(x-x_0)\} & \cosh\{\gamma(x-x_0)\} \end{bmatrix} \tag{17}$$

where cosh and sinh are the hyperbolic cosine and sine respectively. Note that the determinant of the chain parameter matrix is unity. Knowing this quantity, the solution for the voltage and current at any point, x, along the line can be found from (8) in terms of the voltage and current at some reference point, x_0, as

$$V(x) = \cosh\{\gamma(x-x_0)\}\, V(x_0) - Z_C \sinh\{\gamma(x-x_0)\}\, I(x_0) \tag{18a}$$

$$+ \int_{x_0}^{x} [\cosh\{\gamma(x-\hat{x})\}\, V_s(\hat{x}) - Z_C \sinh\{\gamma(x-\hat{x})\}\, I_s(\hat{x})]\, d\hat{x}$$

$$I(x) = -\frac{1}{Z_C}\sinh\{\gamma(x-x_0)\}\, V(x_0) + \cosh\{\gamma(x-x_0)\}\, I(x_0) \tag{18b}$$

$$+ \int_{x_0}^{x} [-\frac{1}{Z_C}\sinh\{\gamma(x-\hat{x})\}\, V_s(\hat{x}) + \cosh\{\gamma(x-\hat{x})\}\, I_s(\hat{x})]\, d\hat{x} \quad .$$

For multiconductor lines, the equations in (4c) may be thought of as "strongly-coupled" state variable equations since the block off-diagonal terms, $\underset{\sim}{Z}$ and $\underset{\sim}{Y}$, are nonzero whereas the block main-diagonal terms are zero, $\underset{n\sim n}{0}$. The chain parameter matrix, $\underset{\sim}{\Phi}(x, x_0)$, however, may be determined in the following manner which is similar to the method for solving the two-conductor line employed above [18, 26, 47]. Assuming for the moment that $\underline{V}_s(x) = \underline{I}_s(x) = n\underline{0}1$, differentiating the second set of equations (4b) again with respect to x, $\underline{\ddot{I}}(x) = -\underset{\sim}{Y}\,\underline{\dot{V}}(x)$, and substituting the first set (4a), $\underline{\dot{V}}(x) = -\underset{\sim}{Z}\,\underline{I}(x)$, one obtains the set of n second-order differential equations

$$\underline{\ddot{I}}(x) = \underset{\sim}{Y}\,\underset{\sim}{Z}\,\underline{I}(x) \quad . \tag{19}$$

Note that even though $\underset{\sim}{Y}$ and $\underset{\sim}{Z}$ are symmetric, it is not necessarily true that the matrix product $\underset{\sim}{Y}\,\underset{\sim}{Z}$ (or $\underset{\sim}{Z}\,\underset{\sim}{Y}$) will be symmetric.

The solution of (19) is usually obtained with similarity transformations [13, 18, 26, 38, 41, 42, 47, 48], which is referred to in the power transmission literature as "modal decomposition" [13]. Define a change of variables, $\underline{I}(x) = \underset{\sim}{T}\,\underline{I}_m(x)$ where $\underset{\sim}{T}$ is an $n\chi n$ nonsingular, complex-valued matrix and $\underline{I}_m(x)$ is an $n\chi 1$ complex-valued vector of "mode currents". Substituting this change of variables into (19) yields

$$\underline{\ddot{I}}_m = \underset{\sim}{T}^{-1}\,\underset{\sim}{Y}\,\underset{\sim}{Z}\,\underset{\sim}{T}\,\underline{I}_m \quad . \tag{20}$$

Suppose there exists an $n\chi n$ similarity transformation, $\underset{\sim}{T}$, which diagonalizes $\underset{\sim}{Y}\,\underset{\sim}{Z}$, i.e.,

$$\underset{\sim}{T}^{-1}\,\underset{\sim}{Y}\,\underset{\sim}{Z}\,\underset{\sim}{T} = \underset{\sim}{\gamma}^2 \tag{21}$$

where $\underset{\sim}{\gamma}^2$ is an $n\chi n$ diagonal matrix with

$$[\underset{\sim}{\gamma}^2]_{ii} = \gamma_i^2 \tag{22a}$$

$$[\underset{\sim}{\gamma}^2]_{\substack{ij \\ i\neq j}} = 0 \tag{22b}$$

and the terms, γ_i^2, $i = 1, ---, n$ are complex-valued scalars. Then (20) becomes a set of n uncoupled differential equations with the simple solution [18, 26, 47]

$$\underline{I}(x) = \underset{\sim}{T}\,\underline{I}_m(x) \tag{23}$$

$$= \underset{\sim}{T}\,(\underset{\sim}{e}^{-\gamma x}\,\underline{I}^{+} - \underset{\sim}{e}^{\gamma x}\,\underline{I}^{-})$$

where $\underset{\sim}{e}^{\gamma x}$ is an $n\chi n$ diagonal matrix with

$$[\underset{\sim}{e}^{\gamma x}]_{ii} = e^{\gamma_i x} \tag{24a}$$

$$[\underset{\sim}{e}^{\gamma x}]_{\substack{ij \\ i\neq j}} = 0 \tag{24b}$$

and $\underline{I}^{+}$ and $\underline{I}^{-}$ are $n\chi 1$ vectors of 2n complex, undetermined constants, $I_i^{+} = [\underline{I}^{+}]_i$ and $I_i^{-} = [\underline{I}^{-}]_i$, which will, in general, be functions of frequency [47]. These undetermined constants will be evaluated by considering the boundary conditions or termination-networks at the ends of the line. Since from (4b) $\dot{\underline{I}}(x) = -\underset{\sim}{Y}\,\underline{V}(x)$, one may obtain from (23)

$$\underline{V}(x) = -\underset{\sim}{Y}^{-1}\,\frac{d\underline{I}(x)}{dx} \tag{25}$$

$$= \underset{\sim}{Y}^{-1}\,\underset{\sim}{T}\,\underset{\sim}{\gamma}\,(\underset{\sim}{e}^{-\gamma x}\,\underline{I}^{+} + \underset{\sim}{e}^{\gamma x}\,\underline{I}^{-})$$

$$= \underset{\sim}{Y}^{-1}\,\underset{\sim}{T}\,\underset{\sim}{\gamma}\,\underset{\sim}{T}^{-1}\left\{\underset{\sim}{T}(\underset{\sim}{e}^{-\gamma x}\,\underline{I}^{+} + \underset{\sim}{e}^{\gamma x}\,\underline{I}^{-})\right\}$$

$$= \underset{\sim}{Z}\,\underset{\sim}{T}\,\underset{\sim}{\gamma}^{-1}\,\underset{\sim}{T}^{-1}\left\{\underset{\sim}{T}(\underset{\sim}{e}^{-\gamma x}\,\underline{I}^{+} + \underset{\sim}{e}^{\gamma x}\,\underline{I}^{-})\right\}$$

where $\underset{\sim}{\gamma}$ is an $n \times n$ diagonal complex-valued matrix with

$$[\underset{\sim}{\gamma}]_{ii} = \gamma_i = \sqrt{\gamma_i^2} \tag{26a}$$

$$[\underset{\sim}{\gamma}]_{\substack{ij \\ i \neq j}} = 0 \quad . \tag{26b}$$

One can easily show from (21) the identity $\underset{\sim}{Y}^{-1}\,\underset{\sim}{T}\underset{\sim}{\gamma} = \underset{\sim}{Z}\underset{\sim}{T}\,\underset{\sim}{\gamma}^{-1}$ which is used in (25).

The solution in the time domain can be found since $\underline{\mathcal{V}}(x, t) = \underline{V}(x)e^{j\omega t}$ and $\underline{\mathcal{J}}(x, t) = \underline{I}(x)e^{j\omega t}$ by multiplying (23) and (25) by $e^{j\omega t}$. It should then be clear that the total solutions consist of forward-traveling waves, $\underline{\mathcal{V}}^+(x, t)$, $\underline{\mathcal{J}}^+(x, t)$, and backward-traveling waves, $\underline{\mathcal{V}}^-(x, t)$, $\underline{\mathcal{J}}^-(x, t)$, on the line with [18]

$$\underline{\mathcal{V}}(x, t) = \underline{\mathcal{V}}^+(x, t) + \underline{\mathcal{V}}^-(x, t) \tag{27a}$$

$$\underline{\mathcal{J}}(x, t) = \underline{\mathcal{J}}^+(x, t) - \underline{\mathcal{J}}^-(x, t) \tag{27b}$$

where

$$\underline{\mathcal{J}}^+(x, t) = \underset{\sim}{T}\,\underset{\sim}{e}^{-\underset{\sim}{\gamma}x}\,\underline{I}^+\,e^{j\omega t} \tag{28a}$$

$$\underline{\mathcal{J}}^-(x, t) = \underset{\sim}{T}\,\underset{\sim}{e}^{\underset{\sim}{\gamma}x}\,\underline{I}^-\,e^{j\omega t} \tag{28b}$$

$$\underline{\mathcal{V}}^+(x, t) = \underset{\sim}{Z}_C\,\underline{\mathcal{J}}^+(x, t) \tag{28c}$$

$$\underline{\mathcal{V}}^-(x, t) = \underset{\sim}{Z}_C\,\underline{\mathcal{J}}^-(x, t) \tag{28d}$$

and $\underset{\sim}{Z}_C$ is the "characteristic-impedance matrix" relating the voltages and currents in the waves with $\underset{\sim}{Z}_C$ defined from (23), (25) and (28) as

$$\underset{\sim}{Z}_C = \underset{\sim}{Y}^{-1}\,\underset{\sim}{T}\,\underset{\sim}{\gamma}\,\underset{\sim}{T}^{-1} = \underset{\sim}{Z}\,\underset{\sim}{T}\,\underset{\sim}{\gamma}^{-1}\,\underset{\sim}{T}^{-1} \tag{29a}$$

$$\underset{\sim}{Z}_C = \underset{\sim}{Y}^{-1}\sqrt{\underset{\sim}{Y}\,\underset{\sim}{Z}} = \underset{\sim}{Z}(\sqrt{\underset{\sim}{Y}\,\underset{\sim}{Z}})^{-1} \quad . \tag{29b}$$

The symbolic notation in (29b) conforms to the scalar characteristic impedance for two-conductor lines discussed above. It can be shown that [18]

$$\sqrt{\underset{\sim}{Y}\,\underset{\sim}{Z}} = \underset{\sim}{T}\,\underset{\sim}{\gamma}\,\underset{\sim}{T}^{-1} \tag{30a}$$

$$\sqrt{\underset{\sim}{Z}\,\underset{\sim}{Y}} = \underset{\sim}{Y}^{-1}\sqrt{\underset{\sim}{Y}\,\underset{\sim}{Z}}\,\underset{\sim}{Y} \tag{30b}$$

$$\sqrt{\underset{\sim}{Y}\,\underset{\sim}{Z}} = \underset{\sim}{Y}\sqrt{\underset{\sim}{Z}\,\underset{\sim}{Y}}\;\underset{\sim}{Y}^{-1} \quad . \tag{30c}$$

The relations in (30) may be easily shown [18] by forming $(\sqrt{\underset{\sim}{Y}\,\underset{\sim}{Z}})\,(\sqrt{\underset{\sim}{Y}\,\underset{\sim}{Z}}) = (\underset{\sim}{T}\,\underset{\sim}{\gamma}\,\underset{\sim}{T}^{-1})\,(\underset{\sim}{T}\,\underset{\sim}{\gamma}\,\underset{\sim}{T}^{-1}) = \underset{\sim}{T}\,\underset{\sim}{\gamma}^{2}\,\underset{\sim}{T}^{-1} = \underset{\sim}{Y}\,\underset{\sim}{Z}$ and $(\sqrt{\underset{\sim}{Z}\,\underset{\sim}{Y}})\,(\sqrt{\underset{\sim}{Z}\,\underset{\sim}{Y}}) = (\underset{\sim}{Y}^{-1}\sqrt{\underset{\sim}{Y}\,\underset{\sim}{Z}}\,\underset{\sim}{Y})\,(\underset{\sim}{Y}^{-1}\sqrt{\underset{\sim}{Y}\,\underset{\sim}{Z}}\,\underset{\sim}{Y}) = \underset{\sim}{Z}\,\underset{\sim}{Y}$. Note that $\sqrt{\underset{\sim}{Y}\,\underset{\sim}{Z}} \neq \sqrt{\underset{\sim}{Z}\,\underset{\sim}{Y}}$ and the order of multiplication of the matrices cannot be interchanged since $\underset{\sim}{Z}$ and $\underset{\sim}{Y}$ do not, in general, commute.

If the mode currents, $\underline{I}_m(x)$, are defined as in (23) and the mode voltages are defined from (25) as $\underline{V}(x) = \underset{\sim}{Z}_C\,\underset{\sim}{T}\underline{V}_m(x)$, then it is clear that the mode quantities consist of n uncoupled waves and each mode has the propagation constant γ_i. The velocities, v_i, and attenuation constants, η_i, associated with each mode are found by writing $\gamma_i = \eta_i + j(\omega/v_i)$ where η_i and v_i are real scalars. Thus one might think of these "mode" quantities as being somewhat basic quantities in the overall propagation of the waves since the total voltages and currents are linear combinations of the mode voltages and mode currents, respectively. This concept, however, is not particularly useful in obtaining numerical solutions to a given problem via machine computation and is only offered as a link to the more familiar two-conductor case discussed above. There are, however, instances where this concept, when related to matrix scattering parameters, can prove useful in certain synthesis problems [19].

The state transition matrix or chain parameter matrix, $\underset{\sim}{\Phi}(x, x_0)$, in (8) which relates voltages and currents at the two ends of a section of the line extending from x_0 to x can also be obtained by eliminating $\underline{I}^+$ and $\underline{I}^-$ from (23) and (25) as [18, 26, 47]

$$\begin{bmatrix} \underline{V}(x) \\ \underline{I}(x) \end{bmatrix} = \underset{\sim}{\Phi}(x, x_0) \begin{bmatrix} \underline{V}(x_0) \\ \underline{I}(x_0) \end{bmatrix} = \begin{bmatrix} \underset{\sim}{\Phi}_{11}(x, x_0) & \underset{\sim}{\Phi}_{12}(x, x_0) \\ \underset{\sim}{\Phi}_{21}(x, x_0) & \underset{\sim}{\Phi}_{22}(x, x_0) \end{bmatrix} \begin{bmatrix} \underline{V}(x_0) \\ \underline{I}(x_0) \end{bmatrix} \quad (31)$$

where the $n \times n$ submatrices, $\underset{\sim}{\Phi}_{ij}(x, x_0)$; i, j = 1, 2 are given by [26, 47]

$$\underset{\sim}{\Phi}_{11}(x, x_0) = 1/2\ \underset{\sim}{Y}^{-1}\ \underset{\sim}{T}\ (\underset{\sim}{e}^{\underset{\sim}{\gamma}(x-x_0)} + \underset{\sim}{e}^{-\underset{\sim}{\gamma}(x-x_0)})\ \underset{\sim}{T}^{-1}\ \underset{\sim}{Y} \quad (32a)$$

$$\underset{\sim}{\Phi}_{12}(x, x_0) = -1/2\ \underset{\sim}{Y}^{-1}\ \underset{\sim}{T}\ \underset{\sim}{\gamma}(\underset{\sim}{e}^{\underset{\sim}{\gamma}(x-x_0)} - \underset{\sim}{e}^{-\underset{\sim}{\gamma}(x-x_0)})\ \underset{\sim}{T}^{-1} \quad (32b)$$

$$= -1/2\ \underset{\sim}{Y}^{-1}\ \underset{\sim}{T}\ \underset{\sim}{\gamma}\ \underset{\sim}{T}^{-1}\left\{\underset{\sim}{T}(\underset{\sim}{e}^{\underset{\sim}{\gamma}(x-x_0)} - \underset{\sim}{e}^{-\underset{\sim}{\gamma}(x-x_0)})\ \underset{\sim}{T}^{-1}\right\}$$

$$\underset{\sim}{\Phi}_{21}(x, x_0) = -1/2\ \underset{\sim}{T}\ (\underset{\sim}{e}^{\underset{\sim}{\gamma}(x-x_0)} - \underset{\sim}{e}^{-\underset{\sim}{\gamma}(x-x_0)})\ \underset{\sim}{\gamma}^{-1}\ \underset{\sim}{T}^{-1}\ \underset{\sim}{Y} \quad (32c)$$

$$= -1/2\left\{\underset{\sim}{T}(\underset{\sim}{e}^{\underset{\sim}{\gamma}(x-x_0)} - \underset{\sim}{e}^{-\underset{\sim}{\gamma}(x-x_0)})\ \underset{\sim}{T}^{-1}\right\}\underset{\sim}{T}\ \underset{\sim}{\gamma}^{-1}\ \underset{\sim}{T}^{-1}\ \underset{\sim}{Y}$$

$$\underset{\sim}{\Phi}_{22}(x, x_0) = 1/2\ \underset{\sim}{T}(\underset{\sim}{e}^{\underset{\sim}{\gamma}(x-x_0)} + \underset{\sim}{e}^{-\underset{\sim}{\gamma}(x-x_0)})\ \underset{\sim}{T}^{-1} \quad . \quad (32d)$$

From (21), one can obtain $\underset{\sim}{Y}^{-1}\underset{\sim}{T}\underset{\sim}{\gamma} = \underset{\sim}{Z}\underset{\sim}{T}\underset{\sim}{\gamma}^{-1}$ and therefore $\underset{\sim}{Y}^{-1}\underset{\sim}{T}\underset{\sim}{\gamma}$ in (32) can be written in terms of $\underset{\sim}{Z}$.

The state transition matrix can also be obtained as an absolutely convergent matrix infinite series [38, 42]

$$\underset{\sim}{\Phi}(x, x_0) = \underset{\sim}{e}^{\underset{\sim}{M}(x-x_0)} = \underset{\sim}{1}_{2n} + \underset{\sim}{M}\frac{(x-x_0)}{1!} + \underset{\sim}{M}^2\frac{(x-x_0)^2}{2!} + \underset{\sim}{M}^3\frac{(x-x_0)^3}{3!} + \cdots \quad (33a)$$

where from (4c)

$$\underset{\sim}{M} = \begin{bmatrix} \underset{n\sim n}{0} & -\underset{\sim}{Z} \\ -\underset{\sim}{Y} & \underset{n\sim n}{0} \end{bmatrix} . \quad (33b)$$

After obtaining the indicated products of $\underset{\sim}{M}$, one can obtain [18]

$$\underset{\sim}{\Phi}_{11}(x, x_0) = \underset{\sim}{1}_n + \underset{\sim}{Z}\underset{\sim}{Y}\frac{(x-x_0)^2}{2!} + (\underset{\sim}{Z}\underset{\sim}{Y})^2\frac{(x-x_0)^4}{4!} + \cdots \tag{34a}$$

$$= \underset{\sim}{Y}^{-1}\left\{\underset{\sim}{1}_n + \underset{\sim}{Y}\underset{\sim}{Z}\frac{(x-x_0)^2}{2!} + (\underset{\sim}{Y}\underset{\sim}{Z})^2\frac{(x-x_0)^4}{4!} + \cdots\right\}\underset{\sim}{Y}$$

$$\underset{\sim}{\Phi}_{12}(x, x_0) = -\underset{\sim}{Z}(x-x_0) - \underset{\sim}{Z}\underset{\sim}{Y}\underset{\sim}{Z}\frac{(x-x_0)^3}{3!} - (\underset{\sim}{Z}\underset{\sim}{Y})^2\underset{\sim}{Z}\frac{(x-x_0)^5}{5!} - \cdots \tag{34b}$$

$$= -\underset{\sim}{Z}(\sqrt{\underset{\sim}{Y}\underset{\sim}{Z}})^{-1}\left\{\sqrt{\underset{\sim}{Y}\underset{\sim}{Z}}(x-x_0) + (\sqrt{\underset{\sim}{Y}\underset{\sim}{Z}})^3\frac{(x-x_0)^3}{3!} + (\sqrt{\underset{\sim}{Y}\underset{\sim}{Z}})^5\frac{(x-x_0)^5}{5!} + \cdots\right\}$$

$$= -\left\{\sqrt{\underset{\sim}{Z}\underset{\sim}{Y}}(x-x_0) + (\sqrt{\underset{\sim}{Z}\underset{\sim}{Y}})^3\frac{(x-x_0)^3}{3!} + (\sqrt{\underset{\sim}{Z}\underset{\sim}{Y}})^5\frac{(x-x_0)^5}{5!} + \cdots\right\}\sqrt{\underset{\sim}{Z}\underset{\sim}{Y}}\ \underset{\sim}{Y}^{-1}$$

$$\underset{\sim}{\Phi}_{21}(x, x_0) = -\underset{\sim}{Y}(x-x_0) - \underset{\sim}{Y}\underset{\sim}{Z}\underset{\sim}{Y}\frac{(x-x_0)^3}{3!} - (\underset{\sim}{Y}\underset{\sim}{Z})^2\underset{\sim}{Y}\frac{(x-x_0)^5}{5!} - \cdots \tag{34c}$$

$$= -\underset{\sim}{Y}(\sqrt{\underset{\sim}{Z}\underset{\sim}{Y}})^{-1}\left\{\sqrt{\underset{\sim}{Z}\underset{\sim}{Y}}(x-x_0) + (\sqrt{\underset{\sim}{Z}\underset{\sim}{Y}})^3\frac{(x-x_0)^3}{3!} + (\sqrt{\underset{\sim}{Z}\underset{\sim}{Y}})^5\frac{(x-x_0)^5}{5!} + \cdots\right\}$$

$$= -\left\{\sqrt{\underset{\sim}{Y}\underset{\sim}{Z}}(x-x_0) + (\sqrt{\underset{\sim}{Y}\underset{\sim}{Z}})^3\frac{(x-x_0)^3}{3!} + (\sqrt{\underset{\sim}{Y}\underset{\sim}{Z}})^5\frac{(x-x_0)^5}{5!} + \cdots\right\}(\sqrt{\underset{\sim}{Y}\underset{\sim}{Z}})^{-1}\underset{\sim}{Y}$$

$$\underset{\sim}{\Phi}_{22}(x, x_0) = \underset{\sim}{1}_n + \underset{\sim}{Y}\underset{\sim}{Z}\frac{(x-x_0)^2}{2!} + (\underset{\sim}{Y}\underset{\sim}{Z})^2\frac{(x-x_0)^4}{4!} + \cdots \tag{34d}$$

$$= \underset{\sim}{Y}\left\{\underset{\sim}{1}_n + \underset{\sim}{Z}\underset{\sim}{Y}\frac{(x-x_0)^2}{2!} + (\underset{\sim}{Z}\underset{\sim}{Y})^2\frac{(x-x_0)^4}{4!} + \cdots\right\}\underset{\sim}{Y}^{-1}.$$

Matrix hyperbolic functions Cosh and Sinh may logically be defined in the following manner. The matrix exponential, $\underset{\sim}{e}^{\sqrt{\underset{\sim}{Y}\underset{\sim}{Z}}(x-x_0)}$, may logically

be defined as the absolutely convergent matrix infinite series [18, 38, 42]

$$\underset{\sim}{e}^{\sqrt{\underset{\sim}{Y}\underset{\sim}{Z}}\,(x-x_0)} = \underset{\sim}{1}_n + \sqrt{\underset{\sim}{Y}\underset{\sim}{Z}}\,\frac{(x-x_0)}{1!} + (\sqrt{\underset{\sim}{Y}\underset{\sim}{Z}})^2\frac{(x-x_0)^2}{2!} + (\sqrt{\underset{\sim}{Y}\underset{\sim}{Z}})^3\frac{(x-x_0)^3}{3!} + \cdots \quad (35)$$

The matrix exponential, $\underset{\sim}{e}^{\underset{\sim}{Y}(x-x_0)}$, can similarly be defined as an absolutely convergent matrix infinite series [18, 38, 42]

$$\underset{\sim}{e}^{\underset{\sim}{Y}(x-x_0)} = \underset{\sim}{1}_n + \underset{\sim}{Y}\frac{(x-x_0)}{1!} + \underset{\sim}{Y}^2\frac{(x-x_0)^2}{2!} + \underset{\sim}{Y}^3\frac{(x-x_0)^3}{3!} + \cdots \quad (36)$$

Since $\underset{\sim}{Y}\underset{\sim}{Z}$ is assumed to be diagonalized by $\underset{\sim}{T}$ as in (21), then the square root of $\underset{\sim}{Y}\underset{\sim}{Z}$ may be defined as $\sqrt{\underset{\sim}{Y}\underset{\sim}{Z}} = \underset{\sim}{T}\,\underset{\sim}{\gamma}\,\underset{\sim}{T}^{-1}$ as shown in (30). Therefore, (35) may be written as [18, 38, 42]

$$\underset{\sim}{e}^{\sqrt{\underset{\sim}{Y}\underset{\sim}{Z}}\,(x-x_0)} = \underset{\sim}{T}\,\underset{\sim}{e}^{\underset{\sim}{\gamma}(x-x_0)}\,\underset{\sim}{T}^{-1} \quad (37)$$

$$= \underset{\sim}{Y}\,\underset{\sim}{e}^{\sqrt{\underset{\sim}{Z}\underset{\sim}{Y}}\,(x-x_0)}\,\underset{\sim}{Y}^{-1}$$

where $\sqrt{\underset{\sim}{Z}\underset{\sim}{Y}}$ is defined in (30b) and (30c). Thus the matrix hyperbolic functions Cosh and Sinh may be defined from (35), (36) and (37) as

$$\mathrm{Cosh}\left\{\sqrt{\underset{\sim}{Y}\underset{\sim}{Z}}\,(x-x_0)\right\} = 1/2\left\{\underset{\sim}{e}^{\sqrt{\underset{\sim}{Y}\underset{\sim}{Z}}\,(x-x_0)} + \underset{\sim}{e}^{-\sqrt{\underset{\sim}{Y}\underset{\sim}{Z}}\,(x-x_0)}\right\} \quad (38a)$$

$$= \underset{\sim}{1}_n + (\sqrt{\underset{\sim}{Y}\underset{\sim}{Z}})^2\frac{(x-x_0)^2}{2!} + (\sqrt{\underset{\sim}{Y}\underset{\sim}{Z}})^4\frac{(x-x_0)^4}{4!} + \cdots$$

$$= 1/2\,\underset{\sim}{T}\left\{\underset{\sim}{e}^{\underset{\sim}{\gamma}(x-x_0)} + \underset{\sim}{e}^{-\underset{\sim}{\gamma}(x-x_0)}\right\}\underset{\sim}{T}^{-1}$$

$$\mathrm{Sinh}\left\{\sqrt{\underset{\sim}{Y}\underset{\sim}{Z}}\,(x-x_0)\right\} = 1/2\left\{\underset{\sim}{e}^{\sqrt{\underset{\sim}{Y}\underset{\sim}{Z}}\,(x-x_0)} - \underset{\sim}{e}^{-\sqrt{\underset{\sim}{Y}\underset{\sim}{Z}}\,(x-x_0)}\right\} \quad (38b)$$

$$= \sqrt{\underset{\sim}{Y}\underset{\sim}{Z}}\,\frac{(x-x_0)}{1!} + (\sqrt{\underset{\sim}{Y}\underset{\sim}{Z}})^3\frac{(x-x_0)^3}{3!} + (\sqrt{\underset{\sim}{Y}\underset{\sim}{Z}})^5\frac{(x-x_0)^5}{5!} + \cdots$$

$$= 1/2\,\underset{\sim}{T}\left\{\underset{\sim}{e}^{\underset{\sim}{\gamma}(x-x_0)} - \underset{\sim}{e}^{-\underset{\sim}{\gamma}(x-x_0)}\right\}\underset{\sim}{T}^{-1}.$$

Therefore, it should be clear by utilizing the relations in (35), (36), (37) and (38) that the expressions for the chain parameter submatrices in (32) and (34) are equivalent and may be written symbolically as [18]

$$\underset{\sim}{\Phi}_{11}(x, x_0) = \text{Cosh}\left\{\sqrt{\underset{\sim}{Z}\,\underset{\sim}{Y}}\,(x-x_0)\right\} = \underset{\sim}{Y}^{-1}\,\text{Cosh}\left\{\sqrt{\underset{\sim}{Y}\,\underset{\sim}{Z}}\,(x-x_0)\right\}\,\underset{\sim}{Y} \tag{39a}$$

$$\underset{\sim}{\Phi}_{12}(x, x_0) = -\underset{\sim}{Z}\left(\sqrt{\underset{\sim}{Y}\,\underset{\sim}{Z}}\right)^{-1}\text{Sinh}\left\{\sqrt{\underset{\sim}{Y}\,\underset{\sim}{Z}}\,(x-x_0)\right\} = -\text{Sinh}\left\{\sqrt{\underset{\sim}{Z}\,\underset{\sim}{Y}}\,(x-x_0)\right\}\sqrt{\underset{\sim}{Z}\,\underset{\sim}{Y}}^{-1}\,\underset{\sim}{Y}^{-1} \tag{39b}$$

$$= -\underset{\sim}{Z}_C\,\text{Sinh}\left\{\sqrt{\underset{\sim}{Y}\,\underset{\sim}{Z}}\,(x-x_0)\right\} = -\text{Sinh}\left\{\sqrt{\underset{\sim}{Z}\,\underset{\sim}{Y}}\,(x-x_0)\right\}\,\underset{\sim}{Z}_C$$

$$\underset{\sim}{\Phi}_{21}(x, x_0) = -\underset{\sim}{Y}\left(\sqrt{\underset{\sim}{Z}\,\underset{\sim}{Y}}\right)^{-1}\text{Sinh}\left\{\sqrt{\underset{\sim}{Z}\,\underset{\sim}{Y}}\,(x-x_0)\right\} = -\text{Sinh}\left\{\sqrt{\underset{\sim}{Y}\,\underset{\sim}{Z}}\,(x-x_0)\right\}\left(\sqrt{\underset{\sim}{Y}\,\underset{\sim}{Z}}\right)^{-1}\,\underset{\sim}{Y} \tag{39c}$$

$$= -\underset{\sim}{Z}_C^{-1}\,\text{Sinh}\left\{\sqrt{\underset{\sim}{Z}\,\underset{\sim}{Y}}\,(x-x_0)\right\} = -\text{Sinh}\left\{\sqrt{\underset{\sim}{Y}\,\underset{\sim}{Z}}\,(x-x_0)\right\}\,\underset{\sim}{Z}_C^{-1}$$

$$\underset{\sim}{\Phi}_{22}(x, x_0) = \text{Cosh}\left\{\sqrt{\underset{\sim}{Y}\,\underset{\sim}{Z}}\,(x-x_0)\right\} = \underset{\sim}{Y}\,\text{Cosh}\left\{\sqrt{\underset{\sim}{Z}\,\underset{\sim}{Y}}\,(x-x_0)\right\}\,\underset{\sim}{Y}^{-1} \tag{39d}$$

where the characteristic-impedance matrix, $\underset{\sim}{Z}_C$, is defined in (29) and (30). (Note that these reduce to the scalar elements for two-conductor (n=1) lines in (17).) For numerical machine computation, however, one would use the forms of the submatrices given in (32) since the equivalent expressions in (34) and (39) would be of little practical value in obtaining numerical results.

Also one can show certain fundamental matrix identities involving the submatrices of the chain parameter matrix [18]:

Identity 1: $$\underset{\sim}{\Phi}_{12}\,\underset{\sim}{\Phi}_{22}\,\underset{\sim}{\Phi}_{12}^{-1}\,\underset{\sim}{\Phi}_{11} - \underset{\sim}{\Phi}_{12}\,\underset{\sim}{\Phi}_{21} = \underset{\sim}{1}_n \tag{40a}$$

Identity 2: $$\underset{\sim}{\Phi}_{21}\,\underset{\sim}{\Phi}_{11}\,\underset{\sim}{\Phi}_{21}^{-1}\,\underset{\sim}{\Phi}_{22} - \underset{\sim}{\Phi}_{21}\,\underset{\sim}{\Phi}_{12} = \underset{\sim}{1}_n \tag{40b}$$

Identity 3: $$\underset{\sim}{\Phi}_{12}\,\underset{\sim}{\Phi}_{22}\,\underset{\sim}{\Phi}_{12}^{-1} = \underset{\sim}{\Phi}_{11} \tag{40c}$$

Identity 4: $$\underset{\sim}{\Phi}_{21}\,\underset{\sim}{\Phi}_{11}\,\underset{\sim}{\Phi}_{21}^{-1} = \underset{\sim}{\Phi}_{22} \tag{40d}$$

Identity 5: $$\underset{\sim}{\Phi}_{11} = \underset{\sim}{\Phi}_{22}^{t} \tag{40e}$$

where $\underset{\sim}{\Phi}_{ij}$ refers to $\underset{\sim}{\Phi}_{ij}(x, x_0)$. Identities 1 and 2 reduce, in the case of two-conductor lines (n=1) where the submatrices become scalars, to familiar results, described above i.e., $\Phi_{22}\Phi_{11} - \Phi_{12}\Phi_{21} = 1$ and the determinant of the chain parameter matrix is equal to unity. Similarly, Identities 3, 4 and 5 also reduce, in the case of two-conductor lines, to familiar results, i.e., $\Phi_{22} = \Phi_{11}$. These identities may be proven by substituting the forms of the submatrices given in (32) and utilizing the fact that $\underset{\sim}{\gamma}$, $\underset{\sim}{e}^{\underset{\sim}{\gamma}(x-x_0)}$ and $\underset{\sim}{e}^{-\underset{\sim}{\gamma}(x-x_0)}$ are diagonal matrices whose products may therefore be interchanged. The identities may be more directly shown, even when $\underset{\sim}{Y}\,\underset{\sim}{Z}$ is not diagonalizable by a similarity transformation, by recalling that the inverse of the chain parameter matrix or state transition matrix is given by $\underset{\sim}{\Phi}^{-1}(x, x_0) = \underset{\sim}{\Phi}(x_0, x)$ [42]. Forming this relation as $\underset{\sim}{\Phi}(x, x_0)\,\underset{\sim}{\Phi}(x_0, x) = \underset{\sim}{1}_{2n}$ yields in partitioned form [18]

$$\begin{bmatrix} \underset{\sim}{\Phi}_{11}(x, x_0) & \underset{\sim}{\Phi}_{12}(x, x_0) \\ \underset{\sim}{\Phi}_{21}(x, x_0) & \underset{\sim}{\Phi}_{22}(x, x_0) \end{bmatrix} \begin{bmatrix} \underset{\sim}{\Phi}_{11}(x_0, x) & \underset{\sim}{\Phi}_{12}(x_0, x) \\ \underset{\sim}{\Phi}_{21}(x_0, x) & \underset{\sim}{\Phi}_{22}(x_0, x) \end{bmatrix} = \begin{bmatrix} \underset{\sim}{1}_n & \underset{\sim}{0}_n \\ \underset{\sim}{0}_n & \underset{\sim}{1}_n \end{bmatrix}. \tag{41}$$

Multiplying this result out and observing from (34) that $\underset{\sim}{\Phi}_{11}(x, x_0) = \underset{\sim}{\Phi}_{11}(x_0, x)$, $\underset{\sim}{\Phi}_{12}(x, x_0) = -\underset{\sim}{\Phi}_{12}(x_0, x)$, $\underset{\sim}{\Phi}_{21}(x, x_0) = -\underset{\sim}{\Phi}_{21}(x_0, x)$, $\underset{\sim}{\Phi}_{22}(x, x_0) = \underset{\sim}{\Phi}_{22}(x_0, x)$ yields Identities 1, 2, 3, 4 directly [18]. Identity 5 is easily shown from (34a) and (34d) since $\underset{\sim}{Y}$ and $\underset{\sim}{Z}$ are symmetric, i.e., $\underset{\sim}{Z} = \underset{\sim}{Z}^t$ and $\underset{\sim}{Y} = \underset{\sim}{Y}^t$, and the transpose of a sum of matrices is equal to the sum of their transposes [18, 38, 42]. This also shows from (34b) and (34c) that $\underset{\sim}{\Phi}_{12}$ and $\underset{\sim}{\Phi}_{21}$ are symmetric, i.e., $\underset{\sim}{\Phi}_{12} = \underset{\sim}{\Phi}_{12}^t$ and $\underset{\sim}{\Phi}_{21} = \underset{\sim}{\Phi}_{21}^t$ [18].

Thus the result conforms (symbolically) to the two-conductor case in which $\underset{\sim}{Y}$ and $\underset{\sim}{Z}$ are complex scalars instead of matrices. This use of symbolic notation for the square root of a matrix and the matrix hyperbolic functions Cosh and Sinh of course makes sense because it was assumed that the matrix product $\underset{\sim}{Y}\,\underset{\sim}{Z}$ was diagonalizable by the similarity transformation, $\underset{\sim}{T}$. It is not necessarily true that the matrix product $\underset{\sim}{Y}\,\underset{\sim}{Z}$ (and also $\underset{\sim}{Z}\,\underset{\sim}{Y}$) will be diagonalizable by a similarity transformation [41, 42]. If the product is not diagonalizable, then a similarity transformation may be found to place $\underset{\sim}{Y}\,\underset{\sim}{Z}$ in the Jordan Canonical form and this result is found in [47] although numerical results become more complicated to obtain.

Thus one of the important simplifying assumptions is that $\underset{\sim}{Y}\,\underset{\sim}{Z}$ is diagonalizable by a similarity transformation as in (21). It is often assumed that $\underset{\sim}{Y}\,\underset{\sim}{Z}$ can be diagonalized by a similarity transformation regardless of the numerical entries in $\underset{\sim}{Y}$ and $\underset{\sim}{Z}$ and this is, of course, not necessarily true [41, 42]. To more completely investigate the problem, determine the eigenvalues of $\underset{\sim}{Y}\,\underset{\sim}{Z}$ as roots of the n-th order complex polynomial in γ^2 [18, 41, 42]

$$\det\left(\gamma^2\,\underset{\sim}{1}_n - \underset{\sim}{Y}\,\underset{\sim}{Z}\right) = 0 \tag{42}$$

where det denotes the determinant. If the resulting eigenvalues, γ_i^2, are distinct, then diagonalization of $\underset{\sim}{Y}\,\underset{\sim}{Z}$ is assured and the $n \times 1$ columns of $\underset{\sim}{T} = [\underline{T}_1, \underline{T}_2, \text{---}, \underline{T}_n]$, $\underline{T}_i$, are eigenvectors of $\underset{\sim}{Y}\,\underset{\sim}{Z}$ satisfying

$$\left(\gamma_i^2\,\underset{\sim}{1}_n - \underset{\sim}{Y}\,\underset{\sim}{Z}\right)\underline{T}_i = \underset{n\text{-}1}{0} \tag{43}$$

for $i = 1, \text{---}, n$ [18, 41, 42]. But, of course, one does not generally know a priori if the eigenvalues will be distinct and considerable computation may

be required to determine this. If there exist repeated eigenvalues, then it may or may not be possible to determine n linearly independent eigenvectors via (43). If n linearly independent eigenvectors can be found, then diagonalization is assured [18, 41, 42]. It can be shown that the eigenvalues of $\underset{\sim}{Y}\,\underset{\sim}{Z}$ are the same as the eigenvalues of $\underset{\sim}{Z}\,\underset{\sim}{Y}$ (see [42], pp. 101-102). When either $\underset{\sim}{Y}$ or $\underset{\sim}{Z}$ are nonsingular, this can be easily shown by forming [18]
$\det\left(\gamma^2\ \underset{\sim}{1}_n - \underset{\sim}{Y}\,\underset{\sim}{Z}\right) = \det\left(\underset{\sim}{Y}\left\{\gamma^2\ \underset{\sim}{1}_n - \underset{\sim}{Z}\,\underset{\sim}{Y}\right\}\underset{\sim}{Y}^{-1}\right) = \det\left(\underset{\sim}{Z}^{-1}\left\{\gamma^2\ \underset{\sim}{1}_n - \underset{\sim}{Z}\,\underset{\sim}{Y}\right\}\underset{\sim}{Z}\right) =$
$\det\left(\gamma^2\ \underset{\sim}{1}_n - \underset{\sim}{Z}\,\underset{\sim}{Y}\right)$ since the determinant of a product of square matrices is equal to the product of their determinants and $\det(\underset{\sim}{Y})\ \det\left(\underset{\sim}{Y}^{-1}\right) =$
$\det\left(\underset{\sim}{Z}^{-1}\right)\det(\underset{\sim}{Z}) = 1$. Also one can form (43) as $\underset{\sim}{Y}(\gamma_i^2\ \underset{\sim}{1}_n - \underset{\sim}{Z}\,\underset{\sim}{Y})\left(\underset{\sim}{Y}^{-1}\ \underset{\sim}{T}_i\right) =$ $\underset{n-1}{0}$ and $\underset{\sim}{Z}^{-1}(\gamma_i^2\ \underset{\sim}{1}_n - \underset{\sim}{Z}\,\underset{\sim}{Y})(\underset{\sim}{Z}\,\underset{\sim}{T}_i) = \underset{n-1}{0}$ so that if $\underset{\sim}{Y}$ is nonsingular then each of the eigenvectors of $\underset{\sim}{Z}\,\underset{\sim}{Y}$ is equal to the product of $\underset{\sim}{Y}^{-1}$ and each of the eigenvectors of $\underset{\sim}{Y}\,\underset{\sim}{Z}$ (within a scalar constant), and if $\underset{\sim}{Z}$ is nonsingular, then each of the eigenvectors of $\underset{\sim}{Z}\,\underset{\sim}{Y}$ is equal to the product of $\underset{\sim}{Z}$ and each of the eigenvectors of $\underset{\sim}{Y}\,\underset{\sim}{Z}$ (within a scalar constant) [18]. These facts can be used to form the relations in (23), (25) and (32) in terms of $\sqrt{\underset{\sim}{Z}\,\underset{\sim}{Y}}$ and its eigenvectors.

When discussing the question of distinct eigenvalues in numerical computation, it is important to consider the question of "how distinct". For example, if two of the eigenvalues are distinct only after the 16-th digit, then although they are technically distinct, the two eigenvectors from (43) associated with these two "almost-distinct" eigenvalues may be very nearly collinear causing $\underset{\sim}{T}$ to be an ill-conditioned matrix with a very small determinant, i.e., $\underset{\sim}{T}$ will be "almost singular". Thus numerical instabilities

and other associated errors can occur when, for example, computing the inverse of $\underset{\sim}{T}$, $\underset{\sim}{T}^{-1}$, since $\underset{\sim}{T}$ may be an ill-conditioned matrix having a very small determinant [49].

This is one of the reasons why determining numerically stable similarity transformations such as orthogonal or unitary transformations are important in numerical machine computations[49]. For example, a real, orthogonal similarity transformation, $\underset{\sim}{T}$, can always be found which will diagonalize a real, symmetric matrix and $\underset{\sim}{T}^{-1} = \underset{\sim}{T}^{t}$ where the transpose of a matrix $\underset{\sim}{M}$ is denoted by $\underset{\sim}{M}^{t}$ [41, 49]. Also, complex,unitary transformations, $\underset{\sim}{T}$, can always be found which diagonalize complex matrices which are either hermitian or normal and $\underset{\sim}{T}^{-1} = \underset{\sim}{T}^{*}$ where the complex conjugate transpose of a matrix $\underset{\sim}{M}$ is denoted by $\underset{\sim}{M}^{*}$ [41, 49]. Hermitian matrices satisfy $\underset{\sim}{M} = \underset{\sim}{M}^{*}$ and normal matrices satisfy $(\underset{\sim}{M})(\underset{\sim}{M}^{*}) = (\underset{\sim}{M}^{*})(\underset{\sim}{M})$ [41].

Machine computation of the eigenvalues and eigenvectors of $\underset{\sim}{Y}\,\underset{\sim}{Z}$ is not generally performed by a direct application of (42) and (43). Instead of directly applying (42) and (43), a more efficient method would be to tranform $\underset{\sim}{Y}\,\underset{\sim}{Z}$ with a similarity transformation to some other more convenient form whose eigenvectors and eigenvalues are related to these of $\underset{\sim}{Y}\,\underset{\sim}{Z}$. For example it is known that it is always possible to obtain an $n\chi n$ complex,similarity tranformation, $\underset{\sim}{U}$, which is unitary that will reduce any $n\chi n$ complex matrix (in particular $\underset{\sim}{Y}\,\underset{\sim}{Z}$) to upper triangular form, i.e., $\underset{\sim}{U}^{*}\,\underset{\sim}{Y}\,\underset{\sim}{Z}\,\underset{\sim}{U} = \underset{\sim}{M}$ and $\underset{\sim}{U}^{*} = \underset{\sim}{U}^{-1}$, where $\underset{\sim}{M}$ has zeros below the main diagonal [41]. Then since $\underset{\sim}{M}$ is similar to $\underset{\sim}{Y}\,\underset{\sim}{Z}$ (in the mathematical sense of similarity), the eigenvalues of $\underset{\sim}{M}$ which are

the elements on the main diagonal of $\underset{\sim}{M}$ are the same as the eigenvalues of $\underset{\sim}{Y}\,\underset{\sim}{Z}$ [41, 49]. A commonly-used algorithm is the QR transformation [49]. The eigenvectors of $\underset{\sim}{Y}\,\underset{\sim}{Z}$, $\underline{T}_i$, are related to the eigenvectors of $\underset{\sim}{M}$, $\underline{S}_i$, by $\underline{T}_i = \underset{\sim}{U}\,\underline{S}_i$ where $\underline{S}_i$ is an $n\chi 1$ eigenvector of $\underset{\sim}{M}$ associated with the eigenvalue γ_i^2 and corresponds to the eigenvector $\underline{T}_i$ associated with eigenvalue γ_i^2 [41, 49]. The transformation to Hessenberg form is also commonly employed [49].

In addition to the question of the existence of a numerically stable similarity transformation which diagonalizes the matrix product $\underset{\sim}{Y}\,\underset{\sim}{Z}$, there is the problem of recomputing the eigenvalues and eigenvectors at each frequency being considered. Since the matrix product $\underset{\sim}{Y}\,\underset{\sim}{Z}$ is a function of frequency, then one is, in general, required to repeat the determination of the eigenvalues and eigenvectors of this complex-valued matrix product, $\underset{\sim}{Y}\,\underset{\sim}{Z}$, at each frequency and this can be a very time-consuming task when the response at a large number of frequencies is desired. There are, however, certain practical cases where $\underset{\sim}{Y}\,\underset{\sim}{Z}$ can be diagonalized by a numerically stable transformation and, moreover, for these cases, $\underset{\sim}{T}$ is independent of frequency and need only be computed once. These important cases will now be discussed.

3.1 Transmission Lines in a Homogeneous Medium

This section will consider the (n+1)-conductor lines in a homogeneous medium represented in Fig. 2. Although the lines in Fig. 2a and Fig. 2b can only logically be considered immersed in free space which is considered lossless, the formulation which will be investigated will assume losses in

the medium in order that the situation in Fig. 2c may be considered. The following important relations which are well known in the case of two-conductor lines in a homogeneous medium are shown in Appendix A for the case of (n+1)-conductor lines in a homogeneous medium which is assumed to be characterized by μ, ϵ, σ:

$$\underset{\sim}{L}\,\underset{\sim}{C} = \underset{\sim}{C}\,\underset{\sim}{L} = \mu\epsilon\,\underset{\sim}{1}_n \tag{44a}$$

$$\underset{\sim}{L}\,\underset{\sim}{G} = \underset{\sim}{G}\,\underset{\sim}{L} = \mu\sigma\,\underset{\sim}{1}_n \quad . \tag{44b}$$

When the dielectric medium is lossy as in Fig. 2c, the conductivity in (44b) refers to the effective conductivity as $\sigma = \sigma_d + \omega\epsilon'' = \omega\epsilon_v\,\epsilon_r \tan\delta$ and includes the combined losses due to ohmic conductivity, σ_d, and dipole relaxation effects. The loss tangent of the medium is denoted by $\tan\delta$, ϵ_v is the permittivity of free space and ϵ_r is the relative dielectric constant. The permittivity, ϵ, refers to the real part of the complex effective permittivity, i.e., $\epsilon = \epsilon_v\,\epsilon_r$, and the permeability, μ, will typically be that of free space, μ_v. In addition, since the medium is homogeneous it can also be shown [54] that $\underset{\sim}{C} = \epsilon\,\underset{\sim}{K}$ and from (44) it follows that

$$\underset{\sim}{C} = \epsilon\underset{\sim}{K} \tag{45a}$$

$$\underset{\sim}{L} = \mu\underset{\sim}{K}^{-1} \tag{45b}$$

$$\underset{\sim}{G} = \sigma\underset{\sim}{K} \tag{45c}$$

where $\underset{\sim}{K}$ is an $n\times n$ real, symmetric, positive definite matrix independent of ϵ(and therefore frequency) and is dependent only upon the cross-sectional structure of the line (conductor separations and wire radii). The matrix product $\underset{\sim}{Y}\,\underset{\sim}{Z}$ with the relations in (44) and (45) becomes

$$\underset{\sim}{Y}\,\underset{\sim}{Z} = (\sigma + j\omega\epsilon)\,\underset{\sim}{K}\,(\underset{\sim}{R}_c + j\omega\underset{\sim}{L}_c) + (j\omega\mu\sigma - \omega^2\mu\epsilon)\,\underset{\sim}{1}_n \qquad (46)$$

and if perfect conductors are assumed, then all n mode velocities and attenuation constants degenerate into one set, which represents the true TEM mode of propagation.

If perfect conductors are assumed, i.e., $\underset{\sim}{R}_c = \underset{\sim}{L}_c = \underset{n\sim n}{0}$, then from (46) $\underset{\sim}{T} = \underset{\sim}{1}_n$ and $\gamma_i^2 = (j\omega\mu\sigma - \omega^2\mu\epsilon)$ in (21) where $\underset{\sim}{1}_n$ is the n x n identity matrix with ones on the main diagonal and zeros elsewhere. Thus, the matrix chain parameters for the homogeneous-medium case with (n+1) perfect conductors become from (32)

$$\underset{\sim}{\Phi}_{11}(x, x_0) = \cosh\left\{\gamma(x-x_0)\right\}\underset{\sim}{1}_n \qquad (47a)$$

$$\underset{\sim}{\Phi}_{12}(x, x_0) = -\sinh\left\{\gamma(x-x_0)\right\}\left[(j\omega/\gamma)\,\underset{\sim}{L}\right] \qquad (47b)$$

$$\underset{\sim}{\Phi}_{21}(x, x_0) = -\sinh\left\{\gamma(x-x_0)\right\}\left[(j\omega/\gamma)\,\underset{\sim}{L}\right]^{-1} \qquad (47c)$$

$$\underset{\sim}{\Phi}_{22}(x, x_0) = \cosh\left\{\gamma(x-x_0)\right\}\underset{\sim}{1}_n \qquad (47d)$$

where $\gamma = \sqrt{j\omega\mu(\sigma + j\omega\epsilon)}$ and the characteristic impedance matrix becomes from (29a)

$$\underset{\sim}{Z}_C = \sqrt{\frac{j\omega\mu}{(\sigma + j\omega\epsilon)}}\;\;\underset{\sim}{K}^{-1} \qquad (48)$$

$$= (j\omega/\gamma)\,\underset{\sim}{L} \quad .$$

For a lossless medium, $\sigma = 0$, $\gamma = j\omega\sqrt{\mu\epsilon}$ and (47) becomes [26]

$$\underset{\sim}{\Phi}_{11}(x, x_0) = \cos\left\{\beta(x-x_0)\right\}\underset{\sim}{1}_n \qquad (49a)$$

$$\underset{\sim}{\Phi}_{12}(x, x_0) = -j\sin\left\{\beta(x-x_0)\right\}[\upsilon\,\underset{\sim}{L}] \qquad (49b)$$

$$\underset{\sim}{\Phi}_{21}(x, x_0) = -j\sin\left\{\beta(x-x_0)\right\}[\upsilon\,\underset{\sim}{L}]^{-1} \qquad (49c)$$

$$\underset{\sim}{\Phi}_{22}(x, x_0) = \cos\left\{\beta(x-x_0)\right\}\underset{\sim}{1}_n \qquad (49d)$$

where the wave number, β, is given by $\beta = 2\pi/\lambda$, $\lambda = \upsilon/f$, $\upsilon = 1/\sqrt{\mu\epsilon}$ and the characteristic-impedance matrix is real and becomes $\underset{\sim}{Z}_C = \upsilon \underset{\sim}{L}$.

If perfect conductors cannot be assumed, then from (46) it is sufficient to find a $\underset{\sim}{T}$ which diagonalizes $\underset{\sim}{K}(\underset{\sim}{R}_c + j\omega\underset{\sim}{L}_c)$, i.e.,

$$\underset{\sim}{T}^{-1}\left\{\underset{\sim}{K}(\underset{\sim}{R}_c + j\omega\underset{\sim}{L}_c)\right\}\underset{\sim}{T} = \underset{\sim}{\Lambda}^2(\omega) \tag{50}$$

where $\underset{\sim}{\Lambda}^2(\omega)$ is an $n\chi n$ diagonal matrix with $[\underset{\sim}{\Lambda}^2(\omega)]_{ii} = \lambda_i^2(\omega)$ and $[\underset{\sim}{\Lambda}^2(\omega)]_{ij} = 0$ for $i \neq j$. The eigenvalues can then be found from (46) and (50) as

$$\gamma_i^2 = (\sigma + j\omega\epsilon)\,\lambda_i^2(\omega) + (j\omega\mu\sigma - \omega^2\mu\epsilon) \quad . \tag{51}$$

In general, diagonalization as in (50) is not assured since $\underset{\sim}{K}(\underset{\sim}{R}_c + j\omega\underset{\sim}{L}_c)$ is a complex matrix with no particular structural properties which would be useful in determining a priori whether the matrix is diagonalizable, i.e., hermitian or normal.

If one neglects the internal inductance of the conductors, i.e., $\underset{\sim}{L}_c = {}_n\underset{\sim}{0}_n$, or neglects the resistance of the conductors, i.e., $\underset{\sim}{R}_c = {}_{n\sim n}^{0}$, then numerically stable transformations can be found which diagonalize each of these cases but not both, i.e., there exists a $\underset{\sim}{T}$ such that [13]

$$\underset{\sim}{T}^{-1}\,\underset{\sim}{K}\,\underset{\sim}{R}_c\,\underset{\sim}{T} = \underset{\sim}{\Lambda}^2(\omega) \rightarrow \left\{\underset{\sim}{L}_c = {}_n\underset{\sim}{0}_n\right\} \tag{52}$$

or there exists a $\underset{\sim}{T}$ such that

$$j\omega\,\underset{\sim}{T}^{-1}\,\underset{\sim}{K}\,\underset{\sim}{L}_c\,\underset{\sim}{T} = \underset{\sim}{\Lambda}^2(\omega) \rightarrow \left\{\underset{\sim}{R}_c = {}_n\underset{\sim}{0}_n\right\} \tag{53}$$

but the same $\underset{\sim}{T}$ will not necessarily simultaneously diagonalize both. That this can be done relies only on the fact that $\underset{\sim}{K}$ is real, symmetric, positive definite and that $\underset{\sim}{R}_c$ and $\underset{\sim}{L}_c$ are real symmetric [13, 41, 42]. The construction of a numerically stable transformation, $\underset{\sim}{T}$, which will diagonalize the

product of a real, symmetric, positive definite matrix and a real, symmetric matrix will be shown in Section 3.2 and may be computed very efficiently with the subroutine NROOT in the IBM Scientific Subroutine Package (SSP) [50]. Generally for high frequencies, the entries in $\underset{\sim}{L}_c$ are much less than the corresponding entries in $\underset{\sim}{L}$ and the approximation in (52) would be relatively accurate [13]. However, in either case, since both $\underset{\sim}{R}_c$ and $\underset{\sim}{L}_c$ are functions of frequency, the transformation matrix, $\underset{\sim}{T}$, and the eigenvalues must be recomputed at each frequency under consideration and this increases the overall computation time.

There are cases where one can include both resistance and internal inductance of the conductors and obtain a numerically stable, frequency-independent transformation. For example, consider Fig. 2a in which all (n+1) wires are assumed to be identical. In this case, (50) becomes (see (6) and (7))

$$(r_c + j\omega\ell_c)\ \underset{\sim}{T}^{-1}\ \underset{\sim}{K}\ \left\{\underset{\sim}{1}_n + \underset{\sim}{U}_n\right\}\ \underset{\sim}{T} = \underset{\sim}{\Lambda}^2(\omega) \qquad (54)$$

where the (n+1) conductors (including the reference wire) have resistance, r_c, and internal inductance, ℓ_c, and $\underset{\sim}{U}_n$ is the $n\times n$ unit matrix with one's in every position, i.e., $[\underset{\sim}{U}_n]_{ij} = 1$ $i, j = 1, \cdots, n$. Note that even though $\underset{\sim}{K}$ and $\left\{\underset{\sim}{1}_n + \underset{\sim}{U}_n\right\}$ each are symmetric, it is not necessarily true that their product will be symmetric. Since $\underset{\sim}{K}$ is real, symmetric and positive definite and $\left\{\underset{\sim}{1}_n + \underset{\sim}{U}_n\right\}$ is real, symmetric then, as discussed before, the product can be diagonalized and NROOT in SSP can be used to perform the reduction [50]. Furthermore, $\underset{\sim}{T}$ will be independent of frequency and need be computed

only once in the frequency response solution and the eigenvalues can be recomputed very simply at each frequency from (51). Assuming that the n wires in Fig. 2b and Fig. 2c are identical, then this technique applies since $\underset{\sim}{U}_n$ does not appear in (54) because the ground plane and circular shield are assumed to be perfect conductors. In this case one only needs to diagonalize $\underset{\sim}{K}$ which can be accomplished with the subroutine EIGEN in SSP [50] since $\underset{\sim}{K}$ is real, symmetric.

3.2 Transmission Lines in Inhomogeneous Media

One of the main problems under consideration in this report is the case of circular wires with circular, dielectric insulation as shown in Fig. 3 which appear in the form of bundles of closely coupled, dielectric-coated wires. These commonly occur in electronic systems in the form of densely packed cable bundles and flat pack or woven cables [51]. The inhomogeneity in the surrounding medium (free space and insulation dielectric) makes the identities in (44) no longer true. However, it is always possible to diagonalize the matrix product $\underset{\sim}{Y}\,\underset{\sim}{Z}$ with a numerically stable transformation, $\underset{\sim}{T}$, when perfect conductors and dielectrics are considered regardless of the entries in $\underset{\sim}{C}$ and $\underset{\sim}{L}$.

First consider the case where losses are neglected, i.e., $\underset{\sim}{G} = \underset{\sim}{R}_c = \underset{\sim}{L}_c = {}_n\underset{\sim}{0}_n$. The matrix product becomes

$$\underset{\sim}{Y}\,\underset{\sim}{Z} = -\omega^2\,\underset{\sim}{C}\,\underset{\sim}{L} \quad . \tag{55}$$

Recall that $\underset{\sim}{L}$ and $\underset{\sim}{C}$ will be real, symmetric and $\underset{\sim}{C}$ will be positive definite even for this inhomogeneous medium case [39]. Since $\underset{\sim}{C}$ is real, symmetric,

then there always exists an nχn real, orthogonal transformation $\underset{\sim}{U}$ such that

$$\underset{\sim}{U}^{-1}\,\underset{\sim}{C}\,\underset{\sim}{U} = \underset{\sim}{D} \tag{56}$$

where $\underset{\sim}{D}$ is an nχn real, diagonal matrix and $\underset{\sim}{U}^{-1} = \underset{\sim}{U}^{t}$ [41, 49]. Furthermore, since $\underset{\sim}{C}$ is positive definite, the eigenvalues of $\underset{\sim}{C}$ which are the elements of the diagonal matrix $\underset{\sim}{D}$ are all positive, real and nonzero. Thus one can quite easily (and meaningfully) form the square root of the matrix $\underset{\sim}{D}$, $\underset{\sim}{D}^{1/2}$, and write

$$\underset{\sim}{D}^{-1/2}\,\underset{\sim}{U}^{-1}\,\underset{\sim}{C}\,\underset{\sim}{U}\,\underset{\sim}{D}^{-1/2}\,\underset{\sim}{D}^{1/2}\,\underset{\sim}{U}^{-1}\,\underset{\sim}{L}\,\underset{\sim}{U}\,\underset{\sim}{D}^{1/2} = \underset{\sim}{D}^{1/2}\,\underset{\sim}{U}^{t}\,\underset{\sim}{L}\,\underset{\sim}{U}\,\underset{\sim}{D}^{1/2} \tag{57}$$

which is real, symmetric. Thus (57) may be diagonalized again by an nχn real, orthogonal transformation, $\underset{\sim}{S}$, such that

$$\underset{\sim}{S}^{t}\,\underset{\sim}{D}^{1/2}\,\underset{\sim}{U}^{t}\,\underset{\sim}{L}\,\underset{\sim}{U}\,\underset{\sim}{D}^{1/2}\,\underset{\sim}{S} = \underset{\sim}{\Lambda}^{2} \tag{58}$$

and one can identify the transformation matrix $\underset{\sim}{T}$ in (21) as

$$\underset{\sim}{T} = \underset{\sim}{U}\,\underset{\sim}{D}^{1/2}\,\underset{\sim}{S} \tag{59}$$

and propagation matrix $\underset{\sim}{\gamma}^{2}$ in (21) becomes

$$\underset{\sim}{\gamma}^{2} = -\underset{\sim}{\omega}^{2}\,\underset{\sim}{\Lambda}^{2}\,. \tag{60}$$

The propagation constants become from (60), $\gamma_i = j\omega\lambda_i$ where $[\underset{\sim}{\Lambda}^{2}]_{ii} = \lambda_i^2$, $[\underset{\sim}{\Lambda}^{2}]_{ij} = 0$, $i \neq j$ and it is a simple matter to verify that

$$\underset{\sim}{T}^{-1} = \underset{\sim}{T}^{t}\,\underset{\sim}{C}^{-1}\,. \tag{61}$$

The matrix chain parameters for this case are given in (32) and [26] and the subroutine NROOT in SSP will again perform this type of reduction [50]. If the real parts of the permittivities of the insulations are independent of frequency (or assumed to be) then this reduction need be performed only once and if the real parts of the permittivities vary significantly with frequency,

one must recompute $\underset{\sim}{T}$ and $\underset{\sim}{\gamma}^2$ (as well as $\underset{\sim}{C}$) at each frequency. In either case, $\underset{\sim}{T}$ will be real-valued and numerically stable.

In the general case, the matrix product $\underset{\sim}{Y}\,\underset{\sim}{Z}$ becomes

$$\underset{\sim}{Y}\,\underset{\sim}{Z} = (\underset{\sim}{G} + j\omega\underset{\sim}{C})\ (\underset{\sim}{R}_c + j\omega\underset{\sim}{L}_c) + (\underset{\sim}{G} + j\omega\underset{\sim}{C})\ (j\omega\underset{\sim}{L}) \quad . \qquad (62)$$

Even if perfect conductors are assumed, i.e., $\underset{\sim}{R}_c = \underset{\sim}{L}_c = {}_n\underset{\sim}{0}_n$, diagonalization of $\underset{\sim}{Y}\,\underset{\sim}{Z}$ would require the diagonalization of the complex matrix $j\omega\underset{\sim}{G}\underset{\sim}{L} - \omega^2\underset{\sim}{C}\underset{\sim}{L}$. However, $\underset{\sim}{G}$ in general bears no simple relationship to $\underset{\sim}{L}$ or $\underset{\sim}{C}$ such as in (45) since the fields associated with conduction current or dipole relaxation losses will be confined to the insulation dielectrics whereas the fields associated with the real parts of the complex, effective permittivities of the dielectrics can fringe into the surrounding free space medium. Thus the diagonalization of $\underset{\sim}{Y}\,\underset{\sim}{Z}$ is not assured a priori. If diagonalization is possible, $\underset{\sim}{T}$ would in general be complex and a function of frequency.

If the dielectrics are assumed to be perfect (no ohmic conductivity or dipole relaxation effects), then assuming all n conductors are identical (including the reference conductor in Fig. 3a) $\underset{\sim}{Y}\,\underset{\sim}{Z}$ becomes for Fig. 3a

$$\underset{\sim}{Y}\,\underset{\sim}{Z} = j\omega(r_c + j\omega\ell_c)\,\underset{\sim}{C}\,(\underset{\sim}{1}_n + \underset{\sim}{U}_n) - \omega^2\,\underset{\sim}{C}\,\underset{\sim}{L} \quad . \qquad (63)$$

For a real, frequency independent transformation, $\underset{\sim}{T}$, which diagonalizes $\underset{\sim}{Y}\,\underset{\sim}{Z}$ to exist, it would be required in general that the same $\underset{\sim}{T}$ diagonalize both $\underset{\sim}{C}\,(\underset{\sim}{1}_n + \underset{\sim}{U}_n)$ and $\underset{\sim}{C}\,\underset{\sim}{L}$. This is, in general, not possible. Even if the reference conductor is assumed lossless, i.e., $\underset{\sim}{U}_n = {}_n\underset{\sim}{0}_n$ in (63) for Fig. 3b and Fig. 3c, the existence of a real, frequency-independent transformation which diagonalizes $\underset{\sim}{Y}\,\underset{\sim}{Z}$ would imply

$$\underset{\sim}{T}^{-1}\,\underset{\sim}{C}\,\underset{\sim}{T} = \underset{\sim}{\Lambda}_1^2 \tag{64a}$$

$$\underset{\sim}{T}^{-1}\,\underset{\sim}{C}\,\underset{\sim}{L}\,\underset{\sim}{T} = \underset{\sim}{\Lambda}_1^2\,\underset{\sim}{T}^{-1}\,\underset{\sim}{L}\,\underset{\sim}{T} = \underset{\sim}{\Lambda}_2^2 \tag{64b}$$

where $\underset{\sim}{\Lambda}_1^2$ and $\underset{\sim}{\Lambda}_2^2$ are $n \times n$ diagonal matrices. This would therefore imply that the same $\underset{\sim}{T}$ would diagonalize both $\underset{\sim}{C}$ and $\underset{\sim}{L}$ and this is generally not possible.

Therefore, the inclusion of losses generally requires that a complex transformation $\underset{\sim}{T}$ be obtained. The existence of a numerically stable transformation is not guaranteed, in general, when losses are included. $\underset{\sim}{T}$ is also a function of frequency which requires that it be recomputed at each frequency which increases the overall computation time.

3.3 Cyclic-Symmetric Matrices

If the n conductors and dielectric insulations are identical and if the cross-sectional structure of the line exhibits certain physical symmetry with respect to each of the n conductors and the reference conductor, then the matrix product $\underset{\sim}{Y}\,\underset{\sim}{Z}$ can be diagonalized a priori with a transformation matrix, $\underset{\sim}{T}$, which although complex, is independent of frequency even when lossy conductors and lossy, inhomogeneous media are considered. For example, if the n conductors are identical with identical dielectrics all of the same thickness, and are equally spaced with respect to each other, on a ring symmetrical about the reference wire or are equally spaced with respect to each other on a ring concentric with the circular-shield reference conductor as shown in Fig. 8, then $\underset{\sim}{Y}\,\underset{\sim}{Z}$ is always diagonalizable by a frequency independent transformation $\underset{\sim}{T}$.

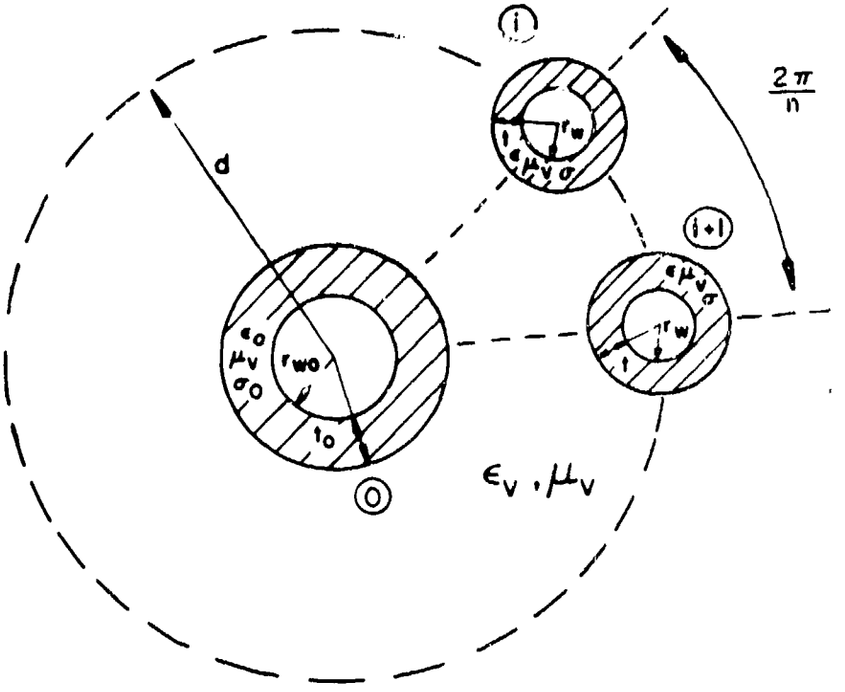

(a)

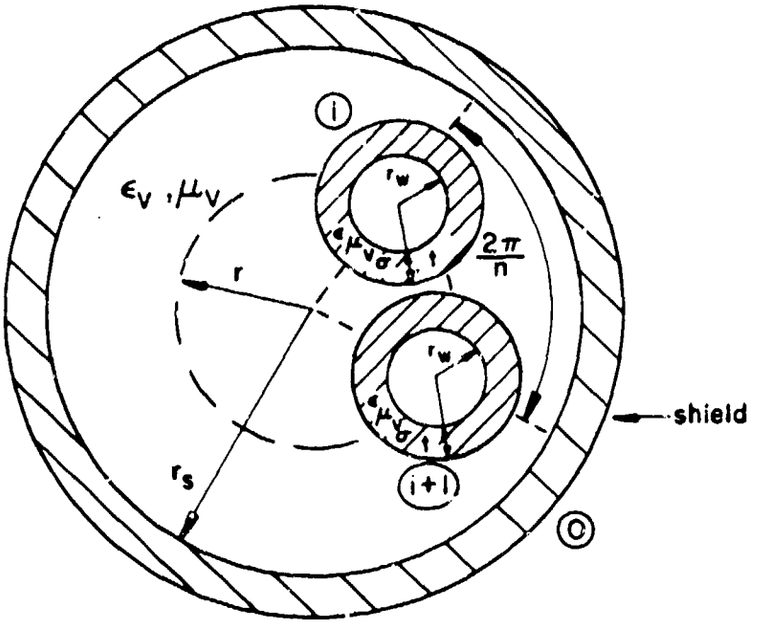

Figure 8. Cyclic-symmetric structures.

For each of the lines in Fig. 8, $\underset{\sim}{Z}$ and $\underset{\sim}{Y}$ will quite obviously be of the form

$$Z = \begin{bmatrix} Z_1 & Z_2 & Z_3 & \cdots & Z_3 & Z_2 \\ Z_2 & Z_1 & Z_2 & Z_3 & & Z_3 \\ Z_3 & Z_2 & \ddots & \ddots & \ddots & \vdots \\ \vdots & \ddots & \ddots & \ddots & \ddots & Z_3 \\ Z_3 & & \ddots & \ddots & Z_1 & Z_2 \\ Z_2 & Z_3 & \cdots & Z_3 & Z_2 & Z_1 \end{bmatrix} \qquad Y = \begin{bmatrix} Y_1 & Y_2 & Y_3 & \cdots & Y_3 & Y_2 \\ Y_2 & Y_1 & Y_2 & Y_3 & & Y_3 \\ Y_3 & Y_2 & \ddots & \ddots & \ddots & \vdots \\ \vdots & \ddots & \ddots & \ddots & \ddots & Y_3 \\ Y_3 & & \ddots & \ddots & Y_1 & Y_2 \\ Y_2 & Y_3 & \cdots & Y_3 & Y_2 & Y_1 \end{bmatrix} \tag{65}$$

where $[\underset{\sim}{Z}]_{ii} \triangleq Z_1$, $[\underset{\sim}{Y}]_{ii} \triangleq Y_1$, $[\underset{\sim}{Z}]_{ij}$, $[\underset{\sim}{Y}]_{ij}$ are defined in (6) and (7). Matrices with this special structure are cyclic-symmetric matrices and the general $n \times n$ cyclic-symmetric matrix, $\underset{\sim}{M}$, is defined by $[\underset{\sim}{M}]_{ij} = M_{|i-j|+1}$ where $M_{j+n} = M_j$, $M_{n+2-j} = M_j$ and indices greater than n and less than 1 are defined by the convention $n+j = j$ and $n+i = i$ [52, 6]. Because of the special structure of the matrices, there always exists a transformation, $\underset{\sim}{T}$, which is independent of frequency and the numerical entries in $\underset{\sim}{Z}$ and $\underset{\sim}{Y}$ which will diagonalize both $\underset{\sim}{Z}$ and $\underset{\sim}{Y}$, i.e., $\underset{\sim}{T}^{-1}\,\underset{\sim}{Y}\,\underset{\sim}{T} = \underset{\sim}{\gamma}^2_{Y}$, $\underset{\sim}{T}^{-1}\,\underset{\sim}{Z}\,\underset{\sim}{T} = \underset{\sim}{\gamma}^2_{Z}$ and $\underset{\sim}{\gamma}^2 = \underset{\sim}{\gamma}^2_{Z}\,\underset{\sim}{\gamma}^2_{Y}$ where $\underset{\sim}{\gamma}^2_{Z}$ and $\underset{\sim}{\gamma}^2_{Y}$ are $n \times n$ diagonal matrices [1, 5, 52, 65]. The elements of $\underset{\sim}{T}$ which diagonalize any cyclic-symmetric matrix of the form in (65) are [5, 52, 65]

$$[\underset{\sim}{T}]_{ij} = \frac{1}{\sqrt{n}} \angle\left(\frac{2\pi}{n}(j-1)(i-1)\right) \tag{66}$$

where a complex number c with magnitude c_m and angle θ_m is written as $c_m \angle\theta_m$. $\underset{\sim}{T}$ is unitary such that $\underset{\sim}{T}^{-1} = \underset{\sim}{T}^*$ and cyclic-symmetric matrices

can be shown to be normal matrices, i.e., $\underset{\sim}{M}\underset{\sim}{M}^* = \underset{\sim}{M}^*\underset{\sim}{M}$, since it can be shown that the product of any two cyclic-symmetric matrices of the same order commute under multiplication [52]. The eigenvalues, of the product of two cyclic-symmetric matrices of the form in (65), $\underset{\sim}{Y}\underset{\sim}{Z}$, can be shown to be [5, 52]

$$\gamma_i^2 = \left\{\sum_{p=1}^{n} [\underset{\sim}{Z}]_{1p} \angle\frac{2\pi}{n}(p-1)\ (i-1)\right\} \left\{\sum_{q=1}^{n} [\underset{\sim}{Y}]_{1q} \angle\frac{2\pi}{n}(q-1)\ (i-1)\right\} \qquad (67)$$

where $[\underset{\sim}{Z}]_{1p}$ and $[\underset{\sim}{Y}]_{1p}$ are the elements in the first row and p-th column of $\underset{\sim}{Z}$ and $\underset{\sim}{Y}$ in (65) respectively, p=1, ---, n.

Thus if the line consists of n identical conductors with identical insulations and thicknesses and exhibits certain cross-sectional symmetry, then the matrix product $\underset{\sim}{Y}\underset{\sim}{Z}$ can always be diagonalized regardless of the numerical entries in $\underset{\sim}{Y}$ and $\underset{\sim}{Z}$ and the transformation matrix is independent of frequency. Neither the transformation matrix $\underset{\sim}{T}$, $\underset{\sim}{T}^{-1}$ nor the eigenvalues need be computed since they are known a priori through (66), (67) and $\underset{\sim}{T}^{-1} = \underset{\sim}{T}^*$.

Cyclic-symmetric matrices are obviously quite desirable from a computational standpoint and have been used in modeling cable bundles under the assumption that the conductors are arranged symmetrically about the axis of an overall shield or occupy all possible positions within the shield randomly [52]. Special cases of cyclic-symmetric matrices are encountered throughout the power transmission literature under the assumption that the power line is balanced or completely transposed and the transformation matrix is often referred to as a symmetrical-component transformation [6, 13].

This method cannot generally be applied when the reference conductor is an infinite ground plane since the special structures of $\underset{\sim}{Y}$ and $\underset{\sim}{Z}$ in (65) will not result unless the system of n wires and the n images used to replace the ground plane possess the required symmetry. However, for the case of a three-conductor line (n=2) consisting of two identical wires both at the same height above a ground plane, i.e., $r_{w1} = r_{w2}$, $t_1 = t_2$, $\epsilon_1 = \epsilon_2$, $\sigma_1 = \sigma_2$, $h_1 = h_2$ in Fig. 2b and Fig. 3b, then $\underset{\sim}{Y}$ and $\underset{\sim}{Z}$ will be cyclic-symmetric regardless of the wire spacing, $d_{1,2}$, or any form of transposition. In this case, the elements of the eigenvectors become real as $T_{11} = 1/\sqrt{2}$, $T_{21} = 1/\sqrt{2}$, $T_{12} = 1/\sqrt{2}$, $T_{22} = -1/\sqrt{2}$ and the eigenvalues are easily shown to be $\gamma_1^2 = (Z + Z_m)(Y + Y_m)$, $\gamma_2^2 = (Z - Z_m)(Y - Y_m)$ where $Z = [\underset{\sim}{Z}]_{11} = [\underset{\sim}{Z}]_{22}$, $Z_m = [\underset{\sim}{Z}]_{12} = [\underset{\sim}{Z}]_{21}$ and $Y = [\underset{\sim}{Y}]_{11} = [\underset{\sim}{Y}]_{22}$, $Y_m = [\underset{\sim}{Y}]_{12} = [\underset{\sim}{Y}]_{21}$.

IV. INCORPORATING THE TERMINATION NETWORKS

Note that in (23) and (25), the only unknowns are the 2n undetermined constants in $\underline{I}^+$ and $\underline{I}^-$. These will be determined by the boundary conditions (termination networks) at $x = 0$ and $x = \ell$ for a line of total length ℓ (see Figure 9). The incorporation of the termination-networks can consume considerable computation time for large numbers of mutually coupled conductors and this necessary step in the total problem solution is generally dismissed as a trivial, straightforward problem. It is straightforward (conceptually) but is certainly not trivial when a large number of mutually coupled conductors are involved.

For two-conductor lines, the terminations (which are assumed to be linear) are represented by Thevenin equivalents as shown in Fig. 6. The terminal equations become

$$V(0) = V_0 - Z_0 I(0) \tag{68a}$$

$$V(\ell) = V_\ell + Z_\ell I(\ell) \tag{68b}$$

where V_0 and V_ℓ are equivalent open-circuit port voltages with respect to the reference conductor.

For multiconductor lines, the termination-networks are similarly considered to be linear n-ports and are characterizable by "Generalized Thevenin Equivalents" as

$$\underline{V}(0) = \underline{V}_0 - \underline{\underline{Z}}_0 \underline{I}(0) \tag{69a}$$

$$\underline{V}(\ell) = \underline{V}_\ell + \underline{\underline{Z}}_\ell \underline{I}(\ell) \tag{69b}$$

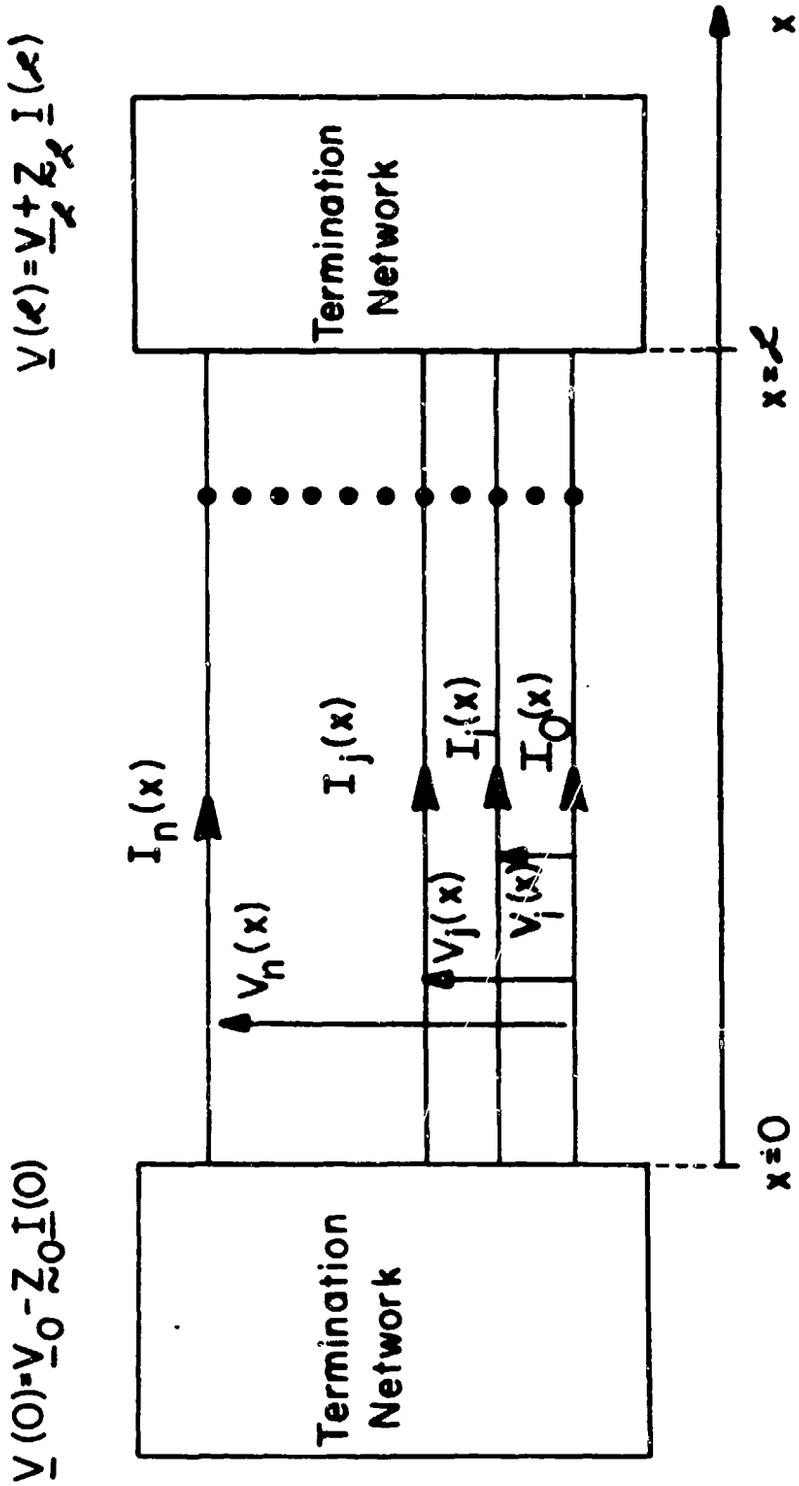

Figure 9. The termination-networks for multiconductor transmission lines.

where $\underline{V}_0$ and $\underline{V}_\ell$ are $n\times 1$ complex-valued vectors of equivalent open-circuit port excitation voltages with respect to the reference conductor and $\underset{\sim}{Z}_0$ and $\underset{\sim}{Z}_\ell$ are $n\times n$ complex-valued, symmetric matrices. The linear n ports can quite obviously be characterized by (69) and $[\underline{V}_0]_i = V_{0i}$, $[\underline{V}_\ell]_i = V_{\ell i}$ as shown in Fig. 10. For arbitrary termination-networks, the entries in (69) can be quite easily obtained by treating $\underline{V}(0)$ and $\underline{V}(\ell)$ as independent voltage sources and writing the loop current equations of the networks. The currents $\underline{I}(0)$ and $\underline{I}(\ell)$ will comprise subsets of the loop currents for the networks and the remaining loop currents can be eliminated to yield (69). If the i-th conductor is connected to the reference conductor only through impedances Z_{0i} and $Z_{\ell i}$, then the entries in $\underset{\sim}{Z}_0$ and $\underset{\sim}{Z}_\ell$ are easily obtained as $[\underset{\sim}{Z}_0]_{ii} = Z_{0i}$, $[\underset{\sim}{Z}_0]_{ij} = 0$, $[\underset{\sim}{Z}_\ell]_{ii} = Z_{\ell i}$, $[\underset{\sim}{Z}_\ell]_{ij} = 0$ for $i, j = 1, \cdots, n$ and $i \neq j$.

Combining (23), (25) and (69) one can obtain straightforwardly [26, 48]

$$\left[\begin{array}{c:c} -\left\{\underset{\sim}{Z}_0\,\underset{\sim}{T} - \underset{\sim}{Y}^{-1}\,\underset{\sim}{T}\,\underset{\sim}{\gamma}\right\} & \left\{\underset{\sim}{Z}_0\,\underset{\sim}{T} + \underset{\sim}{Y}^{-1}\,\underset{\sim}{T}\,\underset{\sim}{\gamma}\right\} \\ \left\{\underset{\sim}{Z}_\ell\,\underset{\sim}{T} + \underset{\sim}{Y}^{-1}\,\underset{\sim}{T}\,\underset{\sim}{\gamma}\right\} e^{\underset{\sim}{\gamma}\ell} & -\left\{\underset{\sim}{Z}_\ell\,\underset{\sim}{T} - \underset{\sim}{Y}^{-1}\,\underset{\sim}{T}\,\underset{\sim}{\gamma}\right\} e^{-\underset{\sim}{\gamma}\ell} \end{array}\right] \left[\begin{array}{c} \underline{I}^- \\ \underline{I}^+ \end{array}\right] = \left[\begin{array}{c} \underline{V}_0 \\ \underline{V}_\ell \end{array}\right]. \tag{70}$$

Since $\underset{\sim}{T}^{-1}\,\underset{\sim}{Y}\,\underset{\sim}{Z}\,\underset{\sim}{T} = \underset{\sim}{\gamma}^2$, then $\underset{\sim}{Y}^{-1}\,\underset{\sim}{T}\,\underset{\sim}{\gamma}$ in (70) can be replaced by $\underset{\sim}{Z}\,\underset{\sim}{T}\,\underset{\sim}{\gamma}^{-1}$. Once this set of $2n$ equations in the $2n$ unknowns, $\underline{I}^+$ and $\underline{I}^-$, are solved (by Gaussian elimination and back substitution, for example, [49]) then the response, $\underline{V}(x)$ and $\underline{I}(x)$, at any point on the line can be determined from (23) and (25). For two-conductor lines, the matrices and vectors in (70) become scalars and $\underset{\sim}{T}$ becomes 1 (see (13) and (14)).

It is also possible to indirectly solve for the response via the matrix chain parameters. With $x = \ell$ and $x_0 = 0$ in (31) and (32) and using (69) one

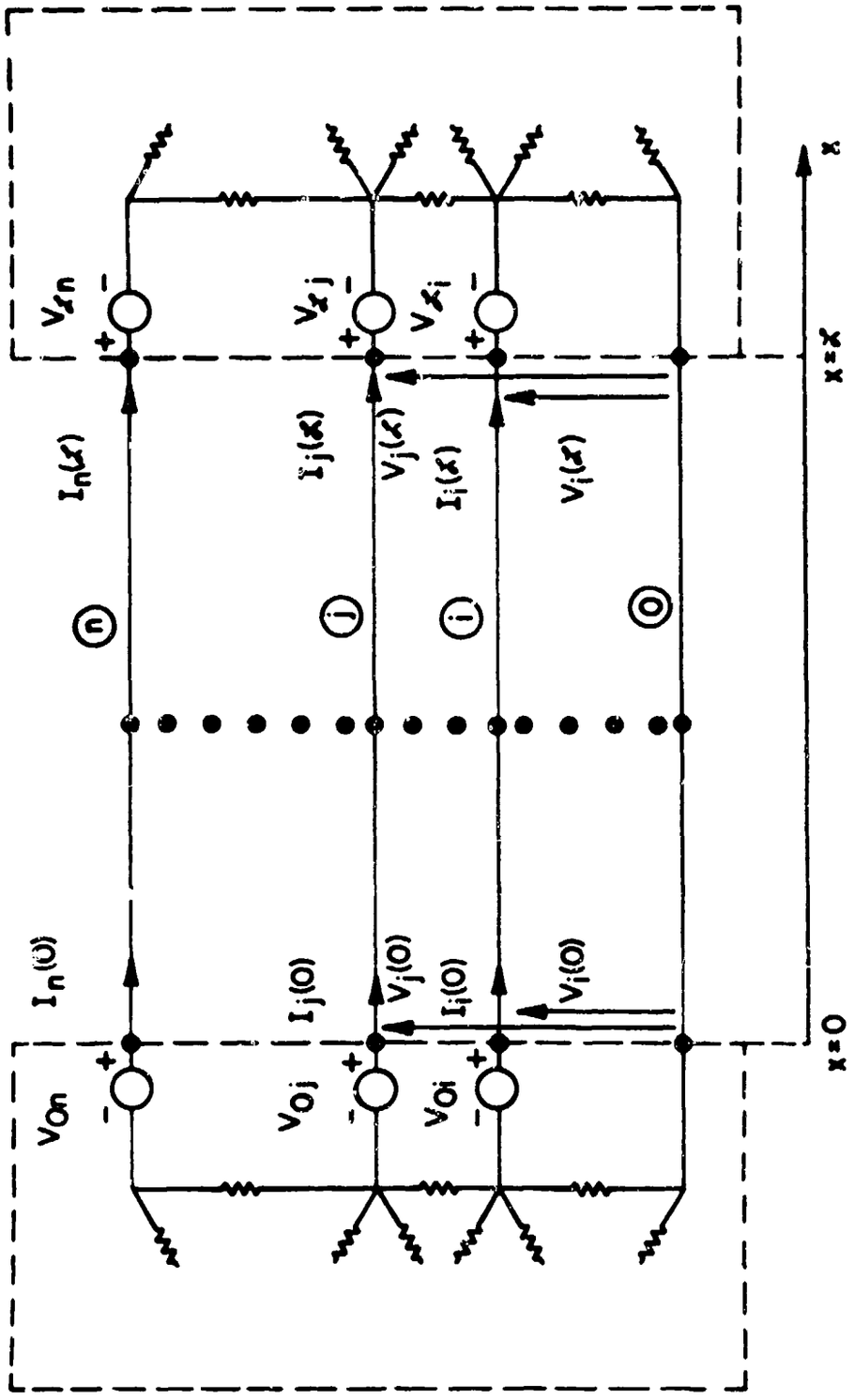

Figure 10. The termination-networks for multiconductor transmission lines.

can straightforwardly obtain [26, 48]

$$[\underset{\sim}{Z}_{\mathcal{L}}\underset{\sim}{\Phi}_{22}(\mathcal{L}) - \underset{\sim}{Z}_{\mathcal{L}}\underset{\sim}{\Phi}_{21}(\mathcal{L})\underset{\sim}{Z}_0 - \underset{\sim}{\Phi}_{12}(\mathcal{L}) + \underset{\sim}{\Phi}_{11}(\mathcal{L})\underset{\sim}{Z}_0]\underline{I}(0) = [\underset{\sim}{\Phi}_{11}(\mathcal{L}) - \underset{\sim}{Z}_{\mathcal{L}}\underset{\sim}{\Phi}_{21}(\mathcal{L})]\underline{V}_0 - \underline{V}_{\mathcal{L}} \quad (71a)$$

$$\underline{I}(\mathcal{L}) = \underset{\sim}{\Phi}_{21}(\mathcal{L})\underline{V}_0 + [\underset{\sim}{\Phi}_{22}(\mathcal{L}) - \underset{\sim}{\Phi}_{21}(\mathcal{L})\underset{\sim}{Z}_0]\underline{I}(0) \quad (71b)$$

where $\underset{\sim}{\Phi}(\mathcal{L}, 0) \triangleq \underset{\sim}{\Phi}(\mathcal{L})$. $\underline{V}(x)$ and $\underline{I}(x)$ can be obtained for any x from (8) with $\underline{I}(0)$ from the solution of (71a) and $\underline{V}(0)$ determined from (69a). Here one need only solve n equations in n unknowns, equation (71a), as opposed to 2n equations in 2n unknowns in (70). However, certain matrix multiplications are required in forming both (70) and (71).

Using the matrix chain parameter identities in (40), it can be shown that (71) may be written in an alternate form [18]

$$\begin{bmatrix} \{\underset{\sim}{\Phi}_{21}(\mathcal{L})\underset{\sim}{Z}_0 - \underset{\sim}{\Phi}_{22}(\mathcal{L})\} & \underset{\sim}{1}_n \\ \underset{\sim}{1}_n & \{\underset{\sim}{\Phi}_{21}(\mathcal{L})\underset{\sim}{Z}_{\mathcal{L}} - \underset{\sim}{\Phi}_{22}(\mathcal{L})\} \end{bmatrix} \begin{bmatrix} \underline{I}(0) \\ \underline{I}(\mathcal{L}) \end{bmatrix} = \begin{bmatrix} \underset{\sim}{\Phi}_{21}(\mathcal{L})\underline{V}_0 \\ -\underset{\sim}{\Phi}_{21}(\mathcal{L})\underline{V}_{\mathcal{L}} \end{bmatrix} \quad (72)$$

which has a highly sparse (large number of zero elements) coefficient matrix with $2(n^2 - n)$ of the $4n^2$ elements identically zero. Equation (72) can also be solved explicitly for $\underline{I}(0)$ and $\underline{I}(\mathcal{L})$ as [18]

$$[\underset{\sim}{1}_n - \{\underset{\sim}{\Phi}_{21}(\mathcal{L})\underset{\sim}{Z}_{\mathcal{L}} - \underset{\sim}{\Phi}_{22}(\mathcal{L})\}\{\underset{\sim}{\Phi}_{21}(\mathcal{L})\underset{\sim}{Z}_0 - \underset{\sim}{\Phi}_{22}(\mathcal{L})\}]\underline{I}(0) = -\underset{\sim}{\Phi}_{21}(\mathcal{L})\underline{V}_{\mathcal{L}} - \{\underset{\sim}{\Phi}_{21}(\mathcal{L})\underset{\sim}{Z}_{\mathcal{L}} - \underset{\sim}{\Phi}_{22}(\mathcal{L})\}\underset{\sim}{\Phi}_{21}(\mathcal{L})\underline{V}_0 \quad (73a)$$

$$\underline{I}(\mathcal{L}) = -\{\underset{\sim}{\Phi}_{21}(\mathcal{L})\underset{\sim}{Z}_0 - \underset{\sim}{\Phi}_{22}(\mathcal{L})\}\underline{I}(0) + \underset{\sim}{\Phi}_{21}(\mathcal{L})\underline{V}_0 \quad . \quad (73b)$$

The advantage of the formulation in (73) as opposed to (71) is that only two of the matrix chain parameters, $\underset{\sim}{\Phi}_{21}$ and $\underset{\sim}{\Phi}_{22}$, need be determined in solving for $\underline{I}(0)$ and $\underline{I}(\mathcal{L})$ via (73) (see (32)).

The most efficient method of solving n linear, algebraic equations in n unknowns is Gaussian elimination with back substitution (LU decomposition)

which requires $(n^3/3 + n^2 - n/3)$ operations (multiplications and divisions) or on the order of $n^3/3$ for large n [49]. Thus solving (70) instead of (71a) or (73a) requires on the order of $(2n)^3/3$ or 8 times the number of operations and the complete solution of the problem requires, at a minimum, the solution of n complex equations in n unknowns. The impact of this requirement on the overall solution times for large cable bundles can be illustrated as follows. The time required to solve 50 complex equations with a standard Gaussian elimination subroutine with full pivoting (DGELG in SSP [50] which was converted for complex arithmetic) was 12.6 seconds on an IBM 360/65 computer. So if it is required to solve for 100 frequencies, then the overall computation time would be, at a minimum, on the order of 21 minutes. It is not uncommon to find 100 conductors in cable bundles on modern avionics systems and since the number of operations required increases on the order of n^3, then solutions for 100 conductors and 100 frequencies would require, at a minimum, 2.8 hours! Of course, additional time will be required for matrix multiplications (as well as the computation of $\underset{\sim}{Y}$ and $\underset{\sim}{Z}$ and diagonalization of $\underset{\sim}{Y}\underset{\sim}{Z}$) as indicated in (70), (71), (72) and (73). This could be quite substantial since n^3 multiplications are required to multiply two "full" $n \chi n$ matrices which is precisely the number of operations required to invert an $n \chi n$ matrix which is "full" [49].

Using the matrix chain parameter formulation in (71) and (73) has an additional advantage over (70). It allows a straightforward incorporation of incident electromagnetic fields into the solution. Consider (4) and (8) where

the effects of an incident field are included as distributed sources along the line, $\underline{V}_s(x)$ and $\underline{I}_s(x)$. From (8) and (31), define equivalent sources

$$\hat{\underline{V}}_s(\mathcal{L}) = \int_0^{\mathcal{L}} \left\{ \underline{\Phi}_{11}(\mathcal{L}, \hat{x})\, \underline{V}_s(\hat{x}) + \underline{\Phi}_{12}(\mathcal{L}, \hat{x})\, \underline{I}_s(\hat{x}) \right\} d\hat{x} \tag{74a}$$

$$\hat{\underline{I}}_s(\mathcal{L}) = \int_0^{\mathcal{L}} \left\{ \underline{\Phi}_{21}(\mathcal{L}, \hat{x})\, \underline{V}_s(\hat{x}) + \underline{\Phi}_{22}(\mathcal{L}, \hat{x})\, \underline{I}_s(\hat{x}) \right\} d\hat{x} \quad . \tag{74b}$$

One can modify (71) and (73) to include these sources by simply adding $\hat{\underline{I}}_s(\mathcal{L})$ to the right-hand side of (71b) and (73b) and replacing $\underline{V}_{\mathcal{L}}$ with $\underline{V}_{\mathcal{L}} - \hat{\underline{V}}_s(\mathcal{L}) + \underline{Z}_{\mathcal{L}}\, \hat{\underline{I}}_s(\mathcal{L})$ on the right-hand side of (71a) and (73a). This is quite obvious since (8) shows that for $x = \mathcal{L}$ and $x_0 = 0$, $\underline{I}(\mathcal{L})$ is increased by $\hat{\underline{I}}_s(\mathcal{L})$ and $\underline{V}(\mathcal{L})$ is to be increased by $\hat{\underline{V}}_s(\mathcal{L})$ over the case without incident field illumination. From the boundary conditions (69b), $\underline{V}_{\mathcal{L}} = \underline{V}(\mathcal{L}) - \underline{Z}_{\mathcal{L}}\, \underline{I}(\mathcal{L})$, then $\underline{V}_{\mathcal{L}}$ on the right-hand side of (71a) and (73a) is to be decreased by $\hat{\underline{V}}_s(\mathcal{L}) - \underline{Z}_{\mathcal{L}}\, \hat{\underline{I}}_s(\mathcal{L})$ and $\underline{I}(\mathcal{L})$ is to be increased by $\hat{\underline{I}}_s(\mathcal{L})$ in (71b) and (73b). Thus equations (71) and (73) are quite easily modified to consider incident fields and the final equations become [26]

$$\begin{aligned} \left[\underline{Z}_{\mathcal{L}}\, \underline{\Phi}_{22}(\mathcal{L}) - \underline{Z}_{\mathcal{L}}\, \underline{\Phi}_{21}(\mathcal{L})\, \underline{Z}_0 - \underline{\Phi}_{12}(\mathcal{L}) + \underline{\Phi}_{11}(\mathcal{L})\, \underline{Z}_0 \right] \underline{I}(0) = \\ \left[\underline{\Phi}_{11}(\mathcal{L}) - \underline{Z}_{\mathcal{L}}\, \underline{\Phi}_{21}(\mathcal{L}) \right] \underline{V}_0 - \underline{V}_{\mathcal{L}} \\ + \hat{\underline{V}}_s(\mathcal{L}) - \underline{Z}_{\mathcal{L}}\, \hat{\underline{I}}_s(\mathcal{L}) \end{aligned} \tag{75a}$$

$$\underline{I}(\mathcal{L}) = \underline{\Phi}_{21}(\mathcal{L})\, \underline{V}_0 + \left[\underline{\Phi}_{22}(\mathcal{L}) - \underline{\Phi}_{21}(\mathcal{L})\, \underline{Z}_0 \right] \underline{I}(0) + \hat{\underline{I}}_s(\mathcal{L}) \tag{75b}$$

or [18]

$$\begin{aligned} \left[\underline{1}_n - \left\{ \underline{\Phi}_{21}(\mathcal{L})\, \underline{Z}_{\mathcal{L}} - \underline{\Phi}_{22}(\mathcal{L}) \right\} \left\{ \underline{\Phi}_{21}(\mathcal{L})\, \underline{Z}_0 - \underline{\Phi}_{22}(\mathcal{L}) \right\} \right] \underline{I}(0) = - \underline{\Phi}_{21}(\mathcal{L})\, \underline{V}_{\mathcal{L}} \\ - \left\{ \underline{\Phi}_{21}(\mathcal{L})\, \underline{Z}_{\mathcal{L}} - \underline{\Phi}_{22}(\mathcal{L}) \right\} \underline{\Phi}_{21}(\mathcal{L})\, \underline{V}_0 \end{aligned} \tag{76a}$$

$$+ \underset{\sim}{\Phi}_{21}(\mathcal{L})\, \hat{\underline{V}}_s(\mathcal{L}) - \underset{\sim}{\Phi}_{21}(\mathcal{L})\, \underset{\sim}{Z}_{\mathcal{L}}\, \hat{\underline{I}}_s(\mathcal{L})$$

$$\underline{I}(\mathcal{L}) = \underset{\sim}{\Phi}_{21}(\mathcal{L})\, \underline{V}_0 + [\underset{\sim}{\Phi}_{22}(\mathcal{L}) - \underset{\sim}{\Phi}_{21}(\mathcal{L})\, \underset{\sim}{Z}_0]\, \underline{I}(0) + \hat{\underline{I}}_s(\mathcal{L}) \quad . \tag{76b}$$

A more detailed discussion of efficient incorporation of the boundary conditions is given in [26].

The equations in (75) become particularly simple for the multiconductor line in Fig. 2a consisting of (n+1) perfectly-conducting wires in free space illuminated by an incident electromagnetic field. It is shown in Appendix C that (75) reduces for the case of Fig. 2a with incident field illumination to

$$\begin{aligned}[\cos(\beta\mathcal{L})\, \{\underset{\sim}{Z}_0 + \underset{\sim}{Z}_{\mathcal{L}}\} + j\sin(\beta\mathcal{L})\, \{\underset{\sim}{Z}_C + \underset{\sim}{Z}_{\mathcal{L}}\, \underset{\sim}{Z}_C^{-1}\, \underset{\sim}{Z}_0\}]\, \underline{I}(0) = \\ - \underline{V}_{\mathcal{L}} + [j\sin(\beta\mathcal{L})\, \underset{\sim}{Z}_{\mathcal{L}}\, \underset{\sim}{Z}_C^{-1} + \cos(\beta\mathcal{L})\, \underset{\sim}{1}_n]\, \underline{V}_0 \\ + \int_0^{\mathcal{L}} \{[\cos(\beta(\mathcal{L}-\hat{x}))\, \underset{\sim}{1}_n + j\sin(\beta(\mathcal{L}-\hat{x}))\, \underset{\sim}{Z}_{\mathcal{L}}\, \underset{\sim}{Z}_C^{-1}]\, \underline{E}_{\ell}^{(inc)}(\hat{x})\}\, d\hat{x} \\ - \underline{E}_t^{(inc)}(\mathcal{L}) + \{[\cos(\beta\mathcal{L})\, \underset{\sim}{1}_n + j\sin(\beta\mathcal{L})\, \underset{\sim}{Z}_{\mathcal{L}}\, \underset{\sim}{Z}_C^{-1}]\, \underline{E}_t^{(inc)}(0)\}\end{aligned} \tag{77a}$$

$$\begin{aligned}I(\mathcal{L}) = - j\sin(\beta\mathcal{L})\, \underset{\sim}{Z}_C^{-1}\, \underline{V}_0 + [\cos(\beta\mathcal{L})\, \underset{\sim}{1}_n + j\sin(\beta\mathcal{L})\, \underset{\sim}{Z}_C^{-1}\, \underset{\sim}{Z}_0]\, \underline{I}(0) \\ - j\, \underset{\sim}{Z}_C^{-1} \int_0^{\mathcal{L}} \{\sin(\beta(\mathcal{L}-\hat{x}))\, \underline{E}_{\ell}^{(inc)}(\hat{x})\}\, d\hat{x} \\ - j\, \underset{\sim}{Z}_C^{-1}\, \{\sin(\beta\mathcal{L})\, \underline{E}_t^{(inc)}(0)\}\end{aligned} \tag{77b}$$

where $\underline{E}_{\ell}^{(inc)}(x)$, $\underline{E}_t^{(inc)}(\mathcal{L})$ and $\underline{E}_t^{(inc)}(0)$ are $n\times 1$ column vectors with the entries in the i-th rows given by

$$[\underline{E}_{\ell}^{(inc)}(x)]_i = E_{\ell_i}^{(inc)}(d_{i0},\, x) - E_{\ell_i}^{(inc)}(0, x) \tag{77c}$$

$$[\underline{E}_t^{(inc)}(\mathcal{L})]_i = \int_0^{d_{i0}} E_{t_i}^{(inc)}(\xi_i,\, \mathcal{L})\, d\xi_i \tag{77d}$$

$$[\underset{\sim}{E}_t^{(inc)}(0)]_i = \int_0^{d_{i0}} E_{t_i}^{(inc)}(\xi_i, 0)\, d\xi_i \qquad (77e)$$

for i=1,---,n. $E_{\ell_i}^{(inc)}(d_{i0}, x)$ and $E_{\ell_i}^{(inc)}(0, x)$ are the components of the incident electric field intensity vector in the longitudinal (x) direction along the axis of wire i and wire 0 respectively. The terms $E_{t_i}^{(inc)}(\xi_i, 0)$ and $E_{t_i}^{(inc)}(\xi_i, \ell)$ are the transverse components (lying in the y, z plane) of the incident electric field intensity vector at $x = 0$ and $x = \ell$ respectively along the contour ξ_i between wire i and wire 0. The contour ξ_i is a straight-line path between wire i and wire 0 and perpendicular to these wires. The entries β and $\underset{\sim}{Z}_C$ are the wave number and characteristic-impedance matrix respectively with $\beta = 2\pi/\lambda$, $\lambda = v/f$, $v = 1/\sqrt{u_v \epsilon_v}$ and $\underset{\sim}{Z}_C = v\underset{\sim}{L}$. The corresponding solution for Fig. 2b is also discussed in Appendix C.

4.1 Lumped-Circuit Iterative Approximations

In deriving (4), "electrically short" Δx sections of the line were considered and since the line was assumed to be uniform, all Δx sections will be identical. Requiring that the Δx sections be "electrically short" for all frequencies, the transmission line equations in (4) are obtained in the limit as $\Delta x \to 0$. Alternately, one can construct lumped-circuit models for the line consisting of N identical sections of length ℓ/N so that each of the sections would in itself be "electrically short", e.g., the section would be no more than, for example, 1/10 of a wavelength long for the frequency under consideration. Note that since ℓ/N is assumed to be "electrically short" and the cross-sectional dimensions of the line are assumed to be "electri-

cally small" so that transmission line theory applies, then a lumped-circuit representation of this portion of the line is valid. Perhaps the more common models of the transmission line are the lumped-circuit iterative approximations which use this philosophy. Models are shown for (n+1)-conductor lines in Figure 11 as the lumped Γ model, lumped $\urcorner$ model, lumped Pi (π) model and lumped Tee model. The lumped $\urcorner$ section is similar to the circuit in Figure 7 but with Δx replaced by ℓ/N. The lumped Γ section is the opposite, i.e., the capacitance and conductance elements appearing at the end of the lumped $\urcorner$ section appear at the beginning of the lumped Γ section. The lumped Pi section is similar to the lumped $\urcorner$ section but has half the values of the capacitance and conductance parameters placed at the beginning and at the end of the section. The lumped Tee section is again similar to the lumped $\urcorner$ section but has half the values of resistance and inductance (self and mutual) elements placed at the beginning and at the end of the section. The lumped Γ model has been used in the program STRAP [36]; the lumped Pi model has been used in the program IVEMCAP [34], and lumped Pi and Tee models have been used in power transmission line studies [9].

The $2n \times 2n$ chain parameter matrix of a section of line of length ℓ/N characterized by any of the lumped iterative approximations can easily be shown in terms of $\underset{\sim}{Z}$ and $\underset{\sim}{Y}$ to be (see Appendix D)

$$\underset{\sim}{\Phi}_k = \begin{bmatrix} \{\underset{\sim}{1}_n\} & \{-\underset{\sim}{Z}(\ell/N)\} \\ \{-\underset{\sim}{Y}(\ell/N)\} & \{\underset{\sim}{1}_n + \underset{\sim}{Y}\,\underset{\sim}{Z}(\ell/N)^2\} \end{bmatrix} \text{(Lumped}\urcorner\text{)} \qquad (78a)$$

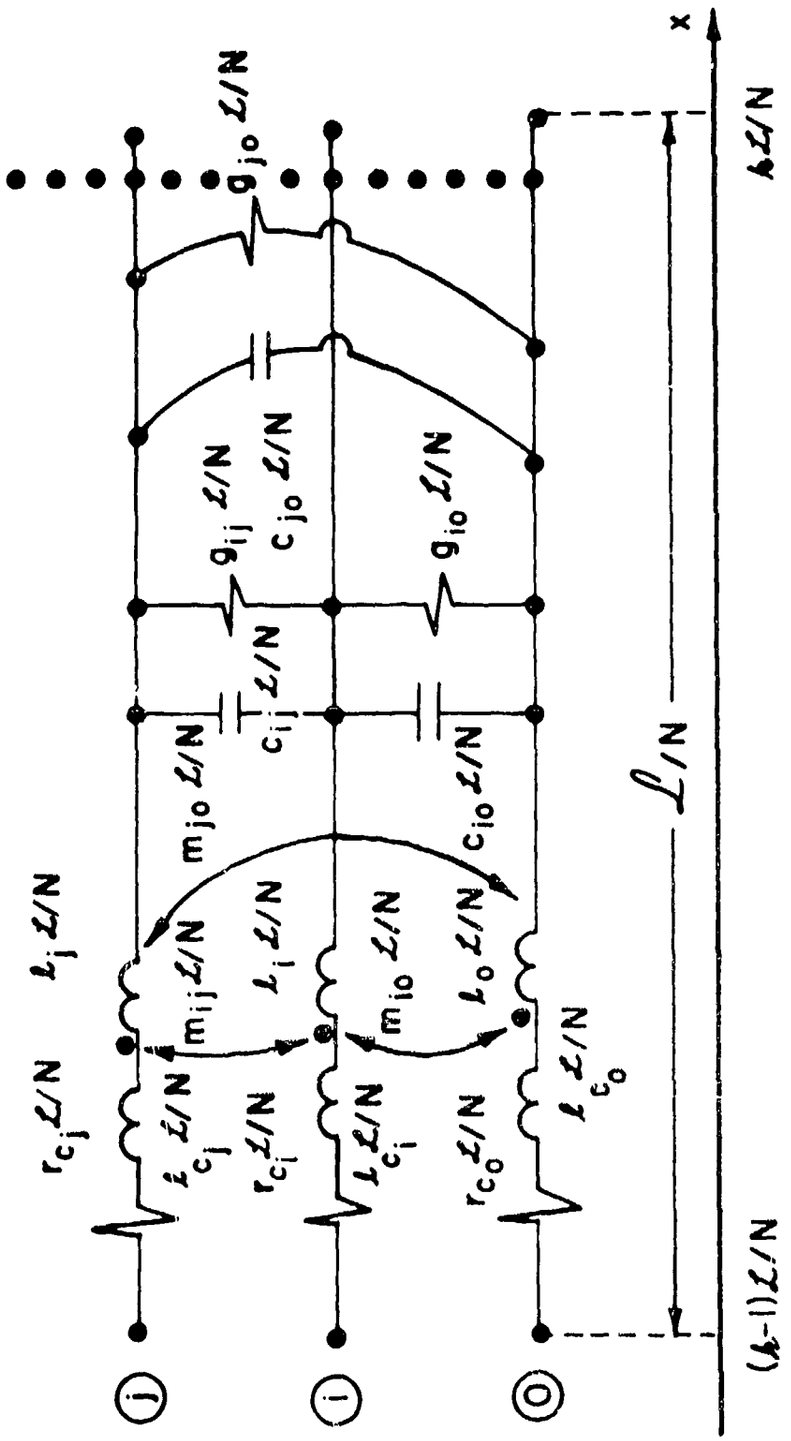

(a) The lumped ⌐ equivalent circuit.

Figure 11. Lumped-circuit iterative models of multiconductor transmission lines (cont.).

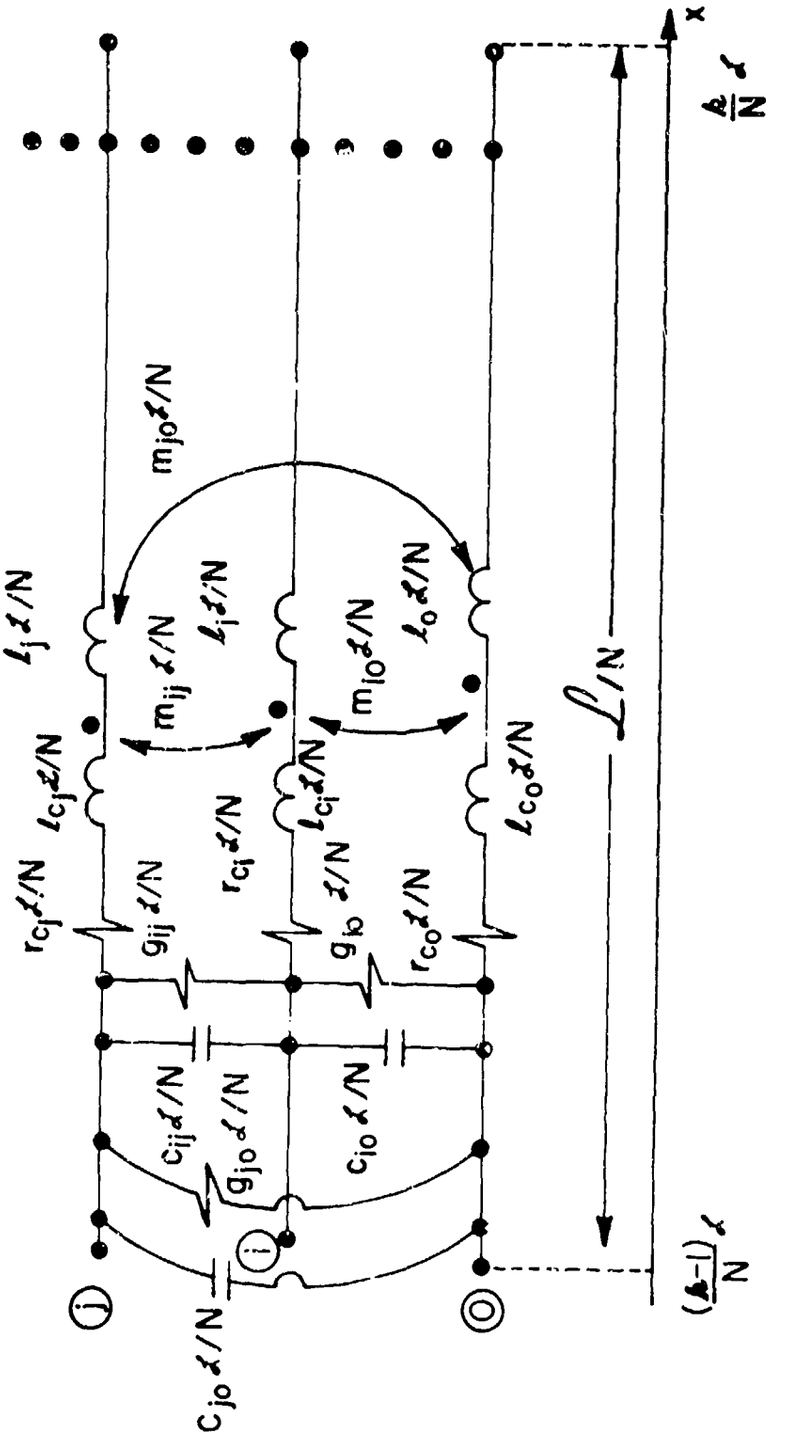

(b) The lumped Γ equivalent circuit.

Figure 11. Lumped-circuit iterative models of multiconductor transmission lines (cont.).

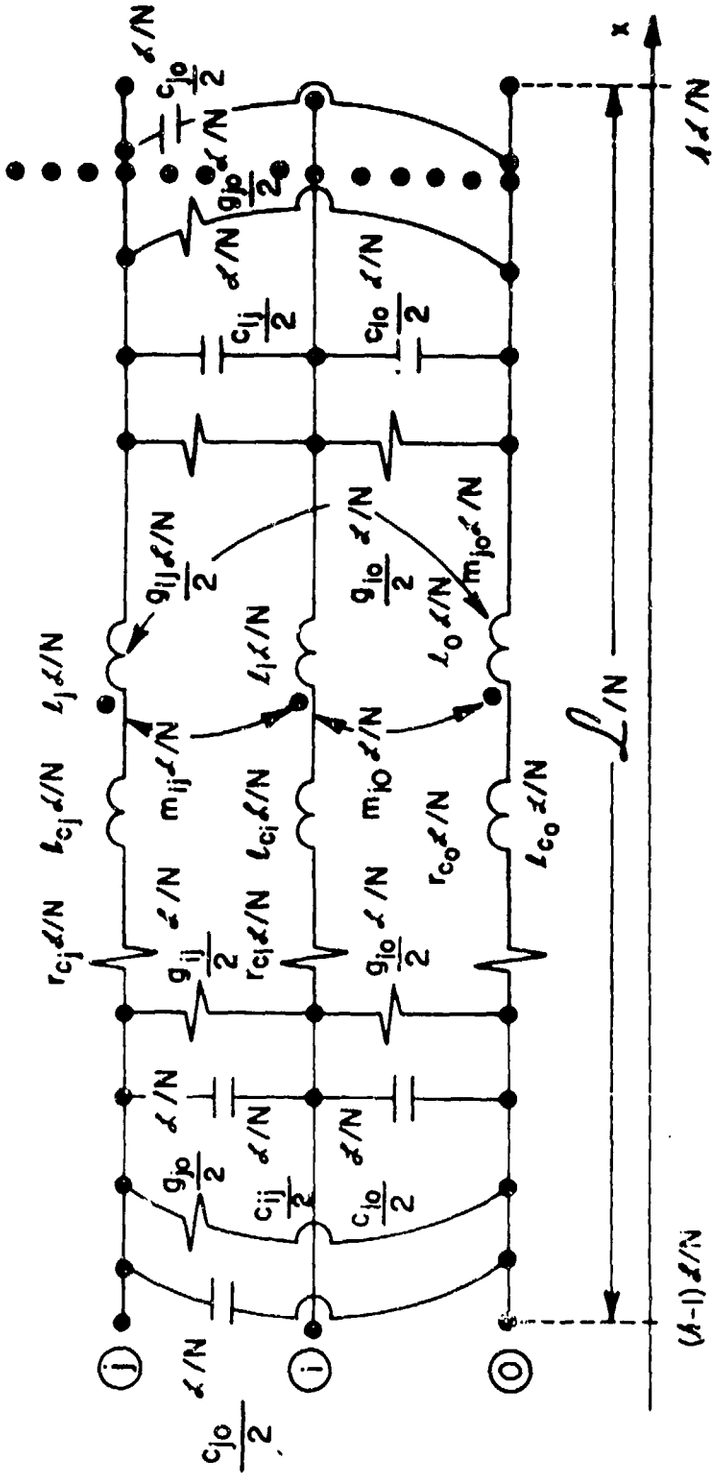

(c) The lumped Pi equivalent circuit.

Figure 11. Lumped-circuit iterative models of multiconductor transmission lines (cont.).

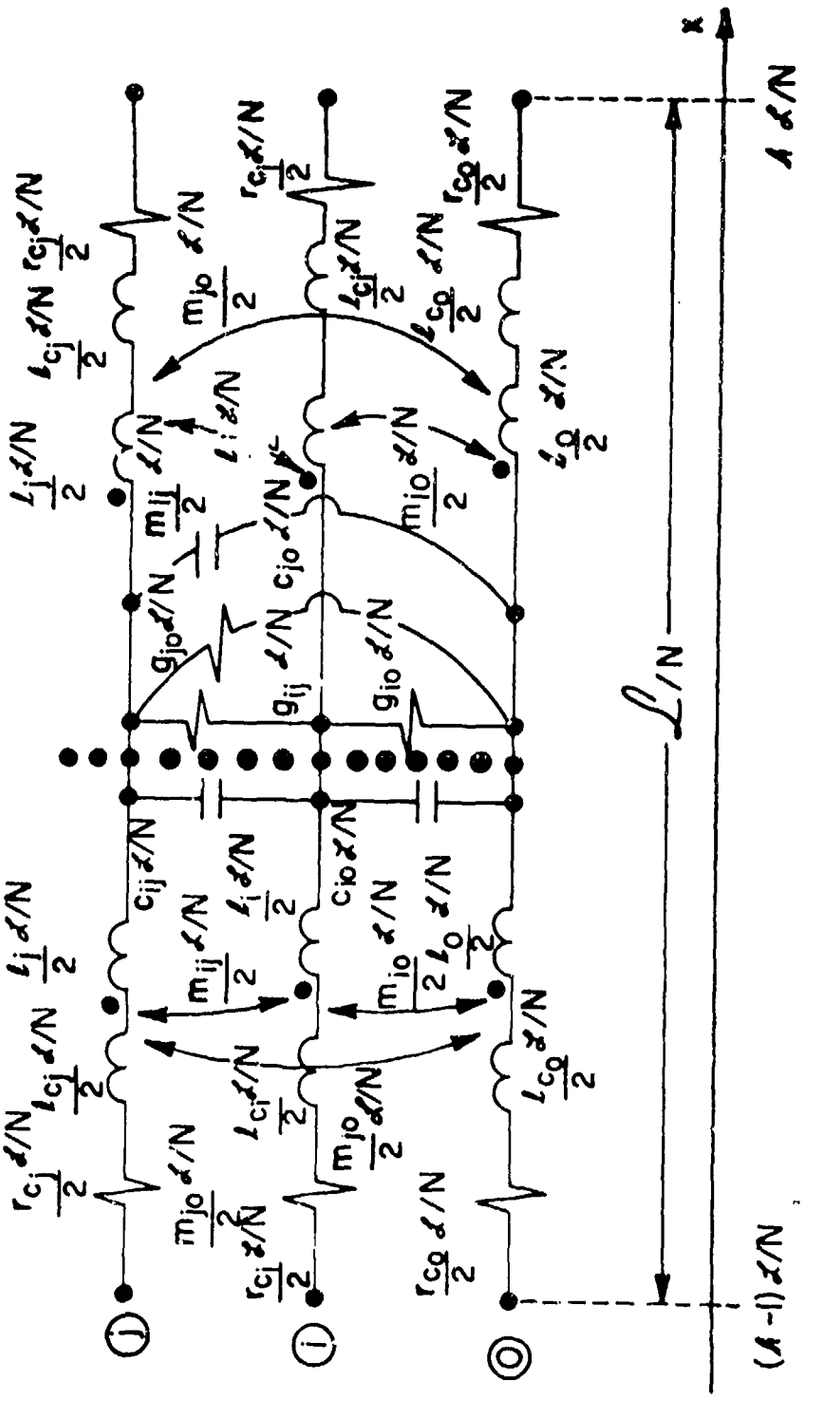

(d) The lumped Tee equivalent circuit.

Figure 11. Lumped-circuit iterative models of multiconductor transmission lines.

$$\underset{\sim}{\Phi}_k = \begin{bmatrix} \left\{\underset{\sim}{1}_n + \underset{\sim}{Z}\,\underset{\sim}{Y}(\mathcal{L}/N)^2\right\} & \left\{-\underset{\sim}{Z}(\mathcal{L}/N)\right\} \\ \left\{-\underset{\sim}{Y}(\mathcal{L}/N)\right\} & \left\{\underset{\sim}{1}_n\right\} \end{bmatrix} \quad \text{(Lumped } \Gamma\text{)} \qquad (78b)$$

$$\underset{\sim}{\Phi}_k = \begin{bmatrix} \left\{\underset{\sim}{1}_n + 1/2\ \underset{\sim}{Z}\,\underset{\sim}{Y}(\mathcal{L}/N)^2\right\} & \left\{-\underset{\sim}{Z}(\mathcal{L}/N)\right\} \\ \left\{-\underset{\sim}{Y}(\mathcal{L}/N) - 1/4\ \underset{\sim}{Y}\,\underset{\sim}{Z}\,\underset{\sim}{Y}(\mathcal{L}/N)^3\right\} & \left\{\underset{\sim}{1}_n + 1/2\ \underset{\sim}{Y}\,\underset{\sim}{Z}(\mathcal{L}/N)^2\right\} \end{bmatrix} \quad \text{(Lumped Pi)} \quad (78c)$$

$$\underset{\sim}{\Phi}_k = \begin{bmatrix} \left\{\underset{\sim}{1}_n + 1/2\ \underset{\sim}{Z}\,\underset{\sim}{Y}(\mathcal{L}/N)^2\right\} & \left\{-\underset{\sim}{Z}(\mathcal{L}/N) - 1/4\ \underset{\sim}{Z}\,\underset{\sim}{Y}\,\underset{\sim}{Z}(\mathcal{L}/N)^3\right\} \\ \left\{-\underset{\sim}{Y}(\mathcal{L}/N)\right\} & \left\{\underset{\sim}{1}_n + 1/2\ \underset{\sim}{Y}\,\underset{\sim}{Z}(\mathcal{L}/N)^2\right\} \end{bmatrix} \quad \text{(Lumped Tee)} \quad (78d)$$

These models are referred to as lumped-circuit iterative approximations since the overall matrix chain parameters for the line of length $\mathcal{L}$ and N sections (all of the same type) is quite obviously $\underset{\sim}{\Phi} = (\underset{\sim}{\Phi}_k)^N$, i.e., multiply the chain parameter matrices in (78) together N times, since the chain parameters for each section only relate the voltages and currents at the two ends of each section as

$$\begin{bmatrix} \underline{V}\left(\frac{k}{N}\mathcal{L}\right) \\ \underline{I}\left(\frac{k}{N}\mathcal{L}\right) \end{bmatrix} = \underbrace{\begin{bmatrix} \underset{\sim}{\Phi}_{k11} & \underset{\sim}{\Phi}_{k12} \\ \underset{\sim}{\Phi}_{k21} & \underset{\sim}{\Phi}_{k22} \end{bmatrix}}_{\underset{\sim}{\Phi}_k} \begin{bmatrix} \underline{V}\left(\frac{k-1}{N}\mathcal{L}\right) \\ \underline{I}\left(\frac{k-1}{N}\mathcal{L}\right) \end{bmatrix} \qquad (79)$$

where each submatrix $\underset{\sim}{\Phi}_{k11}$, $\underset{\sim}{\Phi}_{k12}$, $\underset{\sim}{\Phi}_{k21}$, $\underset{\sim}{\Phi}_{k22}$ is $n \times n$ and corresponds to submatrices in (78) and k = 1, 2, ---, N.

Generally an N section lumped-circuit iterative approximation is solved (the boundary conditions or termination-networks are incorporated) as strictly a lumped, electrical circuits problem with circuit analysis programs such as ECAP, SCEPTRE, TRAFFIC, etc. [53]. The node-voltage equations

or loop-current equations of the network of N sections with termination-networks are written and solved via these programs. It is possible to write, for example, the node-voltage equations directly from the matrix chain parameters without employing a circuit diagram. Using (69) and (79), one can straightforwardly obtain (see Appendix D)

$$\begin{bmatrix} \underset{\sim}{Y}_1 & \underset{\sim}{1}_n & \underset{\sim}{0}_n & \cdots & \underset{\sim}{0}_n \\ \underset{\sim}{1}_n & \underset{\sim}{\hat{Y}} & \underset{\sim}{1}_n & \underset{\sim}{0}_n & \vdots \\ \underset{\sim}{0}_n & \underset{\sim}{1}_n & \ddots & \ddots & \underset{\sim}{0}_n \\ \vdots & \underset{\sim}{0}_n & \ddots & \underset{\sim}{\hat{Y}} & \underset{\sim}{1}_n \\ \underset{\sim}{0}_n & \cdots & \underset{\sim}{0}_n & \underset{\sim}{1}_n & \underset{\sim}{Y}_{N+1} \end{bmatrix} \begin{bmatrix} \underline{V}(0) \\ \underline{V}(\mathcal{L}/N) \\ \vdots \\ \underline{V}\left(\frac{N-1}{N}\mathcal{L}\right) \\ \underline{V}(\mathcal{L}) \end{bmatrix} = \begin{bmatrix} \underset{\sim}{\Phi}_{k12}\ \underset{\sim}{Y}_0 \underline{V}_0 \\ \underset{\sim}{0}_n \underline{1} \\ \vdots \\ \underset{\sim}{0}_n \underline{1} \\ \underset{\sim}{\Phi}_{k12}\ \underset{\sim}{Y}_{\mathcal{L}} \underline{V}_{\mathcal{L}} \end{bmatrix} \tag{80}$$

where

$$\underset{\sim}{Y}_0 = \underset{\sim}{Z}_0^{-1} \tag{81a}$$

$$\underset{\sim}{Y}_{\mathcal{L}} = \underset{\sim}{Z}_{\mathcal{L}}^{-1} \tag{81b}$$

$$\underset{\sim}{Y}_1 = \left\{ \underset{\sim}{\Phi}_{k12}\ \underset{\sim}{Y}_0 - \underset{\sim}{\Phi}_{k11} \right\} \tag{81c}$$

$$\underset{\sim}{\hat{Y}} = - \left\{ \underset{\sim}{\Phi}_{k11} + \underset{\sim}{\Phi}_{k12}\ \underset{\sim}{\Phi}_{k22}\ \underset{\sim}{\Phi}_{k12}^{-1} \right\} \tag{81d}$$

$$\underset{\sim}{Y}_{N+1} = \left\{ \underset{\sim}{\Phi}_{k12}\ \underset{\sim}{Y}_{\mathcal{L}} - \underset{\sim}{\Phi}_{k12}\ \underset{\sim}{\Phi}_{k22}\ \underset{\sim}{\Phi}_{k12}^{-1} \right\} \quad . \tag{81e}$$

In deriving (80) from (69) and (79), use is made of the relation

$$\underset{\sim}{\Phi}_{k22}\ \underset{\sim}{\Phi}_{k12}^{-1}\ \underset{\sim}{\Phi}_{k11} - \underset{\sim}{\Phi}_{k21} = \underset{\sim}{\Phi}_{k12}^{-1} \tag{82}$$

which one can readily verify from the partitioned forms of the chain parameters in (78). In fact, this relationship can be shown to be true in general for any lumped, linear, reciprocal 2n-port characterized by the

chain parameter matrix in (79) by writing (79) from the nodal-admittance-matrix characterizing the 2n-port and invoking symmetry of this nodal admittance matrix via reciprocity.

In (78a), (78b) and (78c), $\underset{\sim}{\Phi}_{k12}^{-1} = -(N/\mathcal{L})\,\underset{\sim}{Z}^{-1}$ and in (78d) $\underset{\sim}{\Phi}_{k12}^{-1} = \left\{\underset{\sim}{1}_n + 1/4\,\underset{\sim}{Y}\,\underset{\sim}{Z}(\mathcal{L}/N)^2\right\}^{-1}\left\{-(N/\mathcal{L})\underset{\sim}{Z}^{-1}\right\}$. Therefore when writing the node-voltage equations in this fashion, it appears that the inverse of the per-unit-length impedance matrix, $\underset{\sim}{Z}$, is required. The inverse of $\underset{\sim}{Z}$ is needed when writing node-voltage equations strictly from a circuit diagram when mutual inductances are present [53]. However, one can show from (78) that

$$\underset{\sim}{\Phi}_{k12}\,\underset{\sim}{\Phi}_{k22}\,\underset{\sim}{\Phi}_{k12}^{-1} = \underset{\sim}{\Phi}_{k22}^{t} \tag{83}$$

which can be used in forming $\hat{\underset{\sim}{Y}}$ and $\underset{\sim}{Y}_{N+1}$ in (80) as

$$\hat{\underset{\sim}{Y}} = -\left\{\underset{\sim}{\Phi}_{k11} + \underset{\sim}{\Phi}_{k22}^{t}\right\} \tag{84a}$$

$$\underset{\sim}{Y}_{N+1} = \left\{\underset{\sim}{\Phi}_{k12}\,\underset{\sim}{Y}_{\mathcal{L}} - \underset{\sim}{\Phi}_{k22}^{t}\right\} \quad . \tag{84b}$$

Thus the inverse of $\underset{\sim}{Z}$ is not needed when writing the node-voltage equations in this fashion as in (80).

It should be noted that the formulation in (80) provides an additional method of obtaining the exact, distributed-parameter solution for $\underline{V}(0)$ and $\underline{V}(\mathcal{L})$. For example, taking N=1 and using the distributed matrix chain parameters $\underset{\sim}{\Phi}_{11}$, $\underset{\sim}{\Phi}_{12}$, $\underset{\sim}{\Phi}_{21}$, and $\underset{\sim}{\Phi}_{22}$ from (31) and (32) one obtains a set of 2n equations in the 2n unknowns, $\underline{V}(0)$ and $\underline{V}(\mathcal{L})$, which can be solved for the exact, distributed-parameter solution instead of using (70), (71), (72) or (73). For the distributed case, one can also show $\underset{\sim}{\Phi}_{22}\,\underset{\sim}{\Phi}_{12}^{-1}\,\underset{\sim}{\Phi}_{11} - \underset{\sim}{\Phi}_{21} = \underset{\sim}{\Phi}_{12}^{-1}$ (see (40)). In addition, one can show that $\underset{\sim}{\Phi}_{12}\,\underset{\sim}{\Phi}_{22}\,\underset{\sim}{\Phi}_{12}^{-1} = \underset{\sim}{\Phi}_{11}$ (see (40)) and this can be

used in forming $\underset{\sim}{Y}_{N+1}$ in (81). Thus, for the distributed case, (80) becomes

$$\begin{bmatrix} \left\{\underset{\sim}{\Phi}_{12}(\mathcal{L})\ \underset{\sim}{Z}_0^{-1} - \underset{\sim}{\Phi}_{11}(\mathcal{L})\right\} & \underset{\sim}{1}_n \\ \underset{\sim}{1}_n & \left\{\underset{\sim}{\Phi}_{12}(\mathcal{L})\ \underset{\sim}{Z}_{\mathcal{L}}^{-1} - \underset{\sim}{\Phi}_{11}(\mathcal{L})\right\} \end{bmatrix} \begin{bmatrix} \underline{V}(0) \\ \underline{V}(\mathcal{L}) \end{bmatrix} = \begin{bmatrix} \underset{\sim}{\Phi}_{12}(\mathcal{L})\ \underset{\sim}{Z}_0^{-1}\ \underline{V}_0 \\ \underset{\sim}{\Phi}_{12}(\mathcal{L})\ \underset{\sim}{Z}_{\mathcal{L}}^{-1}\ \underline{V}_{\mathcal{L}} \end{bmatrix} \qquad (85)$$

and (85) may be explicitly solved for $\underline{V}(0)$ and $\underline{V}(\mathcal{L})$ as was done in obtaining (73) from (72). Note the similarity of (85) to (72).

An important consideration in using the lumped-circuit iterative approximations is that to obtain correlation with the distributed-parameter formulation described by (4) (which these models are intended to approximate), each section must be electrically short and therefore the number of sections used to represent the line must be increased for increasing frequency. For an (n+1)-conductor line with N sections, (N+1)n simultaneous, complex equations in terms of the node voltages, $\underline{V}(0)$, $\underline{V}(\mathcal{L}/N)$,---, $\underline{V}(\mathcal{L})$ must be solved at each frequency as is evident from (80). For N>1, i.e., using more than one section to represent the entire line, the equations become sparse (large number of zero entries) which is clear from (80) and the fact that each section interacts directly with only its two neighboring sections. This high degree of sparsity can be used to drastically reduce the storage and computation times over that which would be required if the nodal-admittance matrix were treated as "full" and no advantage taken of the zero entries. These considerations are implemented in the program, TRAFFIC [53]. Even if only one section were used to represent the entire line, i.e., N=1, (80) shows that 2n complex equations in 2n unknowns must be solved at each frequency. However, these equations can be solved explicitly for $\underline{V}(0)$ or

$\underline{V}(\mathcal{L})$ so that for N=1 a minimum of n simultaneous equations in n unknowns, $\underline{V}(0)$ or $\underline{V}(\mathcal{L})$ need be solved. In obtaining the solution of the distributed-parameter, transmission line equations directly rather than approximating the line with lumped-circuit iterative models, one is also required to solve 2n simultaneous equations in 2n unknowns through a solution of (70), (72) or (85) or n equations in n unknowns through a solution of (71a) or (73a) and the number of simultaneous equations which must be solved need not be increased with increasing frequency as is required with the lumped-circuit iterative approximations.

Incident fields may also be incorporated into the solution via the lumped-circuit iterative approximations. Define from (8)

$$\begin{bmatrix} \underline{V}(k\mathcal{L}/N) \\ \underline{I}(k\mathcal{L}/N) \end{bmatrix} = \underset{\sim}{\Phi}(k\mathcal{L}/N, {}^{(k-1)\mathcal{L}}/N) \begin{bmatrix} \underline{V}({}^{(k-1)\mathcal{L}}/N) \\ \underline{I}({}^{(k-1)\mathcal{L}}/N) \end{bmatrix} + \int_{(k-1)\mathcal{L}/N}^{k\mathcal{L}/N} \underset{\sim}{\Phi}({}^{k\mathcal{L}}/N, \hat{x}) \begin{bmatrix} \underline{V}_s(\hat{x}) \\ \underline{I}_s(\hat{x}) \end{bmatrix} d\hat{x} \tag{86}$$

$$\cong \underset{\sim}{\Phi}_k \left\{ \begin{bmatrix} \underline{V}({}^{(k-1)\mathcal{L}}/N) \\ \underline{I}({}^{(k-1)\mathcal{L}}/N) \end{bmatrix} + \int_{(k-1)\mathcal{L}/N}^{k\mathcal{L}/N} \begin{bmatrix} \underline{V}_s(\hat{x}) \\ \underline{I}_s(\hat{x}) \end{bmatrix} d\hat{x} \right\}$$

for k = 1, 2, ---, N since it is assumed that $\underset{\sim}{\Phi}(k\mathcal{L}/N, {}^{(k-1)\mathcal{L}}/N) \cong \underset{\sim}{\Phi}_k$ for electrically short sections. Thus, for electrically short sections, the lumped-circuit iterative models can logically be modified to include incident fields by adding appropriate voltage and current sources to the beginning of each section as indicated by (86). The node-voltage equations in (80) will be modified by adding appropriate additional forcing functions to the right-hand side vector and the coefficient matrix will remain unchanged.

The question of convergence of the lumped-circuit iterative approximations to the distributed-parameter solution is difficult to answer quantitatively. A preliminary indication can be obtained by observing the convergence of the overall chain parameter matrix for an N section representation, $\underset{\sim}{\Phi}_k^N$, to the distributed-parameter chain matrix (or state transition matrix), $\underset{\sim}{\Phi}$. The state transition matrix $\underset{\sim}{\Phi}(\mathcal{L})$ (equations (31), (32) and (33) with $x = \mathcal{L}$ and $x_0 = 0$) can be expanded into an absolutely convergent infinite series as shown in (34) as

$$\underset{\sim}{\Phi}(\mathcal{L}) = \begin{bmatrix} \underset{\sim}{1}_n & \underset{\sim}{0}_n \\ \underset{\sim}{0}_n & \underset{\sim}{1}_n \end{bmatrix} + \begin{bmatrix} \underset{\sim}{0}_n & -\underset{\sim}{Z} \\ -\underset{\sim}{Y} & \underset{\sim}{0}_n \end{bmatrix} \frac{\mathcal{L}}{1!} + \begin{bmatrix} \underset{\sim}{Z}\underset{\sim}{Y} & \underset{\sim}{0}_n \\ \underset{\sim}{0}_n & \underset{\sim}{Y}\underset{\sim}{Z} \end{bmatrix} \frac{\mathcal{L}^2}{2!} + \begin{bmatrix} \underset{\sim}{0}_n & -\underset{\sim}{Z}\underset{\sim}{Y}\underset{\sim}{Z} \\ -\underset{\sim}{Y}\underset{\sim}{Z}\underset{\sim}{Y} & \underset{\sim}{0}_n \end{bmatrix} \frac{\mathcal{L}^3}{3!} + \cdots \tag{87}$$

Expanding the chain parameter matrices for the lumped iterative approximations in (78) one obtains for the lumped ⌐ model:

$$\underset{\sim}{\Phi}_k = \begin{bmatrix} \underset{\sim}{1}_n & \underset{\sim}{0}_n \\ \underset{\sim}{0}_n & \underset{\sim}{1}_n \end{bmatrix} + \begin{bmatrix} \underset{\sim}{0}_n & -\underset{\sim}{Z} \\ -\underset{\sim}{Y} & \underset{\sim}{0}_n \end{bmatrix} \frac{\mathcal{L}}{N} + \begin{bmatrix} \underset{\sim}{0}_n & \underset{\sim}{0}_n \\ \underset{\sim}{0}_n & \underset{\sim}{Y}\underset{\sim}{Z} \end{bmatrix} \left(\frac{\mathcal{L}}{N}\right)^2 \tag{88a}$$

and for the lumped Γ model:

$$\underset{\sim}{\Phi}_k = \begin{bmatrix} \underset{\sim}{1}_n & \underset{\sim}{0}_n \\ \underset{\sim}{0}_n & \underset{\sim}{1}_n \end{bmatrix} + \begin{bmatrix} \underset{\sim}{0}_n & -\underset{\sim}{Z} \\ -\underset{\sim}{Y} & \underset{\sim}{0}_n \end{bmatrix} \frac{\mathcal{L}}{N} + \begin{bmatrix} \underset{\sim}{Z}\underset{\sim}{Y} & \underset{\sim}{0}_n \\ \underset{\sim}{0}_n & \underset{\sim}{0}_n \end{bmatrix} \left(\frac{\mathcal{L}}{N}\right)^2 \tag{88b}$$

and for the lumped Pi model:

$$\underset{\sim}{\Phi}_k = \begin{bmatrix} \underset{\sim}{1}_n & \underset{\sim}{0}_n \\ \underset{\sim}{0}_n & \underset{\sim}{1}_n \end{bmatrix} + \begin{bmatrix} \underset{\sim}{0}_n & -\underset{\sim}{Z} \\ -\underset{\sim}{Y} & \underset{\sim}{0}_n \end{bmatrix} \frac{\mathcal{L}}{N} + \begin{bmatrix} \underset{\sim}{Z}\underset{\sim}{Y} & \underset{\sim}{0}_n \\ \underset{\sim}{0}_n & \underset{\sim}{Y}\underset{\sim}{Z} \end{bmatrix} 1/2\left(\frac{\mathcal{L}}{N}\right)^2 + \begin{bmatrix} \underset{\sim}{0}_n & \underset{\sim}{0}_n \\ -\underset{\sim}{Y}\underset{\sim}{Z}\underset{\sim}{Y} & \underset{\sim}{0}_n \end{bmatrix} 1/4\left(\frac{\mathcal{L}}{N}\right)^3 \tag{88c}$$

and for the lumped Tee model:

$$\underset{\sim}{\Phi}_k = \begin{bmatrix} \underset{\sim}{1}_n & \underset{\sim}{0}_n \\ \underset{\sim}{0}_n & \underset{\sim}{1}_n \end{bmatrix} + \begin{bmatrix} \underset{\sim}{0}_n & -\underset{\sim}{Z} \\ -\underset{\sim}{Y} & \underset{\sim}{0}_n \end{bmatrix} \frac{\mathcal{L}}{N} + \begin{bmatrix} \underset{\sim}{Z}\underset{\sim}{Y} & \underset{\sim}{0}_n \\ \underset{\sim}{0}_n & \underset{\sim}{Y}\underset{\sim}{Z} \end{bmatrix} 1/2\left(\frac{\mathcal{L}}{N}\right)^2 + \begin{bmatrix} \underset{\sim}{0}_n & -\underset{\sim}{Z}\underset{\sim}{Y}\underset{\sim}{Z} \\ \underset{\sim}{0}_n & \underset{\sim}{0}_n \end{bmatrix} 1/4\left(\frac{\mathcal{L}}{N}\right)^3 . \tag{88d}$$

Note that for N = 1, i.e., one section is used to represent the entire line, the lumped Pi and lumped Tee models appear to be better approximations to the distributed solution, $\underset{\sim}{\Phi}(\mathcal{L})$ in (87) than do the lumped Γ and lumped $\urcorner$ models in the sense that the first three terms of (88c) and (88d) are identical with the first three terms of $\underset{\sim}{\Phi}(\mathcal{L})$ and the fourth term is only partially the fourth term in $\underset{\sim}{\Phi}(\mathcal{L})$. In the expansions (88a) and (88b), only the first two terms agree with the first two terms of $\underset{\sim}{\Phi}(\mathcal{L})$ and the third term partially agrees with the third term in $\underset{\sim}{\Phi}(\mathcal{L})$.

There are certain other lumped approximations which at first glance seem to be not included in this discussion but are, in reality, versions of lumped-circuit iterative models using only one section to represent the entire line and with certain circuit elements neglected [35]. In addition, with these approximations the capacitive and inductive coupling are computed independently of each other and added together which is generally only valid for weakly-coupled lines (see reference [30], pp. 287-291).

V. THE PER-UNIT-LENGTH PARAMETERS

Derivations of the per-unit-length parameters of internal resistance and internal self inductance, i.e., the entries in $\underset{\sim}{R}_c$ and $\underset{\sim}{L}_c$, which account for skin effect associated with imperfect conductors are well known for solid, round-wire conductors and are found in numerous texts [2, 3, 30]. These internal parameters are derived by assuming that the currents internal to the conductors are symmetric with respect to the centers of the conductors. However, for closely-spaced conductors, this assumption may not be valid since proximity effect can alter the internal current distributions (see reference [40], Chapter 9).

The derivations of the per-unit-length external parameters, i.e., the entries in $\underset{\sim}{G}$, $\underset{\sim}{L}$ and $\underset{\sim}{C}$, assume all (n+1) conductors are perfect conductors and are more involved especially for close conductor spacings. These parameters generally only exist in closed form for the simple cases of two-conductor lines in homogeneous media in Fig. 4 consisting of two bare wires in an infinite, homogeneous medium in Fig. 4a (reference [55], pp. 133-136), one bare wire in an infinite homogeneous medium above an infinite ground plane in Fig. 4b (reference [55], pp. 183-185), and one wire within a circular shield which is homogeneously filled with a dielectric in Fig. 4c (reference [55], pp. 125-133).

Having accurate values for the entries in the per-unit-length parameter matrices, especially the external inductance and capacitance matrices $\underset{\sim}{L}$ and $\underset{\sim}{C}$, is obviously important in obtaining accurate solutions and the per-unit-

length parameters must be obtained even when using lumped-circuit iterative approximations discussed in Section 4.1. It is important to remember that with the assumption of TEM mode propagation on the line, the transverse fields at each x along the line satisfy a static distribution and therefore the per-unit-length external parameters, i.e., entries in $\underset{\sim}{G}$, $\underset{\sim}{L}$ and $\underset{\sim}{C}$, are obtained as the solution to a two-dimensional static fields problem [39]. This also is implied in the inhomogeneous medium case under the "quasi-TEM mode" assumption.

5.1 The Per-Unit-Length External Parameters for Lines in a Homogeneous Medium

The per-unit-length parameter matrices, $\underset{\sim}{C}$, $\underset{\sim}{L}$ and $\underset{\sim}{G}$ for lines immersed in a homogeneous medium possess the important properties given in (44), $\underset{\sim}{L}\underset{\sim}{C} = \underset{\sim}{C}\underset{\sim}{L} = \mu\epsilon \underset{\sim}{1}_n$ and $\underset{\sim}{L}\underset{\sim}{G} = \underset{\sim}{G}\underset{\sim}{L} = \mu\sigma \underset{\sim}{1}_n$. It can be shown [54] that, for a homogeneous medium, each of these matrices is related to an $n \times n$ matrix, $\underset{\sim}{K}$, which is independent of the parameters of the medium and dependent only on the cross-sectional structure of the line as

$$\underset{\sim}{C} = \epsilon \underset{\sim}{K} \tag{89a}$$

$$\underset{\sim}{G} = \sigma \underset{\sim}{K} = (\sigma/\epsilon)\, \underset{\sim}{C} \tag{89b}$$

$$\underset{\sim}{L} = \mu \underset{\sim}{K}^{-1} = \mu\epsilon\, \underset{\sim}{C}^{-1} \quad . \tag{89c}$$

For two-conductor lines in a homogeneous medium, the per-unit-length parameters in the transmission line equations in (1) are obtainable, exactly in closed form even for close conductor spacings where proximity effect produces a nonuniform charge distribution around the conductor peripheries [55]. The matrix $\underset{\sim}{K}$ in (89) becomes a scalar K and the parameters in (1)

become $c = \epsilon K$, $g = \sigma K$, $\ell = \mu K^{-1}$.

For two wires in a homogeneous medium in Fig. 4a, the per-unit-length capacitance becomes [56]

$$c = \frac{2\pi\epsilon}{\cosh^{-1}\left[(d^2 - r_{w1}^2 - r_{w0}^2)/(2\, r_{w1}\, r_{w0})\right]} \quad . \tag{90}$$

For widely-separated conductors, (90) can be approximated by [3]

$$c \cong \frac{2\pi\epsilon}{\ell n\left(\frac{d^2}{r_{w1}\, r_{w0}}\right)} \tag{91}$$

where ℓn is the natural logarithm. For identical wires with $r_{w1} = r_{w0} = r_w$, (91) yields less than 5% error for $(d/r_w) > 5$ [55, 56]. For the case of one wire in a homogeneous medium above an infinite ground plane as in Fig. 4b, the per-unit-length capacitance becomes [55]

$$c = \frac{2\pi\epsilon}{\cosh^{-1}(h/r_w)} \quad . \tag{92}$$

and for $(2h/r_w) > 5$, (92) can be approximated by [55]

$$c \cong \frac{2\pi\epsilon}{\ell n\,(2h/r_w)} \tag{93}$$

For the case of one wire within and centered on the axis of a circular shield which is homogeneously filled with a dielectric as in Fig. 4c, the per-unit-length capacitance becomes [55]

$$c = \frac{2\pi\epsilon}{\ell n\,(r_s/r_w)} \quad . \tag{94}$$

In all of the above cases, $c = \epsilon K$ and K is easily identified. In addition, $\ell = \mu_v K^{-1}$ and $g = \sigma K$. For Fig. 4a and Fig. 4b, $\epsilon = \epsilon_v$ and $\sigma = 0$.

The parameters for lines consisting of more than two conductors are, in general, not obtainable in closed form for closely-spaced conductors and numerical approximations must be used. These techniques generally fall into two classes; the method-of-moments techniques [56-62, 22, 66-68] or imaging techniques [63, 64, 65]. A particularly successful technique is the use of harmonic expansion functions to describe the charge distribution around the conductor peripheries [56, 57].

Consider the system of (n+1) bare wires in Fig. 2a. With the moment method using harmonic expansion functions, the free-charge distribution, ρ_i, around the cross-sectional perimeter of the i-th conductor per unit of length in the x direction is described as a Fourier series with respect to a cylindrical coordinate system at the center of the i-th conductor as shown in Fig. 12a, i.e.,

$$\rho_i(\theta_i) = a_{i0} + \sum_{m=1}^{A_i} a_{im} \cos m\theta_i + \sum_{m=1}^{B_i} b_{im} \sin m\theta_i \qquad i = 0, 1, \cdots, n. \tag{95}$$

The absolute potential[1], $\phi_p(r_p, \theta_p)$, at an arbitrary point P located at a radius r_p and angle θ_p shown in Fig. 12a due to this charge distribution over the i-th isolated conductor is [56, 57]

$$\phi_p(r_p, \theta_p) = -\frac{1}{4\pi\epsilon} \left\{ a_{i0} \int_0^{2\pi} I(\theta_i)\, d\theta_i \right. \tag{96}$$

$$\left. + \sum_{m=1}^{A_i} a_{im} \int_0^{2\pi} \cos(m\theta_i)\, I(\theta_i)\, d\theta_i + \sum_{m=1}^{B_i} b_{im} \int_0^{2\pi} \sin(m\theta_i)\, I(\theta_i)\, d\theta_i \right\}$$

1. The term "absolute potential" refers to the potential with respect to infinity and the reference potential terms are omitted in (96). This is valid for a system with zero net charge and is demonstrated in Appendix E.

The parameters for lines consisting of more than two conductors are, in general, not obtainable in closed form for closely-spaced conductors and numerical approximations must be used. These techniques generally fall into two classes; the method-of-moments techniques [56-62, 22, 66-68] or imaging techniques [63, 64, 65]. A particular successful technique is the use of harmonic expansion functions to describe the charge distribution around the conductor peripheries [56, 57].

Consider the system of (n+1) bare wires in Fig. 2a. With the moment method using harmonic expansion functions, the free-charge distribution, ρ_i, around the cross-sectional perimeter of the i-th conductor per unit of length in the x direction is described as a Fourier series with respect to a cylindrical coordinate system at the center of the i-th conductor as shown in Fig. 12a, i.e.,

$$\rho_i(\theta_i) = a_{i0} + \sum_{m=1}^{A_i} a_{im} \cos m\theta_i + \sum_{m=1}^{B_i} b_{im} \sin m\theta_i \qquad (95)$$
$$i = 0, 1, ---, n.$$

The absolute potential,[1] $\phi_p(r_p, \theta_p)$, at an arbitrary point P located at a radius r_p and angle θ_p shown in Fig. 12a due to this charge distribution over the i-th isolated conductor is [56, 57]

$$\phi_p(r_p, \theta_p) = -\frac{1}{4\pi\epsilon} \left\{ a_{i0} \int_0^{2\pi} I(\theta_i)\, d\theta_i \right. \qquad (96)$$
$$\left. + \sum_{m=1}^{A_i} a_{im} \int_0^{2\pi} \cos(m\theta_i)\, I(\theta_i)\, d\theta_i + \sum_{m=1}^{B_i} b_{im} \int_0^{2\pi} \sin(m\theta_i)\, I(\theta_i)\, d\theta_i \right\}$$

1. The term "absolute potential" refers to the potential with respect to infinity and the reference potential terms are omitted in (96). This is valid for a system with zero net charge and is demonstrated in Appendix E.

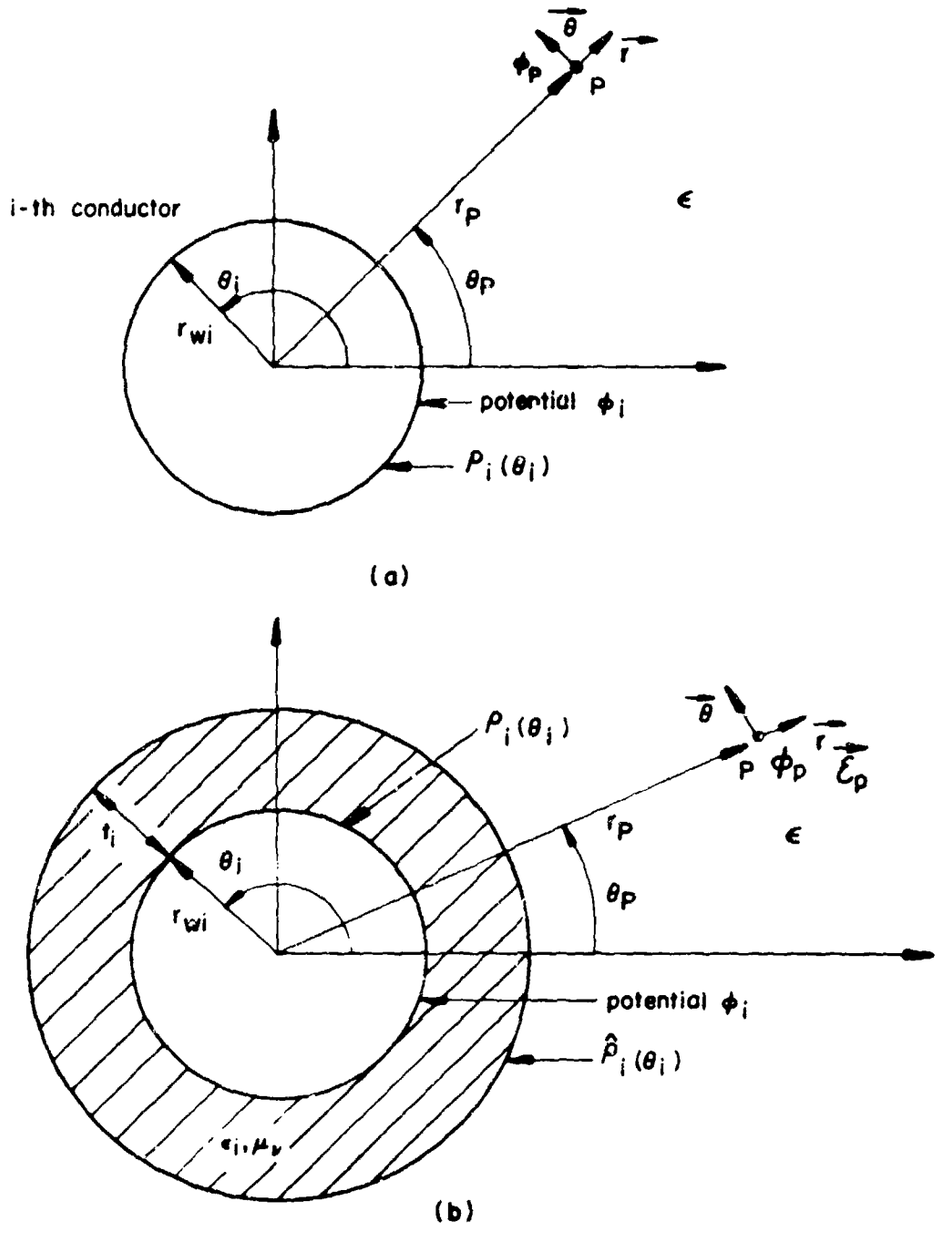

Figure 12. The geometry of the charge distribution problem.

where $I(\theta_i) \quad \ell n \left\{ r_p^2 + r_{wi}^2 - 2r_p\, r_{wi} \cos(\theta_i - \theta_p) \right\} r_{wi}$. These integrals can be evaluated in closed form yielding [56, 57] (See Appendix E)

$$\phi_p(r_p, \theta_p) = -a_{i0} \left(\frac{r_{wi}\, \ell n\, (r_p)}{\epsilon} \right) + \sum_{m=1}^{A_i} a_{im} \left(\frac{r_{wi}^{(m+1)} \cos(m\theta_p)}{2m\epsilon r_p^m} \right) \quad (97)$$

$$+ \sum_{m=1}^{B_i} b_{im} \left(\frac{r_{wi}^{(m+1)} \sin(m\theta_p)}{2m\epsilon r_p^m} \right) \quad .$$

Associated with each conductor in Fig. 2a there are $A_i + B_i + 1$ unknowns; the expansion coefficients a_{i0}, a_{im}, b_{im} in (95). These unknowns will be determined by enforcing the boundary conditions that each conductor (including the reference) is at an absolute potential ϕ_i, i=0, 1, ---n. A total of $\sum_{i=0}^{n}(A_i + B_i + 1)$ match points will be chosen on the (n+1) conductors at which the potential due to all charge distributions in the system (including the charge distribution on the conductor associated with the match point) will be enforced. This results in a set of $\sum_{i=0}^{n}(A_i + B_i + 1)$ equations in the same number of unknowns and can be written as [56, 57]

$$\underset{\sim}{P}\, \underline{\rho} = \underline{\phi} \quad (98)$$

where $\underline{\rho}$ is a vector of length $\sum_{i=0}^{n}(A_i + B_i + 1)$ containing a l of the unknown expansion coefficients a_{i0}, a_{im}, b_{iin} and $\underline{\phi}$ is a vector of the assumed conductor potentials as

$$\underline{\rho} = \begin{bmatrix} \vdots \\ \hline a_{i0} \\ a_{i1} \\ \vdots \\ a_{iA_i} \\ b_{i1} \\ \vdots \\ b_{iB_i} \\ \hline \vdots \end{bmatrix} \qquad \underline{\phi} = \begin{bmatrix} \vdots \\ \hline \phi_j \\ \phi_j \\ \vdots \\ \phi_j \\ \phi_j \\ \vdots \\ \phi_j \\ \hline \vdots \end{bmatrix} \tag{99}$$

where ϕ_j is the potential of the j-th conductor at each of the chosen match points on that conductor surface. Inverting $\underset{\sim}{P}$ in (98), one may write

$$\underline{\rho} = \underset{\sim}{P}^{-1} \underline{\phi} \quad . \tag{100}$$

From the solution in (100) for the expansion coefficients, the total free charge on the i-th conductor is [56, 57]

$$q_i = \int_0^{2\pi} \rho_i(\theta_i)\, r_{wi}\, d\theta_i \tag{101}$$

$$= 2\pi\, r_{wi}\, a_{i0}$$

and an (n+1) $\times$ (n+1) "generalized" capacitance matrix $\underset{\sim}{C}$ may be written as

$$\begin{bmatrix} q_0 \\ \vdots \\ q_n \end{bmatrix} = \begin{bmatrix} C_{00} & C_{01} & \cdots & C_{0n} \\ C_{10} & C_{11} & \ddots & \vdots \\ \vdots & \ddots & \ddots & \vdots \\ C_{n0} & \cdots & \cdots & C_{nn} \end{bmatrix} \begin{bmatrix} \phi_0 \\ \vdots \\ \phi_n \end{bmatrix} \quad . \tag{102}$$

In (102), note that $[\underset{\sim}{C}]_{ij} \triangleq C_{ij} = q_i$ if the excitations are chosen as $\phi_j = 1$ with all other potentials chosen zero, i.e., $\phi_p = 0, p \neq j$, and i, j=0, 1, ---, n.

However, from (101), $q_i = 2\pi r_{w\,i}\, a_{i0}$. Therefore, to find $\mathcal{C}_{ij}$ simply add all elements of $\underset{\sim}{P}^{-1}$ in (100) which are in the row associated with a_{i0} and the columns associated with ϕ_j and multiply the result by $2\pi r_{w\,i}$ [56, 57]. From energy considerations, one can show that $\underset{\sim}{\mathcal{C}}$ is symmetric, i.e., $\mathcal{C}_{ij} = \mathcal{C}_{ji}$ [58].

The $n \times n$ external capacitance matrix, $\underset{\sim}{C}$, used in the transmission line equations in (4), (6) and (7) where potentials V_i, $i=1,---,n$ are defined with respect to the zero-th conductor chosen as reference instead of absolute potentials, ϕ_j, can then be obtained directly from $\underset{\sim}{\mathcal{C}}$. To do this, note that choosing the zero-th conductor as reference, $V_i = (\phi_i - \phi_0)$, $i=1,---,n$ and the transmission line capacitance matrix $\underset{\sim}{C}$ becomes

$$\begin{bmatrix} q_1 \\ \vdots \\ q_n \end{bmatrix} = \begin{bmatrix} C_{11} & ----- & C_{1n} \\ \vdots & & \vdots \\ C_{n1} & ----- & C_{nn} \end{bmatrix} \begin{bmatrix} V_1 \\ \vdots \\ V_n \end{bmatrix} \tag{103}$$

where $[\underset{\sim}{C}]_{ij} \triangleq C_{ij}$ for $i, j=1,---,n$.

Since the system is electrically neutral, we have

$$q_0 = -\sum_{i=1}^{n} q_i \tag{104}$$

and the potentials V_i with respect to the reference conductor become

$$V_i = (\phi_i - \phi_0) \quad . \tag{105}$$

Thus (102) can be written as

$$\begin{aligned} -\sum_{k=1}^{n} q_k &= \mathcal{C}_{01} V_1 + \mathcal{C}_{02} V_2 + --- + \mathcal{C}_{0n} V_n + \left(\sum_{m=0}^{n} \mathcal{C}_{0m}\right) \phi_0 \\ q_1 &= \mathcal{C}_{11} V_1 + \mathcal{C}_{12} V_2 + --- + \mathcal{C}_{1n} V_n + \left(\sum_{m=0}^{n} \mathcal{C}_{1m}\right) \phi_0 \\ &\vdots \\ q_n &= \mathcal{C}_{n1} V_1 + \mathcal{C}_{n2} V_2 + --- + \mathcal{C}_{nn} V_n + \left(\sum_{m=0}^{n} \mathcal{C}_{nm}\right) \phi_0 \quad . \end{aligned} \tag{106}$$

Adding all equations in (106) together we obtain

$$0 = \left(\sum_{m=0}^{n} \mathcal{C}_{m1}\right)V_1 + \left(\sum_{m=0}^{n} \mathcal{C}_{m2}\right)V_2 + \cdots + \left(\sum_{m=0}^{n} \mathcal{C}_{mn}\right)V_n \qquad (107)$$

$$+ \left(\sum_{m=0}^{n} \mathcal{C}_{0m} + \sum_{m=0}^{n} \mathcal{C}_{1m} + \cdots + \sum_{m=0}^{n} \mathcal{C}_{nm}\right)\phi_0$$

or

$$\phi_0 = - \frac{\sum_{k=1}^{n} \left[\left(\sum_{m=0}^{n} \mathcal{C}_{mk}\right) V_k\right]}{\sum_{\ell=0}^{n} \left[\sum_{m=0}^{n} \mathcal{C}_{\ell m}\right]} \quad . \qquad (108)$$

Substituting (108) into the last n equations in (106) and arranging these last n equations in the form of (103) yields the entries in the per-unit-length transmission line capacitance matrix $\underset{\sim}{C}$ as

$$[C]_{ij} = C_{ij} = \mathcal{C}_{ij} - \frac{\left(\sum_{m=0}^{n} \mathcal{C}_{im}\right)\left(\sum_{m=0}^{n} \mathcal{C}_{mj}\right)}{\sum_{\ell=0}^{n} \left(\sum_{m=0}^{n} \mathcal{C}_{\ell m}\right)} \qquad (109)$$

$$= \frac{\mathcal{C}_{ij}\left[\sum_{\ell=0}^{n}\left(\sum_{m=0}^{n} \mathcal{C}_{\ell m}\right)\right] - \left(\sum_{m=0}^{n} \mathcal{C}_{im}\right)\left(\sum_{m=0}^{n} \mathcal{C}_{mj}\right)}{\left(\sum_{\ell=0}^{n} \sum_{m=0}^{n} \mathcal{C}_{\ell m}\right)} \quad .$$

Note that the denominator of (109) is simply the sum of all the elements of $\underset{\sim}{\mathcal{C}}$. The numerator of (109) can be written as

$$\mathcal{C}_{ij}\left[\sum_{\ell=0}^{n} \sum_{m=0}^{n} \mathcal{C}_{\ell m}\right] - \mathcal{C}_{ij}\left(\sum_{\substack{m=0 \\ m\neq i}}^{n} \mathcal{C}_{mj}\right) - \mathcal{C}_{ij}\left(\sum_{\substack{m=0 \\ m\neq j}}^{n} \mathcal{C}_{im}\right) \qquad (110)$$

$$- \left(\sum_{\substack{m=0 \\ m\neq j}}^{n} \mathcal{C}_{im}\right)\left(\sum_{\substack{m=0 \\ m\neq i}}^{n} \mathcal{C}_{mj}\right) - \mathcal{C}_{ij}^{2}$$

$$= \mathcal{C}_{ij}\Big[\underbrace{\sum_{\ell=0}^{n}\sum_{m=0}^{n}\mathcal{C}_{\ell m} - \sum_{\substack{m=0\\ m\neq i}}^{n}\mathcal{C}_{mj} - \sum_{\substack{m=0\\ m\neq j}}^{n}\mathcal{C}_{im} - \mathcal{C}_{ij}}_{\text{sum of all terms in } \underset{\sim}{\mathcal{C}} \text{ except those in the i-th row and j-th column.}}\Big]$$

$$- \underbrace{\Big(\sum_{\substack{m=0\\ m\neq j}}^{n}\mathcal{C}_{im}\Big)}_{\substack{\text{sum of all terms in the i-th row of } \underset{\sim}{\mathcal{C}} \\ \text{except } \mathcal{C}_{ij}}}\underbrace{\Big(\sum_{\substack{m=0\\ m\neq i}}^{n}\mathcal{C}_{mj}\Big)}_{\substack{\text{sum of all terms in the} \\ \text{j-th column of } \underset{\sim}{\mathcal{C}} \\ \text{except } \mathcal{C}_{ij}}} .$$

Therefore, C_{ij} can be written as

$$C_{ij} = \frac{\mathcal{C}_{ij}\left(M_0 - {}_iM - M_j - \mathcal{C}_{ij}\right) - {}_iM\ M_j}{M_0} \qquad (111)$$

where

M_0 = Sum of all terms in $\underset{\sim}{\mathcal{C}}$

${}_iM$ = Sum of all terms in the i-th row of $\underset{\sim}{\mathcal{C}}$ except $\mathcal{C}_{ij}$

M_j = Sum of all terms in the j-th column of $\underset{\sim}{\mathcal{C}}$ except $\mathcal{C}_{ij}$.

For two conductors (n=1) (111) becomes

$$c = q_1/V_1 \qquad (112)$$

$$= \frac{\mathcal{C}_{11}\mathcal{C}_{00} - \mathcal{C}_{01}\mathcal{C}_{10}}{\mathcal{C}_{00} + \mathcal{C}_{01} + \mathcal{C}_{10} + \mathcal{C}_{11}} .$$

This result for n=1 is also obtained in reference [58], pp. 211-213.

This numerical technique can also be applied to the systems in Fig. 2b by replacing the ground plane with the conductor images having equal but opposite charge distributions. As an example, consider the system of n bare wires above an infinite ground plane in Fig. 2b. Replacing the ground plane with images results in Fig. 13. Note that the orientation for θ_i on the image of the i-th conductor is the same as the orientation for θ_i on the i-th conductor however, the charge distribution on the i-th conductor image is $-\rho_i(-\theta_i)$. Also, note that the potential of the i-th image conductor is taken to be $-\phi_i$. By symmetry and the use of image distributions, the voltage of the i-th conductor with respect to the ground plane, V_i, is equal to ϕ_i since the potential difference between the i-th conductor and its image is $\phi_i - (-\phi_i) = 2\phi_i$. Therefore, we only need to enforce the potential ϕ_i at match points on the n conductors above the ground plane due to all charge distributions in the system (those on the n wires and on the n image wires). Thus a set of $\sum_{i=1}^{n}(A_i + B_i + 1)$ equations can be written as in (98). However, these equations will differ from those in (98) in that the expansion coefficients for the zero-th conductor (the ground plane), a_{00}, a_{0m}, b_{0m}, will not be included in the vector $\underline{\rho}$ and the potentials ϕ_0 will not be included in the vector $\underline{\phi}$. These vectors will be of length $\sum_{i=1}^{n}(A_i + B_i + 1)$ instead of $\sum_{i=0}^{n}(A_i + B_i + 1)$. Furthermore, we may replace ϕ_i in $\underline{\phi}$ by V_i. Inverting $\underset{\sim}{P}$ we then may obtain the entries in the transmission line capacitance matrix directly without the need for (111) since $\phi_i = V_i$. Therefore, C_{ij} is simply the sum of all elements

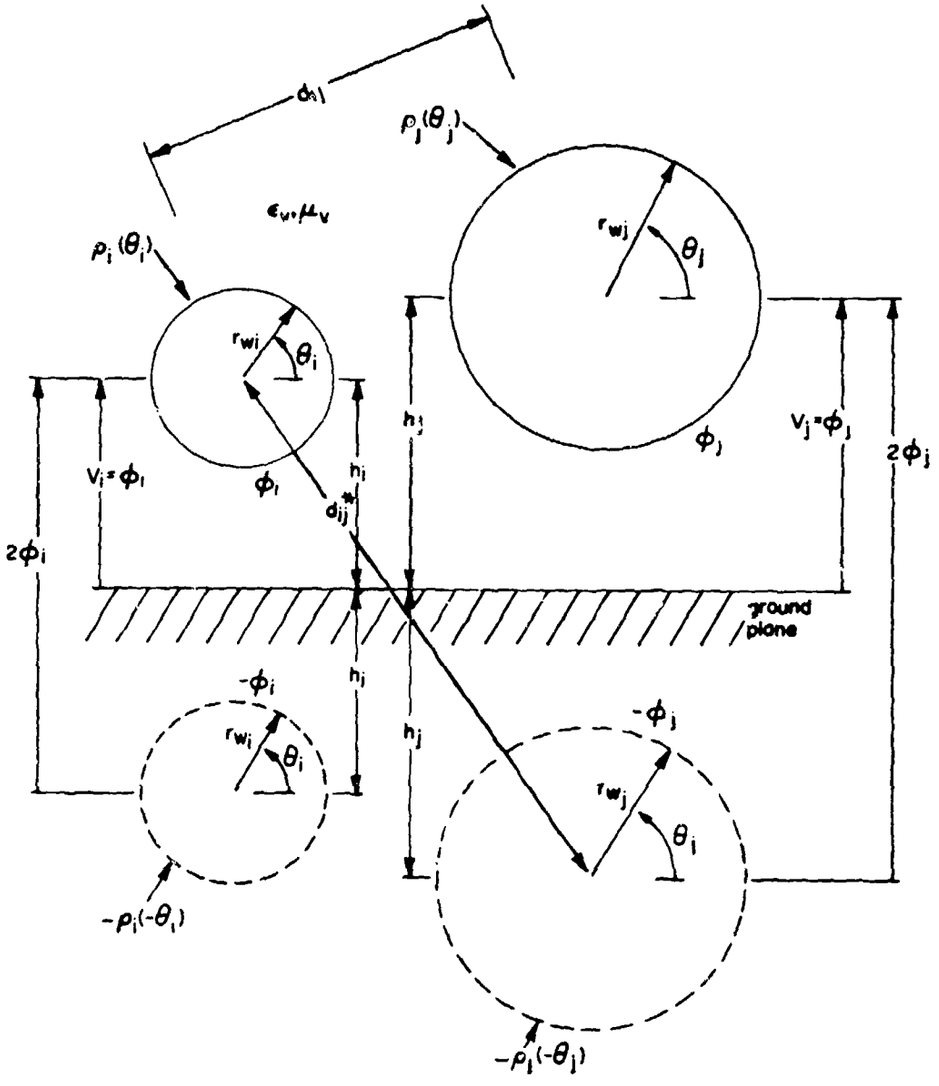

Figure 13. Multiconductor transmission lines above a ground plane and the use of image distributions.

in $\underset{\sim}{P}^{-1}$ which are in the row associated with a_{i0} and the columns associated with $\phi_j = V_j$ multiplied by $2\pi r_{wi}$ for i=1, ---, n and j=1, ---, n.

Consider the case of n wires within a circular shield shown in Fig. 2c. Rather than imaging the conductor charge distributions across the shield boundary, one may expand the per-unit-length free-charge distributions around the n conductor peripheries in a Fourier series and also expand the per-unit-length free-charge distribution around the interior periphery of the shield. Note that in this case, the voltages of the n wires with respect to the shield, V_i, will be $V_i = \phi_i - \phi_0$. Thus (111) can be used to obtain $\underset{\sim}{C}$.

Note that for all these cases, once $\underset{\sim}{C}$ is determined, $\underset{\sim}{L}$ and $\underset{\sim}{G}$ are obtained through (89) as $\underset{\sim}{L} = u_v \epsilon \underset{\sim}{C}^{-1}$ and $\underset{\sim}{G} = (\sigma/\epsilon)\,\underset{\sim}{C}$. For Fig. 2a and Fig. 2b, $\epsilon = \epsilon_v$ and $\sigma = 0$.

It is also possible to obtain closed-form approximations for $\underset{\sim}{C}$, $\underset{\sim}{L}$ and under the assumption that the conductors are widely spaced and these formulas represent the predominant method of computing the entries in these per-unit-length matrices [55, 57]. If it is assumed that the wires in Fig. 2a are sufficiently separated so that the charge distributions around the wire peripheries are constant, i.e., proximity effect [55, 56, 57, 58] is not a factor, then only one expansion function is needed in (95), a_{i0}. In this case there are only (n+1) unknowns , a_{i0}, i=0, 1, ---, n. Furthermore, since the wires are assumed to be widely spaced, then r_p in (97) can be taken to be d_{i0}, d_{j0} or d_{ij}, whichever is appropriate, when computing the contribution to the potential of a conductor due to the charge on

another conductor. When computing the contribution to the potential of a conductor due to the charge distribution on its boundary, the match point is taken on the conductor surface, i.e., $r_p = r_{wi}$. This assumption of widely-spaced conductors has been consistently used in the power transmission area [3, 4, 13, 55, 57] and is generally valid if the smallest ratio of wire separation to wire radius is on the order of 5 or greater [55, 56, 57].

Consider Fig. 2a. Assume as an approximation that the (n+1) wires in Fig. 2a are sufficiently separated such that the per-unit-length charge distributions around the wire peripheries are constant with each wire bearing a per-unit-length total free charge

$$q_i = 2\pi r_{wi} \quad a_{i0} \tag{113}$$

and

$$\rho_i(\theta_i) = a_{i0} \tag{114}$$

for $i = 0, 1, ---, n$. Because of the assumed large separations, this is equivalent to replacing the wires with filamentary line charges [55]. Since the wires are assumed to be widely separated so that the assumption of a constant charge distribution around each periphery is valid, i.e., proximity effect [55] is not a factor, then we may choose match points for the potential at the centers of the conductors rather than at some point on the periphery. However, for a match point on the conductor surface bearing the charge under consideration, we take the match point on the conductor surface, i.e., $r_p = r_{wi}$ in (97).

From the previous results and (113), we may then write (utilizing the first term in (97))

$$\begin{bmatrix} \phi_0 \\ \phi_1 \\ \vdots \\ \phi_n \end{bmatrix} = -\frac{1}{2\pi\epsilon} \begin{bmatrix} \ell n(r_{w0}) & \ell n(d_{10}) & \cdots & \ell n(d_{n0}) \\ \ell n(d_{10}) & \ell n(r_{w1}) & \ddots & \vdots \\ \vdots & \ddots & \ddots & \vdots \\ \ell n(d_{n0}) & \cdots & \cdots & \ell n(r_{wn}) \end{bmatrix} \begin{bmatrix} q_0 \\ q_1 \\ \vdots \\ q_n \end{bmatrix} . \tag{115}$$

Applying (105) to (115) results in a typical equation

$$\begin{aligned} V_i &= \phi_i - \phi_0 \\ &= -\frac{1}{2\pi\epsilon} \left\{ \ell n \left(\frac{d_{i0}}{r_{w0}}\right) q_0 + \cdots + \ell n \left(\frac{r_{wi}}{d_{i0}}\right) q_i \right. \\ &\qquad \left. + \cdots + \ell n \left(\frac{d_{ij}}{d_{j0}}\right) q_j + \cdots + \ell n \left(\frac{d_{in}}{d_{n0}}\right) q_n \right\} \end{aligned} \tag{116}$$

for i, j = 1, ---, n. Applying (104) to (116) yields

$$\begin{aligned} V_i = -\frac{1}{2\pi\epsilon} \left\{ \cdots + \ell n \left(\frac{r_{wi} r_{w0}}{d_{i0} d_{i0}}\right) q_i + \cdots \right. \\ \left. \cdots + \ell n \left(\frac{d_{ij} r_{w0}}{d_{i0} d_{j0}}\right) q_j + \cdots + \ell n \left(\frac{d_{in} r_{w0}}{d_{n0} d_{i0}}\right) q_n \right\} . \end{aligned} \tag{117}$$

Comparing (117) to (103) shows that

$$[\mathcal{C}^{-1}]_{ii} = \frac{1}{2\pi\epsilon} \ell n \left(\frac{d_{i0}^2}{r_{wi} r_{w0}}\right) \tag{118a}$$

$$[\mathcal{C}^{-1}]_{\substack{ij \\ i \neq j}} = \frac{1}{2\pi\epsilon} \ell n \left(\frac{d_{i0} d_{j0}}{r_{w0} d_{ij}}\right) \tag{118b}$$

for i, j=1, -----, n.

Thus the per-unit-length inductance matrix is from (89)

$$[L]_{ii} = \mu\epsilon\,[\mathcal{C}^{-1}]_{ii} = \frac{\mu}{2\pi}\,\ell n\left(\frac{d_{i0}^{\,2}}{r_{wi}r_{w0}}\right) \tag{119a}$$

$$[L]_{\substack{ij\\ i\neq j}} = \mu\epsilon\,[\mathcal{C}^{-1}]_{\substack{ij\\ i\neq j}} = \frac{\mu}{2\pi}\,\ell n\left(\frac{d_{i0}\,d_{j0}}{r_{w0}\,d_{ij}}\right) \tag{119b}$$

for i, j=1, ---, n. Note that for Fig. 2a, $\epsilon = \epsilon_v$, $\mu = \mu_v$ and $\sigma = 0$.

Similarly, large-separation approximations can be obtained for the case of n wires above an infinite ground plane in Fig. 2b. Consider Fig. 13 and assume that the wires are separated sufficiently from each other and the ground plane so that the per-unit-length charge distributions around the peripheries of the wires and their images are constant and given by (113) and (114) for i=1, ---, n. Again, due to the large-separation approximations, we may take the match points at the centers of the conductors when computing the contribution to the potential due to the charge distribution on another conductor and take the match point on the conductor periphery when computing the contribution to the potential of this conductor due to its own charge distribution. From Fig. 13, a typical equation for the i-th conductor may be written as (again using only the first term in (97))

$$\begin{aligned}\phi_i = V_i = \text{----} &+ a_{i0}\left\{\frac{-r_{wi}\ell n(r_{wi})}{\epsilon} + \frac{r_{wi}\ell n(2h_i)}{\epsilon}\right\} + \\ \text{----} &+ a_{j0}\left\{\frac{-r_{wj}\ell n(d_{ij})}{\epsilon} + \frac{r_{wj}\ell n(d_{ij}^{*})}{\epsilon}\right\} + \text{--} \\ = \frac{1}{2\pi\epsilon}&\left\{\text{---} + q_i\,\ell n\left(\frac{2h_i}{r_{wi}}\right) + \text{--} + q_j\,\ell n\left(\frac{d_{ij}^{*}}{d_{ij}}\right) + \text{--}\right\}\end{aligned} \tag{120}$$

for i, j=1, ---, n where d_{ij}^{*} is the center-to-center separation between the i-th wire (j-th wire) and the image of the j-th wire (i-th wire) given by

$$d_{ij}^{*} = \sqrt{(h_i + h_j)^2 + d_{ij}^2 - (h_j - h_i)^2} \qquad (121)$$

$$= \sqrt{d_{ij}^2 + 4\, h_i h_j} \quad .$$

Comparing (120) to (103) and using (89), we obtain

$$[L]_{ii} = \mu\epsilon\, [\underset{\sim}{C}^{-1}]_{ii} = \frac{\mu}{2\pi} \ln\left(\frac{2h_i}{r_{wi}}\right) \qquad (122a)$$

$$[L]_{\substack{ij \\ i\neq j}} = \mu\epsilon\, [\underset{\sim}{C}^{-1}]_{\substack{ij \\ i\neq j}} = \frac{\mu}{2\pi} \ln\left(\frac{d_{ij}^{*}}{d_{ij}}\right) \qquad (122b)$$

for i, j=1, ---, n. Note that for Fig. 2b, $\epsilon=\epsilon_v$, $\mu = \mu_v$ and $\sigma = 0$.

Large-separation approximations may also be obtained for the system of n wires within a circular shield in Fig. 2c. We assume that all n wires are sufficiently separated from each other and the shield so that the wires may be replaced by filamentary line charges. The circular shield (assumed to be perfectly conducting), may then be replaced by filamentary line charge images. Each filamentary line charge has an image on a line joining the line charge and the center of the shield and is at a distance of r_s^2/r_i from the shield center where r_s is the shield radius and r_i is the radial distance of the i-th wire from the shield center [58]. One can then straightforwardly derive, by superposition

$$[\underset{\sim}{C}^{-1}]_{ii} = \frac{V_i}{q_i}\Big|_{q_1, \text{---}, q_{i-1}, q_{i+1}, \text{---}, q_n = 0} \qquad (123a)$$

$$= \frac{1}{2\pi\epsilon} \ln\left(\frac{r_s^2 - r_i^2}{r_s\, r_{wi}}\right)$$

$$[\underset{\sim}{C}^{-1}]_{\substack{ij \\ i\neq j}} = \frac{V_i}{q_j}\Big|_{q_1, \text{---}, q_{j-1}, q_{j+1}, \text{---}, q_n = 0} \qquad (123b)$$

$$= \frac{1}{2\pi\epsilon} \ln\left\{\left(\frac{r_j}{r_s}\right)\sqrt{\frac{(r_i r_j)^2 + r_s^4 - 2 r_i r_j r_s^2 \cos\theta_{ij}}{(r_i r_j)^2 + r_j^4 - 2 r_i r_j^3 \cos\theta_{ij}}}\right\}$$

where θ_{ij} is given in Fig. 2c.

To derive (123), consider an infinitesimal line charge of radius r_w bearing a total per-unit-length free charge q. The potential at a point $r \geq r_w$ with respect to the line charge surface as reference is (see reference [58], page 92)

$$V = - \frac{q}{2\pi\epsilon_v} \ln\left(\frac{r}{r_w}\right) \quad . \tag{124}$$

Equation (123a) can then be derived from Fig. 14a with (124) and $q_j = 0$ as

$$V_i = \frac{q_i}{2\pi\epsilon_v} \left\{ \ln \left(\frac{(r_s^2 / r_i) - r_i}{r_{wi}} \right) - \ln \left(\frac{(r_s^2 / r_i) - r_s}{r_{wi}} \right) + \ln \left(\frac{r_s - r_i}{r_{wi}} \right) \right\}$$

$$= \frac{q_i}{2\pi\epsilon_v} \ln \left(\frac{r_s^2 - r_i^2}{r_s r_{wi}} \right) \quad . \tag{125}$$

Equation (123b) can be derived from Fig. 14b by making use of the result in (124) and the law of cosines. With $q_i = 0$, we obtain

$$V_i = \frac{q_j}{2\pi\epsilon_v} \left\{ \ln\left(\frac{d_2}{r_{wj}}\right) - \ln\left(\frac{d_2^*}{r_{wj}}\right) - \ln\left(\frac{d_1}{r_{wj}}\right) + \ln\left(\frac{d_1^*}{r_{wj}}\right) \right\}$$

$$= \frac{q_j}{2\pi\epsilon_v} \ln \left(\frac{d_2 \, d_1^*}{d_2^* \, d_1} \right) \quad . \tag{126}$$

Utilizing the law of cosines, one may obtain

$$d_2^{*2} = r_s^2 + \left(r_s^2 / r_j\right)^2 - \left(2 r_s^3 / r_j\right) \cos\theta_{ij} \tag{127a}$$

$$d_2^2 = r_i^2 + \left(r_s^2 / r_j\right)^2 - \left(2 r_i r_s^2 / r_j\right) \cos\theta_{ij} \tag{127b}$$

$$d_1^{*2} = r_s^2 + r_j^2 - \left(2 r_s r_j\right) \cos\theta_{ij} \tag{127c}$$

$$d_1^2 = r_i^2 + r_j^2 - \left(2 r_i r_j\right) \cos\theta_{ij} \quad . \tag{127d}$$

Substituting (127) into (126) yields (123b).

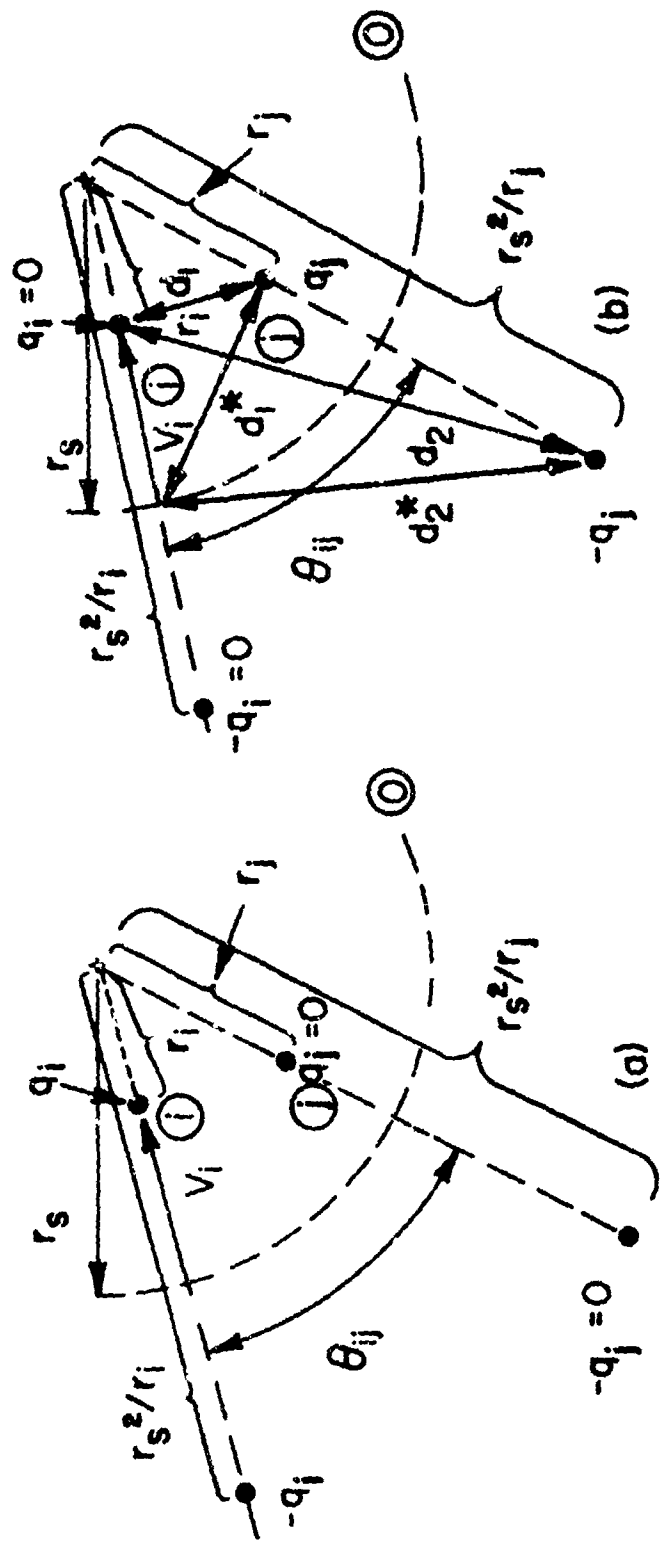

Figure 14. The replacement of the wires and the shield with infinitesimal line charges for shielded, multiconductor lines with large separations in homogeneous media.

5.2 The Per-Unit-Length External Parameters for Lines in an Inhomogeneous Medium

Derivations of the entries in $\underset{\sim}{G}$, $\underset{\sim}{L}$ and $\underset{\sim}{C}$ for the lines in Fig. 3 are complicated by the inhomogeneity of the surrounding medium introduced by the interface between the dielectric insulations and free space. The inhomogeneity is introduced through the permittivities and conductivities of the insulations since the dielectric insulations are characterized by free space permeability, μ_v. Therefore, the per-unit-length external inductance matrix, $\underset{\sim}{L}$, can be found as $\underset{\sim}{L}=\mu_v \epsilon_v \underset{\sim}{C}_0^{-1}$ where $\underset{\sim}{C}_0^{-1}$ is determined as in Section 5.1 with the dielectric insulations removed and may be obtained accurately with moment methods and harmonic expansion functions or may be approximated for large conductor spacings by (119), (122), or (123).

The computation of the entries in $\underset{\sim}{G}$ introduces some conceptual difficulties for the inhomogeneous medium case. Consider the computation of $\underset{\sim}{G}$ for static excitation (reference [39], Chapter 6). The transverse conduction current density $\vec{J}_T$, is related to the transverse electric field, $\vec{e}_T$, in each dielectric as $\vec{J}_T = \sigma_{d_i} \vec{e}_T$. The boundary conditions on the potential function ϕ where $\vec{e}_T = -\text{grad}\ \phi$, is that e_{tan} must vanish over the conductor surfaces (perfect conductors are assumed for this computation) and the derivative of ϕ normal to the dielectric-free space boundaries must vanish at the boundary (see reference [39], chapter 6). The latter requirement insures that the normal component of $\vec{J}_T$ is zero at these

boundaries, i. e. no current flow into the free space medium. The consequence of this is that if none of the dielectric insulations touch each other or the ground plane or circular shield, then $\underset{\sim}{C}$ computed for static conditions with a straightforward application of the above boundary conditions would be identically zero since no conductive path between the conductors would exist for nontouching dielectrics. However, dipole relaxation effects will nevertheless produce certain losses even for a transverse field distribution and nonstatic excitation since the transverse displacement current will have a portion in phase with the transverse electric field. Therefore, equivalent shunt conductances should be determined to represent these non-static losses.

Assuming perfect dielectrics, however, one can compute the entries in $\underset{\sim}{C}$ in a straightforward fashion. A moment method of solution with harmonic expansion functions as in Section 5.1 can be used for this problem [56, 57]. Consider the system of (n+1) dielectric-insulated wires in Fig. 3a. Represent the bound-charge distributions at the dielectric-free space boundaries with Fourier series as [56, 57]

$$\hat{\rho}_i(\theta_i) = \hat{a}_{i0} + \sum_{m=1}^{\hat{A}_i} \hat{a}_{im} \cos m\theta_i + \sum_{m=1}^{\hat{B}_i} \hat{b}_{im} \sin m\theta_i \qquad i=0,\ 1,\ ---,\ n. \tag{128}$$

Represent the charge distributions at the conductor-dielectric boundaries (which is total charge, bound plus free for this case) with Fourier series as in (95). The contributions to the potential and electric field at a point P in Fig. 12b due to each of the components of the charge distributions are given in Table I with respect to Fig. 15 [56, 57].

TABLE I

Contributions to the Potential and Electric Field at a Point **P** in Fig. 15 due to Harmonic Expansion Functions on a Circular Boundary.

Expansion Function	Contribution to the Potential at P	Contribution to the Electric Field at P
1	$-\frac{r_b \ln(r_p)}{\epsilon_v}$	$\frac{r_b}{\epsilon_v r_p}\vec{r}$
$\cos m\theta_b$	$\frac{r_b^{(m+1)} \cos m\theta_p}{2\epsilon_v m r_p^m}$	$\frac{(r_b/r_p)^{m+1}}{2\epsilon_v}\{\cos m\theta_p \vec{r} + \sin m\theta_p \vec{\theta}\}$
$\sin m\theta_b$	$\frac{r_b^{(m+1)} \sin m\theta_p}{2\epsilon_v m r_p^m}$	$\frac{(r_b/r_p)^{m+1}}{2\epsilon_v}\{\sin m\theta_p \vec{r} - \cos m\theta_p \vec{\theta}\}$

(a) $r_p > r_b$

Expansion Function	Contribution to the Potential P	Contribution to the Electric Field at P
1	$-\frac{r_b \ln(r_b)}{\epsilon_v}$	0
$\cos m\theta_b$	$\frac{r_p^m \cos m\theta_p}{2\epsilon_v m (r_b)^{m-1}}$	$-\frac{(r_p/r_b)^{m-1}}{2\epsilon_v}\{\cos m\theta_p \vec{r} - \sin m\theta_p \vec{\theta}\}$
$\sin m\theta_b$	$\frac{r_p^m \sin m\theta_p}{2\epsilon_v m (r_b)^{m-1}}$	$-\frac{(r_p/r_b)^{m-1}}{2\epsilon_v}\{\sin m\theta_p \vec{r} + \cos m\theta_p \vec{\theta}\}$

(b) $r_p < r_b$

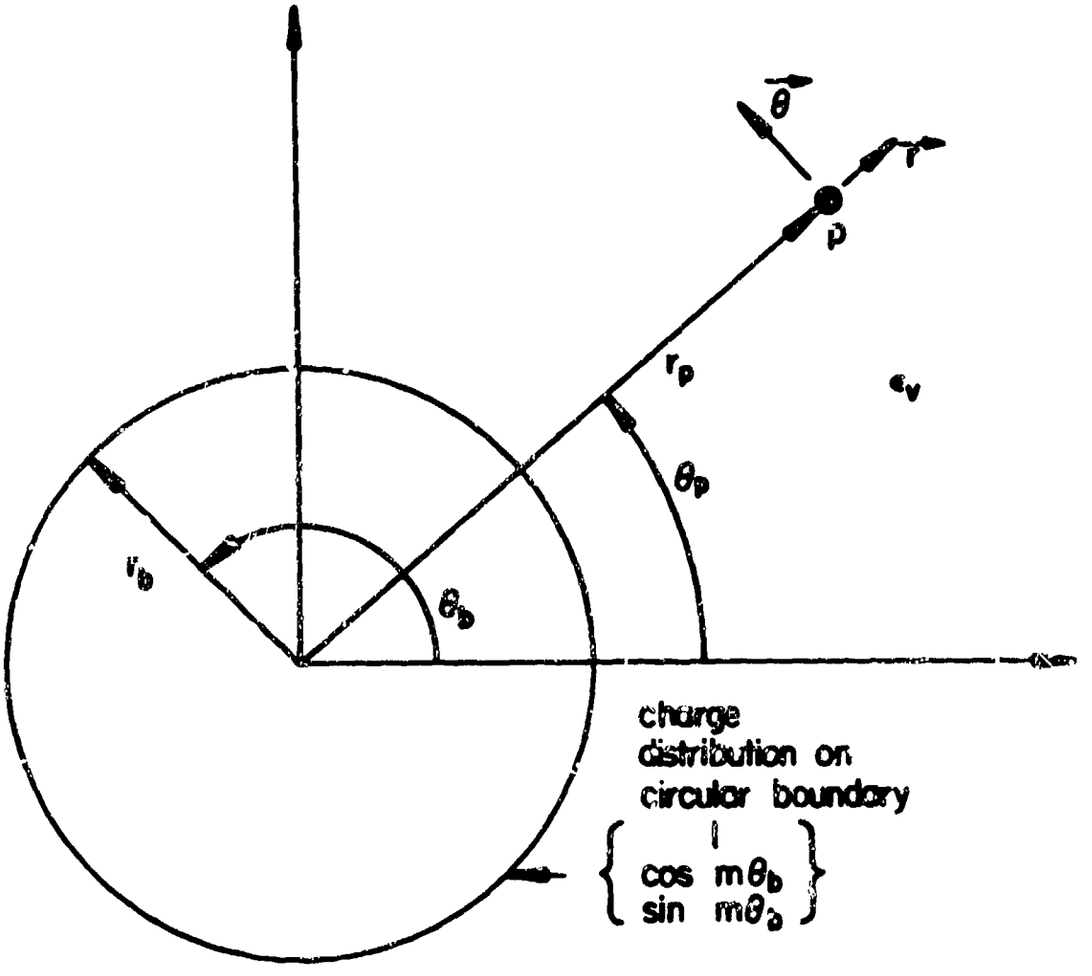

Figure 15. The geometry for Table I.

Thus there are $2 + A_i + B_i + \hat{A}_i + \hat{B}_i$ unknowns associated with each wire, a_{i0}, a_{im}, b_{im}, $\hat{a}_{i0}$, $\hat{a}_{im}$, $\hat{b}_{im}$. The boundary conditions will be enforced by requiring that the potential on the i-th conductor due to all source distributions be ϕ_i and the normal component of the displacement vector due all source distributions be continuous at the dielectric-free space boundaries. Generally $1+A_i + B_i$ match points are selected on the i-th conductor and $1 + \hat{A}_i + \hat{B}_i$ match points are selected on the interface between the i-th dielectric and free space. The component of the total electric field (from all source distributions) normal to and just inside the dielectric-free space surface at each match point on this surface is multiplied by ϵ_i and set equal to the product of ϵ_v and the component of the total electric field (due to all source distributions) normal to and just outside the boundary at this match point. A set of $\sum_{i=0}^{n} (2 + A_i + B_i + \hat{A}_i + \hat{B}_i)$ simultaneous equations can be written to enforce these conditions as [56, 57]

$$\begin{bmatrix} \underset{\sim}{P} \end{bmatrix} \begin{bmatrix} \underline{\rho} \\ \hline \underline{\hat{\rho}} \end{bmatrix} = \begin{bmatrix} \underline{\phi} \\ \hline \underline{0} \end{bmatrix} \tag{129}$$

where $\underline{\rho}$ and $\underline{\phi}$ are defined in (99) and $\underline{\hat{\rho}}$ is a column vector of the expansion coefficients in (128) arranged as in $\underline{\rho}$ and $\underline{0}$ is a column vector of zeros of length $\sum_{i=0}^{n} (1 + \hat{A}_i + \hat{B}_i)$.

Inverting $\underset{\sim}{P}$ in (129), one can obtain [56, 57]

$$\begin{bmatrix} \underline{\rho} \\ \hline \underline{\hat{\rho}} \end{bmatrix} = \begin{bmatrix} \underset{\sim}{P^{-1}} \end{bmatrix} \begin{bmatrix} \underline{\phi} \\ \hline \underline{0} \end{bmatrix} . \tag{130}$$

The total free charge on the i-th conductor (which defines the generalized capacitance matrix) is given by [56, 57]

$$q_{fi} = q_i + \hat{q}_i = \int_0^{2\pi} \rho_i(\theta_i)\, r_{wi}\, d\theta_i + \int_0^{2\pi} \hat{\rho}_i(\theta_i)\,(r_{wi} + t_i)\, d\theta_i \qquad (131)$$

$$= 2\pi r_{wi}\, a_{i0} + 2\pi (r_{wi} + t_i)\, \hat{a}_{i0}$$

since q_i is the total charge at the conductor-dielectric boundary which is the sum of the total free charge and bound charge with the bound charge being identical in magnitude but opposite in sign to the bound charge on the dielectric-free space surface, $\hat{q}_i$, i. e., $q_i = q_{fi} - \hat{q}_i$, and t_i is the thickness of the i-th dielectric. The generalized capacitance matrix can be written as in (102) where q_i in (102) is replaced by q_{fi} from (131). By using the excitation $\phi_j = 1$, $\phi_p = 0, p \neq j$, $[\underset{\sim}{\mathcal{C}}]_{ij}$ equals the sum of two terms. One term is $2\pi r_{wi}$ multiplied by the sum of all elements in $\underset{\sim}{P}^{-1}$ which are in the row associated with a_{i0} and columns associated with ϕ_j and the other term is $2\pi (r_{wi} + t_i)$ multiplied by the sum of all elements in $\underset{\sim}{P}^{-1}$ which are in the row associated with $\hat{a}_{i0}$ and the columns associated with ϕ_j [56, 57]. The entries in the n χ n per-unit-length capacitance matrix, $\underset{\sim}{C}$ used in the transmission line equations can then be straightforwardly obtained from the (n+1) χ (n+1) generalized capacitance matrix, $\underset{\sim}{\mathcal{C}}$, as in (111).

Typical computed results for two dielectric-insulated wires are shown in Fig. 16. By symmetry, the coefficients of the terms in (95) and (128) are zero, i. e. $b_{im} = 0$ and $\hat{b}_{im} = 0$. Therefore the expansion func-

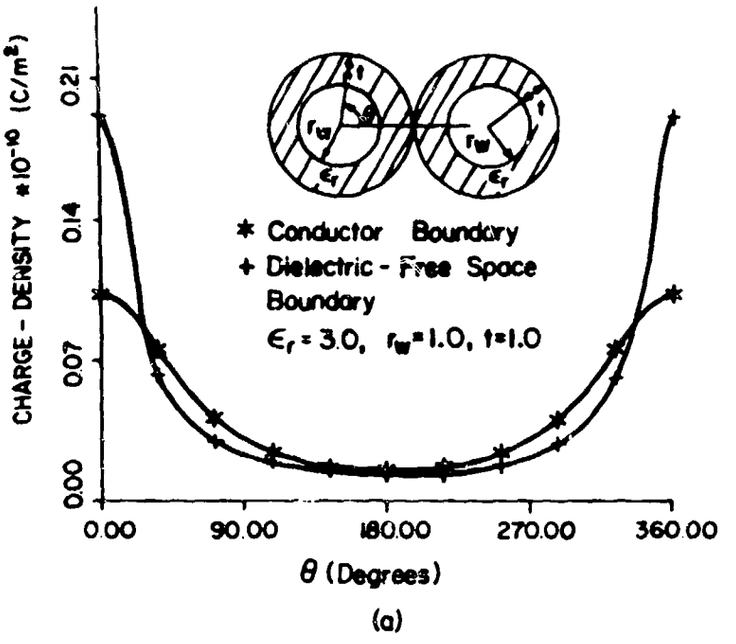

(a)

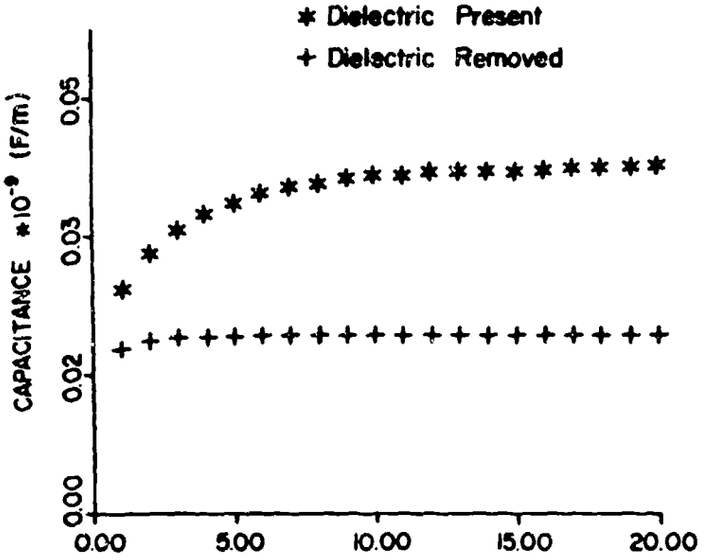

(b)

Figure 16. Computed results for two dielectric-insulated wires.

tions on each boundary consist of the constant term and only cosine terms. Similar results for a 5-wire flat pack cable are shown in Fig. 17. Selected entries in the first row of the generalized capacitance matrix, $C_{00}, C_{01}, C_{02}, C_{03}, C_{04}$ are shown. Again by symmetry, the sine expansion functions are not included since the coefficients of these terms will be zero for wires in a linear array such as flat pack cables.

These results can be extended to include the case of n wires above an infinite ground plane in Fig. 3b in the following manner. Consider the set of n dielectric-insulated wires above an infinite ground plane shown in Fig. 18. To treat these cases, we replace the ground plane with a corresponding set of image wires. The i-th wire image is at a distance of h_i below the ground plane. Each image wire is identical to its corresponding wire above the ground plane and the potential of the i-th conductor image is $-\phi_i$. The charge distributions around the i-th conductor and i-th dielectric-free space boundary are denoted by $\rho_i(\theta_i)$ and $\hat{\rho}_i(\theta_i)$, respectively. The charge distributions on the corresponding boundaries of the image wires are identical in magnitude but opposite in sign to those of the corresponding wires above the ground plane, i.e. $-\rho_i(-\theta_i)$ and $-\hat{\rho}_i(-\theta_i)$. The charge distributions ρ_i and $\hat{\rho}_i$ are again expanded into Fourier series.

A set of simultaneous equations in terms of the unknown expansion coefficients in ρ_i and $\hat{\rho}_i$ can again be formulated to enforce the boundary conditions on the potential of the i-th conductor and the continuity of the normal components of the displacement vector at the dielectric-free space

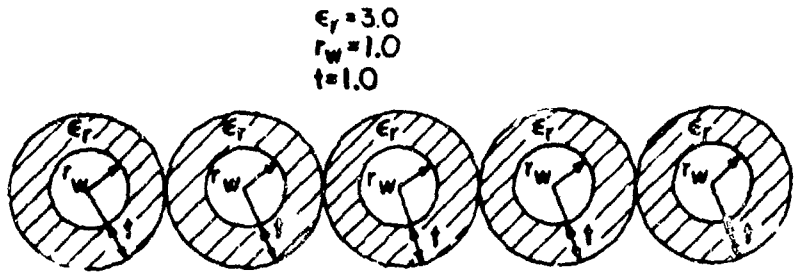

(a)

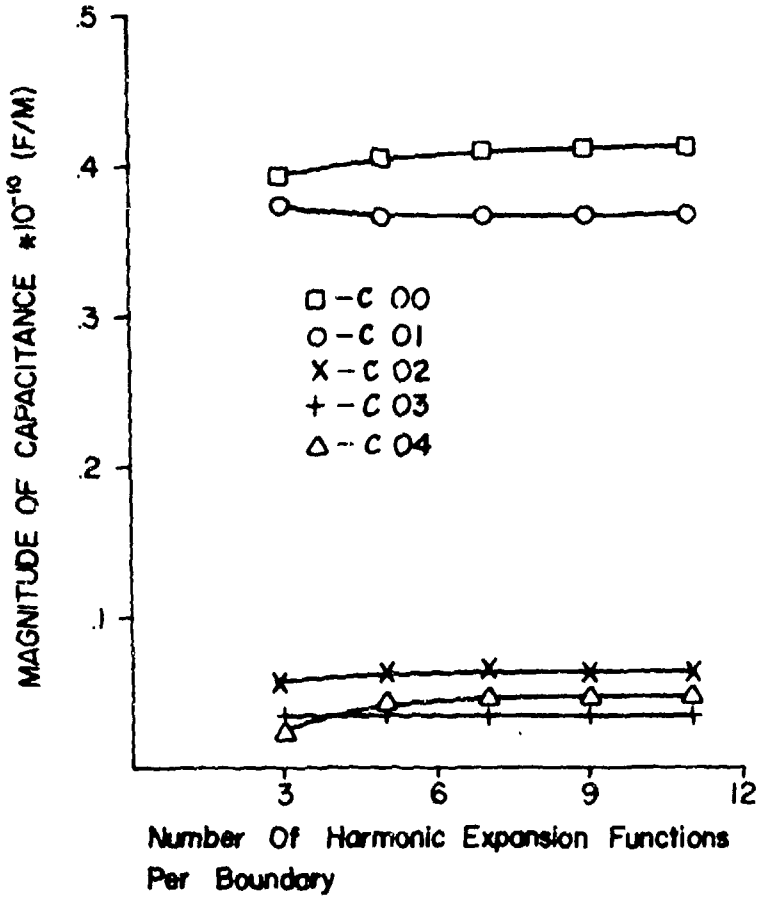

(b)

Figure 17. Computed results for a five-wire ribbon cable.

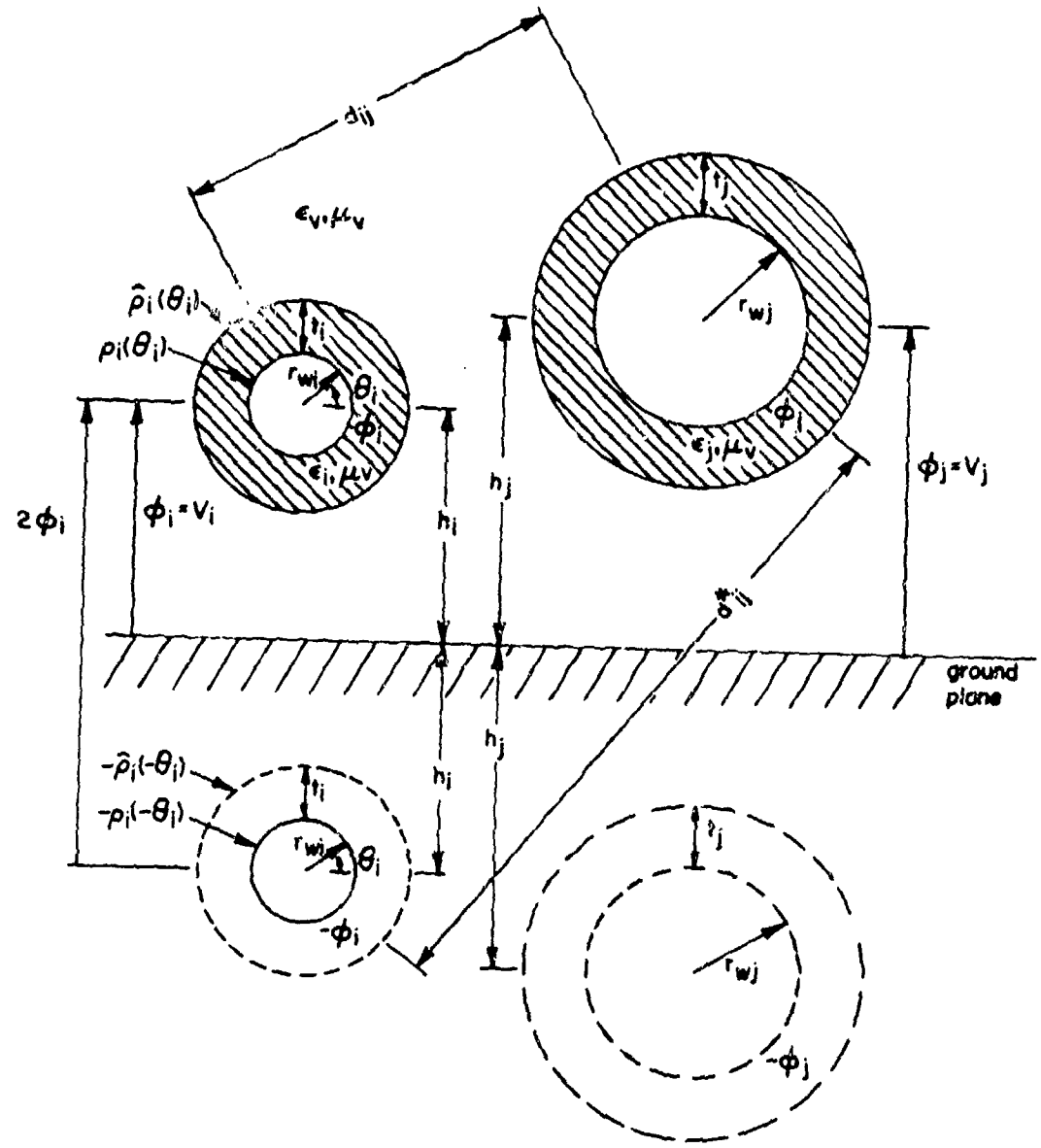

Figure 18. Dielectric-insulated wires above a ground plane and the image distributions.

boundaries of each wire due to all charge distributions in the system (the distributions on the wires and their images). By symmetry and the use of image distributions, we only need to write $\sum_{i=1}^{n} (2 + A_i + B_i + \hat{A}_i + \hat{B}_i)$ equations to enforce these boundary conditions on only the original n wires above the ground plane. Once these equations are solved, the per-unit-length transmission line capacitance matrix, $\underset{\sim}{C}$, can be directly obtained as before since, for this case, $\phi_i = V_i$ where V_i are the transmission line voltages with respect to the ground plane as shown in Fig. 18. Thus for this case as for Fig. 2b, there is no need to reduce the generalized capacitance matrix to the transmission line capacitance matrix via (111).

The per-unit-length transmission line inductance matrix, $\underset{\sim}{L}$, can be obtained accurately by repeating this solution with the insulation dielectrics removed and using (89) as indicated in Section 5.1 or using the large-separation approximation in (122).

The solution for n wires in a circular shield in Fig. 3c can be obtained in the same fashion as discussed in Section 5.1 for the case of Fig. 2c.

The above discussion of the solution for $\underset{\sim}{C}$ assuming perfect dielectrics indicates a method for incorporating dielectric loss and therefore obtaining an equivalent per-unit-length conductance matrix, $\underset{\sim}{G}$, to represent these losses. If each dielectric permittivity is considered to be complex, i.e., $\epsilon_i = \epsilon_i' - j\epsilon_i'' - j(\sigma_{di}/\omega)$ then (129) can be formulated as above with the only difference being that $\underset{\sim}{P}$ will now be complex. In

particular, the last $1 + \hat{A}_i + \hat{B}_i$ rows of $\underset{\sim}{P}$ will be complex. Thus the $n \times n$ complex, capacitance matrix can be obtained as above as $\underset{\sim}{C} = \underset{\sim}{C}_R + j\underset{\sim}{C}_I$ so that $j\omega\underset{\sim}{C} = j\omega\underset{\sim}{C}_R - \omega^2 \underset{\sim}{C}_I$ and the imaginary part of $\underset{\sim}{C}$ can be identified as $\underset{\sim}{G} = -\omega^2 \underset{\sim}{C}_I$. The real part, $\underset{\sim}{C}_R$, is identified as the usual capacitance matrix and will of course not be the same as the matrix which would be computed assuming a perfect dielectric.

Large-separation approximations can also be obtained in a fashion similar to Section 5.1 by requiring that the separation between all wires be large enough so that the charge distributions around the dielectric-free space boundaries and the conductor-dielectric boundaries are essentially constant. However, this is generally not the problem of interest since wires are closely-coupled in densely-packed cable bundles and flat pack and ribbon cables and it is to be expected that the charge distributions around the boundaries will exhibit large variations.

However, to illustrate the application of the technique, the per-unit-length capacitance between two dielectric-insulated wires which are widely separated will be derived. Consider the case of two dielectric-insulated wires shown in Fig. 19. Because of the assumption of large separations, we may assume that the charge distributions around the conductor-dielectric boundaries and the dielectric-free space boundaries are constant. Therefore, only four expansion terms are needed in (95) and (128), a_{00}, $\hat{a}_{00}$, a_{10}, $\hat{a}_{10}$. To facilitate the derivation and provide an upper bound on the per-unit-length capacitance, we will take the match points at the

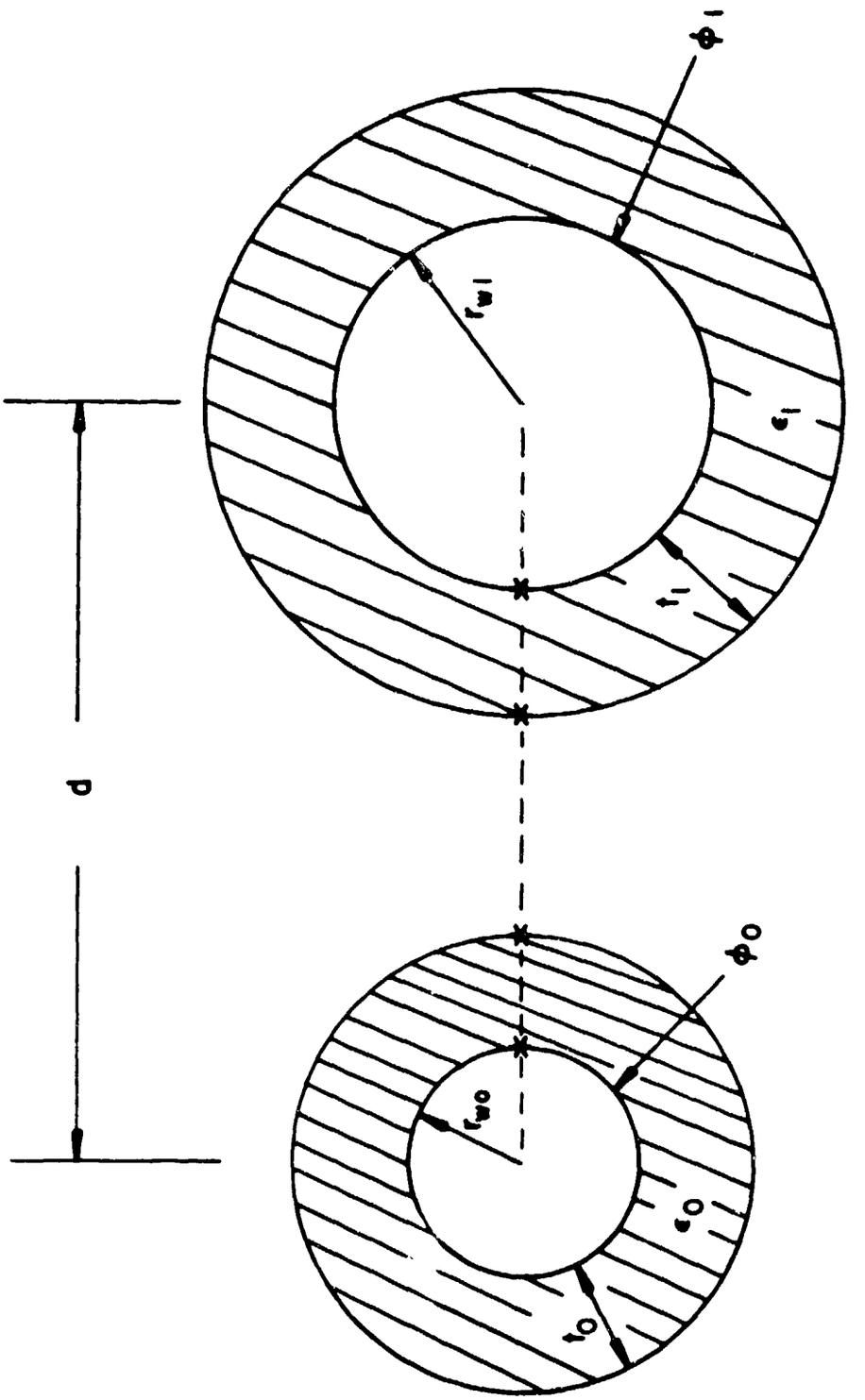

Figure 19. A two-wire line and the selection of the match points.

boundaries on a line joining the centers of the wires as shown in Fig. 19. From the previous results and Table I, one may obtain

$$\phi_0 = -a_{00}\left(\frac{r_{w0}\,\ell n(r_{w0})}{\epsilon_v}\right) - a_{10}\left(\frac{r_{w1}\,\ell n(d-r_{w0})}{\epsilon_v}\right) \qquad (132a)$$

$$-\hat{a}_{00}\left(\frac{(r_{w0}+t_0)\,\ell n\,(r_{w0}+t_0)}{\epsilon_v}\right) - \hat{a}_{10}\left(\frac{(r_{w1}+t_1)\,\ell n\,(d-r_{w0})}{\epsilon_v}\right)$$

$$\phi_1 = -a_{00}\left(\frac{r_{w0}\,\ell n\,(d-r_{w1})}{\epsilon_v}\right) - a_{10}\left(\frac{r_{w1}\,\ell n\,(r_{w1})}{\epsilon_v}\right) \qquad (132b)$$

$$-\hat{a}_{00}\left(\frac{(r_{w0}+t_0)\,\ell n\,(d-r_{w1})}{\epsilon_v}\right) - \hat{a}_{10}\left(\frac{(r_{w1}+t_1)\,\ell n\,(r_{w1}+t_1)}{\epsilon_v}\right)$$

$$a_{00}\left(\frac{r_{w0}\,(\epsilon_{r0}-1)}{(r_{w0}+t_0)}\right) - a_{10}\left(\frac{r_{w1}\,(\epsilon_{r0}-1)}{(d-r_{w0}-t_0)}\right) \qquad (132c)$$

$$+\hat{a}_{00}\left(-1\right) - \hat{a}_{10}\left(\frac{(r_{w1}+t_1)\,(\epsilon_{r0}-1)}{(d-r_{w0}-t_0)}\right) = 0$$

$$a_{00}\left(\frac{r_{w0}\,(\epsilon_{r1}-1)}{(d-r_{w1}-t_1)}\right) - a_{10}\left(\frac{r_{w1}\,(\epsilon_{r1}-1)}{(r_{w1}+t_1)}\right) \qquad (132d)$$

$$+\hat{a}_{00}\left(\frac{(r_{w0}+t_0)\,(\epsilon_{r1}-1)}{(d-r_{w1}-t_1)}\right) + \hat{a}_{10}\left(1\right) = 0$$

where $\epsilon_{r0} = \epsilon_0 / \epsilon_v$ and $\epsilon_{r1} = \epsilon_1 / \epsilon_v$.

These equations may be solved for numerical values of the parameters as outlined previously. However, in literal notation, the solution is quite complicated. Therefore, to simplify the solution and obtain a closed form expression for the per-unit-length capacitance, we will assume that the wires are identical, i.e.,

$$r_{w0} = r_{w1} = r_w \tag{133a}$$

$$t_0 = t_1 = t \tag{133b}$$

$$\epsilon_0 = \epsilon_1 = \epsilon \tag{133c}$$

$$\epsilon_r = \epsilon/\epsilon_v \quad . \tag{133d}$$

With this assumption we may take the charge distributions on wire 0 to be identical to the charge distributions on wire 1 by symmetry. Furthermore,

$$q_1 = 2\pi r_w a_{10} = q \tag{134a}$$

$$q_0 = 2\pi r_w a_{00} = -q \tag{134b}$$

$$\hat{q}_1 = 2\pi (r_w + t) \hat{a}_{10} = \hat{q} \tag{134c}$$

$$\hat{q}_0 = 2\pi (r_w + t) \hat{a}_{00} = -\hat{q} \quad . \tag{134d}$$

Substituting (133) and (134) into (132) yields

$$\phi_0 = \frac{1}{2\pi\epsilon_v} \left\{ \ln\left(\frac{r_w}{d-r_w}\right) q + \ln\left(\frac{r_w+t}{d-r_w}\right) \hat{q} \right\} \tag{135a}$$

$$\phi_1 = \frac{1}{2\pi\epsilon_v} \left\{ \ln\left(\frac{d-r_w}{r_w}\right) q + \ln\left(\frac{d-r_w}{r_w+t}\right) \hat{q} \right\} \tag{135b}$$

$$\left(\frac{(\epsilon_r-1)}{(r_w+t)} + \frac{(\epsilon_r-1)}{(d-r_w-t)}\right) q + \left(\frac{(\epsilon_r-1)}{(d-r_w-t)} - \frac{1}{(r_w+t)}\right) \hat{q} = 0 \tag{135c}$$

$$\left(\frac{(\epsilon_r-1)}{(d-r_w-t)} + \frac{(\epsilon_r-1)}{(r_w+t)}\right) q + \left(\frac{(\epsilon_r-1)}{(d-r_w-t)} - \frac{1}{(r_w+t)}\right) \hat{q} = 0. \tag{135d}$$

Note that (135a) and (135b) show that

$$\phi_0 = -\phi_1 \tag{136}$$

and (135c) and (135d) are identical. Therefore

$$V = \phi_1 - \phi_0 = 2\phi_1 \quad . \tag{137}$$

Note also from (131) that $q_f = q + \hat{q}$ and therefore

$$q = q_f - \hat{q} \quad . \tag{138}$$

Substituting (138) into (135b) and (135c) with (137) yields

$$V = \frac{1}{\pi\epsilon_v}\left\{ \ell n\left(\frac{d-r_w}{r_w}\right) q_f + \ell n\left(\frac{r_w}{r_w+t}\right) \hat{q} \right\} \tag{139}$$

and

$$\hat{q} = \frac{(\epsilon_r - 1)\, d}{\epsilon_r(d-r_w-t)} \quad q_f \quad . \tag{140}$$

Substituting (140) into (139) yields the per-unit-length capacitance as

$$c = \frac{q_f}{V}$$

$$= \frac{\pi \epsilon_v}{\ell n\left(\frac{d-r_w}{r_w}\right) - \left(\frac{(\epsilon_r - 1)\, d}{\epsilon_r(d-r_w-t)}\right) \ell n\left(\frac{r_w+t}{r_w}\right)} \quad . \tag{141}$$

As a check on this result, note that for ϵ_r=1 and t=0, (141) reduces to (91) for identical wires and large separations such that $d - r_w \cong d$.

As a final illustration of these methods, we will compute the entries in the per-unit-length transmission line capacitance matrix for the case of two dielectric-insulated wires above an infinite ground plane. In order to simplify the procedure and to obtain closed-form expressions for these quantities, we will assume that (1) both wires are identical and are at the same height above the ground plane, and (2) the wires are separated sufficiently from each other and the ground plane so that we may assume constant charge distributions around the conductor and dielectric boundaries, i.e.,

$$q_1 = 2\pi r_w a_{10} \tag{142a}$$

$$\hat{q}_1 = 2\pi r_d \hat{a}_{10} \qquad (r_d = r_w + t) \tag{142b}$$

$$q_2 = 2\pi r_w a_{20} \tag{142c}$$

$$\hat{q}_2 = 2\pi r_d \hat{a}_{20} \qquad (r_d = r_w + t) \quad . \tag{142d}$$

The ground plane will be replaced by images as shown in Fig. 20. We choose the match points 1, $\hat{1}$, 2, and $\hat{2}$ on a line joining the two wires (other choices are of course possible).

Applying the results of this section and utilizing symmetry we only need to write constraint equations at match points 1 and $\hat{1}$. The equation for the potential at 1 becomes (see Table I)

$$\begin{aligned}\phi_1 = -\frac{1}{2\pi\epsilon_v}\Big\{ & \ell n(r_w)\, q_1 + \ell n\,(r_d)\,\hat{q}_1 \\ & + \ell n\,(d-r_w) q_2 + \ell n(d-r_w)\hat{q}_2 \\ & + \ell n(d_1)(-q_1) + \ell n(d_1)(-\hat{q}_1) \\ & + \ell n(d_2)(-q_2) + \ell n(d_2)(-\hat{q}_2)\Big\} \quad .\end{aligned} \tag{143}$$

The distances d_1, $\hat{d}_1$, d_2 and $\hat{d}_2$ in Fig. 20 are given by

$$d_1 = \sqrt{4h^2 + r_w^2} \tag{144a}$$

$$\hat{d}_1 = \sqrt{4h^2 + r_d^2} \tag{144b}$$

$$d_2 = \sqrt{4h^2 + (d-r_w)^2} \tag{144c}$$

$$\hat{d}_2 = \sqrt{4h^2 + (d-r_d)^2} \quad . \tag{144d}$$

The equation for the continuity of the normal component of the displacement vector at $\hat{1}$ becomes (see Table I)

$$\frac{1}{\epsilon_v r_d} q_1 + \frac{1}{\epsilon_v r_d} \hat{q}_1 - \frac{1}{\epsilon_v (d-r_d)} q_2 - \frac{1}{\epsilon_v (d-r_d)} \hat{q}_2 \tag{145}$$

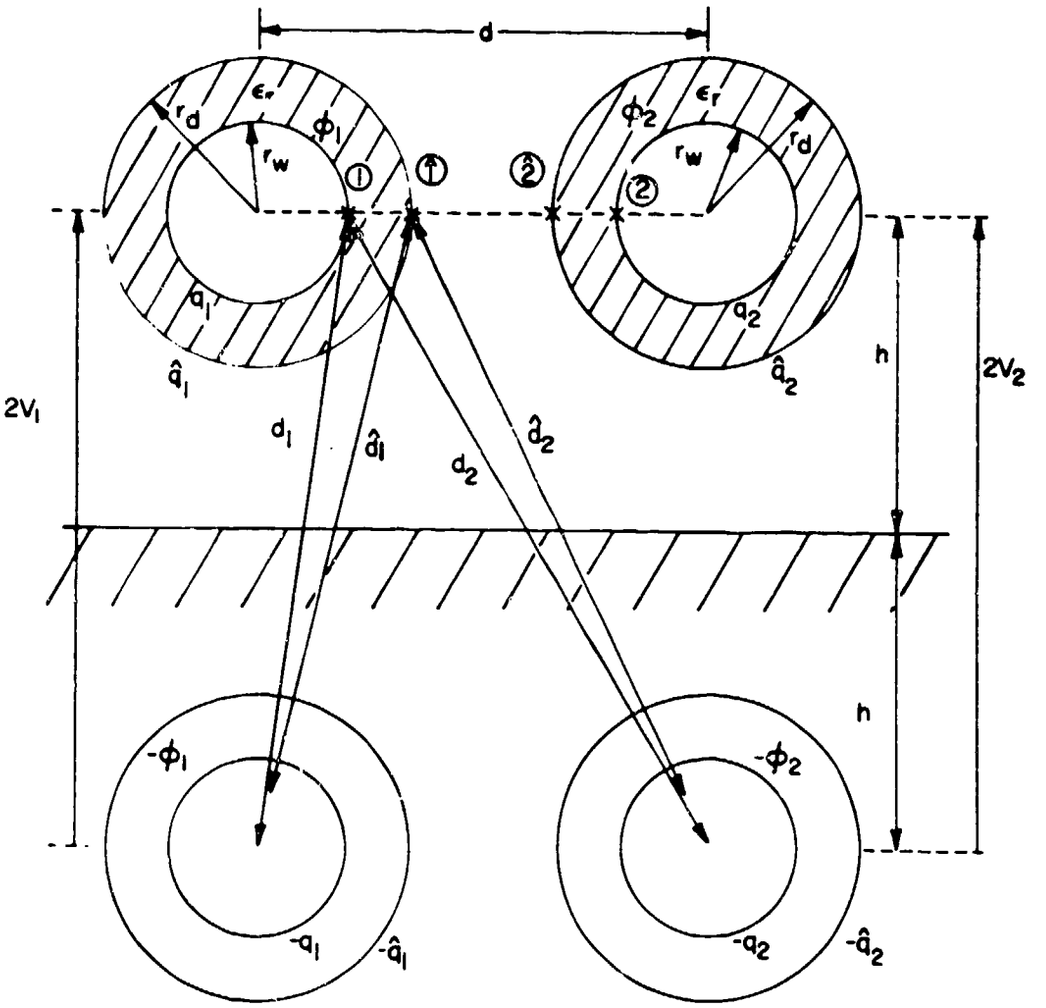

Figure 20. A two-wire line above a ground plane and the selection of the match points.

$$+ \frac{1}{\epsilon_v \hat{d}_1}\left(\frac{r_d}{\hat{d}_1}\right)(-q_1) + \frac{1}{\epsilon_v \hat{d}_1}\left(\frac{r_d}{\hat{d}_1}\right)(-\hat{q}_1)$$

$$- \frac{1}{\epsilon_v \hat{d}_2}\left(\frac{d-r_d}{\hat{d}_2}\right)(-q_2) - \frac{1}{\epsilon_v \hat{d}_2}\left(\frac{d-r_d}{\hat{d}_2}\right)(-\hat{q}_2)$$

$$= \epsilon_r\left\{\frac{1}{\epsilon_v r_d} q_1 + (0)\,\hat{q}_1 - \frac{1}{\epsilon_v(d-r_d)} q_2 - \frac{1}{\epsilon_v(d-r_d)}\hat{q}_2\right.$$

$$+ \frac{1}{\epsilon_v \hat{d}_1}\left(\frac{r_d}{\hat{d}_1}\right)(-q_1) + \frac{1}{\epsilon_v \hat{d}_1}\left(\frac{r_d}{\hat{d}_1}\right)(-\hat{q}_1)$$

$$\left. - \frac{1}{\epsilon_v \hat{d}_2}\left(\frac{d-r_d}{\hat{d}_2}\right)(-q_2) - \frac{1}{\epsilon_v \hat{d}_2}\left(\frac{d-r_d}{\hat{d}_2}\right)(-\hat{q}_2)\right\} .$$

Collecting terms, (145) can be written as

$$\left(\frac{1}{r_d} - \frac{r_d}{(\hat{d}_1)^2} - \frac{\epsilon_r}{r_d} + \frac{\epsilon_r r_d}{(\hat{d}_1)^2}\right) q_1 \qquad (146)$$

$$+ \left(\frac{1}{r_d} - \frac{r_d}{(\hat{d}_1)^2} + \epsilon_r \frac{r_d}{(\hat{d}_1)^2}\right) \hat{q}_1$$

$$+ \left(-\frac{1}{(d-r_d)} + \frac{(d-r_d)}{(\hat{d}_2)^2} + \frac{\epsilon_r}{(d-r_d)} - \frac{\epsilon_r(d-r_d)}{(\hat{d}_2)^2}\right) q_2$$

$$+ \left(-\frac{1}{(d-r_d)} + \frac{(d-r_d)}{(\hat{d}_2)^2} + \frac{\epsilon_r}{(d-r_d)} - \frac{\epsilon_r(d-r_d)}{(\hat{d}_2)^2}\right) \hat{q}_2 = 0 .$$

Since the wires are assumed to be sufficiently separated from each other and the ground plane, we may make the following approximations:

$$d_1 \cong 2h \qquad (147a)$$

$$\hat{d}_1 \cong 2h \qquad (147b)$$

$$d_2 \cong \sqrt{4h^2 + d^2} \qquad (147c)$$

$$\triangleq d^*$$

$$\hat{d}_2 \cong d_2 \tag{147d}$$

$$d - r_w \cong d \tag{147e}$$

$$d - r_d \cong d \quad . \tag{147f}$$

Utilizing these relations in (143) and (146) we obtain ($V_1 = \phi_1$)

$$2\pi\epsilon_v V_1 \cong \left\{ \ell n\left(\frac{2h}{r_w}\right) q_1 + \ell n\left(\frac{2h}{r_d}\right) \hat{q}_1 \right. \tag{148a}$$

$$\left. + \ell n\left(\frac{d^*}{d}\right) q_2 + \ell n\left(\frac{d^*}{d}\right) \hat{q}_2 \right\}$$

$$\left\{ (\epsilon_r - 1)\left(\frac{r_d}{4h^2} - \frac{1}{r_d}\right) \right\} q_1 + \left\{ (\epsilon_r - 1) \frac{r_d}{4h^2} + \frac{1}{r_d} \right\} \hat{q}_1 \tag{148b}$$

$$- \left\{ (\epsilon_r - 1) \left(\frac{d}{(d^*)^2} - \frac{1}{d}\right) \right\} q_2$$

$$- \left\{ (\epsilon_r - 1) \left(\frac{d}{(d^*)^2} - \frac{1}{d}\right) \right\} \hat{q}_2 = 0 \quad .$$

The total free charges on the conductors are given by

$$q_{f1} = q_1 + \hat{q}_1 \tag{149a}$$

$$q_{f2} = q_2 + \hat{q}_2 \quad . \tag{149b}$$

Therefore (148) (along with similar equations at match points 2 and $\hat{2}$) may be written as

$$2\pi\epsilon_v \begin{bmatrix} V_1 \\ V_2 \end{bmatrix} = \begin{bmatrix} A & B \\ B & A \end{bmatrix} \begin{bmatrix} q_1 \\ q_2 \end{bmatrix} + \begin{bmatrix} C & D \\ D & C \end{bmatrix} \begin{bmatrix} \hat{q}_1 \\ \hat{q}_2 \end{bmatrix} \tag{150}$$

$$= \begin{bmatrix} C & D \\ D & C \end{bmatrix} \begin{bmatrix} q_{f1} \\ q_{f2} \end{bmatrix} + \begin{bmatrix} (A-C) & (B-D) \\ (B-D) & (A-C) \end{bmatrix} \begin{bmatrix} q_1 \\ q_2 \end{bmatrix}$$

and

$$\begin{bmatrix} 0 \\ 0 \end{bmatrix} = \begin{bmatrix} E & F \\ F & E \end{bmatrix} \begin{bmatrix} q_1 \\ q_2 \end{bmatrix} + \begin{bmatrix} G & H \\ H & G \end{bmatrix} \begin{bmatrix} \hat{q}_1 \\ \hat{q}_2 \end{bmatrix} \tag{151}$$

$$= \begin{bmatrix} G & H \\ H & G \end{bmatrix} \begin{bmatrix} q_{f1} \\ q_{f2} \end{bmatrix} + \begin{bmatrix} (E-G) & (F-H) \\ (F-H) & (E-G) \end{bmatrix} \begin{bmatrix} q_1 \\ q_2 \end{bmatrix} .$$

where from (148)

$$A = \ell n \left(\frac{2h}{r_w}\right) \tag{152a}$$

$$B = \ell n \left(\frac{d^*}{d}\right) \tag{152b}$$

$$C = \ell n \left(\frac{2h}{r_d}\right) \tag{152c}$$

$$D = B \tag{152d}$$

$$E = (\epsilon_r - 1) \left(\frac{r_d}{4h^2} - \frac{1}{r_d}\right) \tag{152e}$$

$$F = -(\epsilon_r - 1) \left(\frac{d}{(d^*)^2} - \frac{1}{d}\right) \tag{152f}$$

$$G = (\epsilon_r - 1) \frac{r_d}{4h^2} + \frac{1}{r_d} \tag{152g}$$

$$H = F \quad . \tag{152h}$$

The variables q_1 and q_2 can be easily eliminated from equations (150) and (151) since D=B and H=F and the result is

$$\begin{bmatrix} V_1 \\ V_2 \end{bmatrix} = \frac{1}{2\pi\epsilon_v} \left\{ \begin{bmatrix} C & D \\ D & C \end{bmatrix} - \frac{(A-C)}{(E-G)} \begin{bmatrix} G & H \\ H & G \end{bmatrix} \right\} \begin{bmatrix} q_{f1} \\ q_{f2} \end{bmatrix} . \tag{153}$$

Therefore the entries in the inverse of the per-unit-length transmission line capacitance matrix are given by

$$[\underset{\sim}{C}^{-1}]_{ii} = \frac{1}{2\pi\epsilon_v} \left\{ C - \frac{(A-C)}{(E-G)} G \right\} \tag{154a}$$

$$= \frac{1}{2\pi\epsilon_v} \left\{ \ell n \left(\frac{2h}{r_d}\right) + \frac{r_d}{\epsilon_r} \left(\ell n \left(\frac{r_d}{r_w}\right) \right) \left((\epsilon_r - 1) \frac{r_d}{4h^2} + \frac{1}{r_d} \right) \right\}$$

$$[\underset{\sim}{C}^{-1}]_{ij} = \frac{1}{2\pi\epsilon_v}\left\{ D - \frac{(A-C)}{(E-G)} H \right\} \qquad (154b)$$

$$= \frac{1}{2\pi\epsilon_v}\left\{ \ell n \left(\frac{d^*}{d}\right) + \frac{(\epsilon_r - 1) r_d}{\epsilon_r} \left(\ell n \left(\frac{r_d}{r_w}\right)\right)\left(\frac{(d^*)^2 - d^2}{d(d^*)^2}\right) \right\}$$

for i, j=1, 2 and d^* is given by

$$d^* = \sqrt{4h^2 + d^2} \quad . \qquad (155)$$

For this case, we assumed that (1) the two wires are identical, (2) they are at the same height above the ground plane and (3) the wires are sufficiently separated from each other and the ground plane such that the assumption of constant charge distribution is valid. When these assumptions are no longer valid, the expression for the entries in $\underset{\sim}{C}^{-1}$ or $\underset{\sim}{C}$ cannot be easily obtained in closed form and a digital computer must be used. The expressions in (154) for the entries in $\underset{\sim}{C}^{-1}$ will be used in a later publication in the analysis of certain experimental data for which this approximation is reasonably accurate. It should be noted that an approximation for c_{12} for this specific example has been obtained in [33] although the derivation is not presented and evidently relies on certain empirical data.

VI. SUMMARY

A complete and unified discussion of multiconductor transmission line theory has been presented. The general solution of the problem under the assumption of TEM mode propagation in the case of a homogeneous medium or quasi - TEM mode propagation in the case of an inhomogeneous medium has been presented along with parameter derivations and lumped-circuit approximations. If losses can be neglected, then it appears to be as efficient to solve the transmission line equations directly and incorporate the termination networks through the solution of (70), (75) or (76) as it is to use lumped-circuit iterative approximations described in Section 4.1. The matrix chain parameters for the distributed-parameter approach can be easily obtained in closed form suitable for numerical computation so that "abruptly" nonuniform lines can be handled and the per-unit-length parameters must be obtained for either the distributed-parameter or the lumped-circuit iterative approach. When solving the transmission line equations directly, one is not required to solve an increasingly-large (although sparse) set of equations for increasing frequencies when the line is not electrically short as is required with the lumped-circuit iterative approximations. For the homogeneous-medium case, a lossy dielectric can also be included with no additional computational difficulties. Lossy conductors will also present no additional computational problems for the homogeneous-medium case if the n conductors are assumed to be identical. When losses cannot be neglected in the case of an inhomogeneous medium, the question becomes more difficult to answer since

diagonalization of $\underset{\sim}{Y}\underset{\sim}{Z}$, which is required in a direct solution of the transmission line equations, is, in general, required to be performed at each frequency and is not necessarily guaranteed except in the case of cyclic symmetry matrices which assume certain structural symmetries of the line as described in Section 3.3. For this case, it may be preferable to use one of the lumped-circuit iterative models for frequencies where the line is electrically short, e.g., $\ell < {}^{1}/_{10}\,\lambda$, and approximate the line with only one section, i.e., solve (80) with N=1. For frequencies such that $\ell > {}^{1}/_{10}\lambda$, it may be preferable to solve the transmission line equations directly rather than increasing the number of lumped-circuit sections to approximate the line since no quantitative criterion for determining the required number of sections for a given approximation accuracy can evidently be obtained. Numerical techniques for obtaining the per-unit-length parameters for bundles of closely-coupled, dielectric-coated wires as well as large-separation approximations for wires in a homogeneous medium are also given.

APPENDIX A

The purpose of this appendix is to demonstrate certain important properties of the TEM mode assumption given in Section II. An appropriate reference for these results is [40].

The first objective is to show that, for the TEM mode of propagation, the transverse electric field vector and transverse magnetic field vector satisfy the same spatial distributions as static (DC) fields at each x along the line. The electric field intensity vector and the magnetic field intensity vector for the steady state and sinusoidal excitation are written as $\vec{\mathcal{E}}(x, y, z, t) = \vec{E}(x, y, z)\, e^{j\omega t}$ and $\vec{\mathcal{H}}(x, y, z, t) = \vec{H}(x, y, z)\, e^{j\omega t}$ respectively where

$$\vec{E}(x, y, z) = E_x \vec{x} + E_y \vec{y} + E_z \vec{z} \qquad \text{(A-1a)}$$

$$\vec{H}(x, y, z) = H_x \vec{x} + H_y \vec{y} + H_z \vec{z} \qquad \text{(A-1b)}$$

and $\vec{x}, \vec{y}, \vec{z}$ are unit vectors in the x, y and z directions respectively. Assuming the TEM mode of propagation, $E_x = H_x = 0$, the field vectors are entirely transverse to the x direction and are denoted as

$$\vec{E}_T(x, y, z) = E_y \vec{y} + E_z \vec{z} \qquad \text{(A-2a)}$$

$$\vec{H}_T(x, y, z) = H_y \vec{y} + H_z \vec{z} \qquad \text{(A-2b)}$$

Now consider the general (n+1)-conductor, uniform transmission line in Fig. 1a consisting of (n+1) perfect conductors in a linear, isotropic and homogeneous medium. Faraday's law and Ampere's law become for the TEM mode of propagation (in the source-free medium)

$$\nabla \times \vec{E}_T = - j\omega\mu \vec{H}_T \qquad \text{(A-3a)}$$

$$\nabla \times \vec{H}_T = (\sigma + j\omega\epsilon) \vec{E}_T \qquad \text{(A-3b)}$$

where the medium may be lossy through the effective conductivity σ which includes ohmic conductivity and dipole relaxation losses and ϵ refers to the real part of the complex permittivity.

Separating the curl operator into a transverse and a longitudinal component as

$$\nabla = \underbrace{\left(\vec{y}\frac{\partial}{\partial y} + \vec{z}\frac{\partial}{\partial z}\right)}_{\nabla_T} + \vec{x}\frac{\partial}{\partial x} \qquad \text{(A-4)}$$

and applying to (A-3) we obtain

$$\nabla_T \times \vec{E}_T + \frac{\partial}{\partial x}(\vec{x} \times \vec{E}_T) = - j\omega\mu \vec{H}_T \qquad \text{(A-5a)}$$

$$\nabla_T \times \vec{H}_T + \frac{\partial}{\partial x}(\vec{x} \times \vec{H}_T) = (\sigma + j\omega\epsilon) \vec{E}_T \quad . \qquad \text{(A-5b)}$$

However, $\nabla_T \times \vec{E}_T$ and $\nabla_T \times \vec{H}_T$ are vectors in the x direction only. Therefore we have by matching components

$$\nabla_T \times \vec{E}_T = 0 \qquad \text{(A-6a)}$$

$$\frac{\partial}{\partial x}(\vec{x} \times \vec{E}_T) = - j\omega\mu \vec{H}_T \qquad \text{(A-6b)}$$

$$\nabla_T \times \vec{H}_T = 0 \qquad \text{(A-6c)}$$

$$\frac{\partial}{\partial x}(\vec{x} \times \vec{H}_T) = (\sigma + j\omega\epsilon) \vec{E}_T \quad . \qquad \text{(A-6d)}$$

Note also from $\nabla \cdot \vec{D} = \rho$ and $\nabla \cdot \vec{B} = 0$ so that

$$\nabla \cdot \vec{E}_T = \nabla_T \cdot \vec{E}_T = \frac{\rho}{\epsilon} \tag{A-7a}$$

$$\nabla \cdot \vec{H}_T = \nabla_T \cdot \vec{H}_T = 0 \tag{A-7b}$$

(since $E_x = H_x = 0$) where ρ is the free-charge density in the surrounding medium (which will decay to zero with time constant ϵ/σ). Therefore, equations (A-6a), (A-6c), (A-7a) and (A-7b) show that the transverse field vectors $\vec{E}_T$ and $\vec{H}_T$ satisfy the same spatial distributions as static fields in any transverse plane (y, z) at each x along the line.

This may be more easily seen if we write Faraday's law and Ampere's law in integral form by applying Stokes' theorem to $\nabla \times \vec{E} = - j\omega\mu \vec{H}$ and $\nabla \times \vec{H} = (\sigma + j\omega\epsilon)\vec{E} + \vec{J}$ as

$$\oint_C \vec{E} \cdot d\vec{\ell} = - j\omega\mu \int_S \vec{H} \cdot d\vec{a} \tag{A-8a}$$

$$\oint_C \vec{H} \cdot d\vec{\ell} = \int_S \vec{J} \cdot d\vec{a} + (\sigma + j\omega\epsilon) \int_S \vec{E} \cdot d\vec{a} \tag{A-8b}$$

where C is a closed contour enclosing the open surface S. Taking C to be a contour in the transverse (y, z) plane denoted by C_{yz} and S to be a flat surface in the transverse plane denoted by S_{yz} which is bounded by C_{yz} then (A-8) becomes

$$\oint_{C_{yz}} (E_y\, d_y + E_z\, d_z + E_x\, dx) = - j\omega\mu \int_{S_{yz}} H_x\, d_y\, d_z \tag{A-9a}$$

$$\oint_{C_{yz}} (H_y\, d_y + H_z\, d_z + H_x\, dx) = \int_{S_{yz}} J_x\, d_y\, d_z + (\sigma + j\omega\epsilon) \int_{S_{yz}} E_x\, d_y\, d_z \tag{A-9b}$$

where J_x is any source current in the x direction penetrating S_{yz}. However, under the TEM mode assumption $E_x = H_x = 0$ and (A-9) becomes

$$\oint_{C_{yz}} (E_y\, d_y + E_z\, d_z) = \oint_{C_{yz}} \vec{E}_T \cdot (\vec{z}\, dz + \vec{y}\, dy) = 0 \qquad \text{(A-10a)}$$

$$\oint_{C_{yz}} (H_y\, d_y + H_z\, d_z) = \oint_{C_{yz}} \vec{H}_T \cdot (\vec{z}\, dz + \vec{y}\, dy) = \int_{S_{yz}} J_x\, d_y\, d_z \qquad \text{(A-10b)}$$

which are of course indicates that $\vec{E}_T$ and $\vec{H}_T$ are no longer coupled together as is the case for static electromagnetic fields.

Thus we may uniquely define the voltage of the i-th conductor and the current associated with the i-th conductor as

$$V_i(x) = -\int_{C_i} \vec{E}_T \cdot d\vec{\ell} \qquad \text{(A-11b)}$$

$$I_i(x) = \oint_{\hat{C}_i} \vec{H}_T \cdot d\vec{\ell} \qquad \text{(A-11b)}$$

where C_i and $\hat{C}_i$ are shown in Fig. 1b as contours in the transverse plane at a particular x along the line.

The second objective is to demonstrate that for (r+1) perfect conductors in a homogeneous medium, the per-unit-length inductance matrix, $\underset{\sim}{L}$ and per-unit-length capacitance matrix, $\underset{\sim}{C}$ and per-unit-length conductance matrix, $\underset{\sim}{G}$ satisfy the important relations given in (14). From (A-10) and (A-11) we may obtain by taking the partial derivative of each equation with respect to x and taking the curl of $\vec{x}$ with each equation.

$$\frac{\partial^2}{\partial x^2} \vec{H}_T = (j\omega\mu\sigma - \omega^2 \mu\epsilon) \vec{H}_T \qquad \text{(A-12a)}$$

$$\frac{\partial^2}{\partial x^2} \vec{E}_T = (j\omega\mu\sigma - \omega^2 \mu\epsilon) \vec{E}_T \quad . \qquad \text{(A-12b)}$$

From equation (19) assuming perfect conductors

$$\frac{d^2}{dx^2} \underline{I}(x) = \underset{\sim}{Y}\,\underset{\sim}{Z}\,\underline{I}(x) = (j\omega \underset{\sim}{G}\underset{\sim}{L} - \omega^2 \underset{\sim}{C}\underset{\sim}{L})\,\underline{I}(x) \qquad \text{(A-13a)}$$

$$\frac{d^2}{dx^2} \underline{V}(x) = \underset{\sim}{Z}\,\underset{\sim}{Y}\,\underline{V}(x) = (j\omega \underset{\sim}{L}\underset{\sim}{G} - \omega^2 \underset{\sim}{L}\underset{\sim}{C})\,\underline{V}(x) \quad . \qquad \text{(A-13b)}$$

Performing the operations indicated in (A-11) on (A-12) one obtains two sets of n equations

$$\frac{d^2}{dx^2} I_i(x) = (j\omega\mu\sigma - \omega^2 \mu\epsilon)\, I_i(x) \qquad \text{(A-14a)}$$

$$\frac{d^2}{dx^2} V_i(x) = (j\omega\mu\sigma - \omega^2 \mu\epsilon)\, V_i(x) \quad . \qquad \text{(A-14b)}$$

Arranging these for $i = 1, ---, n$ as in (A-13) shows, by matching real and imaginary parts, that

$$\underset{\sim}{L}\underset{\sim}{G} = \underset{\sim}{G}\,\underset{\sim}{L} = \mu\sigma\, \underset{\sim}{1}_n \qquad \text{(A-15a)}$$

$$\underset{\sim}{L}\underset{\sim}{C} = \underset{\sim}{C}\,\underset{\sim}{L} = \mu\epsilon\, \underset{\sim}{1}_n \quad . \qquad \text{(A-15b)}$$

APPENDIX B

The purpose of this appendix is to demonstrate the derivation of the multiconductor transmission line equations in (4), (6) and (7) from the per-unit-length lumped equivalent circuit in Fig. 7.

Utilizing Kirchoff's voltage law counter-clockwise around the loop consisting of the i-th conductor and the zero-th conductor in Fig. 7 yields

$$V_i(x + \Delta x) - V_{s_i}(x)\,\Delta x + j\omega\,\ell_i\,\Delta x\,I_i + \sum_{\substack{k=0 \\ k\neq i}}^{n} j\omega m_{ik}\,\Delta x\,I_k \qquad \text{(B-1)}$$

$$+ (r_{c_i}\,\Delta x + j\omega\,\ell_{c_i}\,\Delta x)\,I_i - V_i(x)$$

$$- (r_{c_0}\,\Delta x + j\omega\,\ell_{c_0}\,\Delta x)\,I_0 - j\omega\ell_0\,\Delta x\,I_0$$

$$- \sum_{k=1}^{n} j\omega m_{k0}\,\Delta x\,I_k = 0 \quad .$$

This equation can be rewritten as

$$\frac{V_i(x + \Delta x) - V_i(x)}{\Delta x} = - j\omega\ell_i\,I_i - \sum_{\substack{k=0 \\ k\neq i}}^{n} j\omega m_{ik}\,I_k \qquad \text{(B-2)}$$

$$- (r_{c_i} + j\omega\ell_{c_i})\,I_i$$

$$+ (r_{c_0} + j\omega\ell_{c_0})\,I_0$$

$$+ j\omega\ell_0\,I_0 + \sum_{k=1}^{n} j\omega m_{k0}\,I_k$$

$$+ V_{s_i}(x)$$

and the current in the reference conductor satisfies

$$I_0 = - \sum_{k=1}^{n} I_k \quad . \tag{B-3}$$

Substituting (B-3) into (B-2) one obtains

$$\begin{aligned} \frac{V_i(x + \Delta x) - V_i(x)}{\Delta x} &= - j\omega \ell_i I_i - j\omega(- m_{i0} I_1 - \cdots - m_{i0} I_n + m_{i1} I_1 + \cdots + m_{in} I_n) \\ &\quad - (r_{c_i} + j\omega \ell_{c_i}) I_i \\ &\quad + (r_{c_0} + j\omega \ell_{c_0} + j\omega \ell_0)(- I_1 - \cdots - I_n) \\ &\quad + j\omega(m_{10} I_1 + \cdots + m_{n0} I_n) \\ &\quad + V_{s_i}(x) \end{aligned} \tag{B-4}$$

which may be rewritten as

$$\begin{aligned} \frac{V_i(x + \Delta x) - V_i(x)}{\Delta x} &= - (r_{c_0} + j\omega \ell_{c_0} + j\omega \ell_0 - j\omega m_{10} - j\omega m_{i0} + j\omega m_{i1}) I_1 \\ &\quad - \cdots - (r_{c_i} + j\omega \ell_{c_i} + j\omega \ell_i + r_{c_0} + j\omega \ell_{c_0} + j\omega \ell_0 \\ &\quad - j\omega m_{i0} - j\omega m_{i0}) I_i - \cdots \\ &\quad \cdots - (r_{c_0} + j\omega \ell_{c_0} + j\omega \ell_0 - j\omega m_{n0} - j\omega m_{i0} + j\omega m_{in}) I_n \\ &\quad + V_{s_i}(x) \quad . \end{aligned} \tag{B-5}$$

Arranging these equations for i=1, ---, n and taking the limit as $\Delta x \to 0$ yields (4a) and the per-unit-length impedance matrix, $\mathcal{Z}$, can be separated as in

(6a) with the entries given in (7a), (7b). (7c).

The derivation of the second transmission line equation, (4b), proceeds similarly. Utilizing Kirchoff's current law for the i-th conductor in Fig. 7, we may write

$$I_i(x + \Delta x) = I_i(x) - (g_{i0}\,\Delta x + j\omega c_{i0}\,\Delta x)\,V_i(x + \Delta x) \qquad \text{(B-6)}$$

$$- \sum_{\substack{k=1 \\ k\neq i}}^{n} (g_{ik}\,\Delta x + j\omega c_{ik}\,\Delta x)(V_i(x + \Delta x) - V_k(x + \Delta x))$$

$$+ I_{s_i}(x)\,\Delta x$$

which may be rewritten as

$$\frac{I_i(x + \Delta x) - I_i(x)}{\Delta x} = (g_{i1} + j\omega c_{i1})\,V_1(x + \Delta x) \qquad \text{(B-7)}$$

$$+ \cdots - (g_{i0} + j\omega c_{i0} + \sum_{\substack{k=1 \\ k\neq i}}^{n} (g_{ik} + j\omega c_{ik}))\,V_i(x + \Delta x)$$

$$+ \cdots + (g_{in} + j\omega c_{in})\,V_n(x + \Delta x) + I_{s_i}(x) \quad .$$

Arranging for i=1,---,n and taking the limit as $\Delta x \to 0$ yields (4b) and the per-unit-length admittance matrix, $\underset{\sim}{Y}$, can be separated as in (6b) with the entries given in (7d) and (7e).

APPENDIX C

The purpose of this appendix is to derive the expressions for the per-unit-length equivalent sources in (5) which are induced by an incident electromagnetic field on the uniform transmission line in Fig. 2a consisting of (n+1) perfect conductors in a lossless, homogeneous medium (see Fig. C-1). The expression for the currents induced in termination networks given in (77) will also be obtained. The solution for Fig. 2b is also discussed.

The solution for the special case of a two-conductor line (n=1) was obtained by Taylor, Satterwhite and Harrison in [20] and later in a more convenient form by Smith in [21]. The solution for the case of a uniform plane wave incident on a three-conductor line in the transverse direction (perpendicular to the system's longitudinal (x) axis) with the electric field intensity vector polarized parallel to the line axis was obtained in [24]. Procedures for extending this result to multiconductor lines were indicated.

It is convenient to consider the effects of the spectral components of the incident field as per-unit-length distributed sources along the line [26]. The sources appear as series voltage sources and shunt current sources as indicated in Fig. C-2 for an "electrically small" Δx section of the line. The multiconductor transmission line equations may then be derived for the Δx subsection and are given in equation (4). The termination networks are given in the form of generalized Thevenin equivalents as in equation (69) and the solution for the termination currents is given in equation (75). Substituting the expressions for the matrix chain parameters given in (49) into (75) for this case of

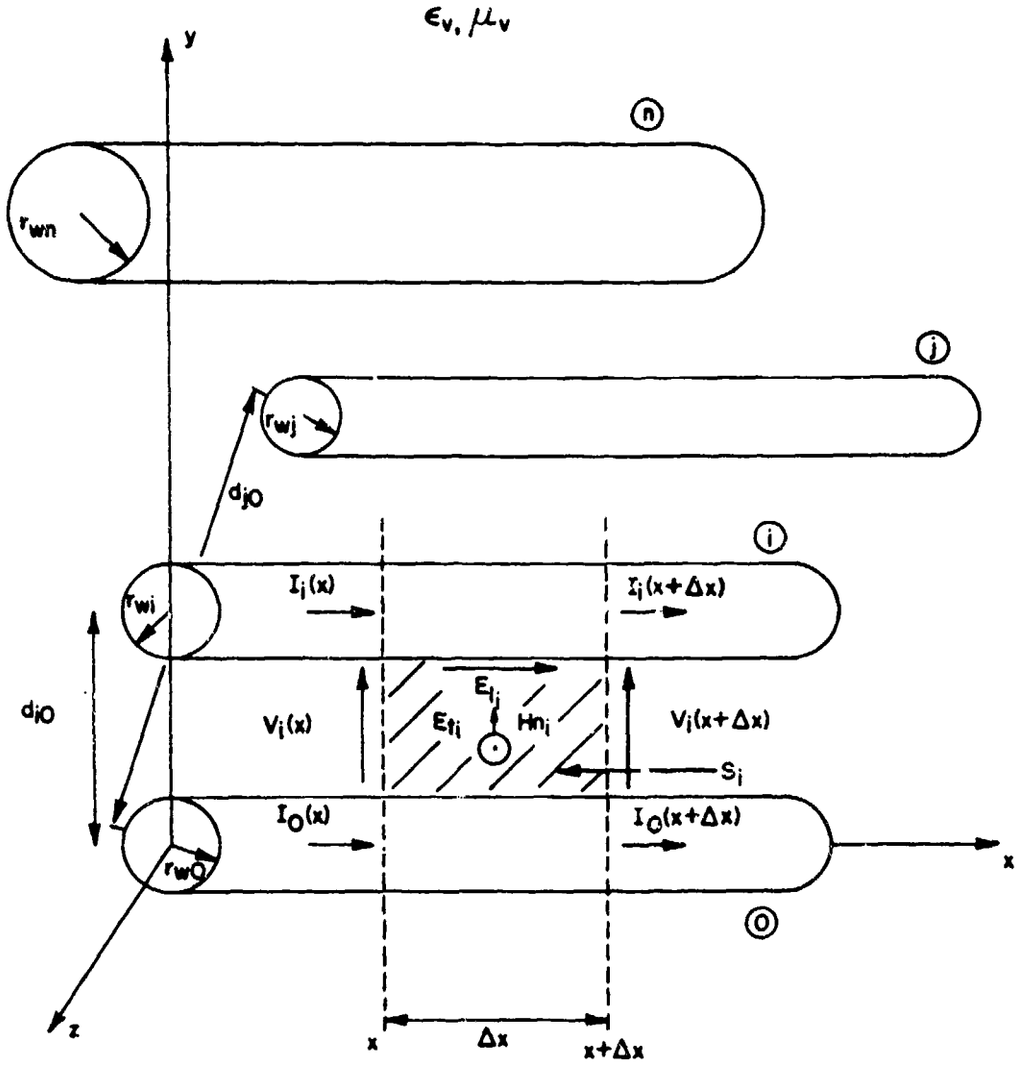

Figure C-1. A multiconductor line with incident field illumination.

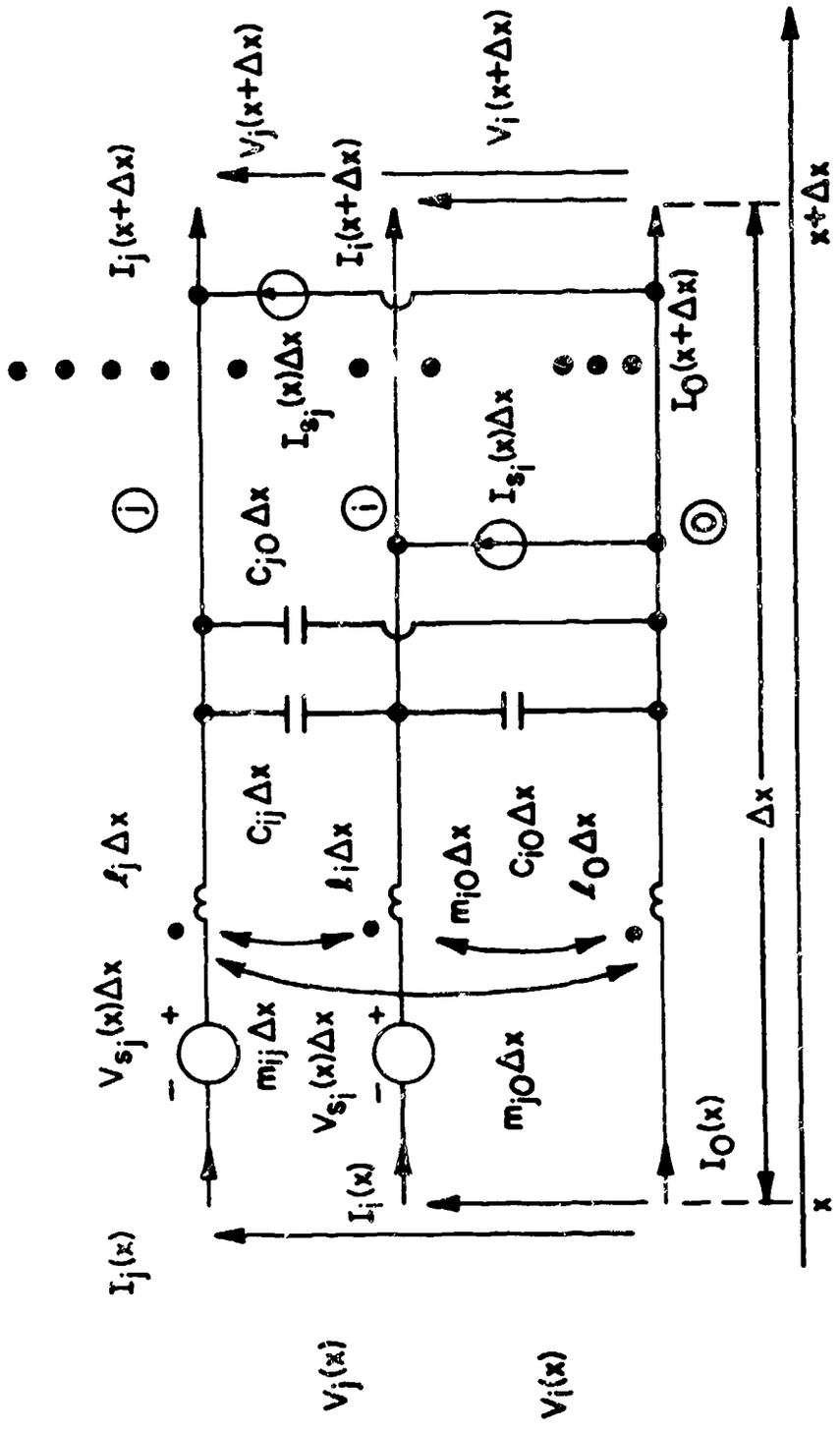

Figure C-2. The per-unit-length equivalent circuit for Fig. C-1.

perfect conductors in a lossless, homogeneous medium (free space) described by ϵ_v and μ_v, we obtain

$$\left[\cos(\beta \mathcal{L})\left\{\underset{\sim}{Z}_0 + \underset{\sim}{Z}_{\mathcal{L}}\right\} + j \sin(\beta \mathcal{L}) \left\{\underset{\sim}{Z}_C + \underset{\sim}{Z}_{\mathcal{L}} \underset{\sim}{Z}_C^{-1} \underset{\sim}{Z}_0\right\}\right] \underline{I}(0) = \tag{C-1a}$$

$$- \underline{V}_{\mathcal{L}} + \left[j \sin(\beta \mathcal{L}) \underset{\sim}{Z}_{\mathcal{L}} \underset{\sim}{Z}_C^{-1} + \cos(\beta \mathcal{L}) \underset{\sim}{1}_n\right] \underline{V}_0$$

$$+ \hat{\underline{V}}_s(\mathcal{L}) - \underset{\sim}{Z}_{\mathcal{L}} \hat{\underline{I}}_s(\mathcal{L})$$

$$\underline{I}(\mathcal{L}) = - j \sin(\beta \mathcal{L}) \underset{\sim}{Z}_C^{-1} \underline{V}_0 + \left[\cos(\beta \mathcal{L}) \underset{\sim}{1}_n + j \sin(\beta \mathcal{L}) \underset{\sim}{Z}_C^{-1} \underset{\sim}{Z}_0\right] \underline{I}(0) \tag{C-1b}$$

$$+ \hat{\underline{I}}_s(\mathcal{L}) \quad .$$

where the wave number is $\beta = 2\pi/\lambda$, $\lambda = \upsilon/f$, $\upsilon = 1/\sqrt{\mu_v \epsilon_v} \cong 3 \times 10^8$ m/sec. The characteristic-impedance matrix $\underset{\sim}{Z}_C$ becomes

$$\underset{\sim}{Z}_C = \upsilon \underset{\sim}{L} \tag{C-2}$$

and $\hat{\underline{V}}_s(\mathcal{L})$ and $\hat{\underline{I}}_s(\mathcal{L})$ are obtained by substituting (49) into (74) as

$$\hat{\underline{V}}_s(\mathcal{L}) = \int_0^{\mathcal{L}} \left\{\cos(\beta(\mathcal{L} - \hat{x})) \underline{V}_s(\hat{x}) - j \sin(\beta(\mathcal{L} - \hat{x})) \underset{\sim}{Z}_C \underline{I}_s(\hat{x})\right\} d\hat{x} \tag{C-3a}$$

$$\hat{\underline{I}}_s(\mathcal{L}) = \int_0^{\mathcal{L}} \left\{\cos(\beta(\mathcal{L} - \hat{x})) \underline{I}_s(\hat{x}) - j \sin(\beta(\mathcal{L} - \hat{x})) \underset{\sim}{Z}_C^{-1} \underline{V}_s(\hat{x})\right\} d\hat{x} \quad . \tag{C-3b}$$

Solution of (C-1a) for the termination current vector, $\underline{I}(0)$, requires the solution of n complex equations in n unknowns ($I_i(0)$). Once (C-1a) is solved, (C-1b) yields the termination currents $\underline{I}(\mathcal{L})$ directly.

Although the equations may appear formidable, they are in a compact form and can be straightforwardly programmed on a digital computer.

Furthermore, the form is not restricted to any particular value of n. The only difficulties are in determining $\underset{\sim}{L}$ and determining $\underline{\hat{V}}_s$ and $\underline{\hat{I}}_s$ (which require that we determine $\underline{V}_s(x)$ and $\underline{I}_s(x)$). The determination of the equivalent sources $V_{s_i}(x)$ and $I_{s_i}(x)$ induced by the incident field will be the next objective.

C.1. Determining the Equivalent Induced Sources

In order to determine the equivalent induced sources, $V_{s_i}(x)$ and $I_{s_i}(x)$, consider Figure C-1. The method used in [20] can be adapted here in a similar fashion. Faraday's law in integral form becomes

$$\oint_{C_i} \vec{E} \cdot d\vec{\ell} = - j\omega\mu_v \int_{S_i} \vec{H} \cdot \vec{n}\, da \qquad \text{(C-4)}$$

where S_i is a flat, rectangular surface in the x,y plane between wire i and wire 0 and between x and $x + \Delta x$ as shown in Figure C-1. The unit normal $\vec{n}$ is $\vec{n} = \vec{z}$ where $\vec{z}$ is the unit vector in the z direction, $da = dx\, dy$ and C_i is a contour encircling S_i in the proper direction (counter-clockwise according to the right-hand rule). Equation (C-4) becomes for the indicated integration[1]

$$\int_0^{d_{i0}} [E_{t_i}(y, x+\Delta x) - E_{t_i}(y, x)]dy \qquad \text{(C-5)}$$

$$- \int_x^{x+\Delta x} [E_{\ell_i}(d_{i0}, x) - E_{\ell_i}(0, x)]dx$$

$$= -j\omega\mu_v \int_x^{x+\Delta x} \int_0^{d_{i0}} H_{n_i}(y, x)\, dy\, dx$$

1. In integrating from y=0 to $y=d_{i0}$, we are implicity assuming that r_{wi} and r_{w0} are much less than d_{i0}, i.e., the wires are sufficiently separated so that they may be replaced by filaments.

where E_{t_i} is the component of the total electric field (incident plus scattered) transverse to the line axis and lying along a straight line joining the two conductors, i.e., $E_{t_i} = E_y$; E_{ℓ_i} is the component of the total electric field along the longitudinal axis of the line, i.e., $E_{\ell_i} = E_x$; and H_{n_i} is the component of the total magnetic field perpendicular to the plane formed by the two wires, i.e., $H_{n_i} = H_z$.

Defining the voltage between the two wires as

$$V_i(x) = - \int_0^{d_{i0}} E_{t_i}(y, x)dy \qquad (C-6)$$

then

$$- \frac{dV_i(x)}{dx} = \lim_{\Delta x \to 0} \frac{1}{\Delta x} \int_0^{d_{i0}} [E_{t_i}(y, x+\Delta x) - E_{t_i}(y, x)]dy \quad . \qquad (C-7)$$

The total electric field along the wire surfaces is zero since we assume perfect conductors. (One can straightforwardly include finite conductivity conductors through a surface impedance as was done in [20]). Therefore (C-5) becomes in the limit as $\Delta x \to 0$

$$\frac{dV_i(x)}{dx} = j\omega\mu_v \int_0^{d_{i0}} H_{n_i}(y, x)dy \quad . \qquad (C-8)$$

The total magnetic field is the sum of an incident and a scattered field:

$$H_{n_i}(y, x) = H_z(y, x) \qquad (C-9)$$

$$= \underbrace{H_z^{(scat)}(y, x)}_{\text{scattered}} + \underbrace{H_z^{(inc)}(y, x)}_{\text{incident}}$$

and the scattered field here is produced by the transmission line currents. The scattered flux passing between the two conductors per unit of line leng is directly related to the scattered magnetic field and the per-unit-length inductance matrix, $\underset{\sim}{L}$, as

$$\phi_i^{(scat)}(x) = -\int_0^{d_{i0}} \mu_v H_{n_i}^{(scat)}(y,x)dy$$

$$= [\ell_{i1}, \ell_{i2}, ----, \ell_{in}] \begin{bmatrix} I_1(x) \\ I_2(x) \\ \cdot \\ \cdot \\ \cdot \\ I_n(x) \end{bmatrix} \qquad \text{(C-10)}$$

where $\ell_{ij} = [\underset{\sim}{L}]_{ij}$. Substituting (C-10) and (C-9) into (C-8) and arranging for i = 1, ----, n yields

$$\underset{\sim}{V}(x) + j\omega \underset{\sim}{L}\underset{\sim}{I}(x) = \begin{bmatrix} \cdot \\ \cdot \\ \cdot \\ j\omega\mu_v \int_0^{d_{i0}} H_{n_i}^{(inc)}(y,x)dy \\ \cdot \\ \cdot \\ \cdot \end{bmatrix} \qquad \text{(C-11)}$$

and the source vector $\underset{\sim}{V}_s(x)$ in (4) is easily identified by comparing (4a) and (C-11).

For transmission line theory to apply, the cross-sectional dimensions of the line (wire spacing, etc.) must be electrically small, i.e., $\beta d_{i0} << 1$ and $\beta d_{ij} << 1$. Thus the result indicates that the voltage, V_{s_i}, induced in the loop between the i-th conductor and the zero-th conductor and between x and $x+\Delta x$ is equal to the rate of change of the incident flux penetrating this "electrically small" loop which, of course, makes sense.

npere's law yields

$$E_y = \frac{1}{j\omega \epsilon_v} \left[\frac{\partial H_x}{\partial z} - \frac{\partial H_z}{\partial x} \right] \quad . \tag{C-12}$$

E_y will consist of scattered and incident field components and is written as

$$E_{t_i}(y,x) = E_y(y,x) \tag{C-13}$$

$$= \underbrace{\overset{(scat)}{E_y}(y,x)}_{\text{scattered}} + \underbrace{\overset{(inc)}{E_y}(y,x)}_{\text{incident}} \quad .$$

Substituting (C-12) into (C-6) we have

$$V_i(x) = -\int_0^{d_{i0}} E_y(y,x)dy = \frac{1}{j\omega \epsilon_v} \int_0^{d_{i0}} \left\{ \frac{\partial \overset{(scat)}{H_z}(y,x)}{\partial x} + \frac{\partial \overset{(inc)}{H_z}(y,x)}{\partial x} \right. \tag{C-14}$$

$$\left. - \frac{\partial \overset{(scat)}{H_x}(y,x)}{\partial z} - \frac{\partial \overset{(inc)}{H_x}(y,x)}{\partial z} \right\} dy \quad .$$

Utilizing (C-10) we obtain

$$V_i(x) = -\frac{1}{j\omega \mu_v \epsilon_v} \frac{d}{dx} \left\{ [\ell_{i1}, \ell_{i2}, ---, \ell_{in}] \underline{I}(x) \right\} \tag{C-15}$$

$$- \frac{1}{j\omega \epsilon_v} \int_0^{d_{i0}} \frac{\partial \overset{(scat)}{H_x}(y,x)}{\partial z} dy - \int_0^{d_{i0}} \overset{(inc)}{E_{t_i}}(y,x)dy \quad .$$

If we assume that the currents on the wires are directed only in the x direction i.e., (there are no transverse components of the currents on the wire surfaces), then $\overset{(scat)}{H_x}(y,x) = 0$ and (C-15) becomes

$$V_i(x) = -\frac{1}{j\omega\mu_v\epsilon_v}\frac{d}{dx}\left\{\left[\ell_{i1}, \ell_{i2}, ---, \ell_{in}\right]\underline{I}(x)\right\} \qquad \text{(C-16)}$$

$$- \int_0^{d_{i0}} E_{t_i}^{(inc)}(y,x)dy \quad .$$

Arranging these equations for i = 1, ---, n we obtain the second transmission line equation

$$\dot{\underline{I}}(x) + j\omega\mu_v\epsilon_v \underset{\sim}{L}^{-1}\underline{V}(x) = -j\omega\mu_v\epsilon_v \underset{\sim}{L}^{-1}\begin{bmatrix} \vdots \\ \int_0^{d_{i0}} E_{t_i}^{(inc)}(y,x)dy \\ \vdots \end{bmatrix} \qquad \text{(C-17)}$$

Utilizing the important relation for a homogeneous medium, $\underset{\sim}{C} = \mu_v\epsilon_v \underset{\sim}{L}^{-1}$ in (C-17) we obtain by comparing (C-11) and (C-17) to (4)

$$\underline{V}_s(x) = j\omega\mu_v \begin{bmatrix} \vdots \\ \int_0^{d_{i0}} H_{n_i}^{(inc)}(y,x)dy \\ \vdots \end{bmatrix} \qquad \text{(C-18a)}$$

$$\underline{I}_s(x) = -j\omega\underset{\sim}{C} \begin{bmatrix} \vdots \\ \int_0^{d_{i0}} E_{t_i}^{(inc)}(y,x)dy \\ \vdots \end{bmatrix} \quad . \qquad \text{(C-18b)}$$

The shunt current sources in $\underline{I}_s(x)$ are therefore a result of the line voltage induced by the incident electric field being applied across the per-unit-length line-to-line capacitances which, of course, satisfies our intuition.

C.2. Solution for $\underline{\hat{V}}_s(x)$ and $\underline{\hat{I}}_s(x)$

The final problem remaining is to obtain simplified versions of $\underline{\hat{V}}_s$ and $\underline{\hat{I}}_s$ in (C-3) to be directly used in (C-1). First consider the determination of $\underline{\hat{V}}_s(\mathcal{L})$. Substituting (C-18) into (C-3a) yields

$$\underline{\hat{V}}_s(\mathcal{L}) = j\omega\mu_v \int_0^{\mathcal{L}} \left\{ \cos(\beta(\mathcal{L}-\hat{x})) \begin{bmatrix} \vdots \\ \int_0^{d_{i0}} H_{n_i}^{(inc)}(y,\hat{x})dy \\ \vdots \end{bmatrix} \right\} d\hat{x} \quad \text{(C-19)}$$

$$- \beta \int_0^{\mathcal{L}} \left\{ \sin(\beta(\mathcal{L}-\hat{x})) \begin{bmatrix} \vdots \\ \int_0^{d_{i0}} E_{t_i}^{(inc)}(y,\hat{x})dy \\ \vdots \end{bmatrix} \right\} d\hat{x} \quad .$$

From Faraday's law we obtain

$$H_{n_i}^{(inc)} = \frac{1}{j\omega\mu_v} \left[\frac{\partial E_{\ell_i}^{(inc)}}{\partial y} - \frac{\partial E_{t_i}^{(inc)}}{\partial x} \right] \quad . \quad \text{(C-20)}$$

Substituting this into (C-19) yields

$$\underline{\hat{V}}_s(\mathcal{L}) = \int_0^{\mathcal{L}} \left\{ \cos(\beta(\mathcal{L}-\hat{x})) \begin{bmatrix} \vdots \\ E_{\ell_i}^{(inc)}(d_{i0},\hat{x}) - E_{\ell_i}^{(inc)}(0,\hat{x}) \\ \vdots \end{bmatrix} \right\} d\hat{x} \quad \text{(C-21)}$$

$$- \int_0^{\mathcal{L}} \left\{ \cos(\beta(\mathcal{L}-\hat{x})) \begin{bmatrix} \vdots \\ \int_0^{d_{i0}} \frac{\partial E_{t_i}^{(inc)}(y,\hat{x})}{\partial \hat{x}} dy \\ \vdots \end{bmatrix} \right\} d\hat{x}$$

$$- \beta \int_0^{\ell} \left\{ \sin(\beta(\ell - \hat{x})) \begin{bmatrix} \vdots \\ \int_0^{d_{i0}} E_{t_i}^{(inc)}(y, \hat{x})\, dy \\ \vdots \end{bmatrix} \right\} d\hat{x} \quad .$$

Utilizing Leibnitz's rule, (C-21) is equivalent to

$$\underline{\hat{V}}_s(\ell) = \int_0^{\ell} \left\{ \cos(\beta(\ell - \hat{x})) \begin{bmatrix} \vdots \\ E_{\ell_i}^{(inc)}(d_{i0}, \hat{x}) - E_{\ell_i}^{(inc)}(0, \hat{x}) \\ \vdots \end{bmatrix} \right\} d\hat{x} \qquad (C\text{-}22)$$

$$- \int_0^{\ell} \frac{\partial}{\partial \hat{x}} \left\{ \cos(\beta(\ell - \hat{x})) \begin{bmatrix} \vdots \\ \int_0^{d_{i0}} E_{t_i}^{(inc)}(y, \hat{x})\, dy \\ \vdots \end{bmatrix} \right\} d\hat{x}$$

and this may be written as

$$\underline{\hat{V}}_s(\ell) = \int_0^{\ell} \left\{ \cos(\beta(\ell - \hat{x})) \begin{bmatrix} \vdots \\ E_{\ell_i}^{(inc)}(d_{i0}, \hat{x}) - E_{\ell_i}^{(inc)}(0, \hat{x}) \\ \vdots \end{bmatrix} \right\} d\hat{x} \qquad (C\text{-}23)$$

$$- \begin{bmatrix} \vdots \\ \int_0^{d_{i0}} E_{t_i}^{(inc)}(y, \ell)\, dy \\ \vdots \end{bmatrix} + \cos(\beta \ell) \begin{bmatrix} \vdots \\ \int_0^{d_{i0}} E_{t_i}^{(inc)}(y, 0)\, dy \\ \vdots \end{bmatrix} \quad .$$

Similarily $\underline{\hat{I}}_s(\mathcal{L})$ may be obtained as

$$\underline{\hat{I}}_s(\mathcal{L}) = -\, j\underset{\sim}{Z}_C^{-1} \int_0^{\mathcal{L}} \left\{ \sin(\beta(\mathcal{L}-\hat{x})) \begin{bmatrix} \vdots \\ E_{\ell_i}^{(inc)}(d_{i0}, \hat{x}) - E_{\ell_i}^{(inc)}(0, \hat{x}) \\ \vdots \end{bmatrix} \right\} d\hat{x} \quad \text{(C-24)}$$

$$- j\underset{\sim}{Z}_C^{-1} \left\{ \sin(\beta \mathcal{L}) \begin{bmatrix} \vdots \\ \int_0^{d_{i0}} E_{t_i}^{(inc)}(y, 0)\, dy \\ \vdots \end{bmatrix} \right\} .$$

The important quantity in (C-1a) is $\underline{\hat{V}}_s(\mathcal{L}) - \underset{\sim}{Z}_{\mathcal{L}}\, \underline{\hat{I}}_s(\mathcal{L})$. Combining (C-23) and (C-24), this becomes

$$\underline{\hat{V}}_s(\mathcal{L}) - \underset{\sim}{Z}_{\mathcal{L}}\, \underline{\hat{I}}_s(\mathcal{L}) = \int_0^{\mathcal{L}} \Big\{ \left[\cos(\beta(\mathcal{L}-\hat{x}))\, \underset{\sim}{1}_n + j \sin(\beta(\mathcal{L}-\hat{x})\, \underset{\sim}{Z}_{\mathcal{L}}\, \underset{\sim}{Z}_C^{-1} \right] \quad \text{(C-25)}$$

$$\times \begin{bmatrix} \vdots \\ E_{\ell_i}^{(inc)}(d_{i0}, \hat{x}) - E_{\ell_i}^{(inc)}(0, \hat{x}) \\ \vdots \end{bmatrix} \Big\} d\hat{x} - \begin{bmatrix} \vdots \\ \int_0^{d_{i0}} E_{t_i}^{(inc)}(y, \mathcal{L})\, dy \\ \vdots \end{bmatrix}$$

$$+ [\cos(\beta \mathcal{L})\, \underset{\sim}{1}_n + j \sin(\beta \mathcal{L})\, \underset{\sim}{Z}_{\mathcal{L}}\, \underset{\sim}{Z}_C^{-1}] \begin{bmatrix} \vdots \\ \int_0^{d_{i0}} E_{t_i}^{(inc)}(y,0)\, dy \\ \vdots \end{bmatrix} .$$

Note that the equivalent forcing function on the righthand side of (C-1a), $\hat{\underline{V}}_s(\mathcal{L}) - \underset{\sim}{Z}_{\mathcal{L}}\, \hat{\underline{I}}_s(\mathcal{L})$, given in (C-25) is simply determined as a convolution of differences of the incident electric field vector along the wire axes, $E_{\ell_i}^{(inc)}(d_{i0}, x) - E_{\ell_i}^{(inc)}(0, x)$, and a linear combination of integrals of components of the electric field vectors at the endpoints of the line which are transverse to the line, $E_{t_i}^{(inc)}(y, \mathcal{L})$ and $E_{t_i}^{(inc)}(y, 0)$. This is, of course, precisely the result obtained by Smith [21] for two conductor lines. Substituting (C-25) into (C-1a) and setting $\underline{V}_{\mathcal{L}} = \underset{n-1}{0}$, $\underline{V}_0 = \underset{n-1}{0}$, i.e., no independent sources in the termination-networks, one can verify that the result reduces for two-conductor lines (n=1) to the result given by Smith [21] since $\underset{\sim}{Z}_C$, $\underset{\sim}{Z}_{\mathcal{L}}$, $\underset{\sim}{Z}_0$ become scalars for two-conductor lines and (C-1a) becomes one equation in only one unknown I(0). For uniform plane wave illumination of the line (which is usually the case of interest), (C-25) reduces to a much simpler form although the result allows for the more general case.

The final equations for the line currents then become (substituting (C-25) into (C-1))

$$[\cos(\beta \mathcal{L}) \left\{ \underset{\sim}{Z}_0 + \underset{\sim}{Z}_{\mathcal{L}} \right\} + j \sin(\beta \mathcal{L}) \left\{ \underset{\sim}{Z}_C + \underset{\sim}{Z}_{\mathcal{L}}\, \underset{\sim}{Z}_C^{-1}\, \underset{\sim}{Z}_0 \right\}]\, \underline{I}(0) = \qquad \text{(C-26a)}$$

$$- \underline{V}_{\mathcal{L}} + \left[j \sin(\beta \mathcal{L})\, \underset{\sim}{Z}_{\mathcal{L}}\, \underset{\sim}{Z}_C^{-1} + \cos(\beta \mathcal{L})\, \underset{\sim}{1}_n \right] \underline{V}_0$$

$$+ \int_0^{\mathcal{L}} \left\{ \left[\cos(\beta(\mathcal{L} - \hat{x}))\, \underset{\sim}{1}_n + j \sin(\beta(\mathcal{L} - \hat{x}))\, \underset{\sim}{Z}_{\mathcal{L}}\, \underset{\sim}{Z}_C^{-1} \right] \underline{E}_{\ell}^{(inc)}(\hat{x}) \right\} d\hat{x}$$

$$- \underline{E}_t^{(inc)}(\mathcal{L}) + \left\{ \left[\cos(\beta \mathcal{L})\, \underset{\sim}{1}_n + j \sin(\beta \mathcal{L})\, \underset{\sim}{Z}_{\mathcal{L}}\, \underset{\sim}{Z}_C^{-1} \right] \underline{E}_t^{(inc)}(0) \right\}$$

$$\underline{I}(\mathcal{L}) = - j \sin(\beta \mathcal{L})\, \underset{\sim}{Z}_C^{-1}\, \underline{V}_0 + \left[\cos(\beta \mathcal{L})\, \underset{\sim}{1}_n + j \sin(\beta \mathcal{L})\, \underset{\sim}{Z}_C^{-1}\, \underset{\sim}{Z}_0 \right] \underline{I}(0) \qquad \text{(C-26b)}$$

$$- j \underset{\sim}{Z}_C^{-1} \int_0^{\mathcal{L}} \left\{ \sin(\beta(\mathcal{L} - \hat{x}))\, \underline{E}_{\ell}^{(inc)}(\hat{x}) \right\} d\hat{x}$$

$$- j \underset{\sim}{Z}_C^{-1} \left\{ \sin(\beta \mathcal{L})\, \underline{E}_t^{(inc)}(0) \right\}$$

where $\underline{E}_{\ell}^{(inc)}(x)$, $\underline{E}_t^{(inc)}(\mathcal{L})$ and $\underline{E}_t^{(inc)}(0)$ are n χ 1 column vectors with the entries in the i-th rows given by

$$\left[\underline{E}_{\ell}^{(inc)}(x) \right]_i = E_{\ell_i}^{(inc)}(d_{i0}, x) - E_{\ell_i}^{(inc)}(0, x) \qquad \text{(C-26c)}$$

$$\left[\underline{E}_t^{(inc)}(\mathcal{L}) \right]_i = \int_0^{d_{i0}} E_{t_i}^{(inc)}(\xi_i, \mathcal{L})\, d\xi_i \qquad \text{(C-26d)}$$

$$\left[\underline{E}_t^{(inc)}(0) \right]_i = \int_0^{d_{i0}} E_{t_i}^{(inc)}(\xi_i, 0)\, d\xi_i \qquad \text{(C-26e)}$$

for i = 1, ----, n which are equations(77).

A word of caution in the interpretation of the notation is in order. Although it should be clear from the derivation, the reader should nevertheless be reminded that the integration path for the component $E_{t_i}^{(inc)}$ is in the y direction when the i-th conductor is concerned. When other conductors are concerned, the integration path is a straight line in the y, z plane which

joins the conductor and the zero-th conductor and is perpendicular to these two conductors. This is designated as ξ_i in (C-26) and replaces the y variable for the path associated with conductors i and 0. The notation may be cumbersome but the idea and implementation is quite simple.

C.3. The Per-Unit-Length Inductance Matrix, $\underset{\sim}{L}$

One final calculation remains; the determination of the per-unit-length inductance matrix, $\underset{\sim}{L}$. Ordinarily this is a difficult calculation as discussed in Section V. However, if we assume that the conductors are separated sufficiently such that the charge distribution around the periphery of each conductor is constant, then the conductors can be replaced by filamentary lines of charge. Typically, this will be quite accurate if the smallest ratio of conductor separation to wire radius is greater than 5 [56]. In this case, the entries in $\underset{\sim}{L}$ are shown in Section V to be

$$\left[\underset{\sim}{L}\right]_{ii} = \mu_v \epsilon_v \left[\underset{\sim}{C}^{-1}\right]_{ii} \cong \frac{\mu_v}{2\pi} \ell n \left(\frac{d_{i0}^2}{r_{wi}\, r_{w0}}\right) \qquad \text{(C-27a)}$$

$$\left[\underset{\sim}{L}\right]_{\substack{ij \\ i\neq j}} = \mu_v \epsilon_v \left[\underset{\sim}{C}^{-1}\right]_{ij} \cong \frac{\mu_v}{2\pi} \ell n \left(\frac{d_{i0}\, d_{j0}}{r_{w0}\, d_{ij}}\right) \quad . \qquad \text{(C-27b)}$$

For closer conductor spacings, proximity effect will alter the charge distributions from constant ones and numerical approximations must be employed to find $\underset{\sim}{L}$ as was discussed in Section V.

The entries in the per-unit-length inductance matrix for large wire spacing given in (C-27) can be derived in an alternate manner

which more clearly illustrates its relation to the total scattered flux passing between the wires. The matrix $\underset{\sim}{L}$ relates the scattered flux $\underline{\phi}^{(scat)}$ passing between the wires to the wire currents as

$$\underline{\phi}^{(scat)} = \begin{bmatrix} \phi_1^{(scat)} \\ \cdot \\ \cdot \\ \cdot \\ \phi_n^{(scat)} \end{bmatrix} = \underbrace{\begin{bmatrix} \ell_{11} & \cdots & \ell_{1n} \\ \cdot & & \cdot \\ \cdot & & \cdot \\ \cdot & & \cdot \\ \ell_{n1} & \cdots & \ell_{nn} \end{bmatrix}}_{\underset{\sim}{L}} \begin{bmatrix} I_1 \\ \cdot \\ \cdot \\ \cdot \\ I_n \end{bmatrix} . \qquad \text{(C-28)}$$

The respective entries are determined as

$$\ell_{ii} = \left. \frac{\phi_i^{(scat)}}{I_i} \right|_{I_1, \text{ ----}, I_{i-1}, I_{i+1}, \text{ ----}, I_n = 0} \qquad \text{(C-29a)}$$

$$\ell_{\substack{ij \\ i \neq j}} = \left. \frac{\phi_i^{(scat)}}{I_j} \right|_{I_1, \text{ ----}, I_{j-1}, I_{j+1}, \text{ ----}, I_n = 0} \qquad \text{(C-29b)}$$

and $\ell_{ij} = \ell_{ji}$. Large wire separations are assumed so that the wires may be replaced by filaments of current.

Consider Fig. C-3a. The magnitude of the magnetic field intensity vector due to I_i on wire i at a distance $r > r_{wi}$ away from wire i is

$$H_r = \frac{I_i}{2\pi r} \qquad \text{(C-30)}$$

and the total flux passing between wire i and wire 0 due to both currents is

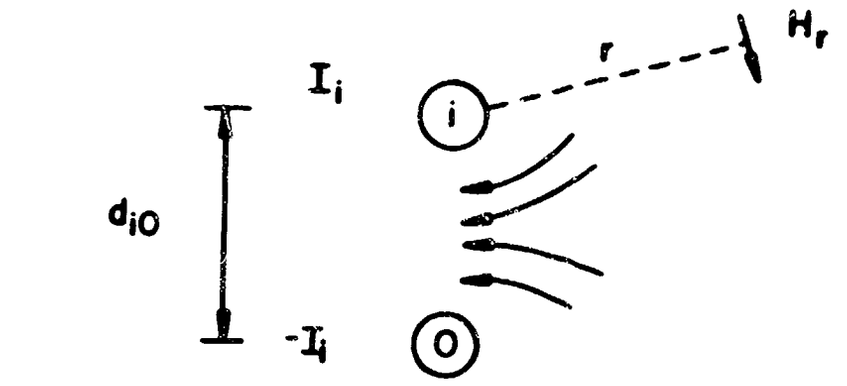

(a)

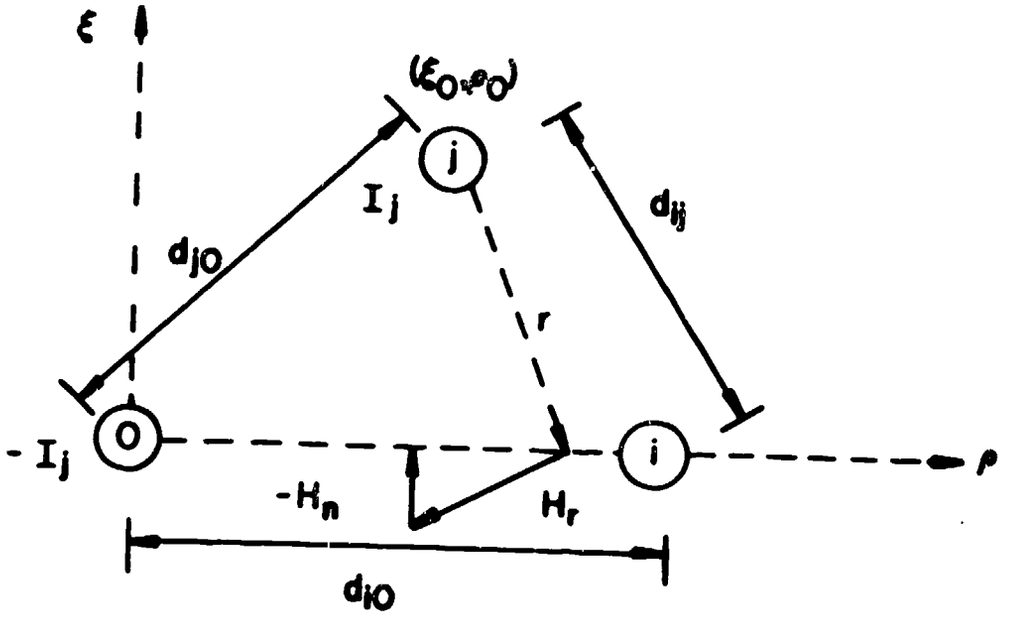

(b)

Figure C-3. The problem geometry for the calculation of the entries in the per-unit-length inductance matrix.

$$\phi_i^{(scat)} = \frac{\mu_v I_i}{2\pi} \left\{ \int_{r_{wi}}^{d_{i0}} \frac{1}{r}\, dr + \int_{r_{w0}}^{d_{i0}} \frac{1}{r}\, dr \right\} \qquad \text{(C-31)}$$

$$= \frac{\mu_v I_i}{2\pi} \ln \left(\frac{d_{i0}^2}{r_{wi}\, r_{w0}} \right) \quad .$$

Thus ℓ_{ii} is easily identified as in (C-27a).

Consider Fig. C-3b. The portion of the flux $\phi_i^{(scat)}$ passing between wire i and wire 0 due to $-I_j$ in the reference conductor is as above

$$\phi_{i0}^{(scat)} = \frac{\mu_v I_j}{2\pi} \ln \left(\frac{d_{i0}}{r_{w0}} \right) \qquad \text{(C-32)}$$

and the portion of the flux passing between wire i and wire 0 due to I_j in the j-th conductor can be found to be

$$\phi_{ij}^{(scat)} = -\mu_v \int_0^{d_{i0}} H_n d\rho = -\frac{\mu_v}{2\pi} I_j \left\{ \int_{\rho=0}^{\rho=d_{i0}} \frac{(\rho - \rho_0)}{\xi_0^2 + (\rho - \rho_0)^2]}\, d\rho \right\} \qquad \text{(C-33)}$$

$$= \frac{\mu_v}{2\pi} I_j \left\{ \frac{1}{2} \ln \left[\frac{(\xi_0^2 + \rho_0^2)}{\xi_0^2 + (d_{i0} - \rho_0)^2} \right] \right\} \quad .$$

Combining (C-32) and (C-33) we obtain

$$\phi_i^{(scat)} = \phi_{i0}^{(scat)} + \phi_{ij}^{(scat)} = \frac{\mu_v I_j}{2\pi} \ln \left(\frac{d_{j0}\, d_{i0}}{d_{ij}\, r_{w0}} \right) \qquad \text{(C-34)}$$

since

$$d_{ij}^2 = \xi_0^2 + (d_{i0} - \rho_0)^2 \qquad \text{(C-35a)}$$

$$d_{j0}^2 = \xi_0^2 + \rho_0^2 \qquad \text{(C-35b)}$$

and ℓ_{ij} is easily identified as given in (C-27b).

C.4. Computed Results

To show the simplicity of the result and indicate its equivalence to the result obtained by Harrison in [24], Example 1 considered in [24] will be computed by this method. Three wires all of radius 10^{-3}m lie in the x, y plane as shown in Figure C-4. A uniform plane wave with an electric field intensity magnitude of 1V/m is propagating in the y direction and 500Ω (purely resistive) loads connect each line to common nodes. The various distances in Figure C-1 are $d_{10} = 10^{-2}$m, $d_{20} = 2 \times 10^{-2}$m and $d_{12} = 10^{-2}$m. $\underset{\sim}{Z}_0$ and $\underset{\sim}{Z}_\ell$ can be easily shown to be

$$\underset{\sim}{Z}_\ell = \underset{\sim}{Z}_0 = \begin{bmatrix} 1000 & 500 \\ 500 & 1000 \end{bmatrix} .$$

The characteristic-impedance matrix, using the values for the per-unit-length inductance matrix given in (C-27), becomes

$$\underset{\sim}{Z}_C = v\underset{\sim}{L} = 60 \begin{bmatrix} \ell n(100) & \ell n(20) \\ \ell n(20) & \ell n(400) \end{bmatrix} .$$

$E_{t_i}^{(inc)} = 0$ in (C-26) and the electric field intensity of the wave is

$$E_\ell^{(inc)}(y, x) = E_x e^{-j\beta y}$$

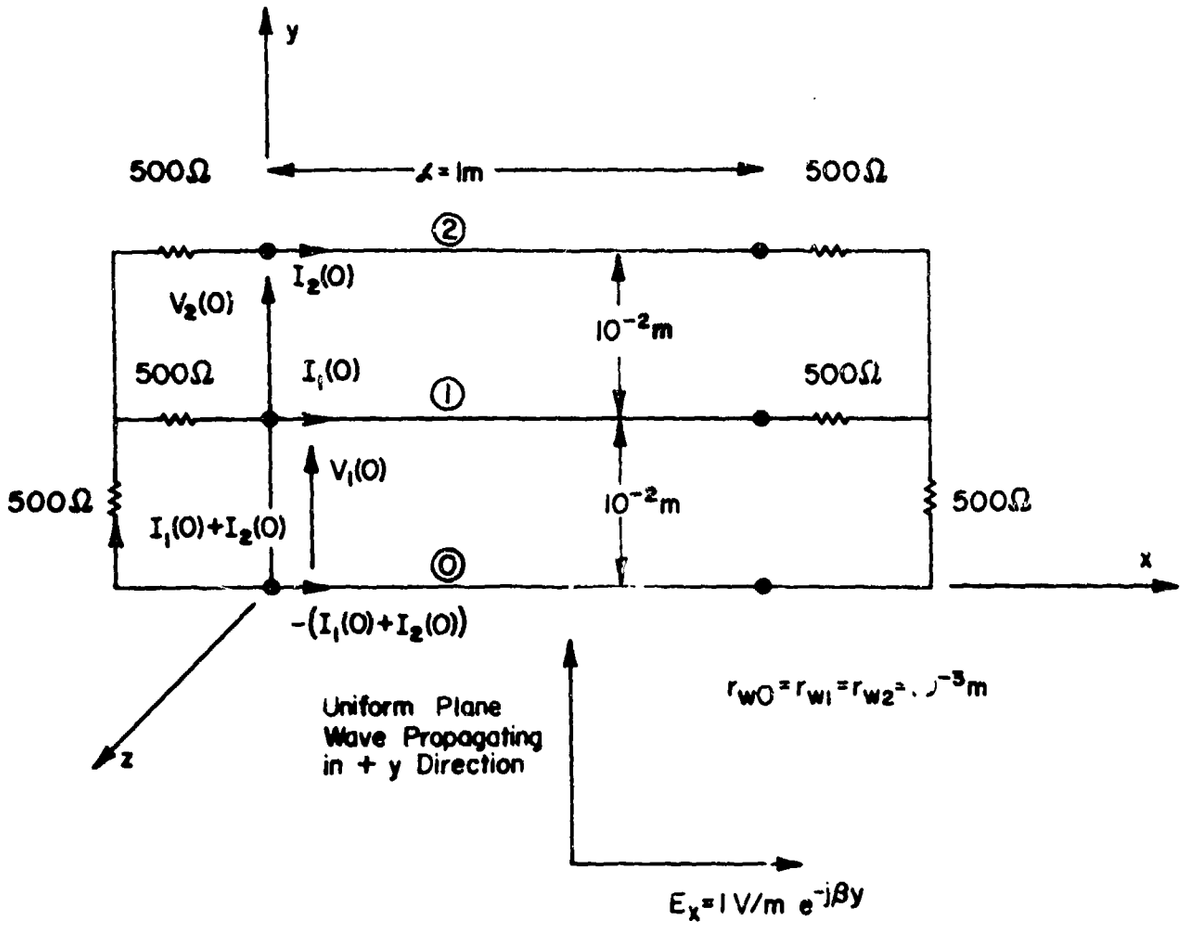

Figure C-4. The geometry for the example.

From this, one can determine

$$E^{(inc)}_{\ell_1}(d_{10}, x) - E^{(inc)}_{\ell_1}(0, x) = e^{-j\beta 10^{-2}} - 1$$

$$E^{(inc)}_{\ell_2}(d_{20}, x) - E^{(inc)}_{\ell_2}(0, x) = e^{-j2\beta 10^{-2}} - 1 \quad .$$

Two frequencies are considered in [24] in terms of $\beta\mathcal{L}$; $\beta\mathcal{L} = 1.5$, $\beta\mathcal{L} = 3.0$. Equations (C-26) with the above items were programmed on an IBM 370/165 computer in double precision arithmetic. The execution time (cpu time) was .01 seconds (1/100 sec) and the results are

$$\beta\mathcal{L} = 1.5 \begin{cases} |I_0(0)| = 1.7662556E - 5A & \angle I_0(0) = 70.77° \\ |I_1(0)| = 9.0756083E - 8A & \angle I_1(0) = -13.9° \\ |I_2(0)| = 1.7671218E - 5A & \angle I_2(0) = -109.52° \end{cases}$$

$$\beta\mathcal{L} = 3.0 \begin{cases} |I_0(0)| = 5.4543875E - 5A & \angle I_0(0) = 9.845° \\ |I_1(0)| = 7.7363155E - 7A & \angle I_1(0) = -75.8° \\ |I_2(0)| = 5.4608110E - 5A & \angle I_2(0) = -170.96° \end{cases} \quad .$$

The computed results obtained by Harrison' method and given in [24] are

$$\beta\mathcal{L} = 1.5 \begin{cases} |I_0(0)| = 1.766E - 5A \\ |I_1(0)| = 9.076E - 8A \\ |I_2(0)| = 1.767E - 5A \end{cases}$$

$$\beta \mathcal{L} = 3.0 \begin{cases} |I_0(0)| = 5.454E - 5A \\ |I_1(0)| = 7.736E - 7A \\ |I_2(0)| = 5.461E - 5A \end{cases}$$

The results computed by this method are exactly those computed by Harrison's method in [24]. However, with this method only 2 simultaneous equations in the 2 unknowns, $I_1(0)$ and $I_2(0)$, are required to be solved ($I_0(0) = -I_1(0) - I_2(0)$). Harrison's method required the solution of 10 simultaneous equations in 10 unknowns. Furthermore, Harrison's method was restricted to uniform plane wave illumination of the line with the wave incident perpendicular to the line. Since $\underset{\sim}{Z}_{\mathcal{L}} = \underset{\sim}{Z}_0$ for this example and since the uniform plane wave is propagating broadside to the line, $\underline{I}(0) = \underline{I}(\mathcal{L})$.

C-5. Extension of the Method to Wires Above a Ground Plane.

Consider the system of n wires in free space above an infinite ground plane shown in Fig. 2(b). The result for (n+1) wires given in (C-26) can be extended to this case with the following observations. Consider Fig. C-5. Clearly we may apply Faraday's law in (C-4) and the previous development to the flat, rectangular surface in the x, y plane shown in Fig. C-5b between the ground plane and the i-th wire and between x and x+Δx. This flat, rectangular surface S_i lies in the x, y plane. Equations (C-26a) and (C-26b) will again be obtained. Equations (C-26c), (C-26d) and (C-26e) become for this case

$$\left[\underline{E}^{(inc)}_{\ell}(x)\right]_i = E^{(inc)}_{\ell_i}(h_i, x) - E^{(inc)}_{\ell_i}(0, x) \qquad \text{(C-36a)}$$

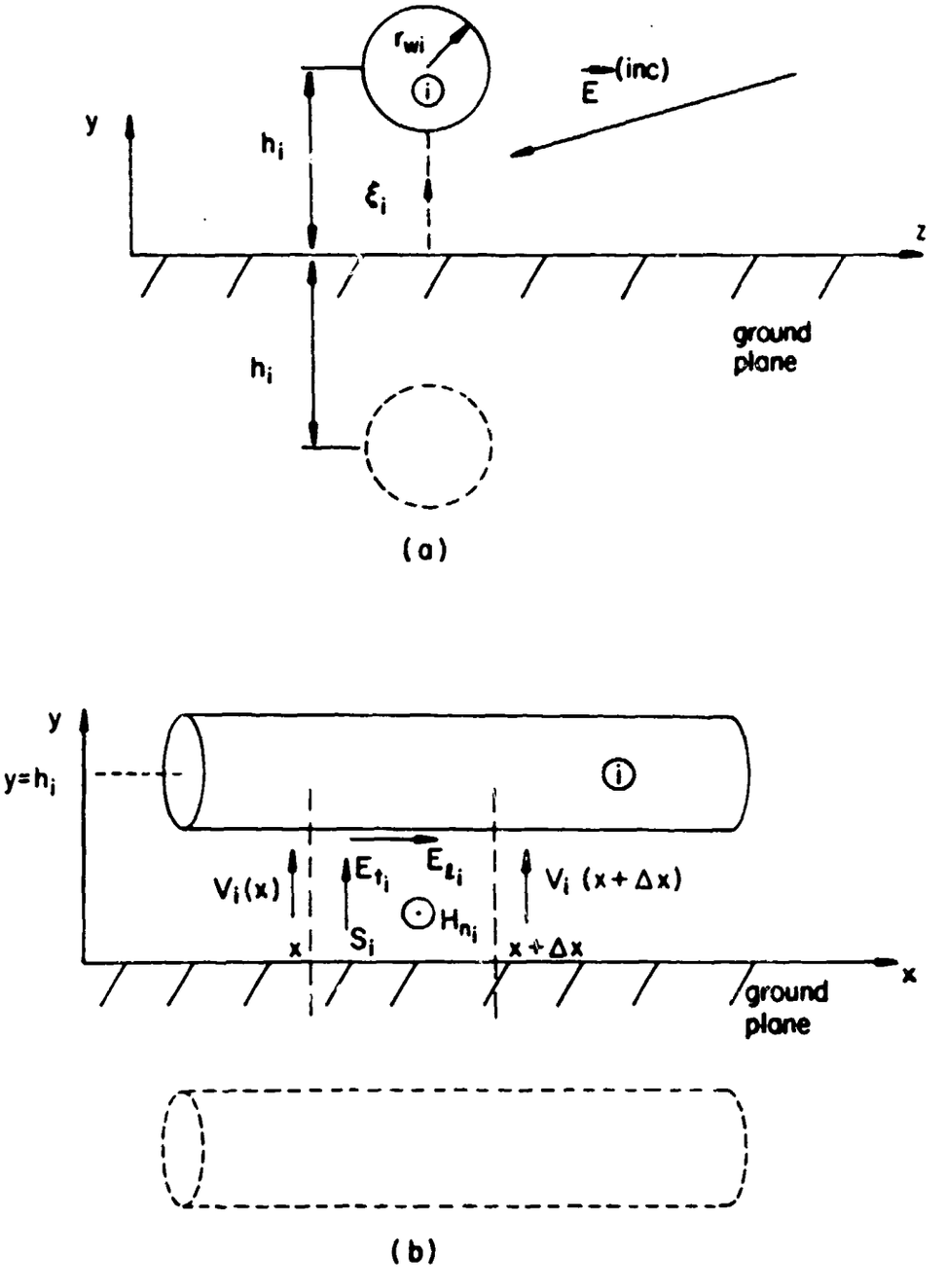

Figure C-5. Multiconductor lines above a ground plane.

$$[\underset{\sim}{E}_t^{(inc)}(\mathcal{L})]_i = \int_0^{h_i} E_{t_i}^{(inc)}(\xi_i, \mathcal{L})\, d\xi_i \qquad \text{(C-36b)}$$

$$[\underset{\sim}{E}_t^{(inc)}(0)]_i = \int_0^{h_i} E_{t_i}^{(inc)}(\xi_i, 0)\, d\xi_i \qquad \text{(C-36c)}$$

where ξ_i is a straight-line contour in the x, y plane between the position of the ground plane, y=0, and the i-th wire which is perpendicular to the ground plane, i.e. $\xi_i = y$. This is indicated in Fig. C-5a.

$E_{\ell_i}^{(inc)}(h_i, x)$ is the component of the incident electric field parallel to the axis of the i-th wire at $y=h_i$ and $E_{\ell i}^{(inc)}(0, x)$ is the component of the incident field parallel to the ground plane directly beneath the i-th wire. $E_{t_i}^{(inc)}$ is the component of the incident electric field parallel to ξ_i and directed in the +y direction.

The per-unit-length inductance matrix, $\underset{\sim}{L}$, can be obtained in a fashion similar to Section C.3 by determining the scattered magnetic flux passing through the surface S_i between the i-th wire and the position of the ground plane (the ground plane is replaced by image wires) and is given in (122) as

$$[\underset{\sim}{L}]_{ii} = \frac{\mu_v}{2\pi} \ell n \left(\frac{2h_i}{r_{wi}}\right) \qquad \text{(C-37a)}$$

$$[\underset{\sim}{L}]_{\substack{ij \\ i\neq j}} = \frac{\mu_v}{2\pi} \ell n \left(\frac{d_{ij}^*}{d_{ij}}\right) \qquad \text{(C-37b)}$$

for i, j=1, ---, n where

$$d_{ij}^* = \sqrt{d_{ij}^2 + 4h_i h_j} \qquad \text{(C-38)}$$

APPENDIX D

The purpose of this appendix is to derive the simplified form of the nodal-admittance matrix for the lumped-circuit iterative approximations given in (80) and the forms of the matrix chain parameters given in (78).

To derive the first equation in (80) consider the equations for the termination-networks in (69):

$$\underline{V}(0) = \underline{V}_0 - \underset{\sim}{Z}_0 \underline{I}(0) \tag{D-1a}$$

$$\underline{V}(\ell) = \underline{V}_\ell + \underset{\sim}{Z}_\ell \underline{I}(\ell) \tag{D-1b}$$

and the matrix chain parameter equations for the lumped-circuit iterative models given in (79) for a line of N sections:

$$\underline{V}\left(\frac{k}{N}\ell\right) = \underset{\sim}{\Phi}_{k11} \underline{V}\left(\frac{k-1}{N}\ell\right) + \underset{\sim}{\Phi}_{k12} \underline{I}\left(\frac{k-1}{N}\ell\right) \tag{D-2a}$$

$$\underline{I}\left(\frac{k}{N}\ell\right) = \underset{\sim}{\Phi}_{k21} \underline{V}\left(\frac{k-1}{N}\ell\right) + \underset{\sim}{\Phi}_{k22} \underline{I}\left(\frac{k-1}{N}\ell\right) . \tag{D-2b}$$

For the first subsection rewrite (D-1a) as

$$\underline{I}(0) = \underset{\sim}{Y}_0 \underline{V}_0 - \underset{\sim}{Y}_0 \underline{V}(0) \tag{D-3}$$

where $\underset{\sim}{Y}_0 = \underset{\sim}{Z}_0^{-1}$ and substitute into (D-2a) with k=1 to yield

$$\underline{V}(\ell/N) = \underset{\sim}{\Phi}_{k11} \underline{V}(0) + \underset{\sim}{\Phi}_{k12} (\underset{\sim}{Y}_0 \underline{V}_0 - \underset{\sim}{Y}_0 \underline{V}(0)) \tag{D-4}$$

$$= (\underset{\sim}{\Phi}_{k11} - \underset{\sim}{\Phi}_{k12} \underset{\sim}{Y}_0) \underline{V}(0) + \underset{\sim}{\Phi}_{k12} \underset{\sim}{Y}_0 \underline{V}_0$$

which is the first equation in (80).

To derive the last equation in (80), rewrite (D-1b) as

$$\underline{I}(\mathfrak{L}) = \underset{\sim}{Y}_{\mathfrak{L}} \underline{V}(\mathfrak{L}) - \underset{\sim}{Y}_{\mathfrak{L}} \underline{V}_{\mathfrak{L}} \tag{D-5}$$

where $\underset{\sim}{Y}_{\mathfrak{L}} = \underset{\sim}{Z}_{\mathfrak{L}}^{-1}$. Substitute this into (D-2b) for k = N to obtain

$$\underset{\sim}{Y}_{\mathfrak{L}} \underline{V}(\mathfrak{L}) - \underset{\sim}{Y}_{\mathfrak{L}} \underline{V}_{\mathfrak{L}} = \underset{\sim}{\Phi}_{k21} \underline{V}\left(\frac{N-1}{N}\mathfrak{L}\right) + \underset{\sim}{\Phi}_{k22} \underline{I}\left(\frac{N-1}{N}\mathfrak{L}\right) . \tag{D-6}$$

Substitute (D-2a) for k = N into (D-6) to obtain

$$\underset{\sim}{Y}_{\mathfrak{L}} \underline{V}(\mathfrak{L}) - \underset{\sim}{Y}_{\mathfrak{L}} \underline{V}_{\mathfrak{L}} = \underset{\sim}{\Phi}_{k21} \underline{V}\left(\frac{N-1}{N}\mathfrak{L}\right) + \underset{\sim}{\Phi}_{k22}\left\{\underset{\sim}{\Phi}_{k12}^{-1} \underline{V}(\mathfrak{L}) - \underset{\sim}{\Phi}_{k12}^{-1} \underset{\sim}{\Phi}_{k11} \underline{V}\left(\frac{N-1}{N}\mathfrak{L}\right)\right\} \tag{D-7}$$

which can be rewritten as

$$\left\{\underset{\sim}{\Phi}_{k21} - \underset{\sim}{\Phi}_{k22} \underset{\sim}{\Phi}_{k12}^{-1} \underset{\sim}{\Phi}_{k11}\right\} \underline{V}\left(\frac{N-1}{N}\mathfrak{L}\right) + \left\{\underset{\sim}{\Phi}_{k22} \underset{\sim}{\Phi}_{k12}^{-1} - \underset{\sim}{Y}_{\mathfrak{L}}\right\} \underline{V}(\mathfrak{L}) = - \underset{\sim}{Y}_{\mathfrak{L}} \underline{V}_{\mathfrak{L}} \tag{D-8}$$

However, one can easily prove the identity in (82)

$$\underset{\sim}{\Phi}_{k21} - \underset{\sim}{\Phi}_{k22} \underset{\sim}{\Phi}_{k12}^{-1} \underset{\sim}{\Phi}_{k11} = - \underset{\sim}{\Phi}_{k12}^{-1} \tag{D-9}$$

associated with the forms of the lumped iterative matrix chain parameters in (78). Therefore, substituting (D-9) into (D-8) and multiplying on the left by $-\underset{\sim}{\Phi}_{k12}$ yields the last equation in (80).

The derivation of the intermediate equations proceeds similarly. Substituting (D-2b) for k=m into (D-2a) for k=m+1 yields

$$\underline{V}\left(\frac{m+1}{N}\mathfrak{L}\right) = \underset{\sim}{\Phi}_{k11} \underline{V}\left(\frac{m}{N}\mathfrak{L}\right) + \underset{\sim}{\Phi}_{k12}\left\{\underset{\sim}{\Phi}_{k21} \underline{V}\left(\frac{m-1}{N}\mathfrak{L}\right) + \underset{\sim}{\Phi}_{k22} \underline{I}\left(\frac{m-1}{N}\mathfrak{L}\right)\right\} \tag{D-10}$$

Writing (D-2a) for k=m as

$$\underline{I}\left(\frac{m-1}{N}\ell\right) = \underset{\sim}{\Phi}_{k12}^{-1}\ \underline{V}\left(\frac{m}{N}\ell\right) - \underset{\sim}{\Phi}_{k12}^{-1}\ \underset{\sim}{\Phi}_{k11}\ \underline{V}\left(\frac{m-1}{N}\ell\right) \tag{D-11}$$

and substituting into (D-10) yields

$$\left\{ \underset{\sim}{\Phi}_{k12}\ \underset{\sim}{\Phi}_{k21} - \underset{\sim}{\Phi}_{k12}\ \underset{\sim}{\Phi}_{k22}\ \underset{\sim}{\Phi}_{k12}^{-1}\ \underset{\sim}{\Phi}_{k11} \right\} \underline{V}\left(\frac{m-1}{N}\ell\right) \tag{D-12}$$

$$+\left\{ \underset{\sim}{\Phi}_{k11} + \underset{\sim}{\Phi}_{k12}\ \underset{\sim}{\Phi}_{k22}\ \underset{\sim}{\Phi}_{k12}^{-1} \right\} \underline{V}\left(\frac{m}{N}\ell\right)$$

$$- \underline{V}\left(\frac{m+1}{N}\ell\right) = \underset{n-1}{0} \quad .$$

Again substituting the identity in (D-9) into (D-12) we obtain

$$\underline{V}\left(\frac{m-1}{N}\ell\right) - \left\{ \underset{\sim}{\Phi}_{k11} + \underset{\sim}{\Phi}_{k12}\ \underset{\sim}{\Phi}_{k22}\ \underset{\sim}{\Phi}_{k12}^{-1} \right\} \underline{V}\left(\frac{m}{N}\ell\right) + \underline{V}\left(\frac{m+1}{N}\ell\right) = \underset{n-1}{0} \tag{D-13}$$

which is the form of any of the intermediate equations in (80).

In addition, it can easily be verified from the forms of the matrix chain parameters for the lumped-circuit iterative models given in (78) that

$$\underset{\sim}{\Phi}_{k12}\ \underset{\sim}{\Phi}_{k22} = \underset{\sim}{\Phi}_{k22}^{t}\ \underset{\sim}{\Phi}_{k12} \tag{D-14a}$$

or

$$\underset{\sim}{\Phi}_{k12}\ \underset{\sim}{\Phi}_{k22}\ \underset{\sim}{\Phi}_{k12}^{-1} = \underset{\sim}{\Phi}_{k22}^{t} \quad . \tag{D-14b}$$

Substituting (D-14b) into (D-8) (along with the identity in (D-9)) and substituting (D-14b) into (D-13) along with (D-4) yield the final nodal-admittance matrix equations in (80):

$$\left(\underset{\sim}{\Phi}_{k12}\ \underset{\sim}{Y}_0 - \underset{\sim}{\Phi}_{k11}\right)\ \underline{V}(0) + \underline{V}(\ell/N) = \underset{\sim}{\Phi}_{k12}\ \underset{\sim}{Y}_0\ V_c \tag{D-15}$$

$$\vdots$$

$$\underline{V}\left(\frac{m-1}{N}\ell\right) - \left(\underset{\sim}{\Phi}_{k11} + \underset{\sim}{\Phi}_{k22}^{t}\right)\underline{V}\left(\frac{m}{N}\ell\right) + \underline{V}\left(\frac{m+1}{N}\ell\right) = \underset{n-1}{0}$$

$$\vdots$$

$$\underline{V}\left(\frac{N-1}{N}\ell\right) + \left(\underset{\sim}{\Phi}_{k12}\underset{\sim}{Y}_{\ell} - \underset{\sim}{\Phi}_{k22}^{t}\right)\underline{V}(\ell) = \underset{\sim}{\Phi}_{k12}\underset{\sim}{Y}_{\ell}\underline{V}_{\ell}$$

for m=1, ----, N-1.

The forms of the matrix chain parameters for the lumped-circuit iterative approximations given in (78) can be derived in the following manner.

For the lumped π model, the terminal equations are (see Fig. 11(a))

$$\underline{V}\left(\frac{k}{N}\ell\right) = \underline{V}\left(\frac{k-1}{N}\ell\right) - \underset{\sim}{Z}\left(\frac{\ell}{N}\right)\underline{I}\left(\frac{k-1}{N}\ell\right) \qquad \text{(D-16a)}$$

$$\underline{I}\left(\frac{k}{N}\ell\right) = \underline{I}\left(\frac{k-1}{N}\ell\right) - \underset{\sim}{Y}\left(\frac{\ell}{N}\right)\underline{V}\left(\frac{k}{N}\ell\right) \qquad \text{(D-16b)}$$

Equation (D-16a) corresponds to the first matrix chain parameter equation in (78a). Substituting (D-16a) into (D-16b) yields

$$\underline{I}\left(\frac{k}{N}\ell\right) = -\underset{\sim}{Y}\left(\frac{\ell}{N}\right)\underline{V}\left(\frac{k-1}{N}\ell\right) + \left\{\underset{\sim}{1}_{n} + \underset{\sim}{Y}\underset{\sim}{Z}\left(\frac{\ell}{N}\right)^{2}\right\}\underline{I}\left(\frac{k-1}{N}\ell\right) \qquad \text{(D-17)}$$

which is the second matrix chain parameter equation in (78a).

For the lumped Γ model, the terminal equations are (see Fig. 11(b))

$$\underline{V}\left(\frac{k}{N}\ell\right) = \underline{V}\left(\frac{k-1}{N}\ell\right) - \underset{\sim}{Z}\left(\frac{\ell}{N}\right)\underline{I}\left(\frac{k}{N}\ell\right) \qquad \text{(D-18a)}$$

$$\underline{I}\left(\frac{k}{N}\ell\right) = -\underset{\sim}{Y}\left(\frac{\ell}{N}\right)\underline{V}\left(\frac{k-1}{N}\ell\right) + \underline{I}\left(\frac{k-1}{N}\ell\right) \qquad \text{(D-18b)}$$

Equation (D-18b) is the second matrix chain parameter equation in (78b). Substituting (D-18b) into (D-18a) yields

$$\underline{V}\left(\frac{k}{N}\ell\right) = \left\{\underset{\sim}{1}_{n} + \underset{\sim}{Z}\underset{\sim}{Y}\left(\frac{\ell}{N}\right)^{2}\right\}\underline{V}\left(\frac{k-1}{N}\ell\right) - \underset{\sim}{Z}\left(\frac{\ell}{N}\right)\underline{I}\left(\frac{k-1}{N}\ell\right) \qquad \text{(D-19)}$$

which is the first matrix chain parameter equation in (78b).

For the lumped Pi model, the terminal equations are (see Fig. 11(c))

$$\underline{V}\left(\frac{k}{N}\mathcal{L}\right) = \underline{V}\left(\frac{k-1}{N}\mathcal{L}\right) - \underset{\sim}{Z}\left(\frac{\mathcal{L}}{N}\right)\left\{\underline{I}\left(\frac{k-1}{N}\mathcal{L}\right) - \frac{1}{2}\underset{\sim}{Y}\left(\frac{\mathcal{L}}{N}\right)\underline{V}\left(\frac{k-1}{N}\mathcal{L}\right)\right\} \qquad \text{(D-20a)}$$

$$= \left\{\underset{\sim}{1}_n + \frac{1}{2}\underset{\sim}{Z}\underset{\sim}{Y}\left(\frac{\mathcal{L}}{N}\right)^2\right\}\underline{V}\left(\frac{k-1}{N}\mathcal{L}\right) - \underset{\sim}{Z}\left(\frac{\mathcal{L}}{N}\right)\underline{I}\left(\frac{k-1}{N}\mathcal{L}\right)$$

$$\underline{I}\left(\frac{k}{N}\mathcal{L}\right) = \underline{I}\left(\frac{k-1}{N}\mathcal{L}\right) - \frac{1}{2}\underset{\sim}{Y}\left(\frac{\mathcal{L}}{N}\right)\underline{V}\left(\frac{k-1}{N}\mathcal{L}\right) \qquad \text{(D-20b)}$$

$$- \frac{1}{2}\underset{\sim}{Y}\left(\frac{\mathcal{L}}{N}\right)\underline{V}\left(\frac{k}{N}\mathcal{L}\right) \quad .$$

Equation (D-20a) is the first matrix chain parameter equation in (78c). Substituting (D-20a) into (D-20b) yields

$$\underline{I}\left(\frac{k}{N}\mathcal{L}\right) = \left\{-\underset{\sim}{Y}\left(\frac{\mathcal{L}}{N}\right) - \frac{1}{4}\underset{\sim}{Y}\underset{\sim}{Z}\underset{\sim}{Y}\left(\frac{\mathcal{L}}{N}\right)^3\right\}\underline{V}\left(\frac{k-1}{N}\mathcal{L}\right) \qquad \text{(D-21)}$$

$$+\left\{\underset{\sim}{1}_n + \frac{1}{2}\underset{\sim}{Y}\underset{\sim}{Z}\left(\frac{\mathcal{L}}{N}\right)^2\right\}\underline{I}\left(\frac{k-1}{N}\mathcal{L}\right)$$

which is the second matrix chain parameter equation in (78c).

For the lumped Tee model, the terminal equations are (see Fig. 11(d))

$$\underline{V}\left(\frac{k}{N}\mathcal{L}\right) = \underline{V}\left(\frac{k-1}{N}\mathcal{L}\right) - \frac{1}{2}\underset{\sim}{Z}\left(\frac{\mathcal{L}}{N}\right)\underline{I}\left(\frac{k-1}{N}\mathcal{L}\right) \qquad \text{(D-22a)}$$

$$- \frac{1}{2}\underset{\sim}{Z}\left(\frac{\mathcal{L}}{N}\right)\underline{I}\left(\frac{k}{N}\mathcal{L}\right)$$

$$\underline{I}\left(\frac{k}{N}\mathcal{L}\right) = \underline{I}\left(\frac{k-1}{N}\mathcal{L}\right) - \underset{\sim}{Y}\left(\frac{\mathcal{L}}{N}\right)\left\{\underline{V}\left(\frac{k-1}{N}\mathcal{L}\right)\right. \qquad \text{(D-22b)}$$

$$\left. - \frac{1}{2}\underset{\sim}{Z}\left(\frac{\mathcal{L}}{N}\right)\underline{I}\left(\frac{k-1}{N}\mathcal{L}\right)\right\}$$

$$= -\underset{\sim}{Y}\left(\frac{\mathcal{L}}{N}\right)\underline{V}\left(\frac{k-1}{N}\mathcal{L}\right) + \left\{\underset{\sim}{1}_n + \frac{1}{2}\underset{\sim}{Y}\underset{\sim}{Z}\left(\frac{\mathcal{L}}{N}\right)^2\right\}\underline{I}\left(\frac{k-1}{N}\mathcal{L}\right) \quad .$$

Equation (D-22b) is the second matrix chain parameter equation in (78d).

Substituting (D-22b) into (D-22a) yields

$$\underline{V}\left(\frac{k}{N}\,\mathfrak{L}\right) = \left\{\underline{1}_n + \frac{1}{2}\,\underline{Z}\,\underline{Y}\left(\frac{\mathfrak{L}}{N}\right)^2\right\}\underline{V}\left(\frac{k-1}{N}\mathfrak{L}\right) \qquad \text{(D-23)}$$

$$+\left\{-\underline{Z}\left(\frac{\mathfrak{L}}{N}\right) - \frac{1}{4}\,\underline{Z}\,\underline{Y}\,\underline{Z}\left(\frac{\mathfrak{L}}{N}\right)^3\right\}\underline{I}\left(\frac{k-1}{N}\,\mathfrak{L}\right)$$

which is the first matrix chain parameter equation in (78d).

APPENDIX E

The purpose of this appendix is to provide justification for omitting the reference potential terms in the potential expressions in Chapter V. Consider Fig. E-1(a) in which infinitesimal line charges lie on a cylindrical surface of radius r_w. The potential $\phi_p(r_p, \theta_p)$ with respect to the potential reference point due to one of the line charges is (reference [58], pp. 91-92)

$$\phi_p(r_p, \theta_p) = \frac{-\lambda}{2\pi\epsilon} \ln\left(\frac{d_p}{d_r}\right) \qquad \text{(E-1)}$$

where the distances from the line charge to the potential and reference points are given by

$$d_p^2 = r_p^2 + r_w^2 - 2r_p r_w \cos(\theta - \theta_p) \qquad \text{(E-2a)}$$

$$d_r^2 = r_r^2 + r_w^2 - 2r_r r_w \cos(\theta - \theta_r) \quad . \qquad \text{(E-2b)}$$

If the cylindrical surface supports a per-unit-length charge distribution of the form

$$\rho(\theta) = a_0 + \sum_{m=1}^{A} a_m \cos m\theta + \sum_{m=1}^{B} b_m \sin m\theta \quad , \qquad \text{(E-3)}$$

then the potential $\phi_p(r_p, \theta_p)$ can be obtained as the limiting case of an infinite number of infinitesimal line charges with appropriate weighting given in (E-3) as [56]

$$\phi_p(r_p, \theta_p) = \frac{-a_0}{2\pi\epsilon} \int_0^{2\pi} \ln\left(\frac{d_p}{d_r}\right) r_w \, d\theta \qquad \text{(E-4)}$$

$$- \frac{1}{2\pi\epsilon} \sum_{m=1}^{A} \int_0^{2\pi} a_m \cos m\theta \ln\left(\frac{d_p}{d_r}\right) r_w \, d\theta$$

$$- \frac{1}{2\pi\epsilon} \sum_{m=1}^{B} \int_0^{2\pi} b_m \sin m\theta \ln\left(\frac{d_p}{d_r}\right) r_w \, d\theta$$

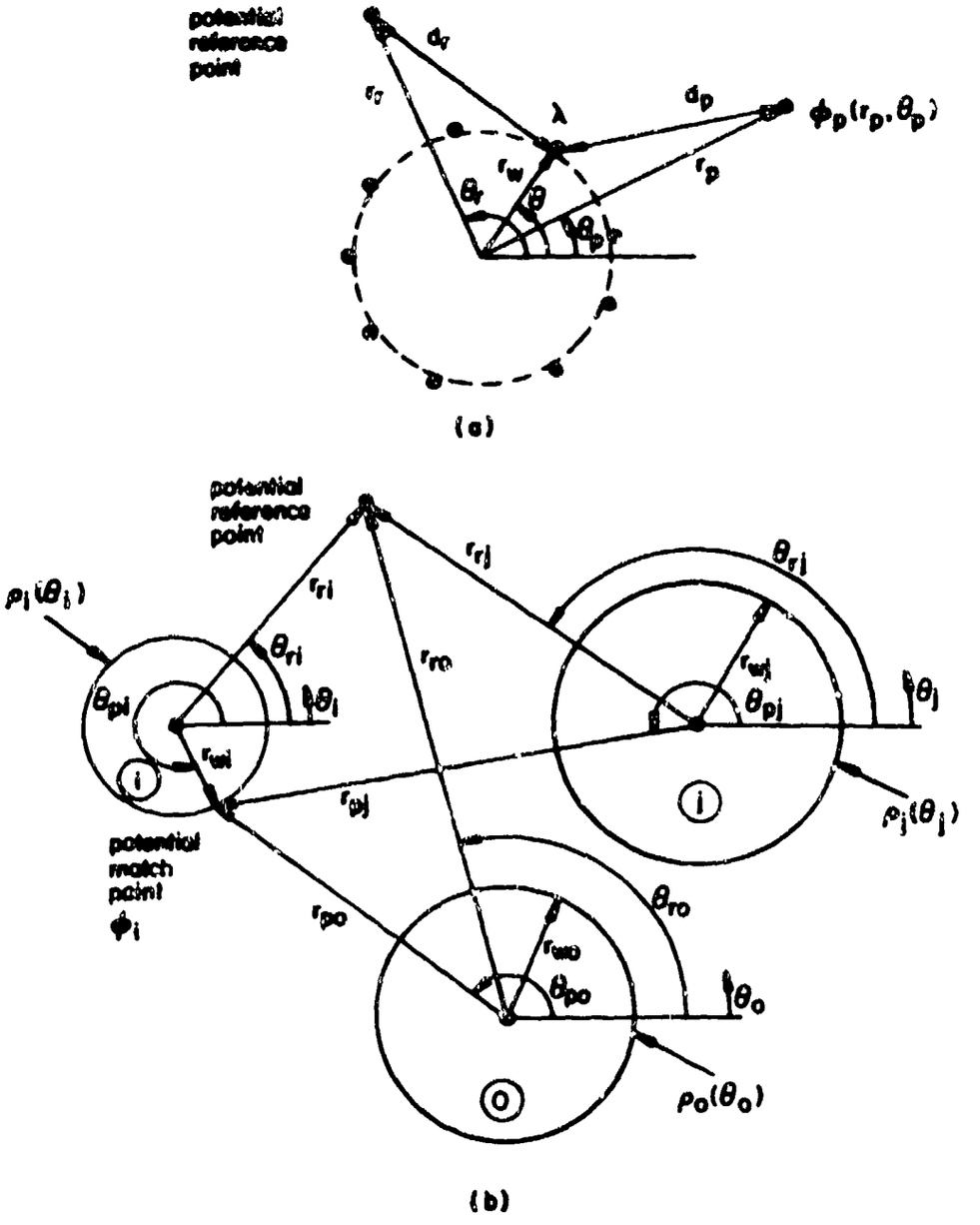

Figure E-1. The geometry for the derivation of the potential expression.

Substituting the expressions for d_p and d_r given in (E-2) into (E-4) yield integrals which can be evaluated in closed form. The result is [56]

$$\phi_p(r_p, \theta_p) = a_0 D_0 (r_p, \theta_p, r_w) - a_0 D_0(r_r, \theta_r, r_w) \qquad \text{(E-5)}$$

$$+ \sum_{m=1}^{A} \left\{ a_m D_m^c (r_p, \theta_p, r_w) - a_m D_m^c(r_r, \theta_r, r_w) \right\}$$

$$+ \sum_{m=1}^{B} \left\{ b_m D_m^s (r_p, \theta_p, r_w) - b_m D_m^s(r_r, \theta_r, r_w) \right\}$$

where

$$D_0(r_p, \theta_p, r_w) = \begin{cases} -\dfrac{r_w \ln r_p}{\epsilon} & r_p \geq r_w \\ -\dfrac{r_w \ln r_w}{\epsilon} & r_p \leq r_w \end{cases} \qquad \text{(E-6a)}$$

$$D_m^c (r_p, \theta_p, r_w) = \begin{cases} \dfrac{(r_w)^{m+1}}{2\epsilon m (r_p)^m} \cos m\theta_p & r_p \geq r_w \\ \dfrac{(r_p)^m}{2\epsilon m (r_w)^{m-1}} \cos m\theta_p & r_p \leq r_w \end{cases} \qquad \text{(E-6b)}$$

$$D_m^s (r_p, \theta_p, r_w) = \begin{cases} \dfrac{(r_w)^{m+1}}{2\epsilon m (r_p)^m} \sin m\theta_p & r_p \geq r_w \\ \dfrac{(r_p)^m}{2\epsilon m (r_w)^{m-1}} \sin m\theta_p & r_p \leq r_w \end{cases} \qquad \text{(E-6c)}$$

The third argument in the expressions of (E-6) will designate the radius of the boundary supporting the charge distribution. The terms $D_0(r_r, \theta_r, r_w)$, $D_m^c(r_r, \theta_r, r_w)$ and $D_m^s(r_r, \theta_r, r_w)$ in (E-5) are the reference potential terms which were omitted from the potential expressions in (96) and (97).

Consider a typical system of (n+1) wires shown in Fig. E-1(b) bearing per-unit-length charge distributions of the form

$$\rho_i(\theta_i) = a_{i0} + \sum_{m=1}^{A_i} a_{im} \cos m\theta_i + \sum_{m=1}^{B_i} b_{im} \sin m\theta_i \qquad \text{(E-7)}$$

for i = 0, 1, ---, n. A typical expression for the potential at a match point on the i-th conductor in Fig. E-1(b) is

$$\begin{aligned}
\phi_i = {} & a_{00} D_0 (r_{p0}, \theta_{p0}, r_{w0}) - a_{00} D_0 (r_{r0}, \theta_{r0}, r_{w0}) \qquad \text{(E-8)} \\
& + \sum_{m=1}^{A_0} \left\{ a_{0m} D_m^c (r_{p0}, \theta_{p0}, r_{w0}) - a_{0m} D_m^c (r_{r0}, \theta_{r0}, r_{w0}) \right\} \\
& + \sum_{m=1}^{B_0} \left\{ b_{0m} D_m^s (r_{p0}, \theta_{p0}, r_{w0}) - b_{0m} D_m^s (r_{r0}, \theta_{r0}, r_{w0}) \right\} \\
& + \text{---------} \\
& + a_{i0} D_0 (r_{wi}, \theta_{pi}, r_{wi}) - a_{i0} D_0 (r_{ri}, \theta_{ri}, r_{wi}) \\
& + \sum_{m=1}^{A_i} \left\{ a_{im} D_m^c (r_{wi}, \theta_{pi}, r_{wi}) - a_{im} D_m^c (r_{ri}, \theta_{ri}, r_{wi}) \right\} \\
& + \sum_{m=1}^{B_i} \left\{ b_{im} D_m^s (r_{wi}, \theta_{pi}, r_{wi}) - b_{im} D_m^s (r_{ri}, \theta_{ri}, r_{wi}) \right\} \\
& + \text{---------} \\
& + a_{j0} D_0 (r_{pj}, \theta_{pj}, r_{wj}) - a_{j0} D_0 (r_{rj}, \theta_{rj}, r_{wj}) \\
& + \sum_{m=1}^{A_j} \left\{ a_{jm} D_m^c (r_{pj}, \theta_{pj}, r_{wj}) - a_{jm} D_m^c (r_{rj}, \theta_{rj}, r_{wj}) \right\} \\
& + \sum_{m=1}^{B_j} \left\{ b_{jm} D_m^s (r_{pj}, \theta_{pj}, r_{wj}) - b_{jm} D_m^s (r_{rj}, \theta_{rj}, r_{wj}) \right\} \\
& + \text{---------}
\end{aligned}$$

If we allow the reference point for the potentials to move to infinity, the reference potential terms for the $a_{im}\cos m\theta_i$ and $b_{im}\sin m\theta_i$ terms, i.e., $D^c_m(r_{ri}, \theta_{ri}, r_{wi})$ and $D^s_m(r_{ri}, \theta_{ri}, r_{wi})$ go to zero for i=0, 1, ---, n as is clear from (E-6b) and (E-6c). In addition, if the total per-unit-length charge on the system of (n+1) conductors is zero, then the reference potential terms due to the constant expansion terms a_{i0}, i.e., $D_0(r_{ri}, \theta_{ri}, r_{wi})$, may also be removed for all i=0, 1, ---, n. This can be shown in the following manner. The total per-unit-length charge on the i-th conductor is

$$q_i = \int_0^{2\pi} \rho_i(\theta_i)\, r_{wi}\, d\theta_i \qquad \text{(E-9)}$$

$$= 2\pi r_{wi} a_{i0}$$

and the portion of the potential expression in (E-8) consisting of the reference potential terms due to the constant charge expansion terms is

$$\begin{aligned} &--- \quad -a_{00} D_0(r_{r0}, \theta_{r0}, r_{w0}) \quad ---- \\ &--- \quad -a_{i0} D_0(r_{ri}, \theta_{ri}, r_{wi}) \quad ---- \\ &--- \quad -a_{j0} D_0(r_{rj}, \theta_{rj}, r_{wj}) \quad ---- \\ &= -\sum_{k=0}^{n} a_{k0} D_0(r_{rk}, \theta_{rk}, r_{wk}) \end{aligned} \qquad \text{(E-10)}$$

Utilizing the expression for D_0 of the form given in (E-6a), equation (E-10) can be written as

$$-\sum_{k=0}^{n} a_{k0} \left(\frac{-r_{wk} \ln(r_{rk})}{\epsilon}\right) . \qquad \text{(E-11)}$$

With the expression for the total per-unit-length charge on the i-th conductor

given in (E-9), equation (E-11) can be written as

$$\sum_{k=0}^{n} q_k \frac{\ell n(r_{rk})}{2\pi\epsilon} \quad . \qquad \text{(E-12)}$$

Requiring the system to be electrically neutral, i.e.,

$$\sum_{k=0}^{n} q_k = 0 \qquad \text{(E-13)}$$

equation (E-12) can be written as

$$-\left(\sum_{k=1}^{n} q_k\right)\frac{\ell n(r_{r0})}{2\pi\epsilon} + \sum_{k=1}^{n} q_k \frac{\ell n\,(r_{rk})}{2\pi\epsilon} \quad . \qquad \text{(E-14)}$$

By combining associated terms, equation (E-14) can be written as

$$\sum_{k=1}^{n} \frac{q_k}{2\pi\epsilon} \ell n \left(\frac{r_{rk}}{r_{r0}}\right) \quad . \qquad \text{(E-15)}$$

As the reference potential point moves to infinity, the distances from the centers of the conductors to the reference point become equal, i.e., $r_{r0} = r_{r1} = \text{----} = r_{rn}$, and (E-15) approaches zero. Therefore, the reference potential terms in the potential expressions may be omitted. Implicit in this is the fact that the potentials, ϕ_i, are with respect to infinity. This is permissible as was shown in this appendix only if the net per-unit-length charge on the system is zero, i.e.,

$$\sum_{k=0}^{n} q_k = 0 \quad . \qquad \text{(E-16)}$$

REFERENCES

[1] S. Hayashi, Surges on Transmission Systems. Kyoto, Japan: Denki-Shoin, Inc., 1955.

[2] W. C. Johnson, Transmission Lines and Networks. New York: McGraw-Hill, 1950.

[3] J. Zaborszky and J. W. Rittenhouse, Electric Power Transmission. New York: Ronald Press, 1954.

[4] L. A. Pipes, "Matrix Theory of Multiconductor Transmission Lines", Phil. Mag., Vol. 24, No. 159, pp. 97-113, July 1937.

[5] L. A. Pipes, "Steady-State Analysis of Multi-Conductor Transmission Lines", Jour. Appl. Phys., Vol. 12, No. 11, pp. 782-789, November 1941.

[6] H. W. Dommel and W. S. Meyer, "Computation of Electromagnetic Transients", Proc. IEEE, Vol. 62, No. 7, pp. 983-993, July 1974.

[7] R. H. Galloway, W. B. Shorrocks, and L. M. Wedepohl, "Calculation of Electrical Parameters for Short and Long Polyphase Transmission Lines", Proc. IEE, Vol. 111, No. 12, pp. 2051-2059, December 1964.

[8] D. E. Hedman, "Propagation on Overhead Transmission Lines I - Theory of Modal Analysis II - Earth-Conduction Effects and Practical Results", Trans. IEEE, Vol. PAS-84, pp. 200-211, March 1965.

[9] W. I. Bowman and J. M. McNamee, "Development of Equivalent Pi and T Matrix Circuits for Long Untransposed Transmission Lines", IEEE Trans. on Power Apparatus and Systems, pp. 625-632, June 1964.

[10] M. Ushirozawa, "High-Frequency Propagation on Nontransposed Power Line", Trans. IEEE , Vol. 83, pp. 1137-1145, November, 1964.

[11] P.Chowdhuri and E. T. B. Gross, "Voltages Induced on Overhead Multiconductor Lines by Lightning Strokes", Proc. IEE, Vol. 116, No. 4, pp. 561-565, April 1969.

[12] L. M. Wedepohl, "Application of Matrix Methods to the Solution of Traveling Wave Phenomena in Polyphase Systems", Proc. IEE, Vol. 110, No. 12, pp. 2200-2212, December 1963.

[13] C. R. Paul, "Solution of the Transmission Line Equations for Lossy Conductors and Imperfect Earth," Proc. IEE(London), Vol. 122, No. 2, pp. 177-182, February 1975.

[14] F. Y. Chang and O. Wing, "Multilayer RC Distributed Networks", IEEE Trans. Circuit Theory, Vol. CT-17, pp. 32-40, February 1970.

[15] F. Y. Chang, "Transient Analysis of Lossless Coupled Transmission Lines in Inhomogeneous Dielectric Medium", IEEE Trans. Microwave Theory and Tech., Vol. MTT-18, No. 9, pp. 616-626, September 1970.

[16] K. D. Marx, "Propagation Modes, Equivalent Circuits, and Characteristic Terminations for Multiconductor Transmission Lines with Inhomogeneous Dielectrics", IEEE Trans. Microwave Theory and Tech., Vol. MTT-21, No. 7, pp. 450-457, July 1973.

[17] C. W. Ho, "Theory and Computer-Aid d Analysis of Lossless Transmission Lines", IBM J. Research and Develop., pp. 249-255, May 1973.

[18] C. R. Paul, "Useful Matrix Chain Parameter Identities for the Analysis of Multiconductor Transmission Lines", IEEE Trans. on Microwave Theory and Techniques, Vol. MTT-23, No. 9, pp. 756-760, September 1975.

[19] E. Ott, A Network Approach to the Design of Multi-line 2N-Port Directional Couplers, Rome Air Development Center, Griffiss AFB, New York, RADC-TR-65-41, April 1965. (AD614 650)

[20] C. D. Taylor, R. S. Satterwhite and C. W. Harrison, Jr., "The Response of a Terminated Two-Wire Transmission Line Excited by a Nonuniform Electromagnetic Field", IEEE Trans. on Antennas and Propagation, pp. 987-989, November 1965.

[21] A. A. Smith, "A More Convenient Form of the Equations for the Response of a Transmission Line Excited by Nonuniform Fields", IEEE Trans. Electromagnetic Compatibility, Vol. EMC-15, pp. 151-152, August 1973.

[22] Electromagnetic Pulse Handbook for Missles and Aircraft in Flight, Sandia Laboratories, SC-M-710346, Albuquerque, N. M., September 1972.

[23] Aeronautical Systems EMP Technology Review (Chapter 5), The Boeing Company, Aerospace Group, Boeing Document D224-10004-1, April 15, 1972.

[24] C. W. Harrison, Jr., "Generalized Theory of Impedance Loaded Multiconductor Transmission Lines in an Incident Field," IEEE Trans. on Electromagnetic Compatibility, Vol. EMC-14, No. 2, pp. 56-63, May 1972.

[25] S. Frankel, "Terminal Response of Braided-Shield Cables to External Monochromatic Electromagnetic Fields", IEEE Trans. on Electromagnetic Compatibility, Vol. EMC-16, No. 1, pp. 4-16, February 1974.

[26] C. R. Paul, "Efficient Numerical Computation of the Frequency Response of Cables Illuminated by an Electromagnetic Field", IEEE Trans. on Microwave Theory and Tech., Vol. MTT-22, No. 4, pp. 454-457, April 1974.

[27] C. R. Paul, "Frequency Response of Multiconductor Transmission Lines Illuminated by an Electromagnetic Field", 1975 IEEE International Symposium on Electromagnetic Compatibility, San Antonio, Texas, October 1975.

[28] J. C. Isaacs, Jr. and N. A. Strakhov, "Crosstalk in Uniformly Coupled Lossy Transmission Lines", Bell System Tech. J., Vol. 52, No. 1, pp. 101-115, January 1973.

[29] J. R. Carson, "Wave Propagation in Overhead Wires With Ground Return", Bell Syst. Tech. J., Vol. 5, pp. 539-559, 1926.

[30] R. E. Matick, Transmission Lines for Digital and Communication Networks. New York: McGraw-Hill, 1969.

[31] W. T. Weeks, "Mathematical Analysis of Ferrite Core Memory Arrays", IEEE Trans. on Computers, Vol. C-18, No. 5, pp. 409-416, May 1969.

[32] K. A. Chen, "Computer-Aided Memory Design Using Transmission Line Models", IEEE Trans. on Computers, Vol. C-17, No. 7, pp. 640-648, July 1968.

[33] B. L. Carlson, W. R. Marcelja and D. A. King, Computer Analysis of Cable Coupling for Intra-system Electromagnetic Compatibility, AFAL-TR-65-142, Wright Patterson AFB, Ohio, The Boeing Company, May 1965.

[34] J. Bogdanor, M. Siegel and G. Weinstock, Intra-vehicle Electromagnetic Compatibility Analysis, AFAL Contract No. F33615-70-C-1333, Wright Patterson AFB, Ohio, The McDonnell-Douglas Corporation, April 1971.

[35] W. R. Johnson, A. K. Thomas, et. al., Development of a Space Vehicle Electromagnetic Interference/Compatibility Specification, NASA Contract Number 9-7305, The TRW Company 08900-6001-T000, June 1968.

[36] Digital Computer Program for EMR Effects on Electronic Systems, Test and Reliability Evaluation Laboratory, U. S. Army Missle Command, Contract DAA H01-69-C-1381, GTE Sylvania Incorporated, June 1972.

[37] J. L. Bogdanor, R. A. Pearlman and M. D. Siegel, Intrasystem Electromagnetic Compatibility Analysis Program, Technical Report, RADC-TR-74-342 Rome Air Development Center, Griffiss AFB, N.Y., December 1974. Vols I - III (AD A008 526 - A008528)

[38] C. R. Paul, Linear Systems, Technical Report, RADC-TR-71-134, Rome Air Development Center, Griffiss AFB, N. Y., July 1971. (AD728 631)

[39] R. M. Fano, L. J. Chu and R. B. Adler, Electromagnetic Fields, Energy and Forces. New York: Wiley, 1960.

[40] R. B. Adler, L. J. Chu and R. M. Fano, Electromagnetic Energy Transmission and Radiation. New York: Wiley, 1960.

[41] F. E. Hohn, Elementary Matrix Algebra. New York: Macmillan, Second Edition, 1964.

[42] K. Ogata, State Space Analysis of Control Systems. Englewood Cliffs, N. J.: Prentice-Hall, 1967.

[43] E. N. Protonotarios and O. Wing, "Analysis and Intrinsic Properties of the General Nonuniform Transmission Line", IEEE Trans. on Microwave Theory Tech., Vol. MTT-15, No. 3. pp. 142-150, March 1967.

[44] K. Singhal and O. Wing, "Network Functions of a Class of Non-uniform Multi-layer Distributed Networks", IEEE Trans. Circuit Theory, Vol. CT-17, No. 2, pp. 275-277, May 1970.

[45] H. Hagiwara and S. Okugawa, "Time-Domain Analysis of Multiconductor Exponential Lines", Proceedings IEEE, pp. 1111-1112, June 1968.

[46] E. C. Bertnolli, "Analysis of the N-Wire Exponential Line", Proceedings IEEE, pp. 1225, June 1967.

[47] C. R. Paul, "On Uniform Multimode Transmission Lines", IEEE Trans. Microwave Theory and Techniques, Vol. MTT-21, No. 8, pp. 556-558, August 1973.

[48] C. R. Paul and J. C. Clements, "Coupled Transmission Lines", 1972 IEEE SOUTHEAST-CON, Louisville, Ky., May 1972.

[49] A. Ralston, A First Course in Numerical Analysis. New York: McGraw-Hill, 1965.

[50] System/360 Scientific Subroutine Package, Version III, Fifth Edition, International Business Machines Corporation, Technical Publications Department, 112 East Post Road, White Plains, New York, August 1970.

[51] R. L. Goldberg, "Focus on Flexible Flat Cable and PC's", Electronic Design, Vol. 20, No. 25, pp. 60-68, December 7, 1972.

[52] D. F. Strawe, Analysis of Uniform Symmetric Transmission Lines, The Boeing Company, Boeing Document, D2-19734-1, August 1971.

[53] A. M. Erisman and G. E. Spies, "Exploiting Problem Characteristics in the Sparse Matrix Approach to Frequency Domain Analysis", IEEE Trans. Circuit Theory, Vol. CT-19, No. 3, pp. 260-264, May 1972.

[54] W. T. Weeks, "Multiconductor Transmission Line Theory in the TEM Approximation", IBM J. Research and Development, pp. 604-611, November 1972.

[55] W. B. Boast, Vector Fields. New York: Harper & Row, Second Edition, 1964.

[56] J. C. Clements and C. R. Paul, Computation of the Capacitance Matrix for Dielectric-Coated Wires, Technical Report, TR-74-59, Rome Air Development Center, Griffiss AFB, N. Y., March 1974. (AD 778 148)

[57] J. C. Clements, C. R. Paul and A. T. Adams, "Computation of the Capacitance Matrix for Systems of Dielectric-Coated Cylindrical Conductors", IEEE Trans. on Electromagnetic Compatibility, Vol. EMC-17, No. 4, pp. 238-248, November 1975.

[58] A. T. Adams, Electromagnetics for Engineers. New York: Ronald Press, 1971.

[59] A. T. Adams and J. R. Mautz, "Computer Solution of Electrostatic Field Problems by Matrix Inversion", Proceedings 1969 National Electronics Conference, pp. 198-201.

[60] M. P. Sarma, "Application of Moment Methods to the Computation of Electrostatic Fields-Part I - Parallel Cylindrical Conductor Systems", IEEE PES Summer Meeting, San Francisco, CA., July 9-14, 1972.

[61] D. W. Kammler, "Calculation of Characteristic Admittances and Coupling Coefficients for Strip Transmission Lines", IEEE Trans. Microwave Theory Tech., Vol. MTT-16, No. 11, pp. 925-937, November 1968.

[62] J. W. Craggs, "The Determination of Capacity for Two-Dimensional Systems of Cylindrical Conductors", Quarterly J. of Mathematics (Oxford Series), Vol. 17, pp. 131-137, 1946.

[63] M. P. Sarma and W. Janischewskyj, "Electrostatic Field of a System of Parallel Cylindrical Conductors", IEEE Trans. on Power Apparatus and Systems, Vol. PAS-88, No. 7, pp. 1069-1079, July 1969.

[64] M. S. Abou - Seada and E. Nasser, "Digital Computer Calculation of the Potential and its Gradient of a Twin Cylindrical Conductor", IEEE Trans. on Power Apparatus and Systems, Vol. PAS-88, No. 12, pp. 1802-1814, December 1969.

[65] A. Matsumoto, Network Synthesis with Multiwire Lines, RADC-TDR-63-369, Rome Air Development Center, Griffiss AFB, N. Y., August 1963. (AD 417 757)

[66] J. W. Craggs and C. J. Tranter, "The Capacity of Two-Dimensional Systems of Conductors and Dielectrics With Circular Boundaries", Quarterly J. of Mathematics (Oxford Series), Vol. 17, pp. 138-144, 1946.

[67] W. T. Weeks, "Calculation of Coefficients of Capacitance of Multiconductor Transmission Lines in the Presence of a Dielectric Interface," IEEE Trans. Microwave Theory Tech., Vol. MTT-18, p. 35, 1970.

[68] L. Young, Parallel Coupled Lines and Directional Couplers. Dedham, Mass: Artech House, 1972.

MISSION
of
Rome Air Development Center

RADC is the principal AFSC organization charged with planning and executing the USAF exploratory and advanced development programs for information sciences, intelligence, command, control and communications technology, products and services oriented to the needs of the USAF. Primary RADC mission areas are communications, electromagnetic guidance and control, surveillance of ground and aerospace objects, intelligence data collection and handling, information system technology, and electronic reliability, maintainability and compatibility. RADC has mission responsibility as assigned by AFSC for demonstration and acquisition of selected subsystems and systems in the intelligence, mapping, charting, command, control and communications areas.